Activation of LFA-1 through mutations within the IDAS site of the I domain : their effects on ligand binding and the capacity of LFA-1 to signal to other integrins

Thesis

ACTIVATION OF LFA-1 THROUGH MUTATIONS WITHIN THE IDAS SITE OF THE I DOMAIN: THEIR EFFECTS ON LIGAND BINDING AND THE CAPACITY OF LFA-1 TO SIGNAL TO OTHER INTEGRINS

Bernadette Mary Sweeney

A thesis submitted in part fulfilment of the requirements of the Open University for the degree of Doctor of Philosophy

February 2004

Department of Project Biology

Celltech

216 Bath Road, Slough, Berkshire, UK

Submission date: 3 March 2004
Award date: 12 May 2004

Abstract

Evidence is now emerging which suggests that in addition to the ability of integrins to regulate cell adhesion through signalling events to other cell surface receptors they may also play a role in the regulation of other integrins expressed on the same cell surface. While the data on LFA-1 is limited, published reports suggest that this integrin when activated can both down- and up-regulate the binding of $\alpha 4\beta 1$ and $\alpha 5\beta 1$ to their respective ligands. Using a novel method we expressed a soluble form of LFA-1 which was subsequently used to identify a series of constitutively activated forms of LFA-1 generated through introduction of novel and published mutations into the I Domain IDAS. Having established their increased activity over wild type LFA-1, the mutant forms of LFA-1 were used to investigate the ability of full length LFA-1 to regulate the binding of $\alpha 4\beta 1$ and $\alpha 5\beta 1$ when expressed on the same cell surface. While mutations in the LFA-1 I domain currently known to promote ligand binding were not sufficient alone to promote integrin crosstalk in either the K562 or JB2.7 cell systems, in the presence of mAb KIM127, crosstalk between $\alpha 5\beta 1$ and all forms of K562 surface expressed LFA-1 was effectively induced. However, the lack of crosstalk with the JB2.7 cell line, even in the presence of KIM127, suggests that this phenomenon may be further complicated by cell-line specific differences.

Acknowledgements

I am deeply indebted to Dr. Martyn Robinson and Dr Tony Shock for all the time, encouragement, and advise they have given to me over the course of this Ph.D. Thanks also to Dr Nancy Hogg, my external supervisor, for her constructive comments and helpful discussions through out my studies. This work however could not have been completed without the support and advise from all my friends and work colleagues at Celltech including Alistair, Al, Andy, Andrew, Dave, Hishani, Jean, Mark, Paul, Paul, Ralph, Sadiqua and Sue, and especially Viv, who always willing gave of her time and expertise to help me. Thanks also to the other PhD students, most especially Lisa, with whom I have been able to share all the highs and lows of this journey. And last but not least, I would like to thank Steve whose practical, emotional and intellectual support throughout has been immeasurable.

Go raibh míle míle maith agaibh as bhur gcunamh!

ABBREVIATIONS

Å	Angstrom
Ab	Antibody
abl	Antibody Leader Sequence
ADMIDAS	Adjacent to Metal Ion Dependent Adhesion Site
Amp	Ampicillin
Amp^r	Ampicillin Resistance
APC	Antigen Presenting cell
bp	Base Pairs
BSA	Bovine Serum Albumin
CamKII	Calmodulin-dependent protein kinase II
CD	Cluster of Differentiation
cDNA	Complementary Deoxyribonucleic Acid
CHO	Chinese Hamster Ovary
CIP	Calf Intestinal Phosphatase
DC-SIGN	Dendritic Cell-Specific ICAM-3 grabbing non-integrin
DNA	Deoxyribonucleic Acid
dATP	Deoxyadenosine Triphosphate
dCTP	Deoxycytosine Triphosphate
dGTP	Deoxyguanosine Triphosphate
dTTP	Deoxythymidine Triphosphate
dH_2O	Distilled Water
DGV	Double Gene Vector
DMEM	Dulbecco's Modified Eagles Media
DMSO	Dimethyl Sulphoxide

DS	double stranded (DNA)
DTT	Dithiothreitol
ECL	Enhanced Chemiluminescence
ECM	Extracellular Martix
EDTA	Ethylenediamine tetra-acetic Acid
EGF	Epidermal Growth Factor
ELISA	Enzyme-linked Immunosorbent Assay
FACS	Fluorescence Activated Cell Sorter
FAK	Focal Adhesion Kinase
Fc	Fragment Crystallisable
FCS	Foetal Calf Serum
FITC	Fluorescein Isocyanate
FL	Full Length
g	Acceleration relative to that due to the earths gravitational field (=9.8ms^{-2})
GMEM	Glasgow Modified Eagles Media
gp	Glycoprotein
GS	Glutamine Synthetase
HBS	Hepes-buffered Saline
HBSS	Hank's Balanced Salt Solution
hCMV	Human Cytomegalovirus
HEV	High Endothelial Venules
hFc	human Fragment Crystallisable
HRP	Horse Radish Peroxidase
HUVECs	Human Umbilical Vein Endothelial Cells
ICAM	Intercellular Adhesion Molecule
iC3b	Cleaved complement component C3b

IDAS	I Domain Allosteric Site
Ig	Immunoglobulin
IL-1	Interleukin 1
JAM	Junction Adhesion Molecule
kb	Kilobase
K_D	Dissociation Constant
kDa	Kilodalton(= 1.66 x 10^{-24}kg)
LAD	Leukocyte Adhesion Deficiency
LB	Luria Broth
LFA-1	Lymphocyte Function Associated Antigen-1
LIMBS	Ligand Induced Metal Ion Binding Site
LPS	Lipopolysaccharide
mAb	Monoclonal Antibody
MAdCAM	Mucosal Addressin Cell Adhesion Molecule
mFc	Mouse Fragment Crystallisable
µF	Micro-Faraday
MIDAS	Metal Ion Dependent Adhesion Site
MHC	Major Histocompatability Complex
MSX	Methionine Sulphoximine
NEAA	Non-essential Amino Acids
neo	Neomycin
NIF	Neutrophil Inhibition Factor
NP40	Nonidet P40
org	Original (cell line)
PAGE	PolyAcrylamide Gel Electrophoresis
PBS	Phosphate-buffered Saline
PCR	Polymerase Chain Reaction
PE	Phycoerythrin

PKC	Protein Tyrosine Kinase
PMA	Phorbol 12-Myristate 13-Acetate
PMN	Polymorphonucleated (cells)
POX	Horseradish peroxidase
PSI	Plexins, Semophorins and Integrins
SD	Standard Deviation
SDS	Sodium Dodecyl Sulphate
SGV	Single Gene Vector
sol	refers to soluble region of the integrin
SV40	Simian Virus 40
TAE	Tris-acetate EDTA
TBS	Tris-buffered Saline
TCR	T Cell Receptor
TD	Tail Domain
TE	Tris EDTA
TLN	Telencephalon
TMB	3,3,5,5'-tretramethylethylenediamine
TNFα	Tumour Necrosis Factor-alpha
UV	Ultraviolet
VCAM-1	Vascular Cell Adhesion Molecule –1
VLA	Very Late Antigen
v/v	volume/volume
WT	Wild type
V/cm	Volts per centimetre
w/v	Weigh per volume
Zap70	Zeta Associated Protein

Table Of Contents

LIST OF FIGURES

List of Tables

Chapter 1

Introduction

Chapter 1 Introduction

1.1 General introduction

Adhesive interactions of cells with other cells and with the extracellular matrix are required for a diverse range of physiological processes that include tissue morphogenesis, inflammation, immune responses, leucocyte trafficking and regulation of cell growth and differentiation (Hynes, 1992; Springer, 1994). Integrins and their ligands play a central role in regulating such processes by bridging the gap between the cell cytoskeleton and the extracellular environment, mediating both cell adhesion and activation of many intracellular signalling pathways.

Integrins are a protein family of noncovalently associated, type 1 transmembrane α and β-subunits. To date the family consists of 24 members, made up of 18 α-chains and 8 β-chains which combine in a partly restricted manner to form the 24 different dimers (Figure.1.1). Both the α and β subunits contain large extracellular domains of more than 940 and 640 residues, respectively (Gahmberg *et al.*, 1997(a)) as well as short but functionally important intracellular domains of ~50 residues (Figure.1.2). Integrins bind to a diverse range of ligands, including components of the extracellular matrix, cell surface Ig superfamily receptors, components of microorganisms, and certain plasma proteins (Ginsberg *et al.*, 1983; Marlin and Springer, 1987). Individual integrins can bind more than one ligand, and, although specific ligands can be recognised by more than one integrin, differences in affinity ensure that there is very little functional redundancy in such interactions.

The integrin of particular interest for this work is LFA-1. LFA-1 (αLβ2) is a member of the leucocyte-specific branch of the integrin family which also includes αMβ2 (Arnaout *et al.*, 1988; Corbi *et al.*, 1988), αXβ2 (p150, 95) (Sanchez-Madrid *et al.*, 1983) and αDβ2 (Van Der Vieren *et al.*, 1995). While LFA-1 is constitutively expressed on the cell surface, the other family

members require cell activation for expression on the cell surface. Table 1.1 illustrates the cellular distribution of the β2 integrins and their known ligands. There is a significant degree of overlap in ligand specificity amongst the different β2 integrins, where the predominant ligands are members of the Ig superfamily. Although LFA-1 expression is limited to leucocytes, it is involved in a broad range of immunological processes including leucocyte extravasation, antigen presentation, and T-lymphocyte alloantigen-induced proliferation (Springer *et al.*, 1987). The functional importance of LFA-1 and the other β2 integrins was first recognized by the clinical condition LAD-1 (leucocyte adhesion deficiency type 1), where a mutation within the β2 chain results in loss of expression of LFA-1 (and other members of the β2 family) leading to a number of leucocyte defects including greatly diminished neutrophil emigration into inflammatory sites, leaving patients susceptible to life-threatening bacterial infections (Gahmberg, *et al.*, 1997(b)). A wealth of data from knock-out animal and *in vivo* studies with monoclonal antibodies (mAbs) have highlighted the important role LFA-1 plays in both normal and pathological conditions (reviewed by de Fougerolles, 2003).

Because of the importance of LFA-1 and integrins in general, both in normal and disease states, much research over the last few years has focused on increasing our knowledge of how integrins function and the processes that are involved in their activation and regulation. In particular, the elucidation of the crystal structure of the extracellular domains of αVβ3 integrin heterodimer and the crystal structures of I domains complexed with ligand, along with extensive mapping of mAb epitopes and mutagenesis studies, have suggested that integrins are molecules in dynamic equilibrium at the cell surface, capable of interacting with a wide range of proteins both intracellularly and extracellularly.

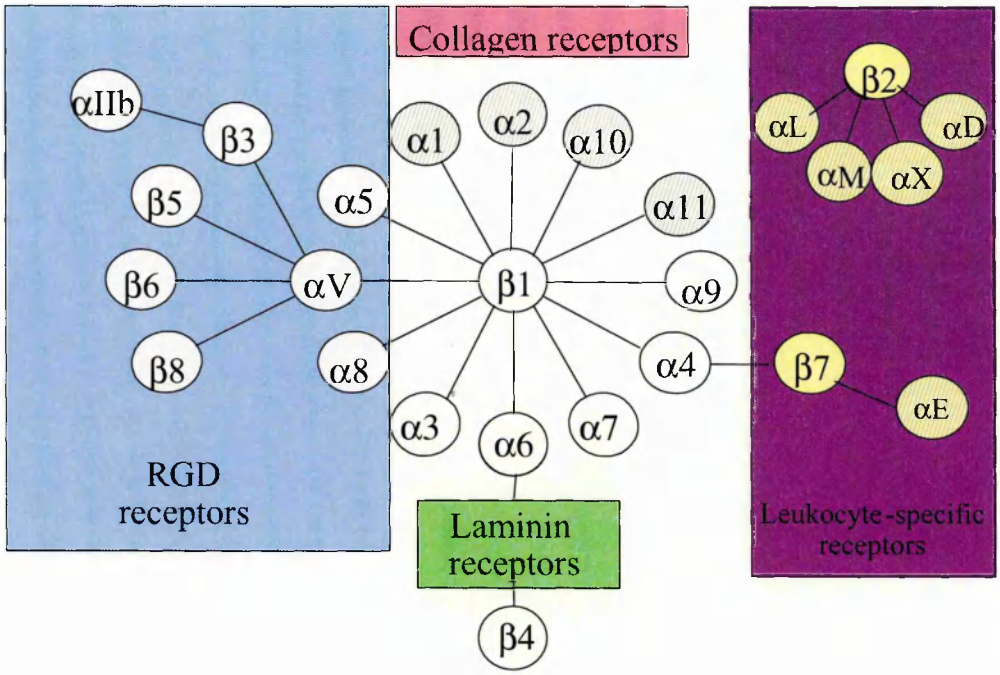

Figure 1.1 **The Integrin Receptor Family.** This figure represents the 24 distinct integrins made up of pairings between 18α-subunits and 8β-subunits. The family can further be divided into several subfamilies based on ligand specificity, and in the case of the β2 and β7 integrins, their restricted expression on leucocytes. α subunits with hatched lines contain an inserted /I domain. Diagram taken from Hynes (2002).

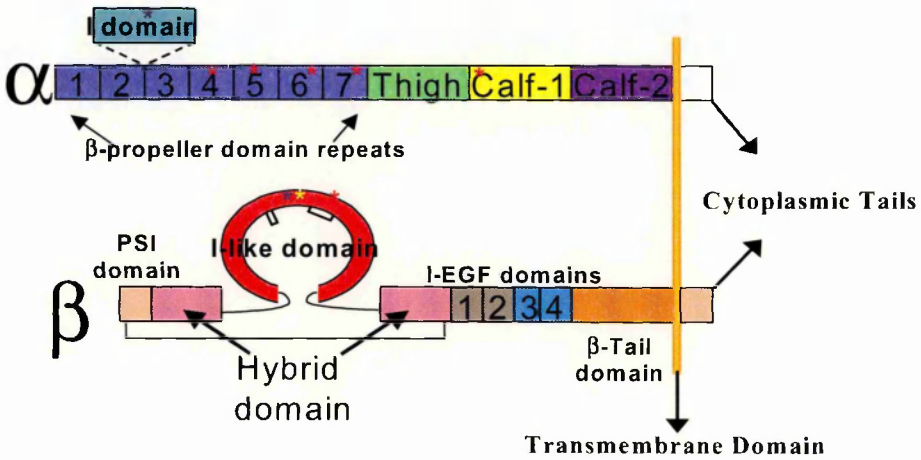

Figure 1.2 **Schematic of the overall structure of an I domain containing integrin.** This diagram illustrates the organisation of the 6 distinct domains of the αL subunit and the 9 distinct domains of the β2 subunit within the primary structure of an I domain-containing integrin. The blue asterisks depict the MIDAS (Metal Ion Dependent Adhesion Site) present in both the I domain and I-like domain. The red asterisks depict putative Ca^{2+} binding sites and the yellow asterisk depicts the ADMIDAS (Adjacent Metal Ion Dependent Adhesion Site)

	LFA-1(αLβ2) CD11a/CD18	MAC-1(αMβ2) CD11b/CD18	P150,95(αXβ2) CD11c/CD18	αDβ2 CD11d/CD18
CELLULAR DISTRIBUTION	All leukocytes	Myeloid cells, Monocytes, Macrophages	Monocytes, Macrophages, Dendritic cells	Macrophages, Neutrophils, Monocytes
LIGANDS	ICAM-1, ICAM-2, ICAM-3, ICAM-4, JAM-1	ICAM-1, ICAM-2, ICAM-3, Fibrinogen, NIF, Factor X, iC3b, JAM-3? CD23	ICAM-1, Fibrinogen, iC3b CD23	ICAM-1, ICAM-3, VCAM-1
FUNCTION	Leukocyte extravasation, Ag presentation, T- lymphocyte alloantigen-induced proliferation	Phagocytœsis, leukocyte extravasation, chemotaxis, activation of neutrophils and monocytes.	Monocyte adhesion and chemotaxis	

Table 1.1 **Cellular distribution and function of the various β2 integrins.** This table describes the cellular distribution, ligand specificity and major functions of each of the β2 integrins. [ICAM = intracellular adhesion molecule; VCAM = vascular cell adhesion molecule 1; NIF = neutrophil inhibitory factor; JAM = junction adhesion molecule; TLN = telencephalon]

This introduction will summarise what is known about the general structure of integrins based on the X-ray crystal and NMR data published to date. This will be followed by a review of how the various integrin and I domain structural conformations can be interpreted to explain integrin activation and ligand binding with particular reference to LFA-1. The remainder of the introduction will cover in detail the function, ligand binding and activation of LFA-1.

1.2 General Integrin Structure

For many years the only structural information about integrins came from images generated in electron microscopy studies of the extracellular region of αIIbβ3 (Du *et al.*, 1993). This showed that the extracellular segment consisted of a globular head and two long stalk regions which connect the globular head to the cell membrane. However, within the last few years resolution of the crystal structure of the extracellular portion of αVβ3 (Xiong *et al.*, 2001, 2002) has greatly enhanced our understanding of the overall structure of integrins. In addition to this information the high level of sequence homology (the α and β-subunits of all integrins share an overall amino acid identity of 25% and 37-45% respectively) and correlation of computer-based predictions of several integrin domain structures allows one to use this structure as a representation of a composite integrin tertiary structure from which the possible mechanisms of activation can be postulated. The crystal structure, resolved to 3.1Å, predicted the presence of 12 domains within the αβ heterodimer extracellular portion of the integrin (Figure.1.3). Of these 12 domains, 8, and a portion of the ninth were fully resolved. A complementary NMR structure of a β2 integrin fragment (Beglova *et al.*, 2002) later revealed the structure of some of the missing domains and helped to further define the overall integrin structure. The structure of the twelve domains (13 for I domain-containing integrins) that assemble into an ovoid head and two legs will be described in detail in the following section.

1.2.1. The α-chain head region

The head region of the α subunit is formed from a seven bladed β-propeller domain (Tuckwell *et al.*, 1994; Springer, 1997) and in 9 out of the 18 integrin α-subunits there is an inserted domain (known as the I domain) between blades 2 and 3.

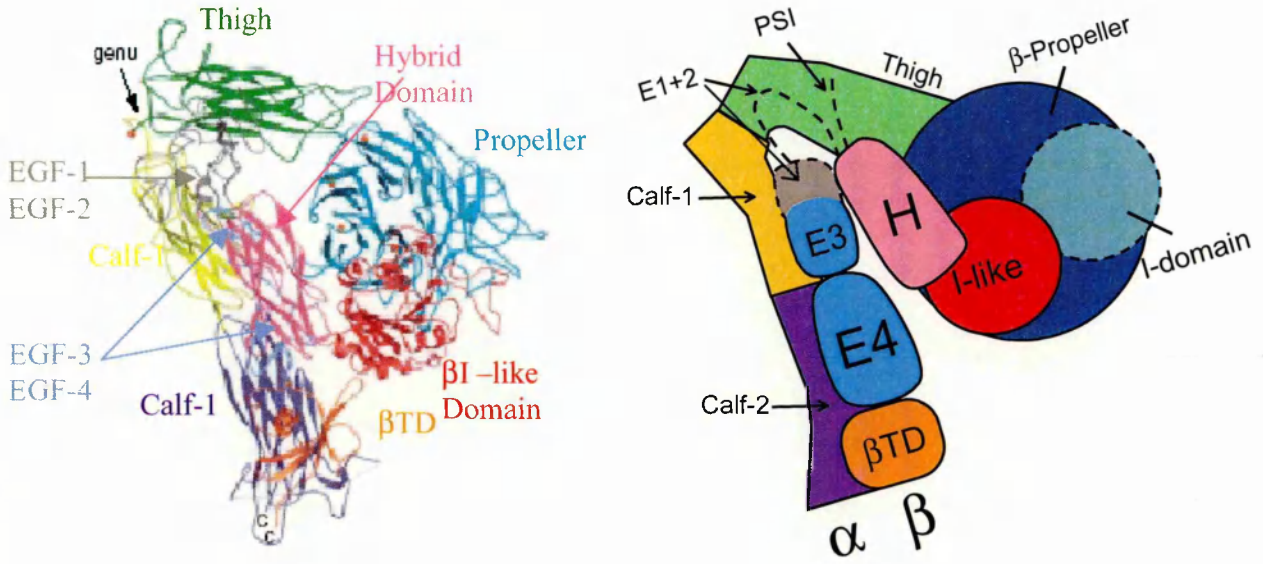

Figure 1.3 **Ribbon diagram of the three-dimensional structure of αVβ3 and schematic of a general integrin with an I Domain based on the αVβ3 structure**. The structure shown on the left hand side is of the unliganded αVβ3 structure (Xiong *et al.*, 2001) with the schematic on the right hand side giving a clearer view of the position of the domains relative to each other. The schematic also includes an I domain which is not present in the αVβ3 integrin. In the crystal structure the integrin is folded over with the head region bent over towards the C termini of the stalks. The structure of the PSI domain and I-EGF repeats 1 and 2 are not well resolved and are estimates only. Ribbon diagram from Xiong *et al.* (2001). Schematic is based on diagram from Beglova *et al.* (2002).

1.2.1.1 β propeller

The N-terminal region of the α-chain contains 7 weakly homologous segments of approximately 60 amino acids each. The crystal structure shows that β-strands of each of the seven homologous segments are arranged around a central axis like blades resembling a propeller (See Figure 1.4). A β-propeller conformation had previously been predicted by Springer, T.A., (1997) and was later confirmed with mAb binding studies which identified several discontinuous epitopes in the region (Oxvig and Springer, 1998). The similarity of the Ca^{2+} binding motifs in β-strands 4-7 of the propeller to turns between β-strands in domains of other proteins such as the

trimeric G -protein β-unit also helped to define the structure (Springer *et al.*, 1997, 2000). Ca^{2+} binding sites, all solvent exposed in the Ca^{2+} complexed crystal structure, were also identified in the β-hairpin loops of blades 4-7 at the bottom of the propeller.

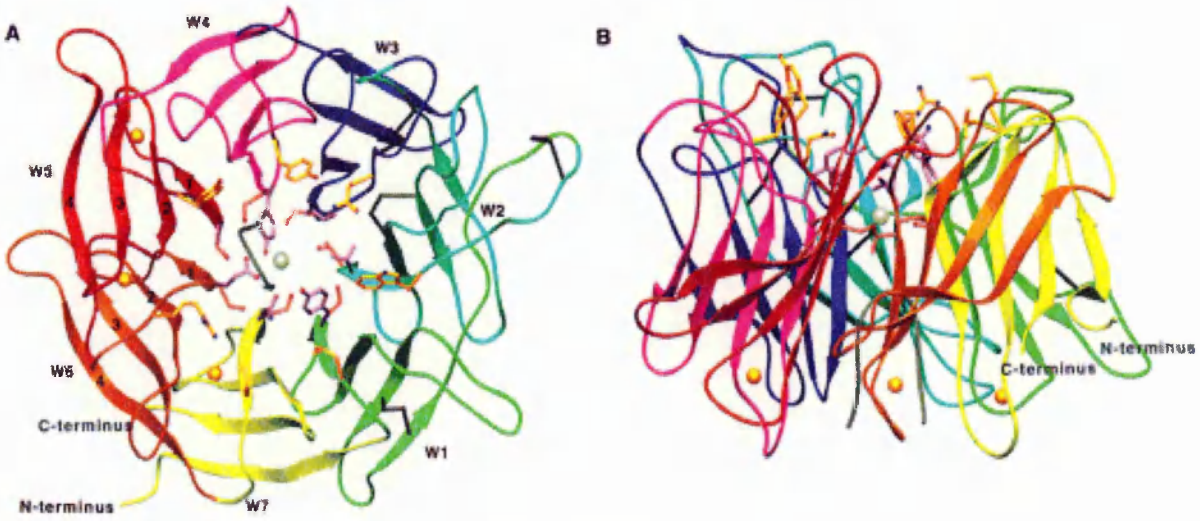

Figure 1.4 **Ribbon Structure of a β-propeller.** This ribbon structure represents the top (A) and side (B) view of the α4 β-propeller containing seven four stranded β-sheet blades (each in a different colour arranged around a central core. The thick arrows depict the β-strands. Putative Ca^{2+} and Mg^{2+} binding sites are represented by gold and silver spheres respectively. When present, the I domain would be inserted between blades 2 and 3. (Springer 1997).

1.2.1.2 I domain

Nine of the known integrin α-subunits, including all those that pair with the β2 subunit, contain a 200 amino acid inserted domain, known as the I domain, between blades 2 and 3 of the β-propeller. Independent crystal structures have now been determined for the I domains of αM (Baldwin *et al.*, 1998; Lee *et al.*, 1995*a, 1995b*), αL (Kallen *et al.*, 1999; Legge *et al.*, 2000; Qu and Leahy, 1995, 1996), α2 (Emsley *et al.*, 1997, 2000), and α1 (Nolte *et al.*, 1999) integrin subunits. Initial studies showed that all 4 of these I domains, which have ~30% sequence

homology adopt the same 3D structure. They consist of a dinucleotide-binding or Rossmann fold, with α-helices surrounding a central β-sheet containing five parallel and one anti-parallel β-strand (Figure 1.5). The β-strands and α-helices tend to alternate in the secondary structure, with the α-helices wrapping around the domain in a clockwise order. Five residues located in the β1-α1, α2-α3 and β4-α4 loops on the top face of the I domain form a central pocket and their side chains coordinate with a Mg^{2+} or Mn^{2+} ion, either directly or via water molecules, to form a metal ion-dependent adhesion site (MIDAS). The metal-coordinating MIDAS residues, DxSxS, are invariant amongst all I domains and mutagenesis of any of these residues has been shown to abrogate ligand binding (Edwards *et al.*, 1995 & 1998). This data, and ligand binding studies with isolated I domains, suggest that this is the major ligand binding site of I domain-containing integrins. This will be discussed in more detail in Section 1.4.

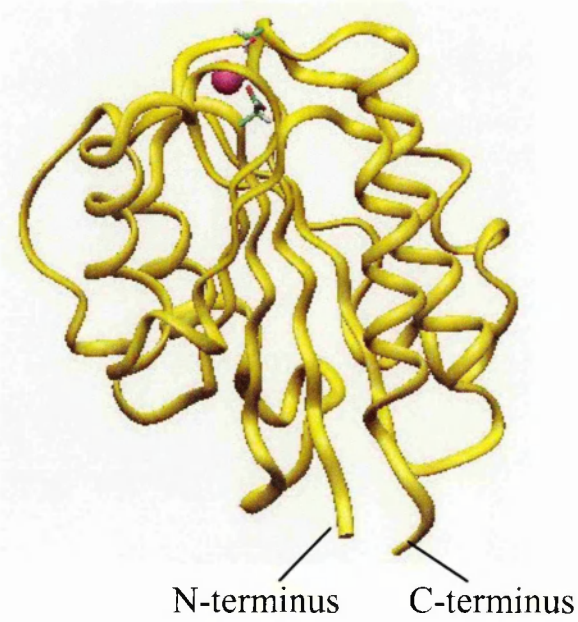

Figure 1.5 **Ribbon structure of the I domain**. This structure shows the tertiary structure of the αL I domain as determined by X-ray crystallography. The protein adopts a Rossmann fold, with a central sheet of β-strands surrounded by seven α-helices. The bound cation in the MIDAS is represented by the pink sphere (Qu and Leahy, 1995).

For integrins that do not contain an I domain it is proposed that the β-propeller participates directly in ligand binding (Humphries, 2000). Mutagenesis studies initially indicated that ligand binding residues cluster at the top and side of the β-propeller (Kamata, 1995) and the αVβ3/ligand crystal structure data is in agreement with this (discussed in more detail in Section 1.4).

1.2.2. The β-chain head region

The N-terminal globular head region of the β-chain within the αVβ3 crystal structure was shown to resemble one of the conformations of the α-subunit I domain and is referred to as the I-like domain or A-domain (Xiong *et al.*, 2000). The existence of an I-like domain which approximately spans residues 100-340 of the integrin β-chain had previously been predicted based on the conserved DXSXS sequence of the MIDAS motif within the region and a predicted secondary structure which had a weak but detectable sequence homology with the α-chain I domain (Lee *et al.*, 1995(a&b); Tuckwell and Humphries, 1997). Epitope mapping with 6 different mAbs had also suggested a Rossmann-like fold as residues 133 of α-helix 1, and residues 332 and 339 of α-helix 6 were predicted to be in close proximity to one another (Huang *et al.*, 2000). The I-like domain MIDAS region contains the same residues as that of the α I domain, except that the threonine is replaced by a glutamic acid residue. This domain appears to be involved in binding ligand in integrins that lack I domains, and to indirectly regulate ligand binding in integrins that contain I domains.

The I-like domain is connected to its stalk via a hybrid domain which is a β-sandwich fold comprised of amino acid segments on either side of the I-like domain (See Figure 1.2). Hydrophilic and hydrophobic contacts contributed from residues on two loops of the hybrid

domain, and residues at the base of the I-like domain form a circular interface between the 2 domains. Takagi and Springer (2002) suggest that movement of one of these connections relative to the other may be an important mechanism for relating conformational change within domains. They predict that changes in the orientation of neighbouring domains in both the α and β subunits could propagate global conformational changes within the integrin.

1.2.3. Contact points between the α-β subunits of the globular head

Several lines of investigation suggest that there is a large interaction between the β-propeller and the I-like domain in all integrins. These include the findings that (a) the anti-LFA-1 mAb YTA-1 can recognize an epitope formed by a combination of the integrin αL and β2 subunits of LFA-1 but does not see the individual subunits alone (Zang *et al.*, 2000), (b) the epitopes of the αIIbβ3 mAbs, PAC-1, LJ-CP3 and OP-G2 consist of several discontinuous sites in both the αIIb and β3 subunits (Puzon-Mclaughlin *et al.*, 2000), (c) several attempts at generating an isolated, correctly folded form of the I-like domain without the presence of the β-propeller have been unsuccessful, and (d) mutations within the region of the I-like domain which contacts the β-propeller including the natural mutations that occur in LAD-1, lead to a lack of association of the α and β subunits (Bilsland and Springer, 1994). Analysis of the crystal structure has supported these findings and showed that the interface is largely hydrophobic and has a buried surface area of ~1600Å^2 which is typical for a large protein-protein interface. In the propeller, 2 aromatic rings contributed from a conserved ΦΦGlyΦ motif (Φ =aromatic residue) at the beginning of each blade appear to form a cup-like structure, which grasp a basic residue (arginine in β3) in the I-like domain. This was shown to be further strengthened by extensive hydrophobic and hydrophilic contacts surrounding this region (Xiong *et al.*, 2001).

Although the solved structure of the αV subunit does not contain an I domain, it is predicted that the insertion of this domain would have little effect on the overall structure of the αβ globular head. Blades 2 and 3 of the β-propeller are positioned away from the β-propeller/I-like domain interface and the I domain is thought to loop away from the β-propeller. Although the N terminus of the I domain is only separated by a short 3 residue linker from the last β-strand of blade 2, which suggests a close association with the β-propeller, the C-terminus has a ~20 amino acid linker connecting it with the β-strand 1 in blade 3 of the β-propeller. This much longer linker, containing several cysteines, indicates a much more flexible relationship with the propeller and may permit conformational movement. It has been suggested that the 'open' and 'closed' conformations of the I domain may be regulated by the interaction of the C-terminal linker with the β-propeller and /or the I-like domain.

1.2.4. The α-subunit stalk domains

The ~500 residues of the extracellular region of the α-subunit, at the C-terminus of the β-propeller domain, make up the stalk region. The αVβ3 crystal structure reveals that this region consists of a C2-type Ig-like 'thigh' domain and two similar β-sandwich domains, named calf-1 and calf-2. The central axis of the β-propeller is almost perpendicular to the main axis of the thigh domain and residues clustered on one side at the bottom of the propeller insert into an ovoid groove at the top of the thigh domain. The propeller/thigh interface has a mixed hydrophobic and hydrophilic nature but lacks salt bridges suggesting that it has some degree of flexibility (Arnaout *et al.*, 2002).

Calf-1 and -2 make substantial, and largely hydrophobic, interdomain contacts with each other but the lack of an intervening amino acid linker suggests that there is little or no interdomain movement. The proteolytic cleavage site that generates the heavy and light chains in certain integrins is predicted to be located in a loop within calf-2. However, as this region is disordered in the crystal structure, structural information of this area is limited. Xiong *et al.* (2003(b)) suggests that in α-chains that do not contain this site (as in I domain containing integrins) the structure of this loop may be modified.

1.2.5. The β-subunit stalk domains

The β-subunit leg is formed from a PSI domain and four tandem EGF-like domains. The β globular head is preceded in the linear sequence by an N-terminal 54-residue PSI domain (plexins, semaphorins and integrins) which, in the 3D structure, lies below the head region (Bork *et al.*, 1999). It contains seven cysteines, six of which are shared with other PSI domains and is predicted to have 2 α-helices. Crystallographic structural data for the PSI domain is limited and Xiong *et al.* (2001) suggest that a higher resolution than 3.1 Å is required for interpretation of the electron density in this region.

Four cysteine-rich repeats at the C-terminus of the hybrid domain make up the long extracellular stalk that connects the headpiece to the membrane. In the αVβ3 crystal structure, only repeats 3 and 4 were clearly resolved and were both shown to assemble into EGF-like folds and to contain β-strands, arranged in a rod-like fashion. A subsequent NMR structure of the second and third cysteine-rich repeats of β2 (Beglova *et al.*, 2002) confirmed this EGF-like pattern. However, definition of these domain boundaries has proved difficult, due in part to the low sequence homology between the repeats. Analysis of the recent NMR solution structure of the β2 stalk

region led Tagaki *et al.* (2001) to redefine these boundaries as starting one cysteine earlier at position 427 (using β2 numbering) than had previously been predicted (Tamkun *et al.*, 1986; Kishimoto *et al.*, 1987). If one compares this to the previously accepted alignment, only three of the eight cysteines and one of the four disulphide bonds in each domain are equivalently assigned (Berg *et al.*, 1999). Domain deletion and mAb studies show good correlation with these predictions (Takagi, *et al.*, 2001) and such redefinition has shown statistically significant sequence homology to the EGF (epidermal growth factor) domain and EGF-like domains that are found in E-selectin, tenascin X, reelin and ADAM-11 (D'Arcangelo *et al.*, 1995). This realignment also results in a shortening of the interdomain linkers between each repeat, greatly limiting the potential for interdomain flexibility and suggesting a rigid connection between domains.

Contrary to the β2 NMR study which suggests the alternative cysteine pairing, the EGF domains 3 and 4 in the αVβ3 structure also appear to have minor strands that do not fit in with this new realignment. Arnaout *et al.* (2002) have therefore proposed another alternative alignment based on the crystal structure where each of the 4 EGF-like domains contain 7 cysteines, of which 6 form 3 internal pairs (typical of EGF domains) and the seventh forms an interdomain disulphide bridge between consecutive EGF-like domains. These disulphide bridges are thought to resemble the calcium 'ion bridge' of classical EGF domains and provide a similar rigidity to the stalk region as suggested in the Tagaki model. As several mAbs to integrin activation epitopes map to these repeats, and are thought to induce activation through conformational changes, it is interesting to note that these domains have unique structural properties that make the interdomain connection rigid and suited for transmission of structural motion in signalling (Beglova *et al.*, 2002; Takagi *et al.*, 2001)

1.2.6. Contact points between the α and β subunits of the stalk region

Small and only moderate hydrophobic interfaces occur between the β-propeller and hybrid domain, calf-1 and EGF-like domain 3, calf-2 and EGF4, & calf-2 and the β-chain tail domain (Arnaout, 2002). It is believed that during integrin activation major structural rearrangements occur in the stalk regions, particularly in the β-subunit, which results in breaking of these contact points. Evidence to support this comes from a set of activating mAbs that bind in the β2 stalk region which are thought to activate by acting as a wedge to break the α and β domain-domain contacts (Huang, *et al.* 2000). Such mAbs include KIM127 (Figure 1.6) which has been studied extensively.

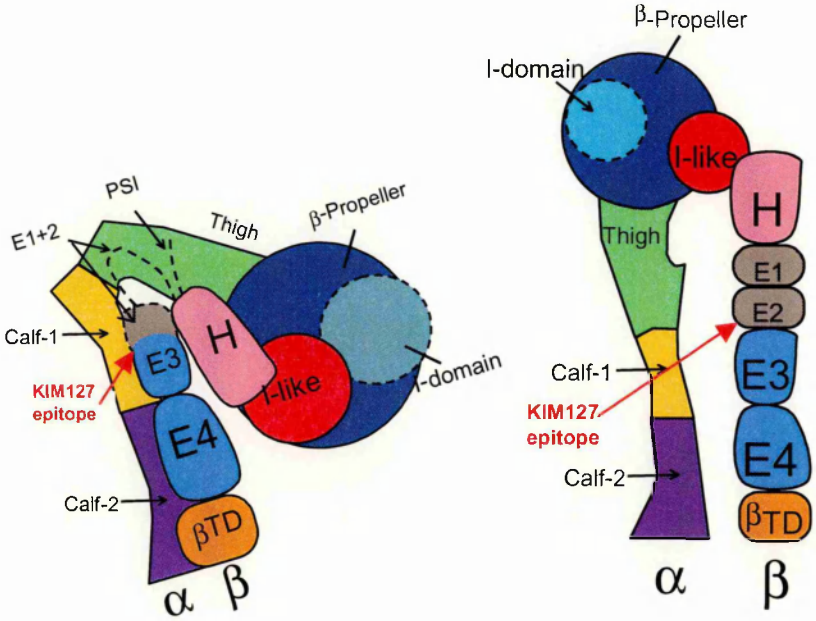

Figure 1.6 **Binding site of KIM127.** Schematic of the approximate spatial relationship among integrin domains and the effect the binding of KIM127 has on wedging the α and β stalk regions apart. The KIM127 mAb epitope has been mapped to EGF domain 2. This schematic is based on the model from Lu *et al.* (2001(b))

1.2.7. Transmembrane and Cytoplasmic domains

The cytoplasmic domains of integrin α and β subunits are relatively short (~50 residues). The 1000 residue cytoplasmic domain of integrin β4 is an exception and contains large fibronectin type III domains which are thought to connect to the cytoskeleton (de Pereda *et al.*, 1999). As a soluble form of αVβ3 lacking its transmembrane domain was used in the elucidation of the crystal structure, no structural data for the transmembrane and cytoplasmic domains is provided by this study. However, a model of the αIIbβ3 cytoplasmic tails derived by NMR spectroscopy (Vinogradova *et al.*, 2002) may provide a generalized model for all integrin cytoplasmic tails (with the obvious exception of α6β4). The structure reveals multiple hydrophobic and electrostatic contacts within the membrane-proximal helices of the α and the β cytoplasmic tails that suggest a method of restraining the integrin in a resting state. These interface interactions are disrupted by point mutations and by binding of the cytoskeletal protein talin, both of which are known to activate the receptor. Conserved sequences of GFFKR in the α subunit (Muir *et al.*, 1994) and LL(XXX)HDR (Hughes *et al.*, 1996) in the β subunits have been shown to play an important role in integrin activation and will be discussed in more detail in Section 1.6.

The transmembrane region of both the α and β chains comprises 23 amino acids that appear to directly contact membrane lipids. Recent investigations reported the presence of an invariant lysine at the carboxy-terminal of both transmembrane domains which may be important for the lateral mobility of integrin subunits in the membrane (Armulik *et al.*, 1999)

1.2.8. Overall crystal structure of αVβ3

The elucidation of the αVβ3 structure has yielded an enormous amount of information on the structure and interactions of many of the domains that make up the heterodimer but the most surprising revelation was the overall shape of the integrin. The αVβ3 crystal structures in the presence of both Ca^{2+} and Mn^{2+}, and with Mn^{2+} plus ligand, have all revealed the same V-shaped organisation, in which the ligand-binding headpiece bends back towards the base of the stalk region and is orientated toward the cell membrane (See Figure 1.3). This contrasts dramatically with the linear and extended form as depicted in EM images (Du *et al.*, 1993). This bend in the structure occurs at the 'integrin knees', between the thigh and calf-1 domains of αV and in the second and third-EGF repeats of β3. This results in the membrane-proximal calf-2 domain lying at an acute angle to the plasma membrane with the ligand-binding face facing away from the membrane and therefore still available for ligand interaction. Interestingly, there is also contact between the F strand/α7 helix loop of the I-like domain and the β3 TD (Tail Domain) although this contact is lost on ligand binding. This bent conformation has led many researchers to rethink the way in which integrins in general bind ligand and the conformational changes that are predicted, by mAb mapping, to take place on ligand binding. Several theories have been put forward to address these issues and will be discussed below in the context of LFA-1.

1.3 LFA-1

1.3.1. LFA-1 Expression

Lymphocyte function-associated antigen (LFA-1) is formed from the association of an 180kDa α subunit (CD11a) with the 95kDa β2 subunit (CD18). It was originally identified in mice (Davignon *et al.* 1981) and the human homologue was later cloned and expressed by Kishimoto *et al.* (1987) and Larson *et al.* (1989). LFA-1 is one of the 9 integrins that contains an I domain and this domain has been reported by many studies to play a critical role in LFA-1/ ligand interactions (see below). Expression of LFA-1 is restricted to leucocytes, being well expressed on the surface of neutrophils, monocytes, macrophages, NK cells, and lymphocytes (Rose *et al.*, 2002; Gahmberg *et al.*, 1997(a)), with expression level and function shown to be dependent on the state of cellular activation and differentiation (Dustin and Springer, 1989; Larson and Springer, 1990)

1.3.2. LFA-1 Function

LFA-1 has been shown to be associated with two major pathways of fundamental importance in inflammation and in the control of specific T-cell immune responses. Firstly, the requirement for β2 integrin activation in the rapid modulation of adhesion and de-adhesion necessary for controlled migration of leucocytes from the bloodstream and across the endothelium, known as extravasation, is well established (Butcher *et al.*, 1999; Imhof and Dunon, 1995). Although selectin molecules are generally thought to be responsible for the rolling of leucocytes along the endothelium, tethering of the rolling leucocytes to the endothelium is mainly controlled by binding of activated integrins, specifically VLA-4 (also shown to mediate rolling) and LFA-1, to

their vascular ligands. For LFA-1, interactions with members of the ICAM family are most relevant in this context. Recent evidence has also suggested the importance of LFA-1 in the initiation of migration through the endothelium to the underlying basement membrane once tight adhesion has occurred through interactions with another ligand, JAM-1 (Ostermann *et al.,* 2002).

Secondly, LFA-1 has been shown to play an important role in the priming of T Cells by antigen presenting cells (APCs). Although MHC class I and class II molecules play a central role by interacting with the T-cell receptor complex (TCR) and forming an immunological synapse, this specific event is dependent on low affinity interactions and, therefore, other molecular interactions including integrin/ligand interactions are required to initiate, strengthen and regulate such adhesion. It has been proposed that ICAM-3, which is highly expressed on T-lymphocytes, mediates the initial low affinity interaction of the T cell and the APC by binding to both LFA-1 and DC-SIGN (Dendritic Cell-specific ICAM-3 grabbing non-integrin) on the APCs (de Fougerolles and Springer, 1992; Montoya *et al.,* 2002; Geijtenbeek *et al.*, 2000). Subsequent TCR /specific peptide-MHC, CD3/CD28 and CD2/LFA-3 interactions appear to induce clustering and high affinity LFA-1/ICAM-1 binding which serves to strengthen the interface which can be sustained for up to 20 hours *in vitro* (Dustin and Springer, 1989; van Kooyk *et al.,* 1989; Dustin and Cooper, 2000). During this process, LFA-1 and ICAM-1 molecules have been shown to initially cluster at the centre of the synapse surrounded by a ring of TCR/MHC peptide but, within minutes, they move to the periphery of the ring with the TCR/MHC taking up the central position (Dustin *et al.,* 2002).

The functional importance of β2 integrins, and in particular LFA-1, is exemplified by the clinical condition known as leucocyte adhesion deficiency type 1 (LAD-1), in which mutations in the common β2 subunit result in the absence (or very low levels) of expression of all β2 integrins. This lack of expression leads to almost complete lack of neutrophil emigration into inflammatory sites, resulting in an increased risk of recurring life-threatening bacterial infections

(Gahmberg *et al.*, 1997(a)). Subsequent studies using αL and β2 knockout mice have shown that, while αL deficient mice have reduced neutrophil migration (Henderson *et al.*, 2001), suffer from impaired T cell proliferation (Shier *et al.*, 1996, 1999) and have defective lymphocyte homing to peripheral lymph nodes (Berlin-Rufenach *et al.*, 1999), they were not as susceptible to bacterial infections as mice lacking the CD18 subunit (Bouvard *et al.*, 2001; Scharffetter-Kochanek *et al.*, 1998).

While LAD-1 highlights the functional importance of LFA-1 in normal immune responses, increased levels of the integrin have been detected in a wide variety of auto-immune and inflammatory conditions such as arthritis, psoriasis and inflammatory bowel disease (Yusuf-Makagiansar *et al,* 2002; Mazzone *et al.,* 1995). The importance of LFA-1 in models of rheumatoid arthritis is supported by studies showing that treatment with αL mAbs reduced inflammatory responses and recruitment of cells to sites of inflammation. Other studies using blocking anti-αL mAbs have also shown that neutrophil and monocyte trafficking to inflamed joints is attenuated in a model of arthritis (Birner *et al.*, 2000), and can prevent disease progression in a collagen induced arthritis model (Kakimoto *et al.*, 1992). A blocking αL mAb has also been shown to be efficacious in treating patients with psoriasis (Gottlieb *et al.*, 2000). Because of these findings, inhibition of LFA-1 function has become a major focus of the pharmaceutical industry in recent years.

1.3.3. LFA-1 Ligands

LFA-1 has been shown to bind all five members of the ICAM Ig family. The ICAM family are a subgroup of the immunoglobulin (Ig) superfamily all of which contain characteristic Ig folds of 80-100 amino acids arranged into two β-sheets and held together by a highly conserved

disulphide bridge (Xie *et al.*, 1995). The ICAM genes are clustered in chromosome region 19q13.2 (Trask *et al.*, 1993; Lewis *et al.*, 1988), except for ICAM-2, which is found on chromosome segment 17q23-25 (Sansom *et al.*, 1991). The ICAMs are type I transmembrane proteins containing between 2 and 9 heavily N-glycosylated Ig domains in their extracellular domains and are attached via a transmembrane domain to relatively short, poorly conserved cytoplasmic domains (Reilly *et al.*, 1995; Miller *et al.*, 1995). Table 1.2 highlights the expression profiles and important properties of each of the ICAMs and the domains involved in ligand binding.

LFA-1 has a greater affinity for ICAM-1 than that for other members of the ICAM family. ICAM-1 exists predominantly as a dimer on the cell surface and studies with soluble forms of the integrin show that LFA-1 binds with much higher affinity to the dimeric form than to the monomeric form (Casasnovas *et al.*, 1995). Most cell types, especially endothelial cells and mesenchymal cells, express some ICAM-1 at a basal level (Hogg *et al.*, 1991) but this is strongly upregulated in response to agents such as lipopolysccharide (LPS), tumour necrosis factor-1 α (TNFα), interleukin-1α (IL-1α), phorbol-myristate-acetate (PMA) and interferon-γ (IFNγ) (Rothlein *et al.*, 1986(a&b); Krutmann *et al.*, 1990).

ICAM-2 is primarily expressed on leucocytes and endothelial cells and is the only ICAM family member expressed on platelets (Diacova *et al.*, 1994). In contrast to ICAM-1, ICAM-2 is expressed as a monomer on the cell surface and is not easily upregulated by cytokines (de Fougerolles *et al.*, 1991). The main function of ICAM-2 is to regulate adhesion of leucocytes to the resting endothelium, but it may be important in regulating cell-cell interactions elsewhere. Recently ICAM-2 has also been shown to be a ligand for DC-SIGN, a C-type lectin expressed on dendritic cells that recognises pathogen-derived carbohydrate structures and, upon binding, allows internalisation of pathogens for antigen processing and T–cell presentation (Geijtenbeek *et al.*, 2000).

ICAM-3 is the major ICAM Ig molecule present on resting leucocytes (de Fougerolles and Springer 1992) and absent from normal endothelial cells but, like ICAM-1 and ICAM-2, is strongly expressed on lymphocytes (Doussis-Anag. *et al.*, 1993). High expression of ICAM-3 mRNA has been shown in cell types involved in antigen presentation (Acevedo *et al.*, 1993) and more recently ICAM-3 has been shown to localize at cell-cell contacts during initial cell aggregation and its low affinity adhesive interactions with DC-SIGN and LFA-1 appear to facilitate the exploration of the APC surface by T-cells (de Fougerolles, *et al.*, 1994; Bleijs *et al.*, 2000).

ICAM-4 is specifically expressed on red cells and carries the LW blood group antigens (Bailly, *et al.*, 1995). It has been proposed that ICAM-4 may be involved in red cell turnover by binding to β2 integrins expressed on spleen macrophages in the red pulp, and also in erythroid maturation to retain immature erythroid precursors in the bone marrow. However, the relevance of ICAM-4 interactions with β2 integrin-expressing cells *in vivo* is still unknown (Bailly *et al.*, 1995; Van Der Vieren *et al.*, 1995).

ICAM-5 is the most complex member of the ICAM family, containing 9 Ig extracellular domains. It is expressed on a subset of neurons, but not on glial cells, within the telencephalon of mammalian brains (Yoshihara *et al.*, 1994). Interactions of T-cells with the somato-dendritic regions of hippocampal neurons is thought to be mediated through binding of LFA-1 to domain 1 of ICAM-5, suggesting a mechanism for immune cell targeting to neurons under normal and pathological conditions (Tian *et al.*, 2000 (a&b)). The sixth domain of ICAM-5 has also been shown to bind T cells but in an integrin-independent manner and the ligand has yet to be identified.

Ostermann *et al.* (2002) have recently identified Junction Adhesion Molecule-1 (JAM-1) as another potential ligand for LFA-1. JAM-1 is a transmembrane protein found associated with tight junctions via cytoplasmic adaptor proteins and its expression appears to be limited to endothelial and epithelial cells. Tight junctions are adhesive complexes consisting of strands of tightly opposed plasma membranes on adjacent cells that contribute to the barrier function of the endothelium. JAM-1 has been shown to be located at the most apical portion of these junctions and is involved in forming close contacts between epithelial cells. Like the ICAM-Ig family, JAM-1 is an Ig superfamily member consisting of two domains, of which the membrane proximal domain is thought to interact with LFA-1. A detailed analysis of LFA-1 binding site on JAM-1 has yet to be carried out.

1.3.4. LFA-1/ ICAM binding interface

Although LFA-1 has been reported to bind all 5 members of the ICAM family, its interaction with ICAM-1, ICAM-2, and ICAM-3 are the most studied. Mutational studies on ICAM-1 and ICAM-3 identified residues E34 and Q73 in ICAM-1 and the corresponding E37 and Q74 of ICAM-3 within domain 1 to be critical for LFA-1 binding (Staunton *et al.*, 1990; Holness *et al.*, 1995). Other mutations within the first domain of these molecules were also shown to affect binding, but loss of reactivity with a panel of mAbs demonstrated that these mutations were associated with larger conformational changes in the molecule. The elucidation of the crystal structures of the first 2 domains of ICAM-1 (Bella *et al.*, 1998; Casasnovas *et al.*, 1998) and ICAM-2 (Casasnovas *et al.*, 1997) and most recently that of the αL I domain complexed with the first three domains of ICAM-1, have not only confirmed the importance of the glutamate residue but also revealed an atomic view of the LFA-1/ICAM-1 interface (Shimaoka *et al.*, 2003).

Property	ICAM-1 (CD54)	ICAM-2 (CD102)	ICAM-3 (CD50)	ICAM-4 (LW)	ICAM-5 Telencephalin
Mol. Wgt(kDa)	90	55	120	42	150
Cellular Distribution :					
Leucocytes					
Resting	+	+	+++	-	-
Activated	+++	+	+++	-	-
Endothelial cells					
Resting	+	++	-	-	-
Activated	+++	++	-	-	-
Lymphomas	+++	+++	+++	-	-
Red Cells	-	-	-	++	-
Telencephalon	-	-	-	-	++
Binding Partners	LFA-1 MAC-1 p150,95	LFA-1 MAC-1	LFA-1 αdβ2, DC-SIGN	LFA-1 MAC-1	LFA-1
No. of Ig Domain	5	2	5	2	9
Ig Domains important for binding	D1(LFA-1) D2(MAC-1)	D1	D1	N.D	D1

Table1.2 Expression profiles of each of the ICAMs and the domains involves in ligand binding.

All four X-ray studies have shown that domains 1 and 2 of ICAM-1 have an extended orientation with an obtuse angle between domains 1 and 2 and with no significant rearrangement in ICAM-1 when bound to integrin. In the integrin /ligand crystal structure, domain 1 appears to lie perpendicular to the 'top' face of the I domain of LFA-1 with a portion of the domain sitting in the shallow groove created by the MIDAS at the top of the I domain (Figure 1.7). The key conserved residues that had previously been shown to interact with the MIDAS, E34 and Q73, are located at the ends of the C strand and the beginning of the G strand, respectively, in domain

1 (Staunton *et al.*, 1990; Casasnovas *et al.*, 1995; Li *et al.*, 1993). In the crystal structure E34 forms a direct contact through its acidic side chain and interacts with the Mg^{2+} ion held in the I domain MIDAS site. Rings of hydrophobic residues surrounding both the Mg^{2+} bound to the I domain (L204, L305 and M140) and the E34 of ICAM-1 (P36, Y66, M64 on β-strands C, D and F) also make contact, and it is thought that this non-polar environment strengthens the electrostatic interaction between E34 and the Mg^{2+} of the MIDAS.

Polar interactions involving hydrogen bonds between T35, P36 and N68 in ICAM-1 and Q143, T243, and H264 in the I domain, as well as a salt bridge between E241 on the I domain and K-39 on ICAM-1, appear to orient ICAM-1 for optimal contact with the I domain and further strengthen the interaction (Shimaoka *et al.*, 2003).

Site directed mutagenesis studies suggest that the β2 binding motifs of ICAM-4 differ from those of the other ICAMs. In ICAM-4, R52 in domain 1 replaces the conserved glutamate residue of the other ICAMs, and mutation of this residue to glutamate has no effect on ICAM binding (Hermand *et al.*, 2000). A recent paper from Ihanus *et al.* (2003) has, however, shown that an epitope recognised by a mAb (MEM83), known to enhance LFA-1 binding to ICAM-1, is also involved in LFA-1/ICAM-4 binding.

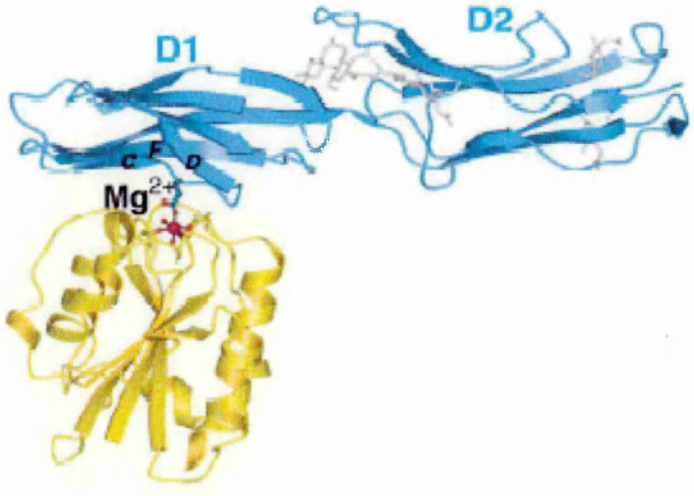

Figure 1.7 **Ribbon structure of ICAM-1 binding to the I domain**. Ribbon diagram of one monomeric unit of αL I domain (gold) complex with ICAM-1 domains 1-2 (blue). The Mg^{2+} ion is shown as a magenta sphere. I domain MIDAS and ICAM-1 Glu-34 side chains are shown as ball-and-stick with red oxygen atoms. The interacting β strands C, D, and F of ICAM-1 are labeled. (Shimaoka *et al.*, 2003).

1.4 I Domain and Ligand Binding

I domains belong to a family of homologous domains of which von Willebrand factor 'A' domains are the prototype (Larson *et al.*, 1989). As discussed earlier LFA-1 is one of the 9 integrins that contains an I domain which is centrally involved in regulating ligand-binding activity. The importance of the αL I domain in ligand binding was first illustrated by the adverse effect that mutations within this region had on the capability of LFA-1 to bind ligand (Edwards, *et al.*, 1995; Huang and Springer, 1995) and by the fact that the majority of mAbs that block the LFA-1/ICAM interaction appear to map to the I domain (Champe *et al.*, 1995). Binding of ICAM-1 to recombinant isolated αL I domain (Randi and Hogg, 1994) also indicated

that this domain was a major ligand-binding site for β2 integrins. More recently, Shimaoka *et al.* (2001) have shown that an isolated I domain under certain conditions can bind ligand with the same specificity as the parental integrin suggesting that LFA-1 ligand binding occurs predominantly through interaction with this domain. Along with this biochemical data, great strides have been made to elucidate the structure of the αL I domain both in the presence and absence of ligand, and the knowledge gained from these studies has further enhanced our understanding of LFA-1 activation and function.

The first crystal structure of an I domain was generated by Lee *et al.* (1995(a)) from the α subunit of integrin αMβ2. As well as confirming the presence of the classic α/β Rossmann fold, it was shown that the I domain contained a Mg^{2+} coordination site at the top of the domain with one of the coordinating points being a glutamate side chain from another I domain molecule. Further structures of the αL and αM I domains with bound Mn^{2+}, and αL I domain in the presence of Mg^{2+}, also confirmed the dinucleotide fold and cation binding site (Qu and Leahy, 1995; Lee *et al.*, 1995(b)). Although comparisons of the crystal structures of the αM I domain with bound Mg^{2+} (Lee *et al.,* 1995(a)) and with bound Mn^{2+} (Lee *et al.*, 1995(b)) showed differences in the residues whose side chains interacted directly with the metal structures, these differences were not noted in the two αL structures. Indeed, only minor rearrangements of the metal-binding site structure were seen when the structures of αL I domain with and without divalent cation were compared and these differences were thought to be the result of normal crystal lattice interactions (Qu and Leahy, 1995; 1996). However, a large movement in the structure of the αL I domain's α7 helix was suggested in the presence of Mn^{2+} compared to the αL I domain in the presence of EDTA. A similar movement of the α7 helix was also noted in the αM I domain crystal structures but this was accompanied by alterations in the metal binding site not seen in the αL I domain crystals (Figure 1.8). Analysis of these αM structures suggested that a glutamate side chain from a neighbouring I domain molecule provided a co-ordination

point in the crystal lattice, essentially mimicking the integrin-ligand interaction. This crystal contact is associated with a change in metal coordination and a shift in the position of the α7 helix that exposes several buried hydrophobic residues. Although the biological relevance of these changes was questioned at the time it was hypothesised that the I domain could exist in two conformations designated as 'open' and 'closed' dependent on the presence of bound ligand (Li *et al.*, 1998).

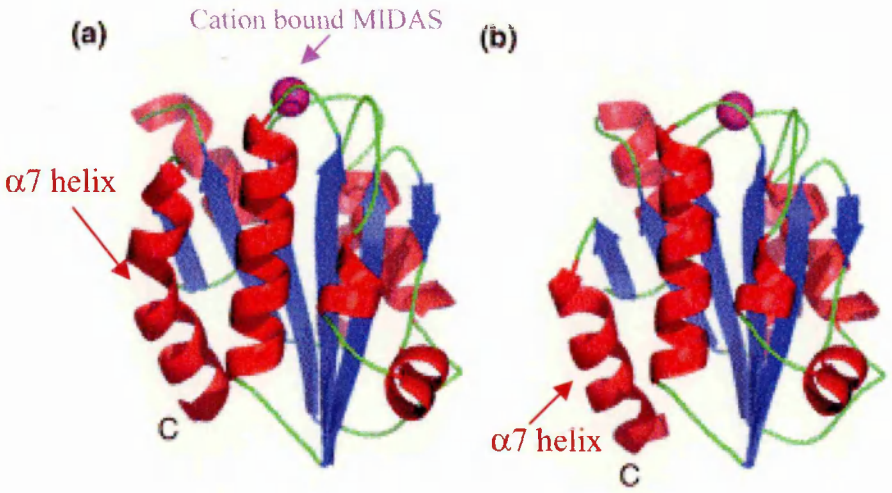

Figure 1.8 **αM I domain in open (a) and closed (b) conformations.** The two conformations illustrate the shift in the α7-helix and the minor shifts in and around the MIDAS (Xiong *et al.* 2000).

The subsequent elucidation of the α2 I domain crystal structure in the absence and presence of a ligand fragment by Emsley *et al.* (2000) confirmed that ligand binding was coupled to the 'open' conformation. In this case the ligand itself contributed the sixth coordination position in the MIDAS site as seen in the αM /ligand mimetic structure (Lee *et al.*, 1995(a)). Three loops on the upper surface of the I domain were shown to engage with the collagen peptide, with a collagen glutamate residue completing the coordination sphere of the metal in the MIDAS. In the unliganded structure ('closed' conformation), the sixth coordination site was contributed by a water molecule. Ligand binding appears to cause a switch in Mg^{2+} coordination in which a

direct bond to the MIDAS threonine is gained while a direct bond to an aspartic acid is lost. These subtle changes in metal coordination were associated with backbone movements of the loops containing the coordinating residues. These in turn were linked to structural shifts in neighbouring loops on the top of the I domain, and to α-helices on the side of the domain. The largest movement in the transition from 'closed' to 'open' conformations involves a 10Å downward shift of the α7 helix which results in a dramatic reshaping of the β6-α7 loop, exposing buried residues at the top of the loop (Lee *et al.*, 1995). These gross structural changes in a region distal to the ligand-binding region provide a mechanism to link conformational movement in I domains to movements elsewhere in the integrin molecule (discussed in Section 1.5.2).

Subsequently, work from Huth *et al.* (2000) using 2D NMR analysis also demonstrated that ICAM-binding to the αL I domain altered the environment of both the MIDAS and a region contained between the β6 strand and α7 helix which has been termed the IDAS (I Domain Allosteric Site). Mutational analysis of the IDAS by other members of this group (Lupher *et al.*, 2001) suggested that the interactions of the large hydrophobic amino acids I306, I235 and I255 create an energy barrier to conformational change in the I domain thus stabilising the conformation seen in the crystal structures. Alanine substitutions at these positions, which presumably reduce this energy barrier, were shown to enhance ligand binding relative to wild type. On the other hand, the hydrophilic amino acids K232, K287, Q303, K304 and K305 present on the surface of the IDAS, appear to stabilize an active state by interacting with other amino acids in LFA-1. Alanine substitution of these amino acids decreased the stability of the activated state presumably by removing polar interactions. Several small molecular inhibitors (Kallen *et al.*, 1999; Kelly *et al.*, 1999; Weitz-Schmidt, 2001) of the LFA-1/ICAM-1 interaction have also been shown to bind at the IDAS site and, since no alteration in the structural arrangement of the MIDAS was shown, these authors concluded that inhibitors block LFA-1 function by binding to the closed conformation of the I domain and prevent the conformational transition to the 'open' form that can bind ligand.

More recently, Shimaoka *et al.* (2003) have solved crystal structures of various mutant forms of αL I domains, unliganded and complexed with a fragment of ICAM-1 containing Ig domains 1-3. By mutating certain pairs of residues to cysteines on either side of the β6 strand and α7 helix (generating new disulphide bridges), they generated locked 'open' (K287C/K294C), locked 'closed' (L289C/K294C) and 'intermediate' (L161C/F299C) activation forms of the αL I domain. Affinity and kinetic measurements showed that the mutant locked 'open' and 'intermediate' αL I domains resulted in a 9000-fold and 400-fold increase in affinity for ICAM-1 over wild type, respectively. Locking the I domain 'open' increased its on-rate, which is consistent with the idea that conformational change is rate limiting for ligand binding by wild type I domain. The affinity and kinetics of ICAM-1 binding are comparable with that measured previously for intact, activated LFA-1 (Labadia *et al.*, 1998). The affinity of the locked-closed conformer was similar to unactivated wild type integrin (Shimaoka *et al.*, 2001).

The 'open' form of αL I domain crystallized in the presence of ligand confirmed that the metal coordination bond between Mg^{2+} and E34 is surrounded on the I domain by a ring of hydrophobic residues (L204, L205 and M140) and the aliphatic portion of T243. Conformational shifts at other points in the I domain were also very similar to those observed in the transition of the α2 and αM I domains from the 'closed' to 'open' conformations (Emsley *et al.*, 2000; Lee *et al.*, 1995). Unfortunately, due to the presence of the disulphide bonds in the 'intermediate' I domains, the β6-α7 loop did not assume the open conformation as seen with α2 and αM. Comparisons of the αL, αM, and α2 I domains which appear in the closed form show an identical conformation of the β6-α7 loop and likewise, the locked 'open' αL I domain had an identical open conformation in the β6 strand and the β6-α7 loop as in the 'open' αM and α2 I domains. However, the conformation of α7 in the locked 'open' αL I domain differs markedly, presumably due to the constraints of the disulphide bond.

Shimaoka *et al.* (2003) argue that the structural details of α7 are not critical as it is the conformations of β-strand 6 and the β6-α7 loop at the top of the I domain that dictate the alterations in the packing of the hydrophobic core during the transition from 'closed' to 'open' conformations. They further suggest that the conformational changes induced by pulling down the β6-α7 loop, as is thought to be the case after signalling to the cytoplasmic tails and mimicked in this case by the introduction of the disulphide bridge, are first propagated to the hydrophobic core of the I domain and then to the MIDAS loops. They argue that if this were not the case, the shift in the position of β6-α7 would just expose the hydrophobic core residues on α1, β4 and β5 and result in a misalignment of the residues within the MIDAS which would render it unable to bind ligand.

They therefore propose that as a result of other conformational changes in the integrin, F292 in the β6-α7 loop at the top of the I domain is removed from its hydrophobic pocket between β strands 4 and 5 and α1 helix by the downward shift of the α7 helix. The α1 helix then moves ~2Å towards the centre of the I domain. The change in coordination is also linked to a movement in the portion of the β1-α1 loop containing S141 of the MIDAS which shifts 2Å to bring it into contact with the side-chain of E34 (ICAM-1) and in turn allows the side chain of Q143 in the β1-α1 loop to form a hydrogen bond with the backbone of P36 on ICAM-1. As a consequence of the movement of S141, L142 pushes D239 in the β4-α5 loop from the primary to the secondary metal coordination sphere. In concert with the movement of the α1 helix, there is a downward movement of the β6-α7 and β4-α5 loops which fill the space left open by the β6-α7 loop. The downward movement of F265 in the β6-α7 loop causes a backbone flip of G240 and results in a 100° rotation of the E241 side chain which is now capable of forming a salt bridge with K39 of ICAM-1, facilitating the positioning of ICAM-1 and the I domain for optimal interaction.

1.4.1. Ligand binding to non-I Domain containing Integrins

In I domain-containing integrins, the I-like domain seems to play predominantly a regulatory role. In non-I domain-containing integrins, the I-like domain plays a direct role in ligand binding (D'Souza *et al.,* 1988; Smith *et al.,* 1990; Lin *et al.,* 1997). Despite the structural diversity of integrin ligands, all appear to contain an exposed aspartic acid or glutamic acid residue, as discussed for I domain-containing integrins, which is critical for recognition by integrins. Many integrins that do not contain an I domain appear to bind to aspartic acid-based sequences such as the RGD motif found in fibronectin, VCAM-1 and vitronectin (Ruoslahti *et al.,* 1996) and crystallisation of the αVβ3 extracellular domains in complex with RGD has for the first time provided an atomic basis for cation-mediated binding of aspartic acid based ligands to integrins (Xiong *et al.,* 2002). In the structure, RGD was shown to fit into a crevice between the β-propeller and the I-like domain of the bent αVβ3 conformation. The ligand arginine side-chain was shown to insert into a groove formed by loops of interconnecting strands D3, A3 and D4, A4 of the β-propeller and is held in place by a salt bridge to D218 at the bottom of the groove and another salt bridge to D150 at the rear of the groove. The hydrophobic portion of the arginine side-chain also interacts with T178 and A215 that form the walls of the groove. The ligand glycine residue contacts the αV subunit via hydrophobic interactions with the carbonyl oxygen of R216. The ligand aspartic acid contacts the metal ion within the MIDAS of the I-like domain and is stabilised by additional contacts with residues T122, R124 and N125 in the same domain. The interaction of the ligand aspartate with the MIDAS is strikingly similar to that seen when T243 of the I domain interacts with cation. The I-like domain MIDAS is formed from the oxygen –containing side-chains of D-X-S-X-S, D119, an invariant glutamic acid (E220, corresponding to the invariant threonine in I domains) and D251. Interestingly, D251 is present on the same loop that continues to form the major interface with the propeller, suggesting that ligand binding may bring about protein movements at the αβ interface.

Unlike the I domain, the MIDAS site of the I-like domain was shown to be unoccupied in the absence of ligand in the αVβ3 crystal structure. Comparison of the unliganded and liganded crystal lattice conformation suggests that in the unliganded state, E220 infringes on the MIDAS preventing the binding of cation whereas, on ligand binding, E220 is moved sufficiently to allow access. A second site (the ADMIDAS) which is cation bound in the unliganded state remains so in the liganded state but changes slightly in its conformation so that it is more closely associated with the MIDAS. In addition to incorporation of Mn^{2+} at the MIDAS and ADMIDAS, a third Mn^{2+} was shown to bind at a site 6Å from the MIDAS. This site, termed the ligand induced metal binding site (LIMBS), is formed from a side chain of E220, the side chains of D158, N215 and D217 and the carbonyl oxygens of D217 and P219. Although the LIMBS Mn^{2+} does not contact the ligand, it appears to be necessary to stabilize the reorientation of E220 and to add conformational stability and structural rigidity to the ligand binding face.

As well as the changes seen at the MIDAS, tertiary changes in the I-like domain and small quaternary changes to the αβ interface are observed in the liganded structure. In the liganded state, the A-α1 loop moved closer to the α2-α3 loop, allowing the MIDAS ion to coordinate residues from both. These movements appear to be initiated by the top of the α1 helix moving closer to the MIDAS, with the ADMIDAS moving in concert. The ligand specificity region of β3 also approaches the ligand, probably as a result of the salt bridge between D179 and R214 in the I-like domain. Several epitopes for activating and inhibitory mAbs have previously been mapped to these regions, underscoring the functional relevance of the observed structural changes. The movements in the A-α1 and α2-α3 loop are very similar in magnitude and direction to those seen when the I domain binds ligand (Emsley *et al.*, 2000). In the I domain, movement of the A-α1 loop causes a buried phenylalanine at the top of the α7 helix to become solvent-exposed which in turn causes a 10Å downward movement of the α7 helix. However, in the I-like domain because the top of the α7 helix is connected through the MIDAS cation to α1

there is minimal movement of the α7 helix when ligand is bound. Small quaternary changes such as the closer interaction of the β-propeller and the I-like domain around the peptide binding site, and rotation at the propeller/thigh interface, are also seen when αVβ3 is occupied with RGD.

As the conformational changes seen in αVβ3 appear to be dependent on ligand binding, the presence of ligand appears to be the controlling factor in integrin activation. An alternative interpretation is that the integrin ectodomain exists in an active /inactive equilibrium and that ligand binds to the pre-existing active form and stabilises the active conformation.

1.5 LFA-1 Activation

Leucocytes circulate throughout the body as non-adherent cells and yet become adherent to their ligands when they transmigrate across the vasculature or encounter APCs in the lymph nodes. Regulation of the activation of integrins, such as LFA-1, on the lymphocyte cell surface has been shown to play a central role in controlling cell adhesion (Faull *et al.*, 1994; Dustin and Springer, 1989; Bazzoni *et al.*, 1998; Diamond and Springer, 1994). External signals triggered by activation of receptors for chemokines, antigens and cytokines can modulate integrin function in a process termed 'inside-out' signalling. The signals generated within the cell are transduced through the integrin cytoplasmic and transmembrane regions to alter the ligand binding capacity of the extracellular domain. Signal transduction can also be transmitted in the opposite direction and initiated after integrins bind ligand, in a process termed 'outside-in' signalling. Like 'inside-out' signalling, this form of signalling is dependent on the cytoplasmic domains of the integrins and their direct or indirect interaction with signalling and cytoskeletal proteins. Integrins can also be activated directly from outside the cell by the divalent cation Mn^{2+}, which binds to the

ectodomain (Dransfield *et al.*, 1992(b); Tominaga *et al.*, 1998(a)), and after stimulation with activating mAbs such as KIM185 (β2) (Andrew *et al.*, 1993), KIM127 (β2) (Stephens *et al.*, 1995), NKI-L16 (αL) (van Kooyk *et al.*, 1991) and MEM83 (αL) (Landis *et al.*, 1993). The mechanisms that initiate activation of integrins are still incompletely understood despite considerable research effort. This section will discuss the data and various theories put forward to explain the activation of LFA-1 (and integrins in general) and will also discuss the structural basis for bidirectional signalling.

1.5.1. Avidity Modulation

Data accumulated over the last 10 years suggests that clustering of integrin receptors in the plane of the membrane, which increases the avidity of the integrin/ligand interaction, strengthens cell-cell adhesion and is a requirement for integrin activation and ligand binding (van Kooyk *et al.*, 1994; Stewart *et al.*, 1998; Yauch *et al.*, 1997; Grabovsky *et al.*, 2000). Initial evidence for avidity alterations of LFA-1 came from the description of the mAb NKI-L16 which detects a Ca^{2+}-dependent epitope and is only expressed when LFA-1 is in a clustered state. Further investigations by the same group showed that lymphocytes only bound to ligand when LFA-1 was clustered on the cell surface, even when the same level of LFA-1 was expressed on different cells (van Kooyk *et al.*, 1994). Increased LFA-1 clustering leading to enhanced avidity is considered to be the dominant mechanism controlling lymphocyte adhesion induced by Ca^{2+} mobilizers and TCR/CD3 ligation (Van Kooyk *et al.*, 1989; Dustin and Springer, 1989; Lub *et al.*, 1995; Stewart *et al.*, 1996). While the precise mechanism by which integrins become clustered remains to be fully clarified, use of agents that disrupt the cytoskeleton such as cytochalasin D have indicated that cytoskeletal rearrangement is involved and that, on activation, LFA-1 molecules are released from restraint, allowing the molecules to move and cluster (Kucik

et al., 1996). Introduction of deletion mutations that result in LFA-1 lacking the complete β2 cytoplasmic tail and/or the conserved KVGFFKR sequence in the αL cytoplasmic tail and hence loss of cytoskeletal interaction also resulted in a clustered cell surface distribution of LFA-1 (Van Kooyk *et al.*, 1999).

Studies of lipid raft dynamics also suggest that integrins are regulated through avidity changes (Krauss *et al.*, 1999). The distribution of lipid molecules such as glycosphingolipids, GPI-anchored proteins and cholesterol in the lipid bilayer is now widely accepted not to be a random process, but rather such lipids are organised into microdomains or 'lipid rafts' and appear to be important in vesicle transport and sorting of membrane proteins in polarized cells (London and Brown, 2000; Cherukuri *et al.*, 2001). At the cell surface, the rafts also serve as platforms for signalling molecules such as Src family members, G-proteins, PI3 kinases and adaptor proteins. It has recently been demonstrated that, on activation, LFA-1, VLA-4, αVβ3 and the β1 integrins α3β1 and α6β1 relocate to these highly organised microdomains and, in doing so, enhance avidity and increase cell adhesion by means of a high local concentration of the integrin (Leitinger *et al.*, 2002; Claas *et al.*, 2001; Thorne *et al.*, 2000).

1.5.2. Affinity Modulation

By definition, high affinity is the consequence of changes in molecular conformation that results in a stable bond between an integrin and its ligand (Chan *et al.*, 2002). Evidence for conformational changes following cell activation is primarily derived from the identification of mAbs that recognize integrin molecules only when they are in an activated state. The first reported activation mAb, PAC-1 (Shattil *et al.*, 1985), was shown to recognize an epitope on the platelet integrin αIIbβ3 only after platelet activation. O'Toole *et al.* (1990) later described two further αIIbβ3 mAbs, mAb62 and P41, which caused both increased binding to fibronectin and a distinct change in conformation as evidenced by the binding of PAC-1. A series of antibodies

described by Luque *et al.* (1996) have also been shown to bind β1 integrins when cells were activated.

Several mAbs that recognise only activated LFA-1, termed reporter mAbs, have also been identified. The epitope of Mab24, which has recently been mapped to the β2 I-like domain, is only induced after ligation of LFA-1 with ICAM-1 and requires the presence of cation (Kamata *et al.*, 2002). Data suggests that this mAb prevents deadhesion of receptor/ligand pairs, by 'locking' the integrin into an active state (Dransfield, *et al.*, 1992(a); Cabanas and Hogg, 1993). Two αL mAbs, CBR LFA-1/1 and H111 have also been identified as activation-sensitive, although both appear to favour the inactive from of LFA-1 as activation by divalent cations reduces binding. H111 binds to the edge of the MIDAS site on the I domain and CBR LFA-1/1 maps to residues 310-338, which includes all of the linker and the last two turns of the C-terminal α-helix. This reduced binding suggests that a change in the conformation around the linker sequence alters the epitope in some way (Ma *et al.*, 2002). However, it must be noted that the affinity changes in LFA-1 reported by these mAbs, and as measured by enhanced binding of ICAM-1, were only demonstrated when the LFA-1 ectodomain was modulated directly through divalent cation binding, presumably bypassing all intracellular signalling mechanisms. The lack of detectable affinity changes in LFA-1 on cellular activation initially suggested that affinity regulation did not have a significant role to play in ligand binding.

Development of *in vitro* and *in vivo* models of leucocyte recruitment have now allowed for the analysis of chemokine-inducible adhesion of leucocytes under flow conditions. Such studies have revealed that chemokines such as SLC (CCL21), ELC (CCL19) and SDF-1α (CXCL20) can induce rapid and transient increases in affinity of LFA-1 for ICAM-1, promote strong adhesion, and initiate arrest of rolling naïve T lymphocytes (Campbell *et al.,* 1998; Constantin *et al.,* 2000). Interestingly, in his study of rapid lymphocyte arrest, Constantin *et al.* (2000) showed that the mechanism of activation employed appears to be dependent on the local

concentration of ligand. Under physiological conditions, affinity regulation of LFA-1 appeared to be sufficient for lymphocyte arrest on ligand-rich high endothelial venules (HEVs), whilst enhanced mobility of integrin appears to be critical for lymphocyte adhesion under conditions of low ligand density. A similar finding by Leitinger *et al.* (2002) showed that there is a mixture of clustered and high affinity LFA-1 molecules present in lipid rafts, suggesting that both affinity and avidity play important and often convergent roles in inducing LFA-1 /ligand interactions. This is dependent on the activation signals received and the concentration of the ligand in the surrounding environment.

Emerging evidence from crystallographic studies of conformational changes within the I domains of αM and α1 on ligand binding does suggest that such conformational changes have a role to play in affinity regulation, although crystallographic studies have yet to yield an αL I domain in this conformation. Shimaoka *et al.* (2001) have shown *in vitro* that conformational changes in the αL I domain confer high affinity binding of LFA-1 to ICAM-1. The identification of areas of flexibility in both the α and β subunits of the αVβ3 integrin also suggests that conformational changes within the integrin may take place on ligand binding. However, the fact that the αVβ3 structure, both in the presence and absence of ligand, remains in the bent conformation has led to researchers questioning how this conformational regulation of affinity actually takes place. Two groups of researchers have published extensively in this area, and have proposed theories on how conformational switching from inactive to active states takes place and have attempted to relate the relevance of these findings to integrin activation and ligand binding. Both theories are based on accumulated data from X-ray crystallographic and NMR studies of integrin structure and mutational analysis of several of the integrin domains. Although both theories agree that dynamic movement through the extracellular domains results in increased ligand binding, there is a conflicting view on the overall structure that constitutes the active state.

The theory proposed by Arnaout (Xiong *et al.*, 2003(b)) is based on the crystal structure of αVβ3 in the presence of ligand which they believe is representative of the active form of the integrin, even though it remains in the bent conformation. To explain how the activation process takes place, the analogy of a 'deadbolt' is employed. A bolt firmly in the latch represents the interaction of the β3 tail domain (bolt) with the F/α7 loop of the I-like domain (clasp) which occurs in the resting state on the cell surface. This interaction locks the I-like domain in an inactive state by preventing the flip of the F/α7 loop required for the movement of the α1 helix which occurs on activation. On transmission of signals through the cytoplasmic domains, movement of the β-tail helices distances the TD domain from the F/α7 loop of the I-like domain and weakens the interactions between the two domains. This renders the integrin competent to bind ligand, causing complete unlocking of the adjacent 'deadbolt'. The authors suggest that the reason one does not observe extensive contacts between the β-tail domain and the I-like domain in the crystal structure is because it is already in the active form due to its truncation before the transmembrane domain. This model, where a movement of ~0.3nm could switch the integrin from active to inactive, is also an attractive explanation for the speed at which some integrins are activated. From their analysis of epitopes recognized by activating mAbs, which are known to bind to various β-subunit C-terminal regions, Arnaout also proposes such mAbs would still be available to bind in this model and could act by unlocking the deadbolt without necessarily straightening the integrin. Analysis by Calzada *et al.* (2002) of epitopes seen by both activating and inactivating αIIbβ3 mAbs also suggests that the structure of the integrin does not appear to require linearisation in order to become active. In conclusion, Arnaout and colleagues suggest that the bent conformation represents the active form of the integrin and extension at the knees is not required for ligand binding but, rather, is a post-binding event linked to extracellular signals.

An alternative model of integrin activation has been proposed by Springer *et al.* (2002) and referred to as the 'switchblade' model. In this model, the bent conformation of αVβ3 is considered to represent the inactive state and activation is associated with the opening of a

"switchblade" which allows the ligand headpiece to move away form the plasma membrane and the legs to separate. Using the αVβ3 structure, superimposed with the β2 I-EGF modules 2 and 3 determined by Beglova *et al.* (2002), Shimaoka *et al.* (2002(b)) have shown the epitopes of mAbs that bind in the stalk region and activate the integrin would be inaccessible if the bent conformation represented the active high affinity ligand binding conformation. The bent structure shows that residues in the β2 I-EGF3, which are involved in the αβ stalk interface that restrains integrins in the inactive state, are on the face pointing toward calf-1 domain of the α-subunit stalk. This being the case, the epitopes of activating mAbs such as KIM127 and MEM148 on I-EGF3 are masked in this conformation, contradicting Arnaout's claim. On transmission of signals to the cytoplasmic domains, Springer's model suggests that the resultant separation of membrane proximal domains leads to the dislocation of the I-EGF3 contact with calf-1 domain. This in turn triggers the 'switch blade'-like opening, which is linked to a change in conformation of the I-like domain. This interpretation fits with the EM images of ligand-bound integrins (Weisel *et al.*, 1992; Du *et al.*, 1993) which show the integrin as an extended structure. Epitope mapping studies (Takagi *et al.*, 2001), which demonstrate that mAbs to specific residues in I-EGF repeats 2 and 3 would be buried in the bent conformation, also add weight to this theory. Furthermore, Takagi *et al.* (2002) have shown by EM that integrins clamped in the inactive state adopt a bent conformation whereas integrins activated by Mn^{2+} or cyclic peptides are presented predominantly in the extended form. They have also presented evidence that tethering of the inactive form to the cell surface using disulphide bridges within the cytoplasmic tails causes the integrin to remain in an inactive state upon cell activation. In I domain-containing integrins, Springer suggests that the conformational change in the I-like domain causes movement of the I domain C-terminal linker sequence, resulting in a downward shift of the α7 helix of the I domain. The consequence of this movement within the I domain was discussed in Section 1.3.

1.5.3. Cations

It is well-established in the integrin field that the divalent cations Mn^{2+} and Mg^{2+} are required to activate integrins and make them competent to bind ligand, whilst Ca^{2+} generally has an inhibitory effect on this binding (Marlin and Springer, 1987; Michishita *et al.*, 1993; Larson *et al.*, 1989; Perruzzelli 1995; Van Kooyk *et al.*, 1994). Although the divalent cation requirements for LFA-1 / ligand interactions have been extensively studied, and several metal binding domains have been identified on both the α and β subunits, the relative importance of the various sites and how the relative site occupancy by cations is regulated *in vivo* is still unclear.

Crystallographic studies have shown that the overall extracellular structure of αVβ3 contains 8 potential cation-binding sites with five on the α subunit and three on the β-subunit (Xiong *et al.*, 2001, 2002). Within the α-subunit, four cation-binding sites are located in the hairpin loops of the β-propeller with the fifth located at a novel site in the α knee region. In the β subunit all 3 sites are located at the top of the I-like domain in close proximity to each other. Crystallisation of αVβ3 in the presence of Mn^{2+} showed that all sites were cation bound while in the presence of Ca^{2+} only six out of the eight sites were occupied. The two sites that remained unbound in the presence of Ca^{2+} were the β-chain I-like domain MIDAS (Metal Ion Dependent Adhesion Site) and LIMBS (Ligand-associated Metal Binding Site) sites.

The binding of both Mn^{2+} and Mg^{2+} to LFA-1 has been suggested to induce a high affinity conformation that promotes ligand binding. This high affinity conformation has been monitored by the binding of certain mAbs known as activation reporter antibodies. These mAbs such as mAb24 appear to only bind to LFA-1 after it has undergone conformational change. Binding of Ca^{2+} however, does not induce the mAb epitope (Dransfield *et al.*, 1989; Dransfield *et al.*, 1992(a +b)). While Mg^{2+} in the MIDAS site is a requirement for ligand binding, it appears to

only enhance binding in response to activation following intracellular signalling or binding of activating mAbs when millimolar levels of Ca^{2+} are also present. In contrast, Mn^{2+} in the presence of low millimolar levels of Ca^{2+} is able to stimulate binding of LFA-1-bearing cells to ligand in the absence of additional stimuli (Dransfield *et al.*, 1992(b); Smith 1994; Michishita *et al.*, 1993). It has been suggested that the difference in the ability of Mg^{2+} and Mn^{2+} to activate LFA-1 is dependent on the affinity of the cations for the MIDAS site. However, Springer *et al.* (2002) have recently suggested that binding of Mn^{2+} to a cation site other than the MIDAS site is the controlling factor for the increased activation over Mg^{2+}, and have proposed the β-I like domain MIDAS site as a potential Mn^{2+} binding site in LFA-1 since this site does not appear to bind Ca^{2+} and hence could be specific for Mn^{2+}. They argue that while there are clear differences in the crystal structures of the αM I domain in the presence of Mn^{2+} compared with Mg^{2+} which in turn has lead to the suggestion that the I domain has a higher affinity for Mn^{2+} when both compete for the same site, the conformation of the αL I domain does not appear to be altered by changes in metal ion binding (Qu and Leahy, 1996). Additionally, the isolated locked-open αL I domain, which they generated to mimic an activated I domain, shows equivalent adhesiveness in the presence of Mg^{2+} or Mn^{2+} in their studies. This led them to propose that the activating effects of Mn^{2+} may in fact be through its binding to one of the other cation binding sites found within the integrin extracellular domains such as the β-I like domain MIDAS site.

Although Mn^{2+} is routinely used to activate integrins *in vitro,* its interaction with cell surface receptors and extracellular matrix proteins (ECM) *in vivo* has received relatively little attention, and Mg^{2+} is thought to be the relevant divalent cation that activates integrins *in vivo*. The theory proposed above, however, suggests that Mn^{2+} may indeed have a role *in vivo*. The concentrations of Mn^{2+} in most adult tissues range between 3-20μM (Chan, A, *et al.*, 1992) and this divalent cation is known to be a required cofactor of important regulatory kinases and phosphatases and can regulate a number of Mn^{2+}-dependent nuclear enzymes, including

endonucleases, nucleotideases, and ribonucleases, required for DNA synthesis and repair (reviewed by Roth *et al.,* 2003).

The data from the αVβ3 crystal structure has also lead to speculation that the ADMIDAS represents a high affinity Ca^{2+} binding site and recently published work from Mould *et al.* (2003) supports this theory. Using the interaction between α5β1 and fibronectin as a model system, they showed that mutation of residues that form the ADMIDAS site inhibit ligand binding. This effect could, however, be partially rescued by the use of activating monoclonal antibodies. Mutation of the ADMIDAS residues also reduced the inhibition of Mn^{2+}-supported ligand binding by Ca^{2+}, suggesting that the ADMIDAS is a Ca^{2+}-binding site involved in the allosteric inhibition of Mn^{2+}-supported ligand binding. Mutations of the ADMIDAS site also perturb transduction of a conformational change from the MIDAS through the C-terminal helix region of the β I-like domain to the underlying hybrid domain, implying an important role for this site in receptor signalling.

Under normal physiological conditions, the concentration of extracellular Mg^{2+} and Ca^{2+} *in vivo* is reported to be approximately 1.5mM and 2.5mM respectively (Olinger, 1989). However, during the early phase of repair following cutaneous injury, levels of Mg^{2+} have been shown to increase significantly with a similar corresponding decrease in the concentration of Ca^{2+}. These changes in cation concentrations correlate with increased migration of inflammatory cells, such as fibroblasts and keratinocytes to the site of injury which is known to be integrin-dependent (Grzesiak and Pierschbacher, 1995). Several other studies (Labadia *et al.*, 1998; Rothlein and Springer, 1986; Stewart *et al.*, 1996) also suggest that the affinity of LFA-1 for ICAM-1 is finely tuned through subtle alterations in the concentrations of Mg^{2+} and Ca^{2+}.

Using surface plasmon resonance, Labadia *et al.* (1998) showed that whilst micromolar concentrations of Ca^{2+} enhance ICAM-1 binding in the presence of Mg^{2+}, increasing Ca^{2+} into the millimolar concentration range results in decreased ICAM-1 binding. At low Ca^{2+} concentrations, binding in the presence of Mg^{2+} appears to be synergistic as evidenced by the affinity measurements of Mg^{2+} in the presence and absence of Ca^{2+} (160μM and 12μM, respectively). However, at high Ca^{2+} concentrations, Ca^{2+} could competitively displace the Mg^{2+} which leads to a form of LFA-1 with a low affinity for ICAM-1 thus suggesting that Ca^{2+} can bind at the MIDAS site and reduce ligand binding dramatically.

A similar study by Griggs *et al.* (1998) investigating the relationship between Ca^{2+} and Mn^{2+}, using isolated αL I domain, showed that while the I domain preferentially bound Mn^{2+} over most cations, this interaction was inhibited by Ca^{2+} and to a lesser extent with other divalent cations. They estimated K_D values of 56μM and 1.4μM for Ca^{2+} and Mn^{2+} respectively, and these values suggest that the MIDAS site may be complexed with Ca^{2+} at physiological concentrations but if the concentration of Ca^{2+} is greatly reduced following cutaneous injury as suggested by Grzesiak and Pierschbacher (1995), then it is possible that Mn^{2+} could bind and initiate integrin-mediated adhesion events.

The LIMBS site could also be a potential Mn^{2+} activation site as it too lacks the presence of a cation in the Ca^{2+} crystal structure. It also contains residues that are conserved in all β I-like domains and appears to add structural stability to the ligand-binding surface. The other cation sites at the base of the β-propeller and in the knee region of the α-subunit could also have potentially important roles to play in the activation of integrins although further research in this area is required before definite roles can be assigned to each of these sites.

1.6 LFA-1 Signalling and Crosstalk

As discussed above, LFA-1 interaction with the ICAMs, like other integrin ligand interactions, requires a signal-induced activation event which causes a transient increase in the capacity of the integrin to bind ligand. Several mutagenesis studies have shown that activation of both avidity and affinity changes appear to be propagated through the cytoplasmic tails. The cytoplasmic tails of most integrins share a similar organisation of polar and apolar amino acids and the conserved sequences of GFFKR in the α subunit (Muir, *et al.*, 1994) and LLxxxHDR in the β subunits appear to form a structural constraint that locks the integrin naturally in a low affinity conformation and, on activation, the two chains separate (Hughes *et al.*, 1996; Ginsberg *et al.*, 2001). Truncation before the GFFKR motif, complete deletion of the motif itself, or point mutations of the individual residues in the motif, results in a constitutively active integrin which is independent of the cell type studied or signalling pathways (O'Toole, *et al.*, 1994; Lu and Springer, 1997). Lu *et al.* (2001(a)) have also shown that replacement of the αL and β2 cytoplasmic domains with acidic and basic peptides that form an α-helical coiled coil cause inactivation of LFA-1, whereas replacement of both tails with basic peptides that prevented formation of an α-helical coiled coil resulted in a constitutively active LFA-1. Induction of ligand binding by the mutated activated cytoplasmic domains also correlated with the induction of activation epitopes in the extracellular domain.

The association of integrin α and β cytoplasmic tails with cytoskeletal proteins appears to be one mechanism by which intracellular signalling events can control the conformation of integrin extracellular domains and promote integrin clustering. Several studies suggest that LFA-1 on lymphocytes is constrained by the actin cytoskeleton in resting cells (Stewart *et al.*, 1998; Kucik *et al.*, 1996). On Ca^{2+}-mediated cell activation, the enzyme calpain releases LFA-1 from this constraint and allows the integrin to cluster (Stewart *et al.*, 1998). Similarly, a study by Sampath

et al. (1998) using neutrophils suggested that talin also tethers β2 integrins to the cytoskeleton and, following activation, proteolysis of talin causes release of integrins from the actin cytoskeleton. PMA- and TCR- induced activation of LFA-1 on T cells, and LPS-induced LFA-1 activation on monocytes, have also been shown to result in association of the protein cytohesin-1 with LFA-1 (Geiger *et al.*, 2000). This appears to be brought about by the activation of PI-3-Kinase through H-ras and Rac pathways which results in phosphoinositide (3,4,5)-triphosphate binding to cytohesin-1 which in turn binds to the cytoplasmic tail of β2 and initiates activation. The KALI motif on the β2 tail has been proposed as a possible binding site for such interactions. Binding of cytohesin and Rac-1 (involved in the PKC intracellular pathway) have both been shown to increase ligand binding following interactions with this motif (Geiger *et al.*, 2000; Valmu *et al.*, 1991; Nagel *et al* 1998).

The precise molecular mechanisms mediating the transduction of signals to the cytoplasmic domains following activation is still unclear, but investigators have identified several signalling pathways that affect both the affinity and avidity of LFA-1 and transmit signals from LFA-1 back into the cell. These transduction events serve to modulate many aspects of cell behaviour including proliferation, shape change, motility, gene expression, and differentiation.

Signalling pathways that are initiated by the upregulation of chemokines have emerged as major activators of integrin activation. Through their interaction with heterotrimeric G protein-coupled receptors (GPCRs) the chemokines SLC (CCL21), ELC (CCL19) and SDF-1α (CXCL20) can rapidly and transiently stimulate an increase in the affinity of LFA-1 for ICAM-1 to promote strong adhesion and induce arrest of rolling naïve T lymphocytes (Campbell *et al.*, 1998). Binding of interleukin-8 (IL-8) to CXCR1 and CXCR2 has also been shown to lead to an increase in intracellular calcium flux, which in turn signals cell shape change, integrin activation and adhesion during the extravasation process (Wolf *et al.*, 1998). In contrast to this transient activation, RANTES and MCP-3 have been shown to trigger prolonged expression of a αMβ2

activation epitope on eosinophils (Weber *et al.*, 1996) suggesting that chemokines can activate β2 integrins through both affinity and avidity changes.

Activation of protein kinases such as Syk, src family tyrosine kinases, and FAK have also been identified as some of the initial signalling events that are triggered by β2 integrin ligation on leucocytes which ultimately lead to β2 integrin-dependent modulation of the cytoskeleton (Berg & Ostergaard, 1997; Fagerholm *et al.*, 2002; Rodriguez-Fernandez *et al.*, 1999). TCR-associated signalling through Lck/Zap70 phosphorylation events have been shown to be initiated at the early stages of synapse formation (Dustin e*t al.*, 2002) while blocking FAK activity by over-expression of a FAK tyrosine phosphatase results in a strong reduction of LFA-1 and TCR co-localization. Antibody-induced clustering of β2 integrins on PMNs has also been shown to trigger an association of Fgr and Hck with PI-3 kinase.

1.6.1. Cross talk

Evidence is now emerging which suggests that, in addition to the effects on other receptors on the cell surface, outside-in signals can also alter the activity of neighbouring integrins in a process termed 'crosstalk' (Blystone *et al.*, 1994; Leitinger and Hogg, 2000). This provides an additional level of complexity at the cellular level and allows one to explain the functional interactions between members of the integrin family. Blystone *et al.* (1994) first noted the 'crosstalk' phenomenon whilst investigating the influence integrins have on the phagocytic ability of cells. Using an αVβ3-transfected K562 cell line which endogenously expresses α5β1, αVβ3 ligation was shown to be capable of inhibiting phagocytic function of α5β1 for fibronectin-opsonized beads without affecting low affinity, α5β1-mediated adhesion. They went on to show that the β3 cytoplasmic tail was both necessary and sufficient for this effect (Blystone

et al., 1995). Further investigation suggested that the mechanism involves calcium- and calmodulin-dependent protein kinase II (CamKII). CamKII is now known to be an important regulator of α5β1-mediated phagocytosis and migration, and co-ligation of αVβ3 or exposure of the isolated β3 tail prevents α5β1-induced CamKII activation (Blystone, *et al.*, 1999). Interestingly, a very recent study by Ly *et al.* (2003) showed, using a COS cell expression system, that *de novo* expression of α5β1 was capable of suppressing αVβ3-mediated adhesive functions and this inhibition was modulated through the α5 integrin cytoplasmic tail.

Pacifici *et al.* (1994) also showed that fibronectin binding to α5β1 was able to induce intracellular signals which increased α2β1-dependent adhesion of monocytes to collagen without modifying α2β1 expression. The α2β1 integrin also induces the release of IL-1 in these cells, an event that is also potentiated by the binding of fibronectin to the α5β1. By using mAbs against the intracellular region of the α5 subunit and specific inhibitors of PKC, the authors showed that the potentiating effects of fibronectin on monocyte IL-1 production and their adherence to collagen was dependent on an intact α5 subunit cytoplasmic domain. Although α2β1 could be activated by several intracellular second messengers, including protein kinase A and intracellular calcium, the potentiating effect of fibronectin was mediated only by PKC. A similar study by Diaz-Gonzalez *et al.* (1996) showed that binding of ligand to integrin αIIbβ3 inhibited the function of other target integrins such as α5β1 and α2β1 by blocking their ability to signal.

Turning our attention to 'crosstalk' involving LFA-1, the first observations were made by Van Kooyk *et al.* (1993) whilst investigating LFA-1/ICAM-1 and VLA-4/VCAM-1 mediated adhesion of T cells to endothelial cells. Using blocking mAbs to both LFA-1 and VLA-4, they observed that the binding of activated T cells to endothelial cells was normally mediated through LFA-1 and not through VLA-4. However, when LFA-1 was not expressed or non-functional, as is the case with several T-cell leukaemia cell lines, VLA-4 was able to mediate adhesion, suggesting that LFA-1 may normally down-regulate VLA-4 although the mechanism has yet to

be identified. Initial work by Porter and Hogg (1997) on LFA-1-mediated crosstalk in primary T cells also showed that the interaction of LFA-1 with ICAM-1 decreased adhesion mediated by VLA-4 and, to a lesser extent, α5β1. Whilst binding studies with mAb 24 suggested that LFA-1 needed to be in the active state for its suppressive effect, ligand binding or prolonged activation of β1 integrins has no effect on LFA-1-mediated adhesion to ICAM-1. However, using a different cell system, the same group published apparently opposing results showing that activation of LFA-1 enhances rather than inhibits the binding of both α5β1 and VLA-4 to their respective ligands (Leitinger & Hogg, 2000). In this study, LFA-1 was expressed without an I domain but appeared to retain features of an activated integrin. Jurkat cell lines expressing this I-domain-less LFA-1 (LFA-1 ΔI and referred to as $JB2.7_{\Delta IDomain}$ in the remainder of this study) demonstrated increased α5β1- and VLA-4- mediated adhesion, and addition of activating β2 mAbs actually enhanced this binding further. In the case of VLA-4, the increased binding likely results from integrin clustering rather than affinity changes since no increase in availability of activation epitopes was observed. The presence of this 'active' LFA-1 in lipid rafts was also shown to promote the movement of VLA-4 into the rafts (Leitinger *et al.,* 2002).

In contrast to the studies above, several researchers have investigated 'cross-talk' leading to LFA-1 activation. May *et al.* (2000) have shown that both LFA-1 and αMβ2 became activated when VLA-4 was ligated by soluble VCAM-1-Fc or by β1 mAbs, leading to rapid induction of adhesion of myelomonocytic cells (HL60, U937) to HUVECs. The activation of the β2 integrins by VLA-4 in this system was further shown to require the presence of the urokinase receptor (uPAR) as depletion of uPAR from the cell surface by phosphatidylinositol-specific phospholipase C reduced cell adhesion dramatically. Chan *et al.* (2000) also showed that treatment of Jurkats or PBMCs with soluble, cross-linked VCAM-1 or activating VLA-4 mAbs, significantly increased adhesion to ICAM-1. Interestingly, as shown with the LFA-1-mediated VLA-4 adhesion described above, this enhanced ICAM-1 binding appeared to be brought about by integrin clustering rather than induction of a high affinity state as evidenced by the lack of

Mab24 binding. Cytochalasin D prevented VLA-4-mediated up regulation of LFA-1 suggesting that rearrangement of the cytoskeleton was involved in the process. That VLA-4 is capable of stimulating LFA-1-dependent ligand binding is further supported by the findings of Rose *et al.* (2001) showing that LFA-1-dependent cell migration is dramatically reduced in a VLA-4-defective Jurkat cell line relative to a cell line expressing normal levels of VLA-4.

The limited data on integrin crosstalk published so far highlights inconsistencies in terms of hierarchy between individual integrins and, indeed, whether the integrin has a positive or negative effect on the function of other integrins. Diaz-Gonzalez *et al.* (1996) suggest that negative versus positive regulation is dependent on the levels of expression of the integrins involved, with negative regulation controlled by high expression of the dominant integrin. Another controlling factor may be the availability of adaptor proteins for cytoskeletal connections or components of critical signalling pathways. Leitinger *et al.* (2002) have suggested that in their initial study which showed negative regulation of VLA-4, the high concentration of LFA-1 on cultured T-cells might sequester such essential adaptor or signalling molecules, whereas in their latter study where there was a low level of LFA-1 expression, the adaptor or signalling molecules would be available for binding to other integrins and hence positively regulate VLA-4.

1.7 Aim of Project

Leitinger *et al.* (2002) reported that the introduction of an I domain-deleted version of LFA-1 into a cell system resulted in crosstalk with other integrins. The authors suggested that the I domain deletion resulted in an LFA-1 molecule that in someway mimicked an active form of the integrin and this resulted in intracellular interactions that enhanced binding through other cell surface integrins. Since an I domain deletion of LFA-1 is unlikely to exactly reproduce the conformation adopted by an activated LFA-1 molecule it was felt that a better picture of integrin crosstalk could be achieved by more subtle alterations of the LFA-1 conformation. The aim of this project was therefore to generate a series of LFA-1 constructs that contained mutations within the I domain which would lead to a more active form of LFA-1. These mutations would be initially characterized in a cell free soluble system to confirm that they did enhance ligand binding. A series of these advantageous mutations would then be transferred into cells to investigate their effects on other endogenous integrins.

Chapter 2

Materials and Methods

Chapter 2 Materials and Methods

2.1 Materials

2.1.1 Reagents and Equipment

Chemical and biological reagents, unless otherwise stated, were obtained from Sigma-Aldrich (UK). Tissue culture components, gel electrophoresis materials and equipment and were obtained from Invitrogen Ltd., (UK). Plastic consumables were obtained from Falcon, BD Biosciences (UK) with the exception of ELISA plates which were Nunc^{TM} brand products, supplied by Fisher Scientific (UK).

Restriction enzymes, AmpliTaq DNA polymerase, T4 DNA ligase and CIP were purchased from Boehringer Mannheim Ltd., (Lewes, East Sussex), New England Biolabs (Beverly, Mass., USA) or Roche Molecular Biochemicals, UK. Antibodies (unlabelled or HRP-, FITC- and PE-labelled) were obtained from Chemicon International Ltd., (Harrow, UK), Cambridge Bioscience (Cambridge, UK) and Jackson Immuno Research, Inc.

The Bio-Rad gene pulser unit and cuvettes were obtained from BIO-RAD (Hemel Hempstead Hertfordshire, UK). FACScalibur was supplied by Becton Dickinson (San Jose CA, USA). Plate washers and plates readers were supplied by Labsystems, UK. All standard curves were constructed and data analysed using Genesis II software (Labsystems, UK). Small-scale centrifugation was carried out using an Eppendorf 5415D benchtop microfuge (Eppendorf Ltd, Germany). Large-scale centrifugation was carried out using a Beckman RC3B or RC5B (Beckman Instrumentation Ltd., CA., USA)

2.1.2 Buffers and Solutions

PBS	120mM NaCl, 2.7mM KCl, 10mM phosphate buffered salts, pH7.4
TBS	20mM Tris-HCl, 150mM NaCl, pH7.4
L-Broth	1% (w/v) Bactotryptone, 0.5% (w/v) Bacto-yeast extract, 17mM NaCl, pH7.4
SOC	2% Bactotryptone (w/v), 0.5% (w/v) Bacto-yeast extract, 10mM NaCl, 25mM KCl, 10mM $MgCl_2$, 10mM $MgSO_4$, 20mM glucose, pH7.4
TE	10mM Tris-HCl pH 7.4, 1mM EDTA
TAE	40mM Tris-acetate pH8, 1mM EDTA
TMB	0.1mg/ml 3,3,5,5'-tetramethylethyene benzidine 0.004%(v/v) hydrogen peroxide in 0.1M acetate-citrate buffer pH 6
FACS Buffer	PBS, 5%(v/v) FCS, 0.02% (v/v) Sodium Azide, pH7.4
Electrophoresis Buffer	2.9g/L Tris Base, 14.4g/L Glycine, 1g/L SDS, pH 8.3
Tris Glycine Blotting Buffer	12g/L Glycine, 3g/L Tris Base, pH 8.3
Blocking Buffer	20mM Tris-HCl, 150mM NaCl, 1mM $MnCl_2$, 1.0% (v/v) Tween, 3% (w/v) BSA, pH7.4
Conjugate Buffer	20mM Tris-HCl, 150mM NaCl, 1mM $MnCl_2$, 0.1%(v/v) Tween, 0.3%(w/v) BSA, pH7.4
Wash Buffer	20mM Tris-HCl, 150mM NaCl, 1mM $MnCl_2$, pH7.4

2.1.3 Bacterial Strains

XL-1 Blue subcloning grade competent cells (Stratagene, CA) were used for most transformations. For site directed mutagenesis transformations, XL-Blue supercompetent grade cells (Stratagene, CA) were used. Where transformations required the use of a dam$^-$ host, competent GM242 cells (M.Cockett, Celltech) were used.

2.1.4 Vectors

EE6hCMV*neo* is a derivative of EE6hCMV (Stephens and Cockett, 1989) carrying a G418 resistance marker. EE12.2 is also a derivative of EE6hCMV but carries a GS selection marker. pEE12.2mFc has a *Sal* I site in the vector removed and replaced by a *Not* I site. It also contains the mouse Fcγ1, *Sal* I / *Eco*R1 gene fragment (Takahashi *et al.*, 1982) (Figure3.3). pV16mFc is also a derivative of pEE6 hCMV in which a *Sal* I site has been removed and replaced with a *Not* I site and a second *Not* I site introduced at the 5' end of the HCMV promoter fragment. This vector also contains the mouse Fcγ1, *Sal* I / *Eco*R1 gene fragment (Figure 3.3).

2.1.5 Antibodies

The name, subclass, host etc. of all antibodies used are described in the table below.

Antibody	Subclass	Host species	Reactivity	Source
MOPC21	1gG1	monoclonal	unknown	ATCC
6.5E	1gG1	monoclonal	hCD18	Celltech
KIM185	1gG1	monoclonal	hCD18	Celltech
KIM127	1gG1	monoclonal	hCD18	Celltech
DA36	1gG1	monoclonal	hCD11a	Celltech
AB38	1gG2a	monoclonal	hCD11a	Chemicon
AB38-PE	1gG2a	monoclonal	hCD11a	Chemicon
MEM83	1gG1	monoclonal	hCD11a	V.Horejsi
MEM95	1gG1	monoclonal	hCD11a	V.Horejsi
MEM48	1gG1	monoclonal	hCD18	V.Horejsi
RR1	1gG2a	monoclonal	hICAM-1	Chemicon

HI 111-PE	1gG1	monoclonal	hCD11a	AutogenBioclear
JB1A	1gG1	monoclonal	hCD29	Chemicon
HA5	1gG1	monoclonal	α5	Chemicon
Mab24	1gG1	monoclonal	hCD18	N. Hogg
KIM215	1gG1	monoclonal	hCD18	Celltech
KIM202	1gG1	monoclonal	hCD18	Celltech
MCA1485	1gG1	monoclonal	hICAM-3	Serotec
MCA1140	1gG1	monoclonal	hICAM-2	Serotec
15.2	1gG1	monoclonal	hICAM-1	Serotec
BR-IC2/2	1gG2a	monoclonal	hICAM-2	Biosource
152-2D11	1gG2a	monoclonal	hICAM-3	Biosource
Y9A2	1gG1	monoclonal	hα9β1	Chemicon
SAM-1	1gG2a	monoclonal	hα5	Celltech
MAX68P	1gG1	monoclonal	hα4	Celltech
HA5	1gG2b	monoclonal	hCD29	Chemicon
BHA2.1	1gG	monoclonal	hα2β1	Chemicon
TS2/7	1gG	monoclonal	hα1	Serotec
C3II.1	1gG	monoclonal	hα3	Pharmingen
TS2/16	1gG1	monoclonal	hβ1	T. Springer
LM609	1gG	monoclonal	hαvβ3	Chemicon
E7P9	1gG1	monoclonal	hαvβ3	Chemicon
7E3	1gG	monoclonal	αIIbβ3	Celltech
AMF-7	1gG	monoclonal	hCD51(αV)	Immunotech
BP6	1gG	monoclonal	hβ7	A. Law
LF61	1gG1	monoclonal	hαE	Serotec
R7.1	1gG1	monoclonal	hCD11a	Biosource
KIM247	1gG1	monoclonal	hCD11b	Celltech
KIM249	1gG1	monoclonal	hCD11b	Celltech
KIM75	1gG1	monoclonal	hCD11b	Celltech
αD	IgG1	monoclonal	hαD	Y.Van Kyook
15.2	1gG1	monoclonal	hICAM-1	Biosource
MCA1140	1gG1	monoclonal	hICAM-2	Serotec
MCA1485	1gG1	monoclonal	hICAM-3	Serotec
Cal3.10	1gG1	monoclonal	hICAM-3	R&D
IG11	1gG1	monoclonal	VCAM-1	Celltech
UPC10	IgG2a	monoclonal	unknown	Sigma
CRB-IC/2	IgG2a	monoclonal	ICAM-2	Biosource
MEM111	IgG2a	monoclonal	ICAM-1	V.Horejsi
P1D6	IgG3	monoclonal	hα5	Chemicon
SC6597	goat	polyclonal	hα6	Santa Cruz
SC6638	goat	polyclonal	hα8	Santa Cruz
SC6628	goat	polyclonal	hα4	Santa Cruz
Ab3.9	1gG	monoclonal	CD11c	N. Hogg

2.1.6 Low Molecular Weight Antagonist

Lovastatin was purchased from Sigma-Aldrich (UK) and was kept as frozen stock solution at a concentration of 50mM in DMSO. Structure is shown below.

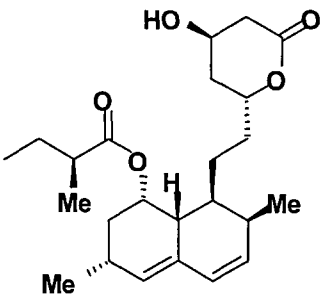

Lovastatin

2.1.7 Cell lines

The mouse myeloma cell line NSO was obtained from C. Milstein (Cambridge) and has previously been described (Galfre and Milstein, 1982).

The cell line CHO-761H was obtained from Celltech (Cockett *et al.*, 1991).

The human erythroleukaemic cell line K562 was obtained from the European collection of Animal Cell Cultures (No.CCL243). The KL4 cell line was obtained from Celltech (Ortlepp *et al.* 1995).

The JB2.7, JB2.7$_{LFA\text{-}1WT}$ and JB2.7$_{\Delta IDomain}$ cell lines were obtained from N. Hogg (London) with kind permission from L. Klickstein.

2.1.8 Assay Reagents

ICAM-1hFc, ICAM-2hFc, ICAM-3hFc and VCAM-1hFc had previously been expressed and purified in house (Celltech) with the original ICAM-Fc fusion genes obtained from D. Simmons.

2.1.9 Oligonucleotides

Vector Primers

HCMV MIE Promoter Primer ***1053 (5' hCMV region)***
Sequence: $^{5'}$GCTGACAGACTAACAGACTGTTCC

Murine γ1 Fc Primer ***V9011 (3' mFc region)***
Sequence: $^{5'}$CGTCTGAGCTGTGTGCACCTCCAC

CD11a Primers

CD11a Primer 1 B3609 (Primer to introduce 3' *Sal* I site)
Sequence: $^{5'}$CCAAGG<u>GTCGAC</u>CTGCTTCTCATACACCACGTCAAC
Sal I

CDlla Primer 2: B6112 (470→)
Sequence: $^{5'}$CTGTGTTACCTCTTCCGCCAG

CDlla Primer 3: B8553 (855→)
Sequence: $^{5'}$ACCAAAGTGCTTATCATCATC

CDlla Primer 4: B8549 (810 ←)
Sequence: $^{5'}$CGCGACATAATTGATGGCACC

CDlla Primer 5: B8550 (1200←)
Sequence: $^{5'}$GGCTCCTACTGCCCCCACGAC

CDlla Primer 6: B8554 (1560→)
Sequence: $^{5'}$ACACCAGAAGTGAGAGCAGGC

CDlla Primer 7: B8551 (1200←)
Sequence: $^{5'}$TCTCTGCTCCCCATAGAACAG

CDlla Primer 8:	B8555 (1680→)
Sequence:	$^{5'}$GCTCTGACAGACATCAACGGC
CDlla Primer 9:	B8552 (2000←)
Sequence:	$^{5'}$GGAGCACTCCACTTCATGCAC
CDlla Primer 10:	B8556 (2070→)
Sequence:	$^{5'}$TACCCCCAGTTCCAAGGCCGC
CDlla Primer 11:	B8557 (2370←)
Sequence:	$^{5'}$CGAGTGCAGGGAGGGTCTCAG
CDlla Primer 12:	B8559 (2450→)
Sequence:	$^{5'}$CCTGCAAGATCCAGAGCCCTG
CDlla Primer 13:	B8558 (2730←)
Sequence:	$^{5'}$CTGTATTAAACATCATCTGCAG
CD11a Primer 14:	B3606 (2790→)
Sequence:	$^{5'}$TGTAACAATGAGGACTCAGACCTC
CDlla Primer 15:	B3607 (3085→)
Sequence:	$^{5'}$CACTATGAGGATCTGGAGAGGCTC
CDlla Primer 16:	B3608 (3200←)
Sequence:	$^{5'}$CAGAGTCCCGATCACTTGGACGAG

Other primers used in the cloning of the various forms of LFA-1 are described in Appendices 1 and 2 and Chapter 3

2.2 Molecular Biology

2.2.1 Gene Cloning by PCR

Approximately 50 ng of template DNA (either cDNA or plasmid DNA) was mixed with 10 pmoles of the appropriate oligonucleotides, and 1unit of AmpliTaq® DNA polymerase, in a PCR buffer containing 0.25mM dNTP (dATP, dCTP, dGTP, dTTP), 50mM KCl, 10mM Tris-HCl pH 8.3, 1.5mM $MgCl_2$, and 0.01% (w/v) gelatin. The reaction was amplified for 30 cycles of 94°C, 1minute; 55°C, 1minute; 72°C, 1-3 minutes; followed by a 15 minute cycle at 72°C, in a T3 thermocycler (Biometra). Samples were then analysed by agarose gel electrophoresis (See Section 2.2.4).

2.2.2 Quick Change Site Directed Mutagenesis

Site directed mutagenesis was carried out using Stratagene's QuikChange® Mutagenesis Kit according to the manufacturer's instructions.

2.2.3 Agarose Gel Electrophoresis

Horizontal submerged gel electrophoresis was carried out as described by Sambrook *et al.* (1989) on 0.5%-1.5% (w/v) agarose gel (depending on fragment size) in TAE buffer containing 0.5µg/ml ethidium bromide. Electrophoresis was typically carried out at 4-6V/cm and the DNA bands were visualised using a 254nm UV light. Agarose gel electrophoresis was used both analytically and preparatively, the latter for purification of fragments after restriction enzyme digestion, prior to ligation. To minimise DNA damage, recovery of DNA fragments for cloning and ligation was carried out using a 366nm wavelength UV light.

2.2.4 Purification of DNA fragments from an agarose gel

DNA fragments were isolated from agarose gel using the Qiaquick® Gel Extraction Kit (QIAGEN Ltd., UK) according to the manufacturer's instructions.

2.2.5 Analysis of DNA by restriction enzyme digest

For general restriction enzyme analysis, 500ng - 2µg DNA was added to the appropriate supplied enzyme buffer with 2-10 units of enzyme for 1 hour at the appropriate temperature.

2.2.6 Phosphatase Treatment

When vector fragments had compatible restriction enzyme overhangs the 5'-phosphate groups were removed by treatment with calf intestinal alkaline phosphatase to prevent self-ligation. Typically, 1 unit of enzyme was added per 100pmoles of DNA and incubated in the recommended buffer at 37°C for 15mins.

2.2.7 Ligation of DNA fragments

Ligations were carried out using the Roche (Germany) DNA Rapid Ligation Kit® according to the manufacturer's instructions.

2.2.8 Transformation of *E.coli*

A small aliquot (2-5µl) of the ligation mixture was transformed into XL-1 Blue sub-cloning grade competent cells (Stratagene, CA) according to the manufacturer's instructions, then plated onto L-broth agar plates containing the appropriate antibiotic selection and propagated over-night in a 37°C incubator.

2.2.9 Transformed *E.coli* / Construct DNA Analysis by PCR

The length of DNA inserts within vectors was estimated by agarose gel electrophoresis following PCR. Appropriate oligonucleotides designed to hybridise in the area flanking the DNA insert were used. A small sample of each colony was inoculated into a PCR reaction mix (0.25mM dNTP (dATP, dCTP, dGTP, dTTP), 50mM KCl, 10mM Tris-HCl pH8.3, 1.5mM $MgCl_2$, 0.01%(v/v) gelatin, 2-20pmol oligo primers, and 1unit of AmpliTaq® DNA polymerase) and the reaction was amplified for 30 cycles of 94°C, 1minute; 55°C, 1minute; 72°C, 1-3 minutes; followed by a 15 minute cycle at 72°C, in a T3 thermocycler (Biometra). Samples were then analysed by agarose gel electrophoresis.

2.2.10 Plasmid DNA preparation from transformed *E.coli*

Single colonies were picked and grown overnight in the appropriate volume of L-broth containing antibiotic selection. For small scale plasmid DNA preparation, QIAprep® spin miniprep kits (QIAGEN Ltd., UK) were used and for large scale QIAfilter plasmid maxi kits (QIAGEN Ltd., UK) were used, both according to manufacturer's instructions.

2.2.11 Optical Density quantitation of DNA

The concentration of DNA was determined using a Beckmann DU-8 spectrophotometer at 260nm, assuming an OD of 1.0 represents a concentration of 50μg/ml of DS DNA for a 1cm path length.

2.2.12 Automated DNA Sequencing

Plasmid DNA was sequenced with the appropriate primers as described in Section 2.1.7 using the Applied Biosystem 373A XL automated sequencer according to the to manufacturer's instructions. Data was analysed by ABI PRISM^{TM} autoassembler software (Perkin Elmer).

2.3 Cell Culture Methods

2.3.1 Mammalian Cell lines

Mammalian cell lines were cultured in either RPMI 1640 or DMEM each supplemented with 10% (v/v) FCS, 2mM glutamine and 50μg/ml penicillin and 50μg/ml streptomycin. For growth of CHO cells 1%(v/v) NEAA was also added. Transfected K562 cells were maintained in media (DMEM) supplemented as above and with 1mg/ml G418. The JB2.7$_{WT}$ and JB2.7$_{\Delta IDomain}$ cells (received from N. Hogg) were maintained in 250μg/ml Zeocin (Invitrogen).

Suspension cells were passaged by diluting 1:10 into fresh growth media (as above). Adherent cells were treated with trypsin/EDTA before passage.

For long term storage, cells in FCS containing 10% (v/v) DMSO were stored in liquid nitrogen. Cells were counted using a Neubauer haemocytometer.

2.3.2 Transient Expression in CHO cells

To test for the integrity and expression of the mutated αL genes, the αL containing vectors were transiently co-transfected with the β2 vector into CHO–761H cells using GenePorter 2000^{TM} according to manufacturer's instructions. For soluble receptors, the supernatants were harvested after 5 days and assayed for the presence of the construct by ELISA. In the case of surface-

expressed receptors, cells were harvested after 2 days and analysed on a fluorescent activated cell sorter (FACScan, Becton Dickinson)

2.3.3 Stable Expression of LFA-1mFc in CHO cells

The generation of stable cells lines expressing the various LFA-1-mFc mutants was performed as above for transient expression using GenePorter 2000™ with the exception, that after 24hrs, the media was replaced with GS selective media, SGMEM + 25μM MSX, and was subsequently replaced every 4-5 days until single colonies of viable cells were visible. These single colonies were then transferred into individual wells using small squares of trypsin-soaked sterilized blotting paper. The most productive clones were identified using mFc assays and assembly ELISAs.

2.3.4 Stable Transfection of K562 Cells

To generate stable K562 cell lines expressing the full-length LFA-1 genes, cells were transfected by electroporation. Using a Bio-Rad gene pulsar unit, $1x10^7$ cells were transfected with 40μg of linearised DGV plasmid DNA and subjected to 1 pulse at 450volts and 960μF. Transfectants were then selected by addition of 1mg/ml G418 (Sigma).

2.3.5 Transfection of JB2.7 Cells

Stable JB2.7 cell lines were generated by electroporation as described by Weber *et al.* (1997). $1x10^7$ cells were transfected with 25μg of linearised plasmid DNA and subjected to 1 pulse at 240volts and 960μF. Transfectants were then selected by addition of 1mg/ml G418.

2.3.6 FACs Analysis

For FACs analysis, 2-5x10^5 cells were incubated with 100µl of FACs buffer containing 20µg/ml of the appropriate labelled antibody at 4°C for 1 hour. Cells were washed twice with FACS buffer and if the labelling antibody was unconjugated, subjected to a further incubation with a second, conjugated antibody for 30 mins, and washed again. Cells were resuspended in 500µl FACS buffer and analysed using a FACScalibur flow cytometer (BD Biosciences). Data was acquired and analysed with CellQuest software (BD Biosciences).

2.4 Soluble Protein Assays

2.4.1 Mouse IgG ELISA

The concentration of LFA-1-mFc fusion proteins in culture supernatants was measured as follows: - Nunc™ 96 well plates were coated with 100µl of 5µg/ml of goat anti-mouse IgG Fc antibody in PBS overnight at 4°C (or 3hrs at room temperature). After washing twice with TBS pH 7.4 using a Wellman Plate washer, plates were blocked with 200µl/well 2% (w/v) BSA, 1% (v/v) Tween20 in TBS for 1 hour at room temperature. Plates were washed again, then purified Max68P (used as standard) at a starting concentration of 100ng/ml, along with sample supernatants, were titrated across the plate in diluent buffer (0.2% (w/v) BSA, 0.1% (v/v) Tween20 in 20mM TBS, pH 7.4) with doubling dilutions. Following 1 hour incubation at room temperature the plates were washed again and 100µl/well anti mFc–HRP 1:10000 dilution in diluent buffer was added across the plate and incubated for 1 hour at room temperature. Following a final wash step, the extent of binding was revealed with addition of 100µl/well TMB and plates read at 630nm with final concentrations calculated using Genesis V3.05 software (Labsystems).

2.4.2 Heterodimer Assembly Assay

To estimate the concentration of correctly assembled αL and β2 heterodimer in culture supernatant and to be able to compare all the mutant forms of LFA-1, a series of assembly ELISAs were developed: the heterodimer was captured by an antibody to one subunit and revealed by another mAb specific for the other subunit or by an antibody that recognises a combinatorial epitope.

Nunc™ 96 well plates were coated with 100µl of 5µg/ml solutions of one of the following mAbs: Ab38, 6.5E, KIM185 or MEM83 in PBS overnight at 4°C. After washing twice with TBS pH 7.4 using a Wellman Plate washer, plates were blocked with 200µl/well 2% (w/v) BSA, 1% (v/v) Tween20 in TBS for 1 hour at room temperature. Plates were washed again and the sample supernatant was titrated down the plate in diluent buffer (0.2% (w/v) BSA, 0.1% (v/v) Tween20 in TBS, pH 7.4) with doubling dilutions. Following a 1 hour incubation at room temperature the plates were washed again and 100µl/well of one of the following biotinylated mAbs at 10µg/ml: 6.5E, KIM185, DA36, in diluent buffer was added across plate. After incubation for 1 hour at room temperature plates were washed and 100µl/well of 1:1500 dilution of streptavidin-peroxidase in diluent buffer was added across the plate and incubated for 30 mins at room temperature. Following a final wash step, the extent of binding was revealed with addition of 100µl/well of TMB and plates read at 630nm.

2.4.3 Ligand- hFc Binding Assays

Nunc™ 96 well plates were coated with 100µl goat anti-mouse IgG Fc antibody at 5µg/ml in PBS overnight at 4°C. After washing twice with TBS pH 7.4 using a Wellman Plate washer, plates were blocked with 200µl/well 2% (w/v) BSA, 1% (v/v) Tween20 in TBS for 1 hour at room temperature. Plates were washed again and the integrin sample supernatants (containing the mFc fusion protein) were titrated down the plate in diluent buffer (0.2% (w/v) BSA, 0.1% (v/v) Tween20 in TBS, pH

7.4, 1mM Mn^{2+}) with doubling dilutions. Following a 1 hour incubation at room temperature the plates were washed again and 100µl/well 200–1000µg/ml sICAM-1, -2, -3hFc diluted in diluent buffer was added across the plate and incubated for 3 hours at room temperature. After washing, 100µl/well anti-hFc–HRP 1:5000 dilution in diluent buffer was added across the plate and incubated for 1 hour at room temperature. Following a final wash step the extent of binding was revealed with addition of 100µl/well of TMB and plates read at 630nm.

2.4.4 Cation Titration Assays

Nunc™ 96 well plates were coated with 100µl of goat anti-mouse IgG Fc antibody at 5µg/ml in PBS overnight at 4°C. After washing twice with TBS pH 7.4 using a Wellman Plate washer, plates were blocked with 200µl/well 2% (w/v) BSA, 1% (v/v) Tween20 in TBS for 1 hr at room temperature. 100µl of LFA-1mFc supernatants was added per well and incubated for 2 hours at room temperature. Plates were washed three times in TBS, 20mM EDTA Buffer followed by three washes in TBS Buffer. 50µl of 2x cation solution were titrated down the plate with tripling dilutions and 50µl of ICAM-1hFc at 0.5µg/ml was added across the plate. After incubation for 3 hours wells were manually washed twice in the corresponding cation concentration buffer and 100µl/well anti hFc–HRP 1:5000 dilution in the corresponding cation concentration buffer was added across plate and incubated for 1 hour at room temperature. Following a final wash step with cation buffer the extent of binding was revealed with addition of 100µl/well of TMB and plates read at 630nm.

2.5 Cell Binding Assays

2.5.1 Rose Bengal ICAM binding Assays

Nunc™ 96 well plates were coated with 100µl of goat anti human IgG Fc antibody (Jackson) at 5µg/ml in PBS overnight at 4°C. After washing twice with TBS using a Wellman Plate washer, plates were blocked with 200µl/well 2% (w/v) BSA, 1% (v/v) Tween20 in TBS for 1 hour at room temperature. 100µl ICAM-1, -2, –3 or VCAM-1hFc diluted in diluent buffer (0.2% (w/v) BSA, 0.1% (v/v) Tween20 in 20mM TBS, pH 7.4) was added across the plate and incubated for 2hours at room temperature. Plates were washed three times in TBS before addition of 100µl 5x 10^4 cells / well in warm cell culture media (DMEM with glutamine). MAbs (final concentration 20µg/ml), PMA (final concentration 100 ng/ml), cytochalasin D (final concentration 5µg/ml) were added to cells to stimulate / inhibit cell adhesion. After incubation at 37°C for 45mins plates were washed with media (DMEM with glutamine) using a multi-channel pipette. 100µl 100% methanol was then added to each well and incubated at room temperature for 10mins followed by a gentle PBS wash. 100µl 0.25% (w/v) Rose Bengal (Sigma R4507) in PBS was then added and plates incubated for 5 mins at room temperature. Following intensive gentle washing in PBS to remove all excess stain, 100µl 1:1 PBS: ethanol solution was added and plates were placed in a shaking incubator undercover for 1 hour. Plates were then read at 570nm.

2.5.2 Rose Bengal Fibronectin Assays

Fibronectin binding assays were carried out as described above in Section 1.5.1 with one exception. Plates were coated directly with 500ng/ml Fibronectin (SIGMA F0895) diluted in PBS and incubated overnight at 4°C before being blocked as above.

2.6 Immunoprecipitation and Western Blotting of mFc-tagged proteins

Western blotting was carried out to confirm the expression of recombinant LFA-1mFc proteins and to ascertain whether the α and β chains were in heterodimeric or homodimeric forms. LFA-1mFc supernatant volumes equivalent to 75ng and 50ng protein (determined by mFc ELISA) for non-reduced and reduced samples, respectively, were incubated with 50µl protein Sepharose A beads in 50mM Tris-HCl, 4M NaCl pH 8 overnight at 4°C. Beads were washed four times in 50mM Tris-HCl, 1%(v/v) NP-40, pH 8, followed by two washes in TBS pH 7.4 and finally suspended in 30µl of TBS containing reduced / non-reduced sample buffer. Samples were heated to 70°C for 5mins and the total sample was loaded onto Novex Tris/Glycine Gels and run at 100mA for the required time for separation. Proteins were transferred to a nitrocellulose membrane for 3 hours using a Novex Mini Cell System in a Tris/Glycine Running Buffer. Following blocking with 5% (w/v) non-fat milk powder in TBS/0.1% NP40 for 1 hour, the membrane was incubated with HRP - labelled-goat anti-mouse IgG Fc antibody at 1:2000 dilution in TBS /0.1% (v/v) NP40 for 1 hour. After extensive washing with TBS/0.1% (v/v) NP40 the bound antibody was detected by non-isotopic enhanced chemiluminescence assay (ECL Kit, Amersham, UK).

2.7 Statistical Analysis of Results

Where appropriate, statistical analysis of data was performed using Graphpad-Prism Version 3 (Graphpad Software, San Diego, CA). To determine if parametric or non-parametric analysis of data was required, Bartletts test of homogeneity of variance was performed. According to this result, either parametric analysis of variance (ANOVA) or non-parametric Kuskal-Wallis ANOVA was performed. For sample comparisons, data was analysed using a two-tailed student's T-test to which a P value of $=< 0.05$ was assigned as significant.

Chapter 3

Mutation Selection, Vector Design and Molecular Cloning

Chapter 3 Mutation Selection, Vector Design and Molecular Cloning

3.1 Introduction

At the time the work described in this thesis was started, two different conformations of the αM and α2 I domains ('open' and 'closed') had been observed in X-ray crystal structures (See Section 1.4). The 'open' conformation involved a change in metal ion coordination and a shift in the position of the C-terminal α-helix that exposed several buried hydrophobic residues (See Figure 1.8). Several X-ray studies of the αL I domain, with and without Mn^{2+} or Mg^{2+}, had also been undertaken but no structural changes in the MIDAS or conformational changes of the buried hydrophobic residues were observed, although a shift in the position of the α7 helix was apparent (Qu and Leahy 1995; 1996). Kallen *et al.* (1999) had also shown that Lovastatin, a small molecular inhibitor of LFA-1, binds in a cleft adjacent to the α7 helix, which became known as the IDAS site. Moreover, since the binding of Lovastatin had no effect on the structural arrangement of the MIDAS site, the authors suggested that inhibition of ICAM-1 binding was through an indirect mechanism. Huth *et al.* (2000) went onto characterise the effects of a series of mutations within the IDAS and identified several residues that were important for ligand binding. Therefore, this data, combined with the I domain X-ray results, suggest that a conformational change in a region distal to the MIDAS is involved in regulating ligand binding. Further investigation of the IDAS site was warranted to determine what influence the position and charge of a selection of residues along the α7 helix had both on conformational change within the IDAS as well as on the activation state of LFA-1. We postulated that it was also possible that a constitutively active form of LFA-1 could be generated by mutations within the IDAS and that this mutated form of LFA-1 would be a useful tool to characterise the interaction of LFA-1 with its ligands.

Also at this time, Stephens *et al.* (2000) expressed the integrin VLA-4 as a soluble, active, heterodimeric immunoglobulin fusion protein. Using a novel approach, the cDNAs encoding the extracellular domains of the integrin α4 and β1 subunits were fused with the human γ1 immunoglobulin Fc domain. Stable heterodimerisation of the α and β chains was brought about by the dimerisation of the CH3 domains and maintained by the formation of disulphide bridges in the hinge region between the CH1 and CH2 domains of the Ig. In addition, the introduction of specific mutations in the Fc region of the molecules helped to induce heterodimeric formation and reduce β–β homodimeric formation. Comparison of this soluble form of VLA-4 with native cell derived VLA-4 showed that the apparent K_D for VCAM-1 binding was similar for both forms of the integrin.

Using this method, it was proposed that it was feasible to generate a soluble form of LFA-1, as previous efforts within this laboratory to generate soluble forms of LFA-1 without some form of tail were unsuccessful (S. Ortlepp personal communication). A soluble form of LFA-1 would allow the study of the function of this integrin in a cell-free system, independent of influences such as signal transduction and clustering. Additionally, we wanted to investigate the possibility of generating a constitutively active form of the integrin by incorporating a series of mutations in and around the IDAS of the LFA-1 I domain. Mutations that conferred an increase in ligand binding in the soluble system would then be introduced into LFA-1 expressed on the cell surface to determine if altering the structure of the α7 helix contained within the IDAS had effects on ligand binding in the presence of cytoplasmic restraints.

3.2 Mutation Selection

Following analysis of the 3D structure of the αL I-domain and information from the literature, the residues listed below were identified as candidates for mutation. Some of the residues chosen were based on mutational analysis of the αL I domain described in the literature, where an increase in activation was observed compared with wild type, when the I domain was expressed in the context of the whole integrin on the cell surface or as an isolated domain. Such mutations were selected to act both as controls to validate the expression systems to be used in this study and as comparisons for the other selected mutations. The other residues selected for mutational analysis were identified based on sequence analysis of other β2 integrin α-subunits and on analysis of the amino acid composition of the α7 helix. Figure 3.1 highlights the positions of the amino acids chosen for mutational analysis within the I domain 3D structure.

I235A: The 235 isoleucine residue is located at the centre of the IDAS cleft on the β1 strand in the I domain and was previously shown by Huth *et al.* (2000) to increase the binding of CHO-expressed LFA-1 to ICAM-1 when the residue was mutated to alanine. Huth *et al.* suggested that replacement of the large hydrophobic isoleucine residue created a cavity in the protein that lowered the energy barrier for conformational change in the I domain. The increased activity seen with the I235A mutation was greater than that seen for the Gly-Ala mutation in the GFFKR motif located in the αL cytoplasmic domain, which when expressed in CHO cells had been shown to also yield a constitutively active LFA-1 phenotype (Lu and Springer, 1997). Interestingly, when the I235A mutation was expressed in a lymphocyte-like cell line (JB2.7), the constitutive activity of the I235A mutant was lost, although increased binding to ICAM-1 was shown at low PMA concentrations relative to wild type (Huth *et al.*, 2000). This result suggested that the cytoplasmic domain also plays a role in the activation state of the integrin.

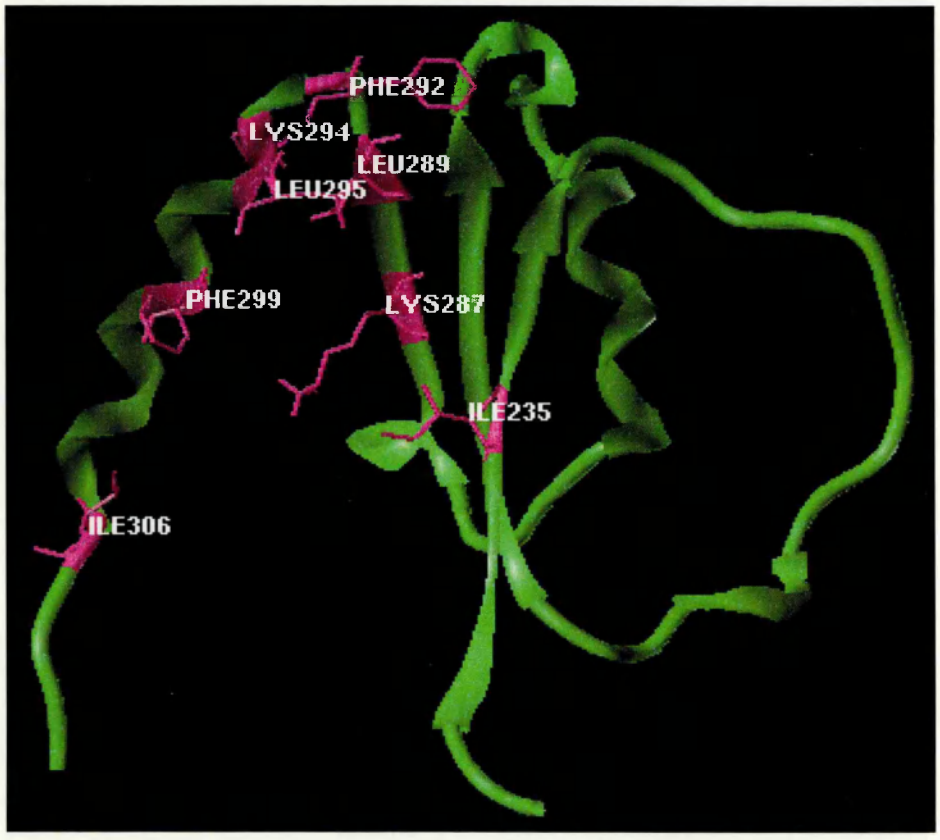

Figure 3.1 **3D-view of sites chosen for mutational analysis within the IDAS site of the αL I domain.** Four of the residues I306, F299, L295 and K294 are located along the length of the α7 helix; F292 is located on the turn between the α7 helix and the β6 strand with L289 and K287 located on the β6- strand. I235 also within the IDAS pocket is located on the β-1 strand. This image was created using the SYBYL6.9 graphics package (Tripos Inc) with kind help from D.Athwal (Celltech).

K287F: Sequence comparison of all the β2 integrins showed that position 287 in all the α-chains contains a conserved phenylalanine except for αL, which contains a lysine residue. Substituting this lysine residue in αL to phenylalanine would introduce a bulky hydrophobic group into the IDAS pocket, which we predicted would induce interactions with side chains of other residues to stabilise the 'closed' form of the I domain by increasing the energy barrier for conformational change. This novel change would, therefore, behave in the opposite manner to the alanine substitution at residue I235. Since LFA-1 has a much higher affinity for each member of the ICAM family compared to other members of the β2 family, substitution of a phenylalanine residue for a lysine residue at this position might also highlight the influence this residue has on the affinity of LFA-1 for its ligands.

F292A: F292 is a large hydrophobic residue situated at the top of the β6-α7 helix loop and is analogous to residue F302 in the αM I domain. Previously, Li *et al.* (1998) expressed an isolated αM I domain containing a F302→W mutation which was shown to increase ligand binding over the wild type version. A similar study of the same mutation by Shimaoka *et al.* (2000) also demonstrated a slight increase in binding of αMβ2 to i3Cb compared to wild type binding. However, two crystallographic studies of αM containing this mutation conducted by the same group (Li *et al.*, 1998; Xhiong *et al.*, 2000) gave conflicting results concerning whether or not this residue was important in converting the I domain from the 'closed' to 'open' conformation. In the first, F302→W was buried in the 'closed' conformation and exposed in the 'open' conformation. In the second study, however, the F302→W mutant crystallised in the 'closed' conformation in the presence and absence of cation and W302 was shown to be buried in both cases. Mutational analysis by Huth *et al.* (2000) and other work by Li *et al.* (1998) have suggested that hydrophilic residues in this area should favour the 'open' conformation. Therefore, in this study F292 was mutated to alanine rather than tryptophan as in the previous

studies. This would allow one to determine if a hydrophilic residue at this position (that is also much smaller in size than a phenylalanine residue) would favour the 'open' ligand binding conformation.

L295A: Like F292, L295 is located at the top of the β6-α7 helix loop and hence could also be involved in conformational changes that take place subsequent to integrin activation. The leucine at this position is hydrophobic and may form polar interactions with surrounding residues, which could stabilise the I domain in either an 'open' or 'closed' conformation. We predicted that substituting this residue to alanine would remove such interactions allowing more flexibility and movement of the helix. It was therefore of interest to establish whether this novel substitution would stabilise either the 'open' or 'closed' conformation, leading to an increase or decrease in ligand binding.

F299A: A further novel substitution was introduced at position F299. This phenylalanine residue is approximately one-third of the way down the α7 helix and its bulky hydrophobic nature suggests that it is involved in interactions with the side chains of other residues, possibly favouring the 'closed' conformation. Substitution of this residue to alanine could alter these side chain interactions and may favour the 'open' conformation as suggested by Huth *et al.* (2000) and Li *et al.* (1998) based on the data where a hydrophobic residue was replaced with a hydrophilic residue.

I306A: I306 is located at the tail of the C-terminal α-helix of αL. It corresponds to I316 in the αM I domain, which has been shown to stabilise the 'closed' conformation of αM by fitting into a hydrophobic pocket between the C-terminal α-helix and the opposing β-sheet of the IDAS site (Xiong *et al.*, 2000). Consistent with these observations, substitution of αL I306 with alanine was shown to increase the adhesion of CHO cells to ICAM-1 relative to wild type. Interestingly, however, the level of binding was not increased to the same extent as the I235 mutation which was also analysed in the same study (Huth *et al.*, 2000). Since this mutation was previously shown to activate LFA-1, inclusion of the same substitution in this study would serve as a control in the soluble Fc system.

L295A + I306A

These residues are at opposite ends of the α7 helix and, whilst it was unknown how the 295 substitution would behave, we predicted that substituting this residue to alanine would allow more flexibility and movement of the helix. As an alanine substitution at residue I306 has previously been shown to increase the activity of LFA-1, pairing it with A295 may increase the overall flexibility of the α-helix, further enhancing the activation state of the integrin.

F292A + L295A + I306A

As with the double mutation described above, it was of interest to see if removal of a second large hydrophobic group on the α7 helix had an additive effect on the activation state of LFA-1 by further lowering the energy barrier required to shift the α7 helix from the 'closed' to the 'open' form. Alternatively, it was possible that substitution of both the 292 and 295 residues to alanine would remove important structural elements within the I domain required for ligand binding.

Other Mutations

Subsequent to identifying the above residues as potential sites for mutational analysis, Shimaoka *et al.* (2001) recently showed that by introducing disulphide bonds at several positions within the IDAS, bracketing the loop between the C-terminal α-helix and the preceding β-strands, an αL I domain in both the 'open' and 'closed' forms could be generated. Introduction of disulphide bonds within the IDAS appeared to lock the αL I domain into conformations similar to that seen in the αM 'open' and 'closed' crystal structures (See Figure 3.2). Mutation of K287 on the β6 strand to a cysteine residue and K294 on the α7 helix also to a cysteine allowed for the formation of a disulphide bridge between β6 and α7. This locked the I domain in an 'open' conformation, as evidenced by high affinity binding to ICAM-1 when expressed as an isolated I domain. By comparison, a disulphide bridge introduced by mutating both L289 and K294 to cysteine residues appeared to present the I domain in a locked 'closed'' conformation. This construct was shown to behave in a similar manner to wild type I domain in ICAM-1-binding experiments.

Taking into account Shimaoka findings, both of these pairs of mutations and mutations that contained single K294→C and K287→C substitutions were also incorporated into this study. We also included a double alanine substitution of residues K287 and K294, to confirm that the presence of cysteine bonds rather than the mutations themselves were responsible for the increased activity. We were interested to know if soluble-expressed integrin containing these mutations behaved in a similar manner to the isolated I domains used in the Shimaoka study (2001), and if this locked 'open' conformation was capable of overriding all other restraints imposed by the other domains of the integrin when expressed on the cell surface. These mutations would also act as controls with which to compare other introduced mutations not previously investigated.

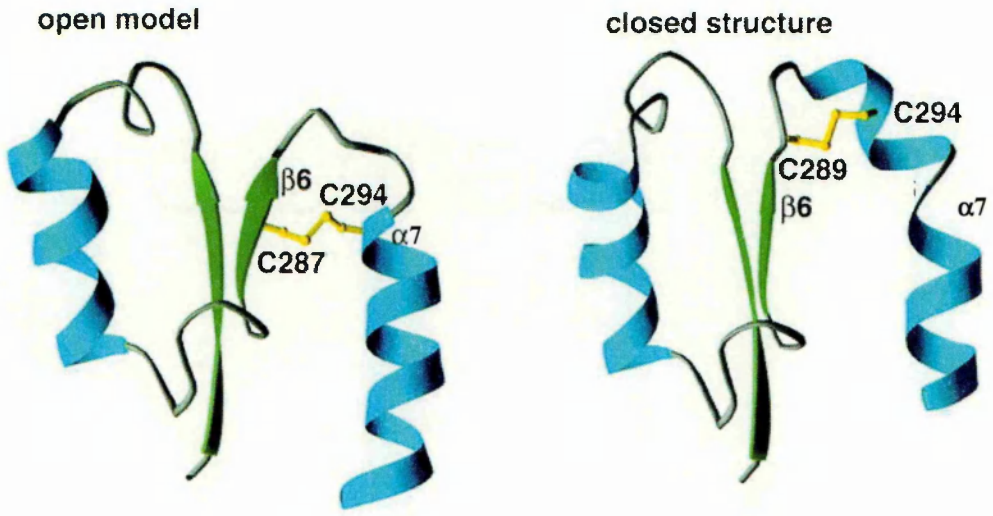

Figure 3.2 **Locked 'open' and 'closed' forms of the αL I domain.** The above illustration taken from Shimaoka *et al.* (2001) depicts the conformational changes that are thought to take place within the I domain on activation of the integrin. These were mimicked by Shimaoka *et al.* by the introduction of cysteine mutations at residues K287/L289 which when paired with a cysteine substitution of residue K294 locks the I domain in an 'open' or 'closed' form.

3.3 Generation Of Soluble mFc Constructs

For the generation of soluble integrin murine Fc constructs, two vectors had previously been designed based on the pEE12.2 and pV16 vectors. Both the pEE12.2mFc and pV16mFc vectors contain a murine γ1 Fc domain cloned in as a *Sal* I-*Eco* RI cDNA fragment encoding 9 residues of the upper hinge, the entire hinge and the constant CH2 and CH3 domain regions (Stephens *et al.*, 2000) (Figure 3.3). To increase the likelihood of stable heterodimerisation of the α and β chains, specific mutations were introduced into the CH3 domains of the murine Fc by oligonucleotide directed PCR mutagenesis creating a 'knob' and 'hole' as described by Ridgeway *et al.* (1996).

A nucleotide change was introduced into the vector which resulted in an amino acid substitution of T→Y (knob) at position 366 in the mFc region of the pEE12.2 vector designed to contain the β integrin subunit and a T→Y substitution (hole) at position 407 in the mFc region of the pV16 vector designed to contain the α integrin subunit. The 'knob' mutation in the mFc tail of the β subunit would help prevent homodimerisation by causing a misalignment of the two CH3 domains whilst the 'neat fit' between the 'knob' and 'hole' would encourage heterodimer formation.

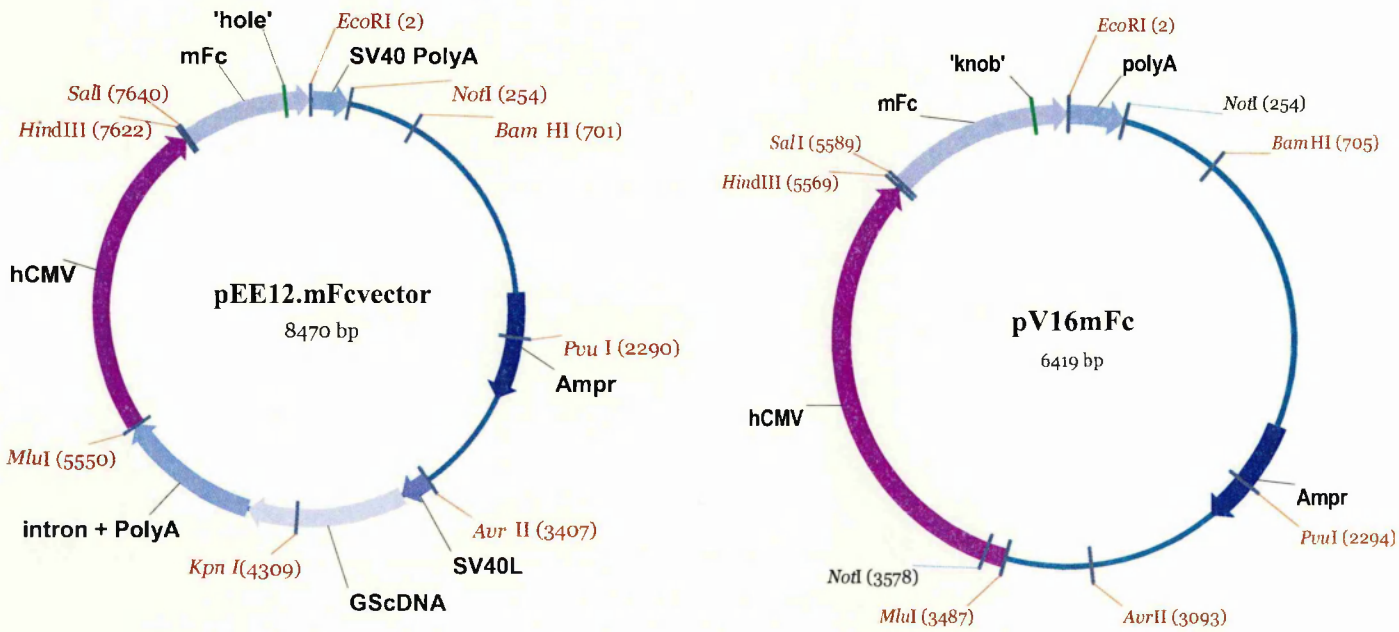

Figure 3.3 **Vector maps of pV16mFc and pEE12.2mFc.** pV16mFc contains the murine γ1 Fc cDNA, an ampicillin resistance marker for selection in a bacterial host (Amp^r), and a transcription unit for the expression of foreign genes. The transcription unit consists of a human cytomegalovirus (hCMV) major immediate early promoter, a polylinker (*Hind* III-*Eco*R I) into which the sequence for the mFc region was later inserted, and the SV40 polyadenylation signals. pEE12.2mFc contains the murine γ1 Fc cDNA, an ampicillin resistance marker for selection in a bacterial host (Amp^r), an SV40 origin for replication in eukaryotic cells, an SV40 late promoter (SV40L) to drive the GS cDNA, the GS cDNA for selection and amplification in mammalian cells and a transcription unit for the expression of foreign genes. The transcription unit consists of an hCMV major intermediate early promoter, a polylinker (*Hind* III-*Eco*R I) into which the sequence for the mFc has been inserted and the SV40 polyadenylation signals.

3.3.1. Cloning and Assembly of the Extracellular Domain of β2 into an Expression Plasmid

In order help with describing the manipulations of the CD18 cDNA its sequence and oligos used to generate the various constructs are shown in Appendix 1. Full length CD18 (2100bps) had previously been cloned into the pEE6hCMV *neo* vector by S.Ortlepp (1997) as a *Hin*d III-*Bcl* I fragment. In order to generate a soluble form of this integrin subunit, the 5' region of CD18 was excised as a *Hin*d III-*Sfu* I fragment (1900bps). The remainder of the extracellular portion of the CD18 sequence was generated by PCR using primers B3611, which incorporated a *Sal* I site at the 3' end of CD18 directly after the end of the extracellular domain sequence, and B3610 which covered the region incorporating the *Sfu* I site. The junction of the extracellular domain and transmembrane domain was predicted based on hydrophobicity plots using Mac Vector (See Figure 3.4). Following digestion with the appropriate restriction enzymes, the *Hin*d III-*Sfu* I (1900bps) and *Sfu* I- *Sal* I (200bps) fragments were subcloned into the *Hin*d III - *Sal* I backbone region of the pV16 vector (Figure 3.6) to generate the V16$\beta 2_{sol}$mFc vector. A PCR screen using primers B3610 and V9011 (reverse primer to the mCH1 region with in the vector backbone) verified the ligation of all three fragments. Further DNA sequencing of both strands in this region revealed that the sequence was the same as that published by Arnaout *et al.* (1988) and S.Ortlepp (1997).

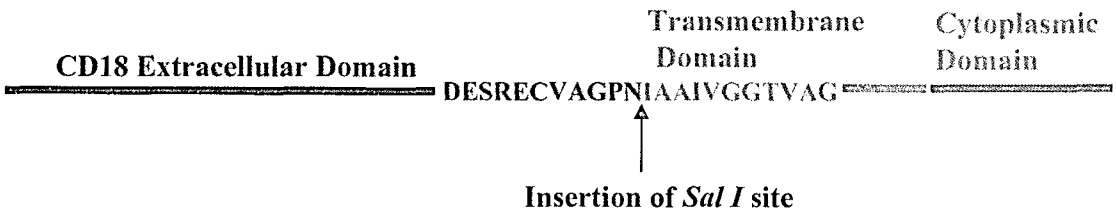

Figure 3.4 Predicted CD18 extracellular – Transmembrane Interface.

3.3.2. Cloning and Assembly of the Extracellular Domain of CD11a into an Expression Plasmid

In order help with describing the manipulations of the CD11a gene its sequence and oligos used to generate the various constructs are shown in Appendix 2. Full length CD11a (3600bps) had also previously been cloned into the pEE12.2 vector (pEE12.2CD11a$_{FL}$) in this laboratory as a *Hind* III-*Bcl* I fragment. In order to generate a soluble form of the subunit, the 5' region of CD11a was excised as a *Hind* III-*Bam*H I fragment (2870bps). The remainder of the extracellular portion of the sequence was generated by PCR using primers B3609, which incorporated a *Sal* I site at the 3' end of CD11a directly after the end of the extracellular domain sequence, and B3606 which covered the region encoding the *Bam*H I site. The junction of the extracellular domain and transmembrane domain was predicted based on hydrophobicity plots using Mac Vector (See Figure 3.5). Following digestion with the appropriate restriction enzymes the *Hind* III-*Bam*H I (2870bps) and *Bam*H I- *Sal* I (400bps) fragments were subcloned into the *Hind* III - *Sal* I backbone region of the pEE12.2 vector to generate the new vector (pEE12.2αL_{sol}mFc) (Figure 3.7). A PCR screen using primers B3606 and V9011 verified the ligation of all three fragments. Further DNA sequencing (Primers listed in Chapter 2 Section 1.1.7) of both strands in this region revealed that the sequence was the same as that published by Larson *et al.* (1989).

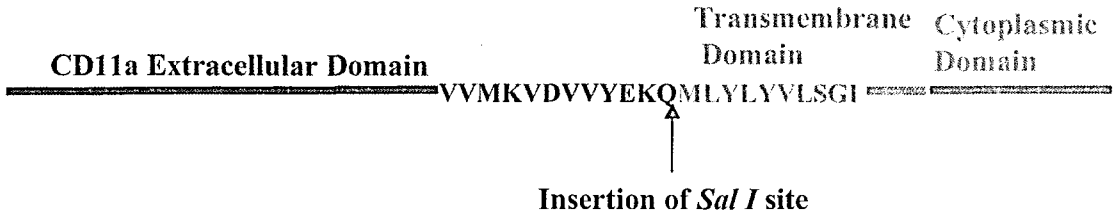

Figure 4.5 Predicted CD11a Extracellular – Transmembrane Interface

3.3.3. Leader Sequence Substitution

Because of low expression levels of soluble LFA-1 after coexpression of the β2 and αL vectors in CHO cells the original leader sequences were substituted with murine antibody light chain (αL) and heavy chain (β2) leader sequences, which had previously been shown in this laboratory to greatly increase integrin expression levels in CHO cells.

1.3.3.1 pEE12.2αL$_{sol}$mFc Vector with Ab Leader Sequence

A PCR fragment that incorporated the 5'*Hin*d III site at the start of the αL construct and the murine κ chain leader sequence of the antibody B72.3 (King *et al.,* 1992) was generated by using a 90mer primer (B6114) and a 3' oligo (B6109) which incorporated a *Nar* I site approximately 530bps distal to the *Hin*d III site (See Appendix 2). The original leader sequence from pEE12.2αLsolmFc was excised using *Hin*d III and *Nar* I restriction enzymes and the remaining backbone as *Nar* I-*Not* I and *Not* 1-*Hin*d III fragments were re-ligated with the *Hin*d III–*Nar* I Ab leader PCR fragment to generate the pEE12.2αL$_{ablsol}$mFc vector with the Ab leader sequence (See Figure 3.7).

CD11a Primer 1 ***B6114 (Primer to introduce 5' Antibody Leader Sequence)***

Sequence: 5'GGCC<u>AAGCTT</u>CCGCCACCATGGCTTGGGTGTGGAAC

(*Hind* III; Kozak Sequence; Antibody Leader Sequence)

TTGCTATTCCTGATGGCAGCTGCCCAAAGTGCCCAA

GCATACAACCTGGACGTG

(CD11a Sequence →)

CD11a Primer 2: ***B6109 (560 ←)***

Sequence: 5'CAGGTCTACGTTGCCCTTGATAC

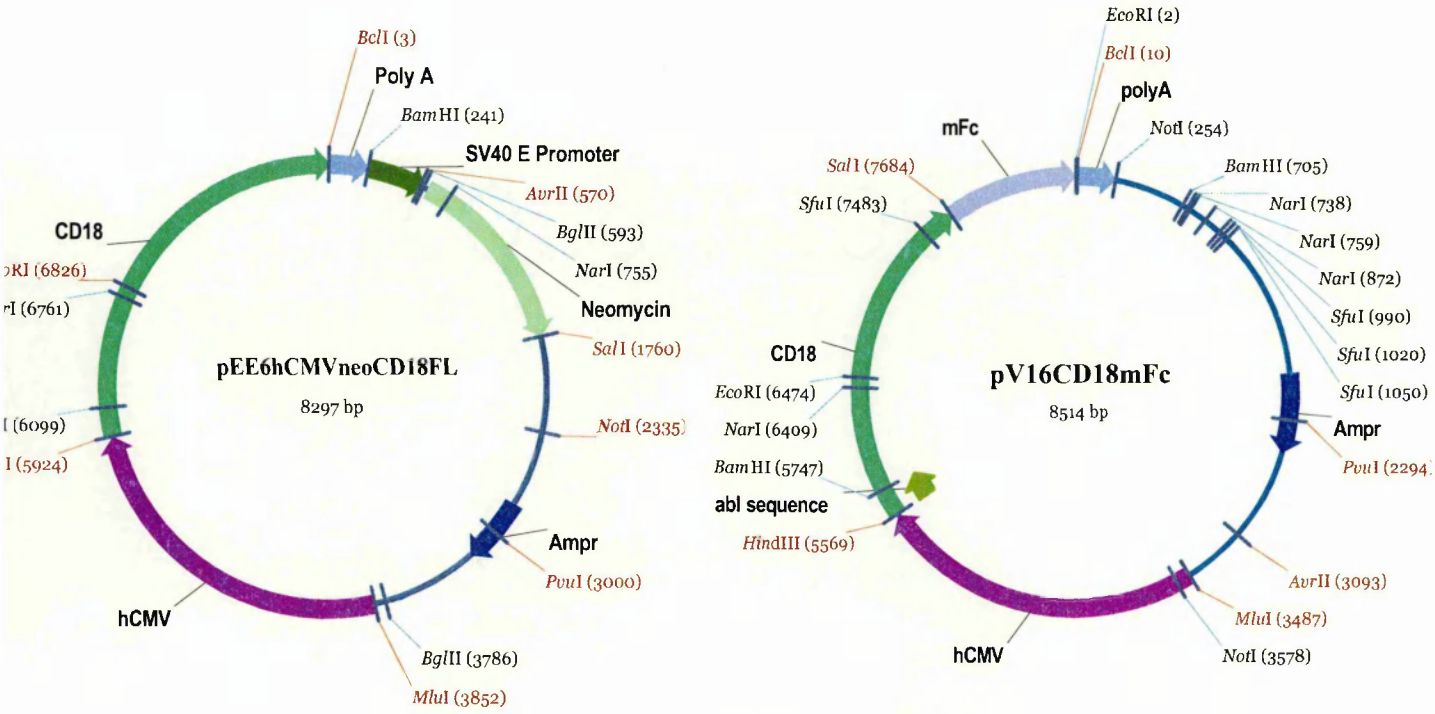

Figure 3.6 **Plasmid Maps of pEE6hCMVneoCD18FL and pV16CD18mFc**
EE6hCMV *neo* contains an ampicillin resistance marker for selection in a bacterial host (Amp^r), a gene encoding neomycin resistance (neo) for selection in mammalian cells and a transcription cassette for foreign gene expression. The transcription unit consists of a human cytomegalovirus (hCMV) major immediate early promoter, a polylinker (*Hind* III-*Bcl* I) into which the sequence for the CD18 full-length gene has been inserted, and the SV40 splice and polyadenylation signals.
The pV16CD18mFc vector backbone is as described above in Figure 3.3 with the cDNA of the extracellular region of CD18 inserted as *Hind* III-*Sfu* I and *Sfu* I-*Sal* I fragments. The antibody leader sequence (abl) was incorporated into the vector as a *Hind* III-*BamH* I PCR fragment at the 5' end of CD18 to generate the pV16CD18ablmFc vector.

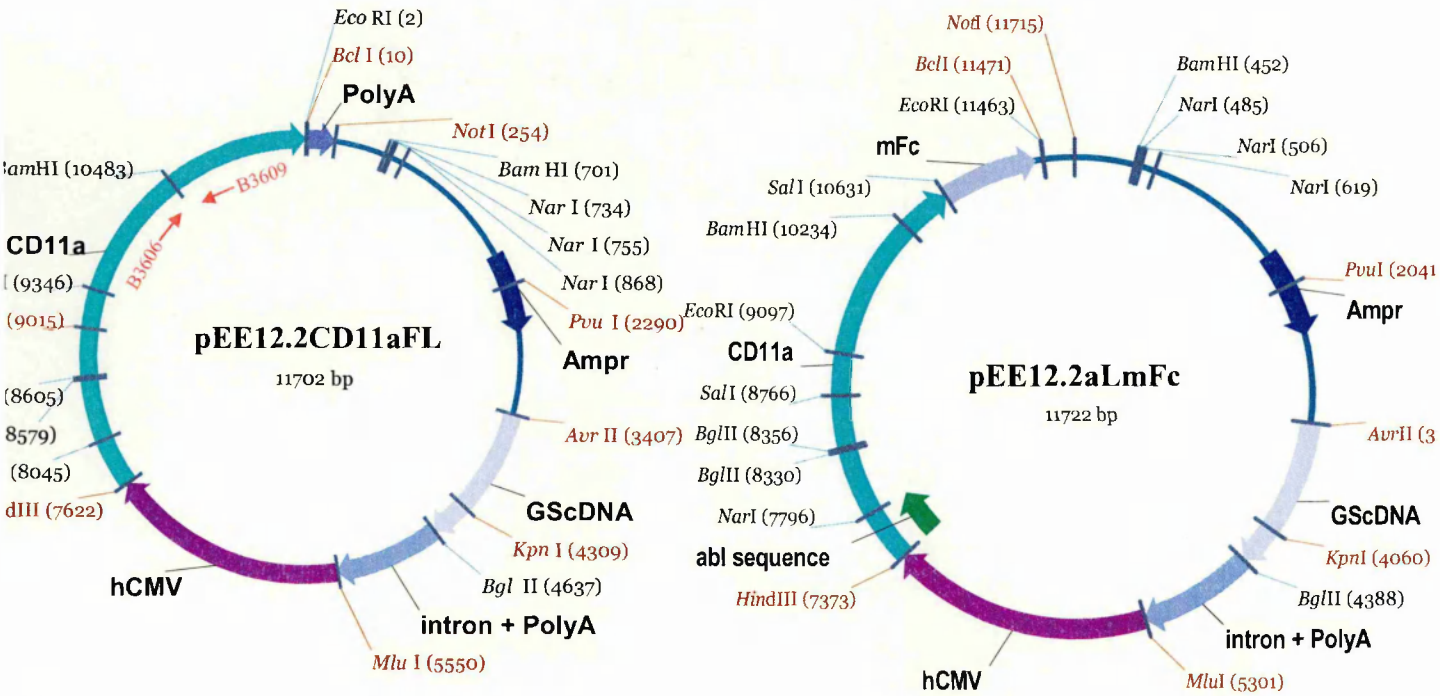

Figure 3.7 **Vector Maps of pEE12.2CD11aFL and pEE12.2αLmFc.** The pEE12.2 CD11aFL vector contains the *CD11a* gene ligated into the pEE12.2 backbone as a *Hind* III – *Bcl* I fragment. For expression of the soluble αL extracellular fragment fused with a mFc tail, the 5' end of the this region was excised as *Hind* III – *Bam*H I fragment and the 3' end incorporating a *Sal* I site was generated by PCR. These two fragments were then ligated into an empty pEE12.2mFc vector cut with *Hind* III and *Sal* I.
The antibody leader sequence (abl) was incorporated into the vector as a *Hind* III-*Not* I PCR fragment at the 5' end of CD11a sequence to generate the pEE12.2αLablmFc vector.

1.3.3.2 pV16β2$_{sol}$mFc Vector with Ab Leader Sequence

A PCR fragment that incorporated the 5'*Hind* III site at the start of the β2 construct and a heavy chain antibody leader sequence also from the antibody B72.3 was generated by using a 108bp primer (B6113) and a 3' oligo (B6110) which incorporated a *Bam*H I site ~200bps distal to the *Hind III* site (See Appendix 1). The original leader sequence from pV16β2$_{sol}$mFc vector was excised using *Hind III* and *Bam*H I restriction enzymes and the remaining backbone as *Bam*H I–*Sal* I and *Sal* I-*Hind* III fragments were religated with the *Hind* III-*Bam*H I Ab leader PCR fragment to generate the pV16β2$_{sol}$mFc vector with the Ab leader sequence (See Figure 3.6).

CD18 Primer 1 ***B6113 (Primer to introduce Antibody Leader Sequence)***

Sequence: 5'GGCCAAGCTTCCGCCACCATGGGCATCAAGATGGAG

(Kozak Sequence; *Hind*III; Antibody Leader Sequence)

TCACAGACCCAGGTCTTTGTATACATGTTGCTGTGGT

TGTCTGGTGTTGATGGACAGGAGTGCACGAAGTTC

(CD18 sequence→)

CD18 Primer 2 ***B6110 (320←)***

Sequence: 5'GTCTTCCTGGGTTTCAGCGAG

3.3.4. Incorporation of IDAS Substitutions into the pEE12.2$_{\alpha Lsol}$ Vector System

The various amino acid substitutions were incorporated into the pEE12.2αL$_{solabl}$mFc vector by site directed mutagenesis using the Stratagene's QuikChange® Mutagenesis Kit. Figure 3.8 illustrates the steps involved in the procedure. The method involves designing two primers both containing the desired mutational change which are complementary to opposite strands of the region of interest within the vector. See below for the list of primers used to incorporate the selected IDAS mutations into the pEE12.2αL$_{solabl}$mFc vector. During temperature cycling, *PfuTurbo* DNA polymerase extended these primers to generate a mutated plasmid containing staggered nicks. Following temperature cycling, the product was treated with *Dpn I.* The *Dpn I*

restriction enzyme (target 5' Gm6ATC-3') is specific for methylated and hemi-methylated DNA and is used to digest the parental DNA template to select for mutation-containing PCR synthesised DNA. The vector DNA containing the desired mutations was then transformed into competent cells in which the nicks were repaired. Plasmid DNA was prepared from the transformants and analysed by DNA sequencing (Chapter 2 Section 2.1.9 for list of primers used) to select clones containing the desired mutation within the αL region. This plasmid was then digested with *Hin*d III and *Bam*H I restriction enzymes to excise the region containing the mutation and religated into an original *Hin*d III-*Bam*H I backbone vector preparation (*Bam*H I-*Eco* RI and *Eco* RI-*Hin*d III fragments) which had not been subjected to the mutagenesis procedure to ensure that random mutations that may have been introduced elsewhere in the vector during the PCR reaction were not carried through. Plasmid preparations of the final construct were also sequenced to confirm the presence of the desired mutation.

I-DOMAIN cloning Oligos

I Domain Primer 1: ***I235A→***
Sequence: 5'ACCAAAGTGCTTGCTATCATCACGGATGGG
Ala

I Domain Primer 2: ***I235A ←***
Sequence: 5'CCCATCCGTGATGATAGCAAGCACTTTGGT
Ala

I Domain Primer 3: ***L287F→***
Sequence: 5'GCGAGCGAGTTTGTGTTTATTCTGGACACA
Phe

I Domain Primer 4: ***L287F ←***
Sequence: 5'TGTGTCCAGAATAAACACAAACTCGCTCGC
Phe

I Domain Primer 5: ***L287C→***
Sequence: 5'GCGAGCGAGTTTGTGTTTATTCTGGACACA
Cys

I Domain Primer 6: ***L287C ←***
Sequence: 5'TGTGTCCAGAATACACACAAACTCGCTCGC
Cys

I Domain Primer 7: ***F292A→***
Sequence: 5'ATTCTGGACACAGCCGAGAAGCTGAAA

Ala

I Domain Primer 8: ***F292A←***
Sequence: 5'TTTCAGCTTCTCGGCTGTGTCCAGAAT
Ala

I Domain Primer 9: ***K294C→***
Sequence: 5'GACACATTTGAGTGTCTGAAAGATCTATTC
Cys

I Domain Primer 10: ***K294C ←***
Sequence: 5'GAATAGATCTTTCAGACACTCAAATGTGTC
Cys

I Domain Primer 11: ***L295A→***
Sequence: 5'ACATTTGAGAAGGCCAAAGATCTATTC
Ala

I Domain Primer 12: ***L295A ←***
Sequence: 5'GAATAGATCTTTGGCCTTCTCAAATGT
Ala

I Domain Primer 13: ***F299A→***
Sequence: 5'CTGAAAGATCTAGCCACTGAGCTGCAG
Ala

I Domain Primer 14: ***F299A ←***
Sequence: 5'CTGCAGCTCAGTGGCTAGATCTTTCAG
Ala

I Domain Primer 15: ***I306A→***
Sequence: 5'CTGCAGAAGAAGGCCTATGTCATTGAG
Ala

I Domain Primer 16: ***I306A ←***
Sequence: 5'CTCAATGACATAGGCCTTCTTCTGCAG
Ala

I Domain Primer 17: ***L295A/ I306A→***
Sequence: 5'ACATTTGAGAAGGCCAAAGATCTATTCACTGAGCTG
Ala

CAGAAGAAGGCCTATGTCATTGAG
Ala

I Domain Primer 18: ***L295A/ I306A←***
Sequence: 5'CTCAATGACATAGGCCTTCTTCTGCAGCTCAGTGAA
Ala

TAGATCTTTGGCCTTCTCAAATGT
Ala

I Domain Primer 19: ***L287A/K294A→***
Sequence: 5'GAGTTTGTGGCTATTCTGGACACATTTGAGGCTCTG
Ala Ala

AAAGAT

I Domain Primer 20: ***L287A/K294A ←***
Sequence: 5'ATCTTTCAGAGCCTCAAATGTGTCCAGAATAGCCAC
Ala Ala

AAACTC

I Domain Primer 21: ***L287C/K294C→***
Sequence: 5'GAGTTTGTGTGTATTCTGGACACATTTGAGTGTCTGA
Cys Cys
AAGAT

I Domain Primer 22: ***L287C/K294C ←***
Sequence: 5'ATCTTTCAGACACTCAAATGTGTCCAGAATACACAC
Cys Cys
AAACTC

I Domain Primer 23: ***L289A/K294A→***
Sequence: 5'TTTGTGAAAATTGCGGACACATTTGAGGCGCTGAAA
Ala Ala
GATCTA

I Domain Primer 24: ***L289A/K294A ←***
Sequence: 5'TAGATCTTTCAGCGCCTCAAATGTGTCCGCAATTTTC
Ala Ala
ACAAA

I Domain Primer 25: ***L289C/K294C→***
Sequence: 5'TTTGTGAAAATTTGTGACACATTTGAGTGTCTGAAAG
Cys Cys
ATCTA

I Domain Primer 26: ***L289C/K294C ←***
Sequence: 5'TAGATCTTTCAGACACTCAAATGTGTCACAAATT
Cys Cys
TTCACAAA

3.3.5. Generation of αLβ2 Double Gene Vectors

The use of DGVs (double gene vectors) containing both integrin subunits had previously been shown to increase expression by up to 3-fold over co-transfection of SGVs (personal communication, P.E. Stephens). A single *Not* I site that had previously been engineered into the pEE12.2 vector allowed for linearisation of this vector and two *Not* I sites engineered into the pV16 vector just before the hCMV region and after the polylinker sequence respectively allowed the entire transcription unit of the β2 gene to be excised as one fragment. Following linearisation and phosphatase treatment of the pEE12.2αL_{ablsol}mFc vector and excision of the

5000bp *Not* I-*Not* I pV16β2$_{ablsol}$mFc fragment, both *Not* I fragments were ligated. Figure 3.9 illustrates the procedure. Following plasmid preparation, diagnostic digestion with a panel of restriction enzymes were carried out to determine that both the αL and β2 genes were present and in the correct orientation.

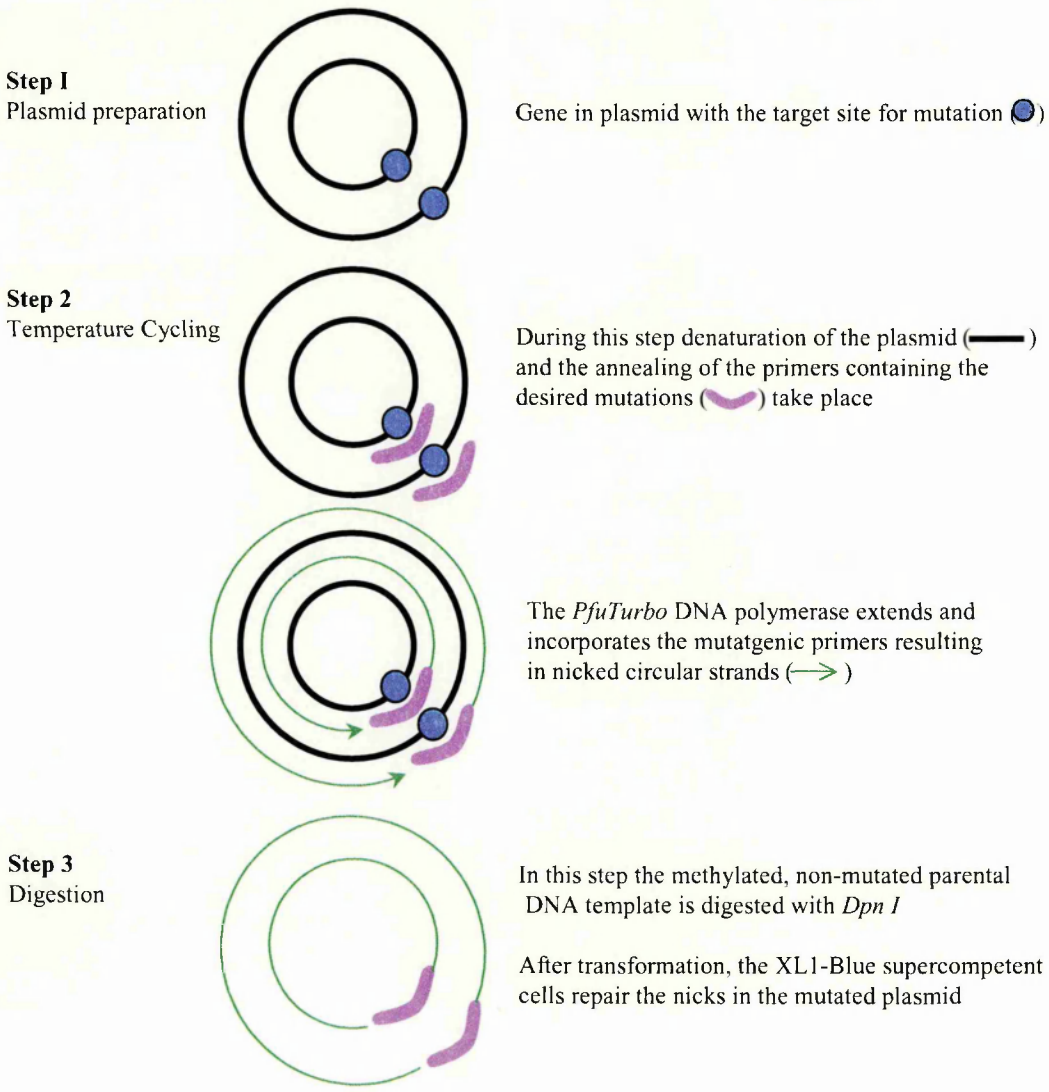

Figure 3.8 Overview of the QuikChange® site-directed mutagenesis method.

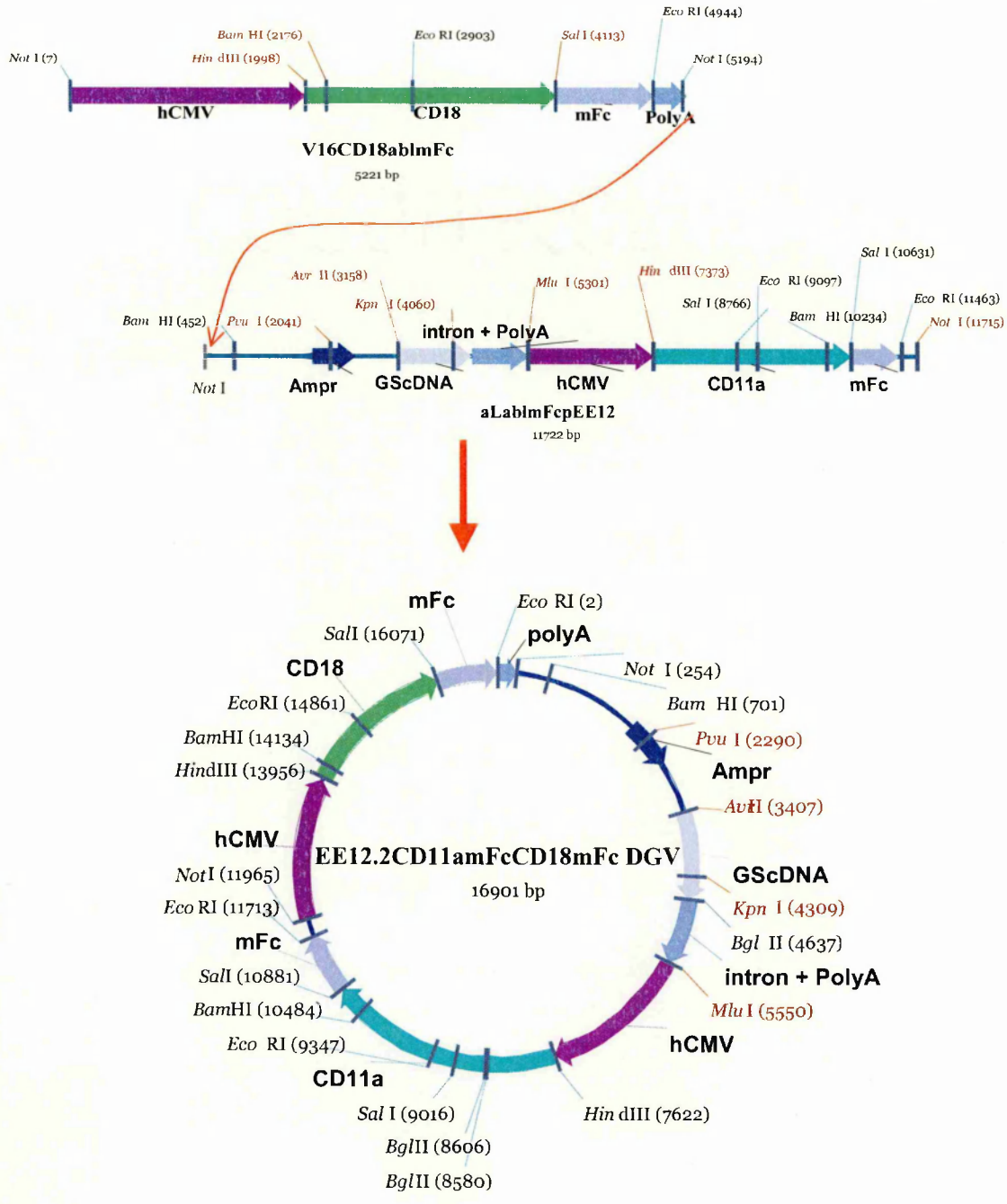

Figure 3.9 **Generation of the DGV containing the CD18 and CD11a extracellular domain gene regions fused with mFc tails.** Digestion of the pEE12.2αLablmFc vector with *Not I* results in linearisation of the molecule while the *Not I* fragment of the pV16β2ablmFc vector contains only the hCMV and the CD18 gene transcription unit. The DGV also contains the GS gene system for selection in mammalian cell systems and the Amp^r gene for selection in bacterial systems.

3.4 αL And β2 Vectors For K562 Transfection And Expression

In order to express LFA-1 on the K562 cell surface, both the αL and β2 full-length genes were required to be transfected into the cell line. Previous work within this laboratory had shown that transfection using a DGV was more efficient than transfection of both integrin chains as SGVs (single gene vectors). The full length CD18 gene was already available in the EE6hCMV*neo* vector system (Figure 3.2), which contained the neomycin resistance gene allowing for positive selection using G418 selection. This vector also contained a unique *Not* I site enabling linearisation of the vector for DGV generation. The V16 vector which contained two *Not* 1 sites was therefore used as the carrier vector for the αL full-length gene.

To incorporate the various IDAS mutations into the full-length version of the αL gene, *Hin*d III-*Sal* I fragments of the 5' end of the αL gene containing the mutated regions were excised from the pEE12.2$_{\alpha LablsolmFc}$ vectors. These fragments were ligated with a *Sal* I-*Bcl* I fragment containing the remaining 3' end of the αL gene which had been excised from the original pEE12.2CD11aFL(see Figure 3.7), and an empty pV16 vector cut with *Hin*d III *and Bcl* I to generate a series of pV16αL$_{mutFL}$ vectors (Figure 3.10). Prior to generation of fragments which required cutting with the *Bcl* I restriction enzyme, the plasmids were grown in the GM242 *dam*$^-$ *E.coli* strain. Following identification of correctly incorporated sequences by DNA sequencing, vectors were transiently co-transfected with pEE6*neo*β2$_{FL}$ into CHO cells and expression was detected by FACs analysis using αL and β2 mAbs. Full-length αLβ2 DGV generation was as described for the DGV containing the soluble constructs as both the pV16αL$_{mutFL}$ vectors and pEE6*neo*β2FL contain the *Not 1* restriction sites in similar positions (See Figure 3.11).

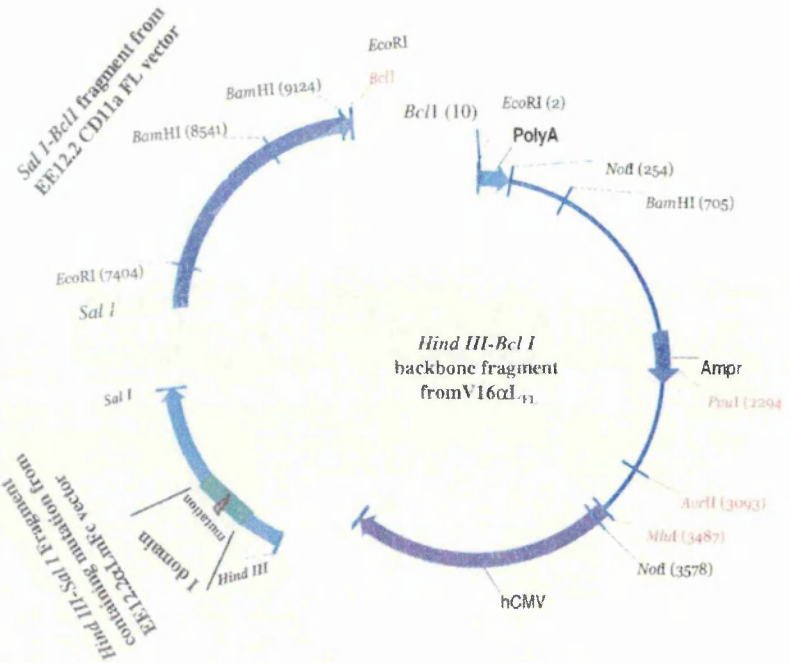

Figure 3.10 **Cloning Strategy to Generate a Vector containing a Full Length version of αL with mutations**. The αL full-length gene containing mutations within the I domain was inserted into the *Hind* III-*Bcl* I backbone fragment of pV16αLFL using a 3-way ligation with an αL 5' *Hind* III-*Sal* I fragment from the pEE12.2αLablmFc vector and a 3' *Sal* I - *Bcl* I fragment from the pEE12.2CD11a FL vector.

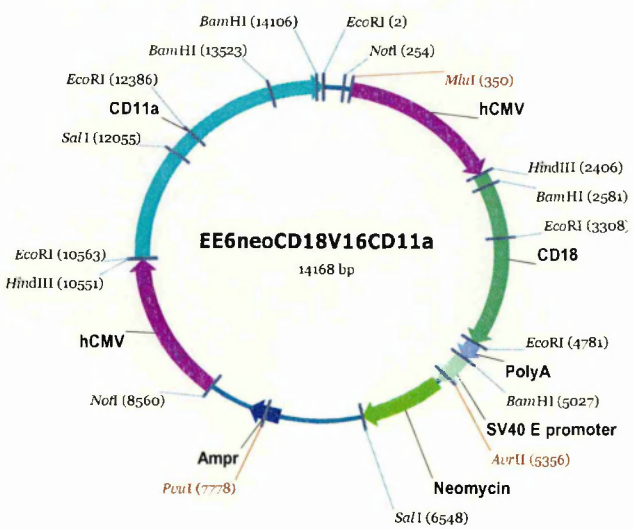

Figure 3.11 **Vector map of DGV used for K562 stable transfection**. The DGV was generated by linearising the pEE6hCMV*neo* vector with *Not* I and inserting a *Not* I-*Not* I fragment of the pV16αL$_{mutFL}$vector containing only the hCMV to drive the CD11a transcription unit. The DGV also contains the neomycin gene for selection in mammalian cell systems with G418 and the Amp^r gene for selection in bacterial systems.

3.5 αL Vectors For JB2.7 Transfection And Expression

Characterisation of the JB2.7 cell line, which is deficient in αL, by Weber *et al.* (1997) showed that the β2 subunit was synthesised and detectable by immunoprecipitation. The β2 subunit however was not expressed on the cell surface but transfection of the cell line with αL cDNA restored surface expression of LFA-1. Therefore, only single gene vectors containing the various full-length αL cDNAs were required to restore functional LFA-1 cell surface expression on JB2.7 cells. As the pV16αL_{mutFL} SGVs generated for the K562 expression system did not contain a selection marker for positive clonal selection, the αL_{mutFL} genes were excised from the pV16αL_{mutFL} SGVs as *Hin*d III-*Bcl* I fragments and ligated into an empty pEE6*neo* vector cut with *Hin*d III and *Bcl* I restriction enzymes (Figure 3.12). Following plasmid preparation, diagnostic digestion with a panel of restriction enzymes to determine the presence of the αL gene and DNA sequencing of the I domain region was carried out to ensure the presence of all the mutated forms of αL.

3.6 Discussion

A panel of expression constructs were generated to give functional vectors capable of either expressing the full length LFA-1 gene or a soluble entity comprising of the extracellular CD11a and CD18 domains fused to murine Fc domains. The inclusion of selection markers such as the neomycin resistance gene for selection in both K562 and JB2.7 cells allowed for an efficient method of identification of cells transfected with the LFA-1 genes. Use of the Stratagene's QuikChange® Mutagenesis Kit enabled the generation of several mutant forms of LFA-1 and proved to be very efficient at incorporating the required mutations without introducing other undesirable mutations. These expression plasmids were then used to transfect mammalian cells to make stable LFA-1 expressing CHO, K562 or JB2.7 cell lines.

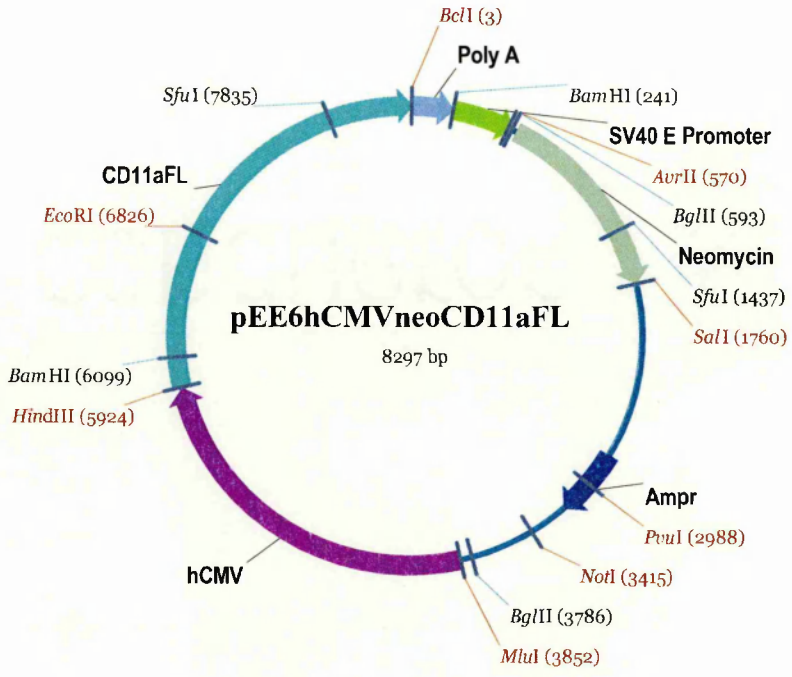

Figure 3.12 **Vector Map of pEE6hCMVneoCD11aFL SGV used for JB2.7 stable transfection.** The transcription unit of pEE6hCMV *neo* consists of a human cytomegalovirus (hCMV) major immediate early promoter, a polylinker (*Hin*d III-*Bcl* I) in to which the sequence for the CD11a full length gene has been inserted as a *Hin*d III-*Bcl* I in 2-way ligation, and the SV40 splice and polyadenylation signals. The SGV also contains the neomycin resistance gene for selection in mammalian cell systems with G418 and the Amp^r gene for selection in bacterial systems from the pEE6 vector.

Chapter 4

Soluble Integrin Expression And Analysis

Chapter 4 Soluble integrin expression and analysis

4.1 Introduction

Studies using both isolated I domain constructs and cell surface expressed I domain-less LFA-1 have shown that the ligand binding site of LFA-1 appears to be solely contained within the I domain (Randi and Hogg, 1994; Leitinger et al., 2000; Shimaoka *et al.*, 2001, 2002). This finding is also supported by work from several other groups, which have shown that mutations within the I domain can dramatically affect the ability of the isolated I domain and LFA-1 expressed on the cell surface to bind ligand. Much of the initial mutational analysis demonstrated the importance in ligand binding of the DXSXS motif within the MIDAS site, and residues surrounding it (Michishita *et al.*, 1993; Edwards *et al.*, 1995 & 1998; Kamata, 1995; Huang and Springer, 1995). This was recently confirmed following the elucidation of a crystal structure of the αL I domain in complex with the first two domains of ICAM-1 (Shimaoka *et al.*, 2002), which demonstrated that residues within the MIDAS of αL and the E34 residue in domain 1 of ICAM-1 form the main point of interaction. Evidence is now emerging that a second region within the I domain, known as the IDAS (I Domain Allosteric Site), also plays a major role in activation and ligand binding. Introduction of select mutations within this region of the I domain have been shown to either abrogate or enhance ligand binding and, in crystal structures of I domains complexed with ligand, a 10Å downward shift of the I domain α7 helix, which forms part of the IDAS, has been observed relative to the unliganded structure. Shimaoka's group have reported the generation of a conformation containing such a 10Å downward shift of the α7 helix by introducing a restraining disulphide bond in the loop between the C-terminal α-helix and the preceding β-strand of the αL IDAS. Such a mutation increases binding of the isolated αL I domain by 9000 fold relative to wild type I domain (Shimaoka *et al.*, 2001). As this site is distal to the MIDAS, its influence on ligand binding is suggested to be through allosteric changes rather than through direct contact with the ligand.

Using isolated I domains to investigate the role of the IDAS in ligand binding, the influence that other extracellular domains, especially the β-propeller, have on I domain mutations cannot be examined. In contrast, in studies using LFA-1 expressed on the cell surface, the influence that signalling molecules and the cytoskeleton have on integrin activation must also be taken into account. As part of this thesis, a soluble form of LFA-1 has been generated which allows one to investigate the role of the IDAS in regulating integrin/ligand interactions in the context of other LFA-1 domains but, importantly, also in a cell free system. The previous chapter, in part, has described the generation of this soluble integrin construct, which contains the extracellular domains of the α and β chains of LFA-1 fused with mouse Ig-Fc domains. This chapter will focus on the expression and characterisation of the LFA-1- mFc construct in relation to ligand binding and cation requirements. In order to investigate further the role of the I domain in ligand binding and its influence on other features of the full length integrin, various mutations within the IDAS domain, some novel and some previously described by other researchers, have also been included in the study (described in Section 3.1).

4.2 Expression of soluble LFA-1mFc

Initial co-transfection of the single gene vectors described in Chapter 3 containing αL with and without I domain mutations and β2 extracellular domain cDNAs was carried out in a CHO transient system to check that the appropriate protein was produced. The plasmids containing the various mutated forms of αLmFc and the β2mFc were introduced into CHO cells using the GenePORTER™ system. GenePORTER™ is a formulation of the lipid dioeoyl phosphatidylethanolamine (DOPE) and a cationic lipid that associates with the negatively charged nucleic acids. The resulting positively-charged complex allows for interaction with the negatively charged cell membrane and, after endocytosis, the nucleic acids are released from endosomes and delivered to the nucleus.

Two days after transfection, the culture supernatant was harvested and assayed for mFc expression by mIgG ELISA and heterodimer formation by sandwich ELISA. The sandwich ELISA involved capturing the soluble integrin with a mAb coated on the plate that recognised the αL subunit and revealing the captured integrin with a mAb that recognised the β2 portion of the integrin. Once it was established that αβ heterodimer was detectable in the transient supernatant, work was undertaken to generate stable cell-lines in order to provide a constant supply of material. Although NS0 stable transfection of the LFA-1 mFc constructs was unsuccessful, stably-transfected CHO cell lines generated nanograms per millilitre quantities of each the constructs and further large-scale production using this system generated sufficient quantities for this study. Each construct was re-sequenced directly before transfection using an altered version of the GenePORTER™ protocol (see Section 2.3.2) to ensure that it contained the correct mutation. Supernatants from the selected clones were concentrated 10-fold in an Amicon™ stirred cell system with a 10 kDa cut off membrane and concentrates were analysed by ELISA which measured the concentration of immunoglobulin Fc (See Section 2.4.1). Verification of the presence of heterodimer was carried out using sandwich ELISAs. Table 4.1 shows the typical results obtained from an IgG assay before concentration. The introduction of select mutations within the IDAS appears to have an advantageous effect on the expression of the LFA-1 mFc construct relative to wild type. This could be due either to increased expression of the αL chain or to more efficient combining of the heterodimer.

To check the integrity of the integrin portion of the fusion proteins and to verify the formation of heterodimer, reduced and non-reduced Western blotting analysis of the samples was carried out using an anti-mFc-HRP detection system. Due to the low concentrations of protein in some of the samples, immunoprecipitation using Protein Sepharose A was first carried out. Figure 4.1 shows a reduced and non-reduced blot of several of the constructs. Under non-reducing conditions the cysteine bond holding the two mFc regions together remains intact and therefore the heterodimer runs as a single high molecular weight species just above the 250kDa marker.

In the presence of a reducing agent, the disulphide bond is reduced and the individual αL and β2 subunits run at approximately 210kDa and 190kDa, respectively.

Construct	Concentration (ng/ml)
WT	30 ng/ml
I235A	15 ng/ml
287C	20ng/ml
287F	20ng/ml
292A	200ng/ml
294C	50 ng/ml
295A	120 ng/ml
299A	50 ng/ml
306A	30 ng/ml
287C294C	30 ng/ml
287A294A	40 ng/ml
289C294C	200 ng/ml
295A306A	250 ng/ml

Table 4.1 **Expression of LFA-1mFc fusion proteins in CHO Cells quantitated by Ig ELISA.** Typical results of IgG ELISAs to measure the concentration of LFA-1mFc fusion protein in CHO cell supernatant. The concentration of the mouse IgG_1 standard (Ab Max68P, Celltech) used was from 0-200ng/ml. For each LFA-1mFc sample the top concentration was neat cell supernatant followed by seven 1:2 dilutions (n=2). These results are representative of 6 or more experiments.

Although the blotting data, which must be noted is only semiquantitative, shows that most of the constructs express the αL and β2 fusion proteins at similar levels, some of the mutants exhibited markedly reduced expression levels. Whilst alanine substitution at residues 295 and 306 show comparable expression to sLFA-1_{WT}mFc, pairing these substitutions in one construct appears to dramatically affect αL subunit expression. In light of the reduced $\alpha L_{295A306A}$ mFc expression it is not surprising that expression of $\alpha L_{292A295A306A}$ mFc is also significantly reduced. Interestingly, in both of these samples, homodimers of the excess β2 subunit appear to form. A minor band at a similar position in samples containing other constructs suggests that some homodimerisation does occur regardless of the expression levels of both subunits. The blots also

highlight that the level of expression of both the β2 subunit, which is invariant in all constructs, and the various αL subunits appears to vary from construct to construct, with some of them containing a much higher proportion of β subunit over α subunit. There are also significant quantities of free mFc (~25kDa on non-reduced gel; ~50kDa on reduced gel) as well as other mFc-containing breakdown products present in each of the samples. The presence of varying levels of heterodimer, homodimer and free Fc in samples suggests that using the mFc ELISA as a quantification method may not truly quantitate the concentration of functional heterodimer in each sample.

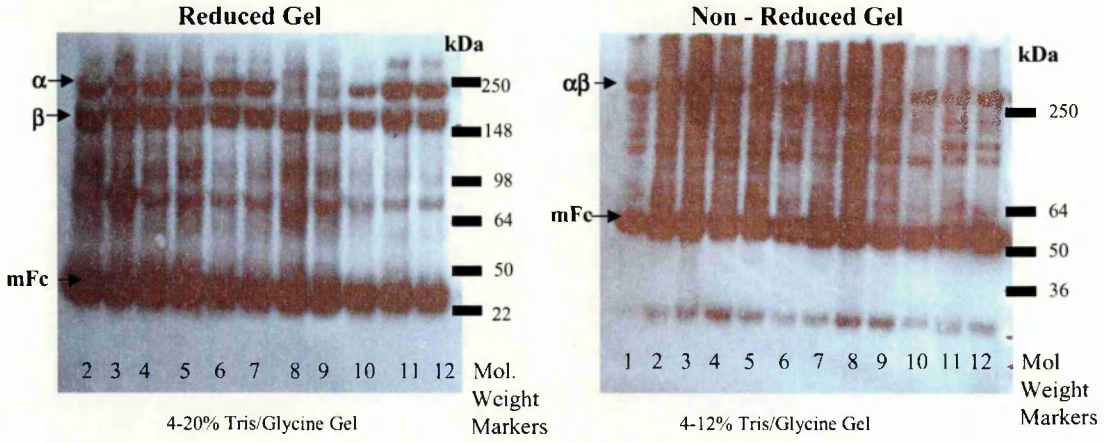

1. **sLFA-1_{235A} mFc**
2. **sLFA-1_{287c} mFc**
3. **sLFA-1_{292} mFc**
4. **sLFA-1_{294C} mFc**
5. **sLFA-1_{295A} mFc**
6. **sLFA-1_{299A} mFc**
7. **sLFA-1_{306A} mFc**
8. **sLFA-$1_{295A306A}$ mFc**
9. **sLFA-$1_{292A295A306A}$ mFc**
10. **sLFA-$1_{287C294C}$ mFc**
11. **sLFA-$1_{289C294C}$ mFc**
12. **sLFA-1_{WT} mFc**

Figure 4. 1 **Western blot of immunoprecipated sLFA-1mFc constructs in the presence and absence of reducing agent.** 50ng/mFc (using IgG ELISA) of each sample was used for each immunopercipitation using 50µl Protein A Sepharose beads in the presence of 4mM NaCl. After incubation overnight at 4°C beads were washed extensively and on addition of sample buffer +/- reducing agent, samples were boiled and loaded onto gels. Following electrophoresis, gels were Western blotted on to nitrocellulose paper overnight at 150mAmps. After blocking and washing, nitrocellulose sheets were incubated with 1:5000 dilution anti-mFc-HRP polyclonal Ab for 1hour. Following extensive washing blots were revealed with an ECL kit and developed as an autoradiograph.

4.3 Assembly Assays

In light of the Western blotting results, a more accurate method of quantifying the heterodimeric content in the supernatants was required. A series of ELISAs, where the αβ heterodimer was captured using an immobilized LFA-1-specific mAb and revealed with a different biotinylated-LFA-1 specific mAb, were therefore developed. Although efforts were made to select antibodies whose binding would not be affected by different I domain mutations it is generally accepted that integrins undergo considerable conformational change on activation. Therefore in order to minimise any effects that this might have on antibody binding and subsequent quantitation, six different pairs of antibodies were used in two site ELISA assays (See Table 4.2).

KIM185 has been mapped to the C-terminal half of the cysteine-rich domain at positions 522-612 in the stalk region of the β2 subunit (Huang *et al.*, 2000). Although it is known to activate LFA-1, Huang *et al.* (2001) suggests that KIM185 binds in a similar manner to both the active and inactive form of the integrin and hence this factor would not affect its ability to capture or reveal the β-chain in this assay. Both DA36 and Ab38 map to the I domain and, although the exact epitopes have not been identified, their ability to completely block ligand binding by all of the LFA-1mFc mutants suggests that the epitopes recognized by these mAbs are not affected by the mutations. Huang *et al.* (2000) have also mapped the 6.5E epitope to the I-like domain and shown that although it binds both LFA-1_{WT} and the locked 'open' form of LFA-1 to the same extent, this mAb is unable to block ICAM-1 binding by locked 'open' LFA-1. This mAb is therefore a useful tool for detecting correctly folded heterodimer.

Figure 4.2 illustrates two representative titrations of the LFA-1mFc supernatants. In most cases the supernatants were titrated from neat and the dilution factor of supernatant for individual mutants that was required to give equal optical density readouts was noted from each experiment. The average dilution factor of each mutant supernatant compared to wild type from

a series of 4 assembly assays was then calculated. Stocks of these dilutions were then used for all subsequent assays and direct aliquots from each were termed as 'neat' for subsequent experiments. The variation from assay to assay in the dilution factor required for most of the supernatants was found to be relatively small with the exception of LFA-$1_{287C294C}$. This result suggests that the introduction of cysteine as opposed to alanine substitutions at positions K287C and K294C has a dramatic effect on the binding of the mAbs used in these assays. The locking of the IDAS in a 'closed' position using the same K287C substitution, and a substitution at position L289C, does not appear to affect the way in which the various mAbs bind. Also, single cysteine substitutions at these positions do not show large variations in binding. Although Shimaoka *et al.* (2001) have show that locking the I domain in the 'closed' conformation does shift the position of the α7 helix, this shift is evidently not as dramatic as locking the protein in the 'open' form. Comparison of the results of the Western blotting experiments with the assembly assay results shown here suggests that the supernatants contain, in addition to free mFc, varying amounts of misfolded and/or homodimeric product.

Capture mAb	Biotinylated Reveal mAb
KIM185	6.5E *bio*
6.5E	DA36 *bio*
Ab38	6.5E *bio*
6.5E	KIM185 *bio*
DA36	KIM185 *bio*
KIM185	DA36 *bio*

Table 4.2 **Combinations of mAbs used in the LFA-1 assembly assay.** This table lists the mAbs and their biotinylated partners that were used in a series of assembly ELISAs designed to quantify the amount of correctly folded heterodimer present in the LFA-1mutant supernatants.

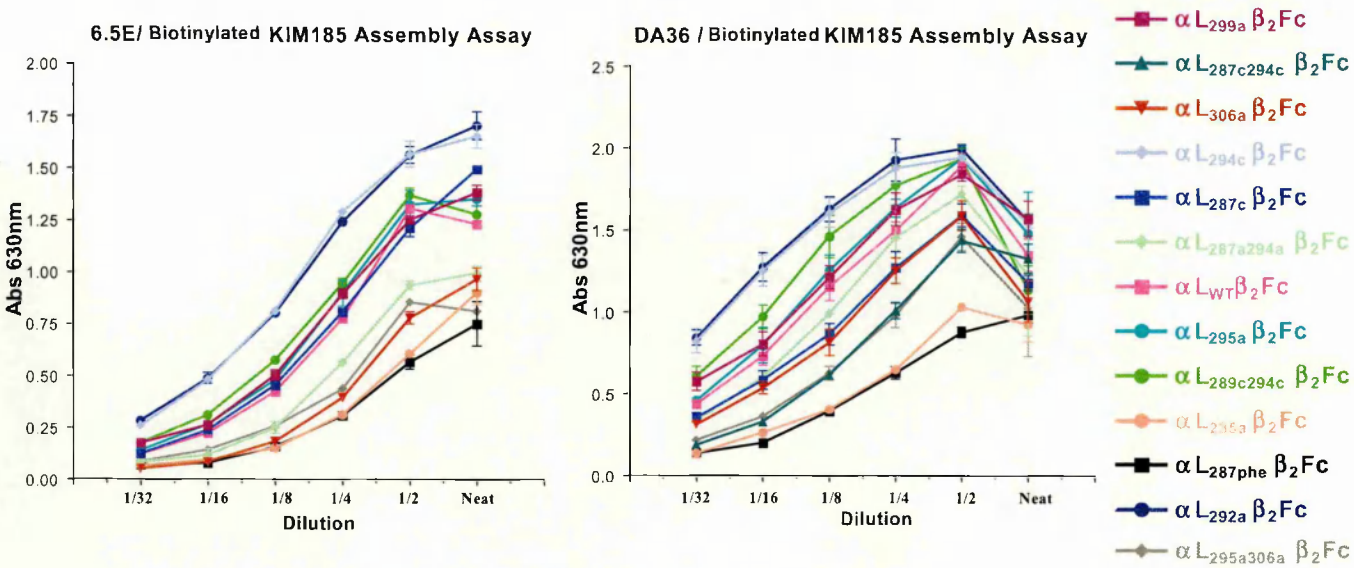

Figure 4. 2 **Assembly Assay Titration curves for the various sLFA-1 mutants in two representative assays.** Supernatants were titrated from neat with doubling dilutions onto plates coated with 5µg/ml 6.5E or DA36. Bound biotinylated KIM185 was revealed with addition of Streptavidin-HRP and the degree of binding was assessed as absorbance at 630nm using TMB substrate. Each data point represents the mean of two values (error bars represent individual values). The data presented here are representative of that obtained in at least three other independently performed experiments.

4.4 ICAM-1, -2 & -3 Ligand Binding

In order to determine the effect each of the mutations had on the function of LFA-1, a series of assays were developed in which the binding of various ICAM-hFc ligands to captured sLFA-1mFc was quantitated by detecting the hFc portion of the ligand molecule with an anti-hFc-HRP polyclonal Ab. The concentrations of ICAM-1, -2, -3 used in the assays were determined by titrating the ligands from 30µg/ml in the presence of sLFA-1_{295A}mFc and selecting a concentration within the linear section of the graph (Figure 4.3). A construct (sLFA-1_{295A}mFc) with high affinity for ligand compared to wild-type (as determined by preliminary ligand binding assays) was chosen to determine the concentrations of ligands to be used in the binding studies so that at no point would saturation of ligand in the case of some of the active constructs become an issue.

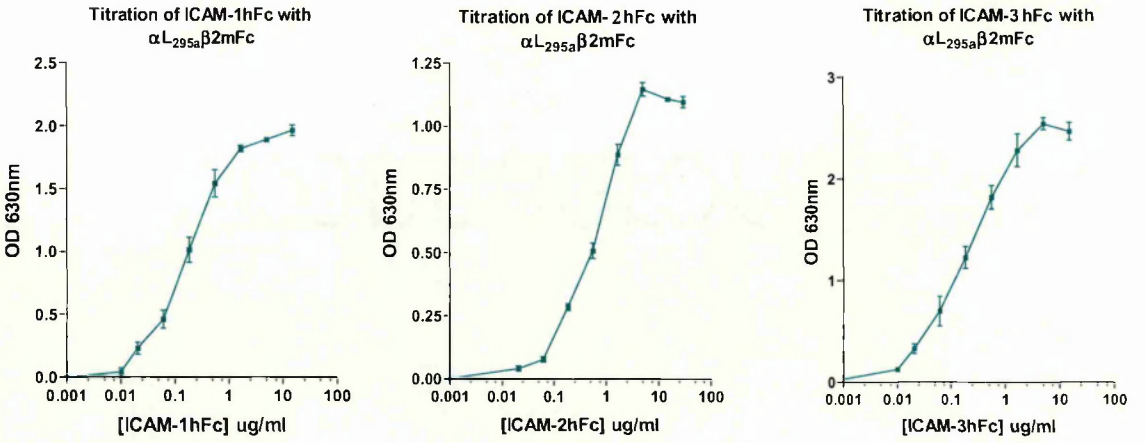

Figure 4.3 **Titration of ICAM-1hFc, ICAM-2hFc and ICAM-3hFc.** Titrations of ICAM-1hFc, ICAM-2hFc and ICAM-3hFc using tripling dilutions from 30μg/ml (start concentration) were incubated with mFc-captured sLFA-1_{295A}mFc for 3hrs. Bound ligand was revealed with an anti-hFc-HRP Ab. Each data point represents mean +/-SD (n=3) and these graphs are representative of 2 or more independently conducted assays.

Figure 4.4 shows the binding curves of the sLFA-1mFc constructs to ICAM-1hFc, ICAM-2hFc and ICAM-3hFc. Where ligand binding was demonstrated, this appeared to be dose-dependent. Moreover, the presence of cation was required for binding as addition of EDTA completely abolished binding. It must however be noted that sigmoidal curves were not achieved in most cases and hence only limited analysis of the data could be carried out. The data does however highlight the increase in ligand affinity of several of the mutants compared to wild type. The introduction of the double cysteine substitution at residues K287 and K294 and single alanine substitutions at positions F295 and I235 showed the greatest increase in ligand binding over wild type. The binding of sLFA-1mFc, containing either the single substitution of K294C or the novel alanine substitution at position 292, to ICAM-1 was also increased relative to wild type. The pairing of the K294C substitution with L289C, which is equivalent to the double mutation introduced by Shimaoka *et al.* (2001) to generate the 'closed' conformation of the I domain, showed similar levels of ICAM-1 binding to sLFA-$1mFc_{WT}$.

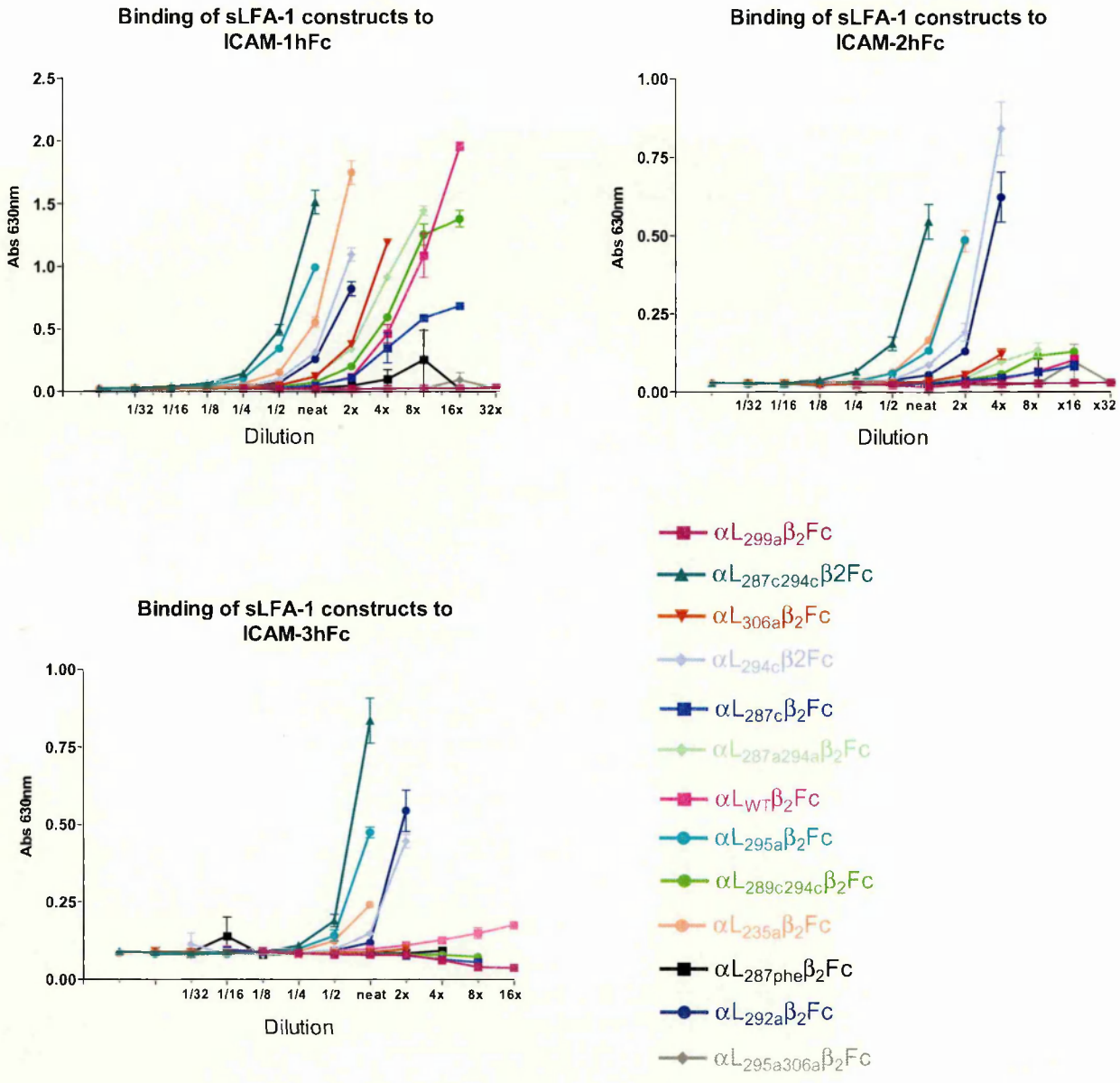

Figure 4.4 **Binding of sLFA-1mFc constructs to ICAM-1, -2, 3hFc.** mFc samples were captured on anti mFc-coated plates and bound ligand was revealed by anti-hFc-HRP Ab binding. All assays were carried out in TBS in the presence of 1mM Mn^{2+}. ICAM-1hFc, ICAM-2hFc, ICAM-3hFc was used at 200ng/ml, 500ng/ml and 500ng/ml, respectively. The initial concentration of each construct used as the starting point for each titration was determined from the assembly assay as in Figure 4.3. Each data point represents the mean of two values (error bars represent individual values). Data presented here are representative of that obtained in at least six other independently performed experiments.

The substitution of alanine residues rather than cysteine residues at positions K287 and K294 resulted in only a slight increase in ligand binding over wild-type and was comparable to that seen for the I306A substitution. This result suggests that the chemical nature of the substitution and possibly the formation of a disulphide bond has an effect on the activation state of the integrin. The introduction of an alanine substitution at residue F299, and a double substitution at positions L295 and I306 within the IDAS completely destroyed the ability of the integrin to bind ligand. Interestingly, the sLFA-1_{299A}mFc construct was one of the more highly expressed constructs and appeared to heterodimerize efficiently, despite having lost ligand-binding capability.

However, the most dramatic effects on ligand binding affinity were seen with ICAM-2hFc and ICAM-3hFc. Whereas sLFA-1mFc$_{WT}$ bond both ligands only at very low levels in the presence of 1mM Mn^{2+}, five of the constructs (those containing mutations at positions 287C294C, 295A, 292A, 294C and 235A) demonstrated relatively high levels of binding to ICAM-2 and -3 with sLFA-1mFc$_{287C294C}$ again appearing to show the greatest increase over wild-type. In agreement with results obtained with ICAM-1, both sLFA-$1_{295A306A}$mFc and sLFA-1_{299A}mFc showed no binding to ICAM-2 or ICAM-3, suggesting that the introduction of these mutations alters the ability of αLβ2 to bind ligand in a fundamental way.

4.5 Activating mAbs

Huth *et al.* (2001) have previously shown that loss of ligand binding in cases where residues within the IDAS were mutated could be rescued in the presence of an activating mAb. As both KIM127 and KIM185 have been extensively shown to be activators of LFA-1/ICAM cell binding events (Andrew *et al.*, 1993, Porter and Hogg, 1997; May *et al.*, 2000; Lu *et al.*, 2001), it was of interest to determine if these mAbs were capable of enhancing the binding of mutant forms of sLFA-1mFc to ICAM ligands. MEM148, another activating mAb, which is thought to

activate ligand binding through a different mechanism from KIM127 and KIM185 (Drbal, 2001), was also used in the study. Data generated during the assembly assay development showed that all three mAbs, including MEM148 which was not used in final assembly assays due to limited supplies, recognised all of the constructs and Figure 4.5 illustrates the percentage increase in binding in the presence of these mAbs over control. Although the baseline binding for each construct was different, in order to highlight the effects each of the activating mAbs had on the constructs, results are plotted as a percentage of increased binding relative to that demonstrated in the absence of activating mAbs for each individual construct.

sLFA-1_{WT}mFc binding to ICAM-1hFc was enhanced by ~40% in the presence of all 3 mAbs and all mAbs enhanced the percentage binding to ICAM-2 and ICAM-3 even further, with MEM148 increasing this binding by ~100% and ~300% with ICAM-2hFc and ICAM-3hFc, respectively. Enhanced binding was also seen for sLFA-1_{287A}mFc, sLFA-1_{306A}mFc, sLFA-$1_{289C294C}$mFc and sLFA-$1_{287A294A}$mFc, all of which gave similar titration curves to sLFA-1_{WT}mFc with cation. This enhanced binding did not, however, reach the level of binding seen for constructs such as sLFA-$1_{287C294C}$mFc, and sLFA-1_{295A}mFc in the presence of cation alone.

Interestingly, most constructs that showed increased binding over sLFA-1_{WT}mFc in the presence of cation alone (see Figure 4.5) could not be further activated to any appreciable degree on addition of the mAbs. The exception to this was sLFA-1_{235A}mFc, which showed increased binding to all 3 ligands in the presence of the activating mAbs, although KIM185 was unable to further activate LFA-1_{235A}mFc binding to ICAM-3. In this case the binding of LFA-1_{235A}mFc reached similar levels to that seen for sLFA-$1_{287C294C}$mFc in the presence of cation alone. The addition of activating mAbs was unable to restore ligand binding to sLFA-1_{299A}mFc, once again indicating the requirement for a phenylalanine at this position to support ligand binding. The lack of binding with sLFA-$1_{295A306A}$mFc also suggests that substitution at both these residues has a major negative effect on ligand binding.

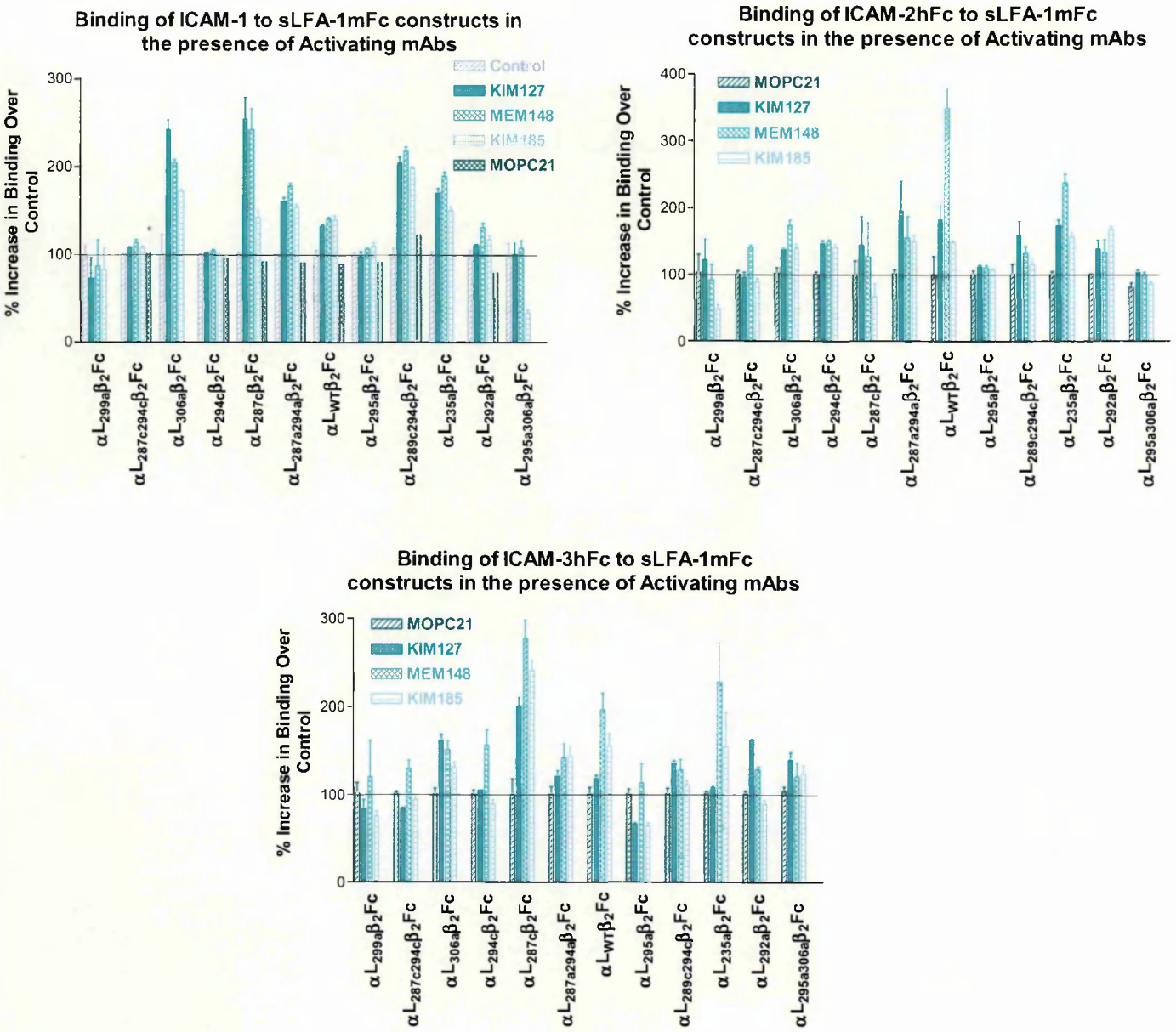

Figure 4.5 **Binding of ICAM-1hFc, ICAM-2hFc and ICAM-3hFc to sLFA-1 constructs in the presence of activating mAbs.** Captured sLFA-1mFc constructs were incubated for 3hrs with 200ng/ml ICAM-1hFc, 500ng/ml ICAM-2hFc ng/ml or 500ng/ml ICAM-3hFc +/- activating mAbs KIM127, KIM185, MEM148 or MOPC21 control, all at 20µg/ml. Assays were performed in the presence of 1mM Mn^{2+}. Bound ICAM-hFc was revealed with an anti-hFc-HRP Ab. % binding for each construct was calculated relative to the readout in the absence of activating mAbs. Each data point represents mean +/-SD (n=4). These graphs are representative of 2 or more independently conducted assays.

4.6 Blocking of Ligand Binding with mAbs and Lovastatin

To confirm that the enhanced binding demonstrated by some of the mutants was LFA-1-dependent, the effects of known LFA-1/ ICAM blocking mAbs and low molecular weight antagonists was investigated. Figure 4.6 (A-E) shows the binding profile of some of the constructs in the presence of DA36 (αL mAb), 6.5E (β2 mAb) and Lovastatin (a fungal metabolite previously shown to inhibit ICAM-1 binding to cell associated and soluble-expressed LFA-1 (Kallen *et al.*, 1999)). DA36 blocks the binding of all of the sLFA-1mFc constructs to all three ICAM ligands. Whether this inhibition is through direct binding around the MIDAS site or through allosteric influences is unknown. 6.5E mAb also completely blocks most sLFA-1mFc construct / ligand interactions with the exception of the interaction of sLFA-1_{295A}mFc with ICAM-1 and sLFA-$1_{287C294C}$mFc with all three ligands. The possible reasons for this reduced inhibition will be discussed in Section 4.9. Lovastatin has previously been shown to bind in the IDAS cleft (Kallen *et al.*, 1999) and has been demonstrated by Shimaoka *et al.* (2001) to bind to the 'closed' form of the I domain. Although Lovastatin had a slight inhibitory effect on sLFA-1_{292A}mFc, and reduced binding of sLFA-1_{WT}mFc to ICAM-1 by ~80%, no blocking of ICAM-1 binding to the sLFA-1mFc constructs containing substitutions at positions 295A, 287C294C or 294C was observed. Inhibition of sLFA-1_{292A}mFc, sLFA-1_{295A}mFc and sLFA-1_{294C}mFc binding to ICAM-2 and ICAM-3 with Lovastatin was greater than that seen with ICAM-1.

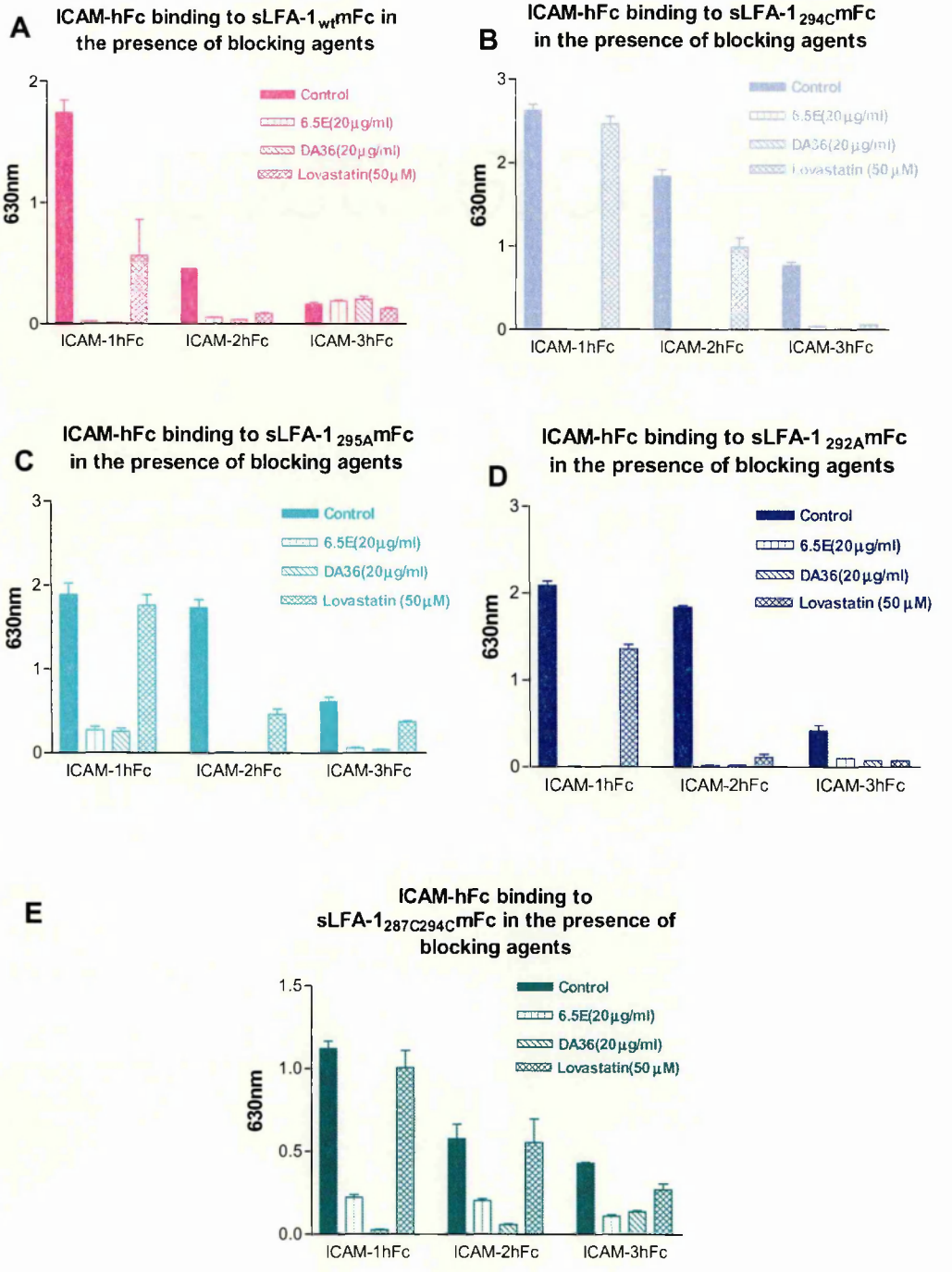

Figure 4. 6 **Binding of ICAM-1hFc, ICAM-2hFc and ICAM-3hFc to sLFA-1mFc constructs in the presence of blocking agents.** Captured sLFA-1mFc constructs were incubated for 3hrs with 200ng/ml ICAM-1hFc, 500ng/ml ICAM-2hFc, 500ng/ml ICAM-3hFc with or without the following; mAbs MOPC21 (control) DA36 or 6.5E at 20µg/ml or 50µM Lovastatin. Bound ICAM-hFc was revealed with an anti-hFc-HRP Ab. Each data point represents mean +/-SD (n=3) and these graphs are representative of 2 or more independently conducted assays.

4.7 6.5E Blocking in the Presence of Activating Abs

Because of the reduced capacity of mAb 6.5E to inhibit the ICAM binding of some of the mutated soluble constructs, it was of interest to see if, when further activated by activating mAbs, sLFA-1_{WT}mFc would behave in a similar manner. The data in Figure 4.7 shows that both KIM127 and MEM148 activation did slightly reduce the inhibitory effect of mAb 6.5E on the sLFA-1_{WT}mFc /ICAM-1hFc interaction but still not to the same extent as that observed by the introduction of the 287C294C mutation. Furthermore, when the same activating mAbs were added in the presence of 6.5E to other constructs, the ability of 6.5E to inhibit was also reduced to some extent even in circumstances where the activating mAb does not further enhance the binding of LFA-1 to the ICAM-1. This was most evident in the case of the sLFA-$1_{287C294C}$mFc construct where, on addition of MEM148, the blocking capacity of 6.5E was almost completely removed.

This result suggests that while sLFA-$1_{287C294C}$mFc appears to achieve maximal binding without the aid of activating mAbs, binding of the mAb still occurs. Indeed this may act to further stabilize the active conformation and, in doing so, reduce the ability of 6.5E to block, presumably through an allosteric mechanism. The inability of 6.5E to block binding when MEM148 is bound is unlikely to be due to steric hindrance as blocking occurs in all the other constructs. This will be discussed further in Section 4.9. In all cases, inhibition with the αL mAb DA36 was greater than 95%.

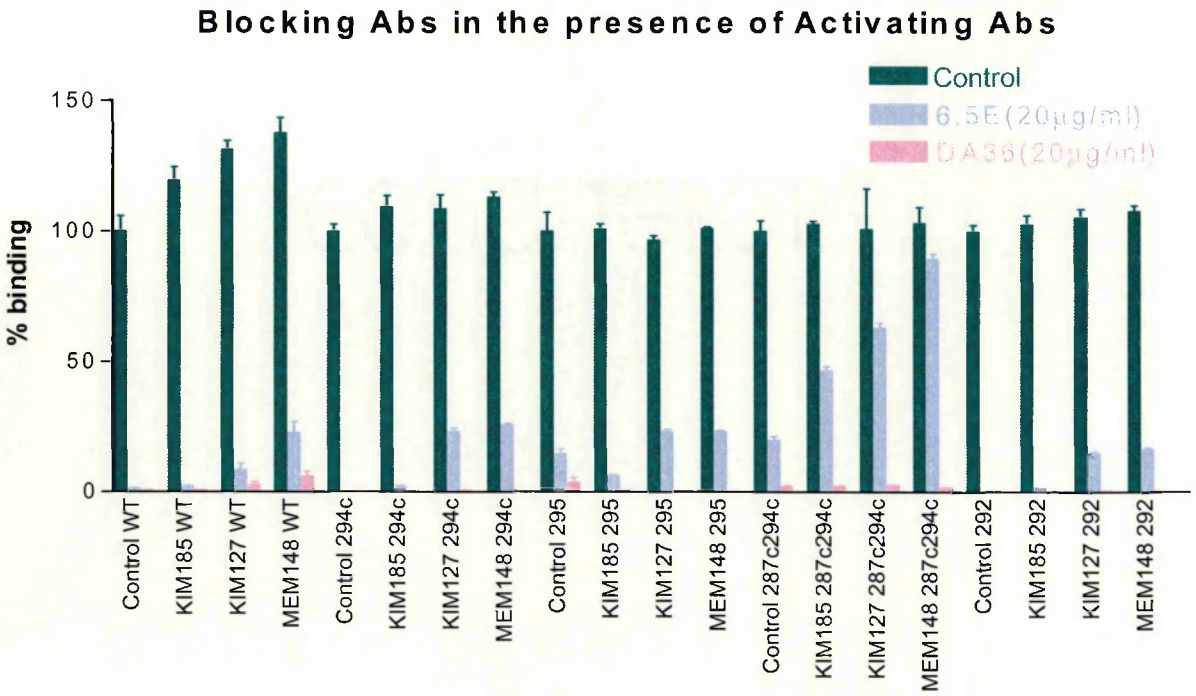

Figure 4.7 **6.5E and DA36 blocking of the sLFA-1mFc/ICAM-1hFc interaction in the presence of activating mAbs.** Captured sLFA-1mFc constructs were incubated for 3hrs with 200ng/ml ICAM-1hFc +/- activating Abs, KIM127, KIM185 or MEM148 and +/- blocking Abs, DA36 or 6.5E or MOPC21 (control). All mAbs used at 20µg/ml. Bound ICAM-1hFc was revealed with an anti-hFc-HRP. Ab. % binding for each construct was calculated relative to the readout in the absence of both activating and blocking mAbs. Each data point represents mean +/-SD (n=3) and this graph is representative of 2 or more independently conducted assays.

4.8 Cation Requirements

4.8.1. Mg^{2+} and Mn^{2+}

Analysis of the increased affinity of some of the constructs for ICAM-1hFc over wild-type seen in previous experiments suggests that the introduction of selected amino acid substitutions within the IDAS constitutively activates the integrin. This activation appeared to be maximal for sLFA-$1_{287C294C}$mFc, sLFA-1_{294C}mFc, sLFA-1_{295A}mFc, since addition of activating Abs did not

appear to further increase the amount of ligand bound. It was therefore of interest to determine if the concentration of cations required by the mutants to give maximal binding was similar to wild type. Although Mn^{2+} is routinely used in this laboratory at 1mM, the possibility that varying the Mn^{2+} concentration could further increase binding affinity was investigated. Figure 4.8 shows Mn^{2+} titration curves for five of the constructs compared to sLFA-1_{WT}mFc.

Titrations over a wide range of cation concentrations were initially carried out (see Figure 4.8) to determine the optimal range for further experiments. In these initial titrations most of the constructs demonstrated an optimal binding at a concentration of approximately 0.5mM for Mn^{2+} and above these concentrations, no further increase in ligand binding was detected. Additionally, varying the Mn^{2+} concentration had no effect on inducing binding of ICAM-1hFc to sLFA-1_{299A}mFc. Further titrations (Figure 4.9) over the optimal ranges indicated that the cation requirements for all the constructs were very similar. These results suggest that activation of the integrin by the introduction of mutations, or restraining the α7 helix in a downward position, has no effect on cation requirements when Mn^{2+} was used.

Similar titration curves were carried out in the presence of Mg^{2+} (Figure 4.10 A&B). Initial titrations showed that maximal binding of all soluble LFA-1 mFc forms occurred around 1mM Mg^{2+}. Further titrations over the optimal range also showed that, similar to Mn^{2+} requirements, the requirement for Mg^{2+} was not affected by introduction of mutations into the IDAS.

4.8.2. Effect of Ca^{2+} on the binding of LFA-1 to ICAM-1

Ca^{2+} has been shown in several studies to inhibit binding of LFA-1 to its ligands (Marlin and Springer, 1987; Dransfield *et al.*, 1992). In order to determine if Ca^{2+} had a similar effect on sLFA-1mFc, a series of checkerboard experiments were conducted where Ca^{2+} and Mn^{2+} were titrated concomitantly. Results from these experiments (Figure 4.11) suggest that Ca^{2+} inhibits

in a dose-dependent manner with almost complete blocking at 10mM. In all cases, as the Mn^{2+} concentration was increased, the amount of Ca^{2+} required to inhibit binding also increased. This suggests that the two cations compete for binding sites on LFA-1 and these sites are not affected by the introduction of mutations within the IDAS.

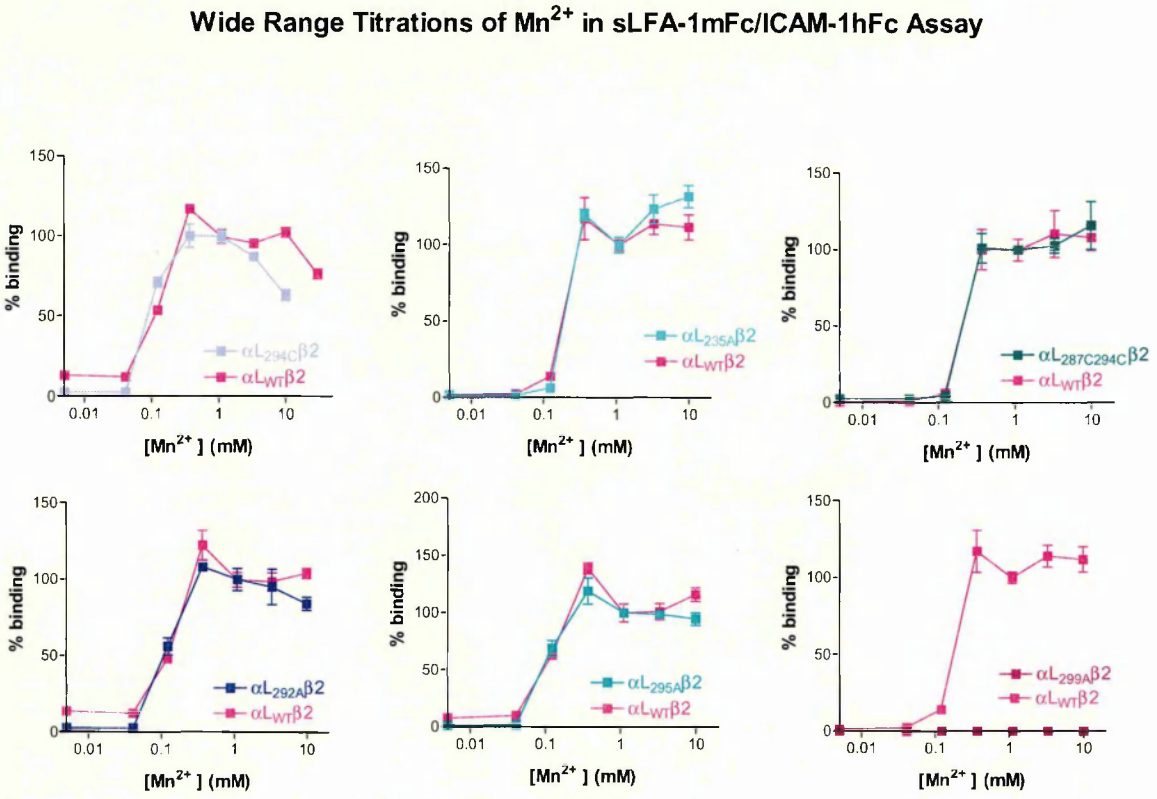

Figure 4.8 **Wide Range Titrations of Mn^{2+} in the sLFA-1mFc/ICAM-1hFc Assay.** These graphs represent the initial Mn^{2+} titrations carried out to determine the range over which any variation in cation concentration from construct to construct could be detected. Captured integrin was depleted of divalent cation by washing (x2) in 20mM EDTA/TBS followed by 4 washes in TBS. 50µl of 400ng/ml ICAM-1hFc in TBS/0.1% BSA, pH7.5 was added to each well along with 50µl of twice the required final concentration of Mn^{2+} in TBS/0.1% BSA, pH7.5. The results are expressed in terms of percentage binding, with 100% binding defined as the maximal signal seen with optimal concentration of Mn^{2+}. Each data point represents Mean +/- SD (n=3) and data presented here are representative of 1 more independently conducted experiment.

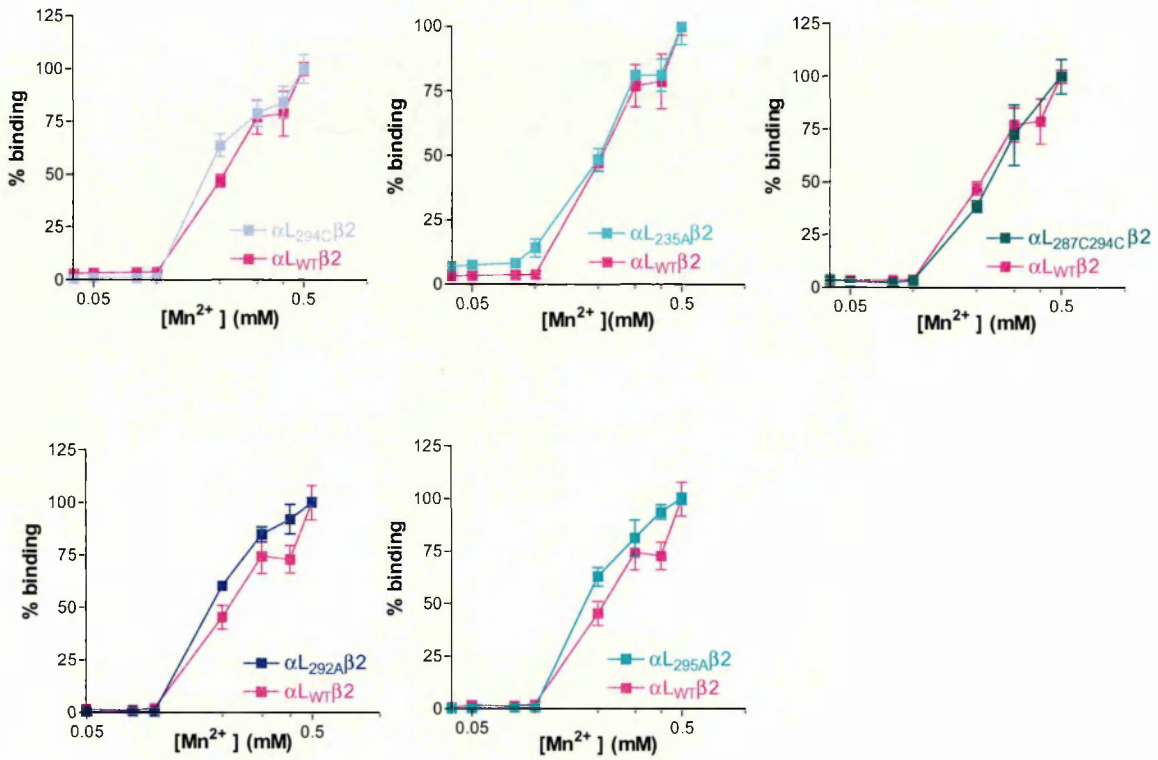

Figure 4.9 **Titrations of Mn^{2+} (0-0.5mM) in the sLFA-1mFc/ICAM-1hFc Assay.** Captured integrin was depleted of divalent cation by washing (x2) in 20mM EDTA/TBS followed by 4 washes in TBS. 50µl of 400ng/ml ICAM-1hFc in TBS/0.1% BSA, pH7.5 was added to each well along with 50µl of twice the required final concentration of Mn^{2+} in TBS/0.1% BSA, pH7.5. The results are expressed in terms of percentage binding, with 100% binding defined as the maximal signal seen with optimal concentration of Mn^{2+}. Each data point represents Mean +/- SD (n=3) and data presented here are representative of 2 or more independently conducted experiments.

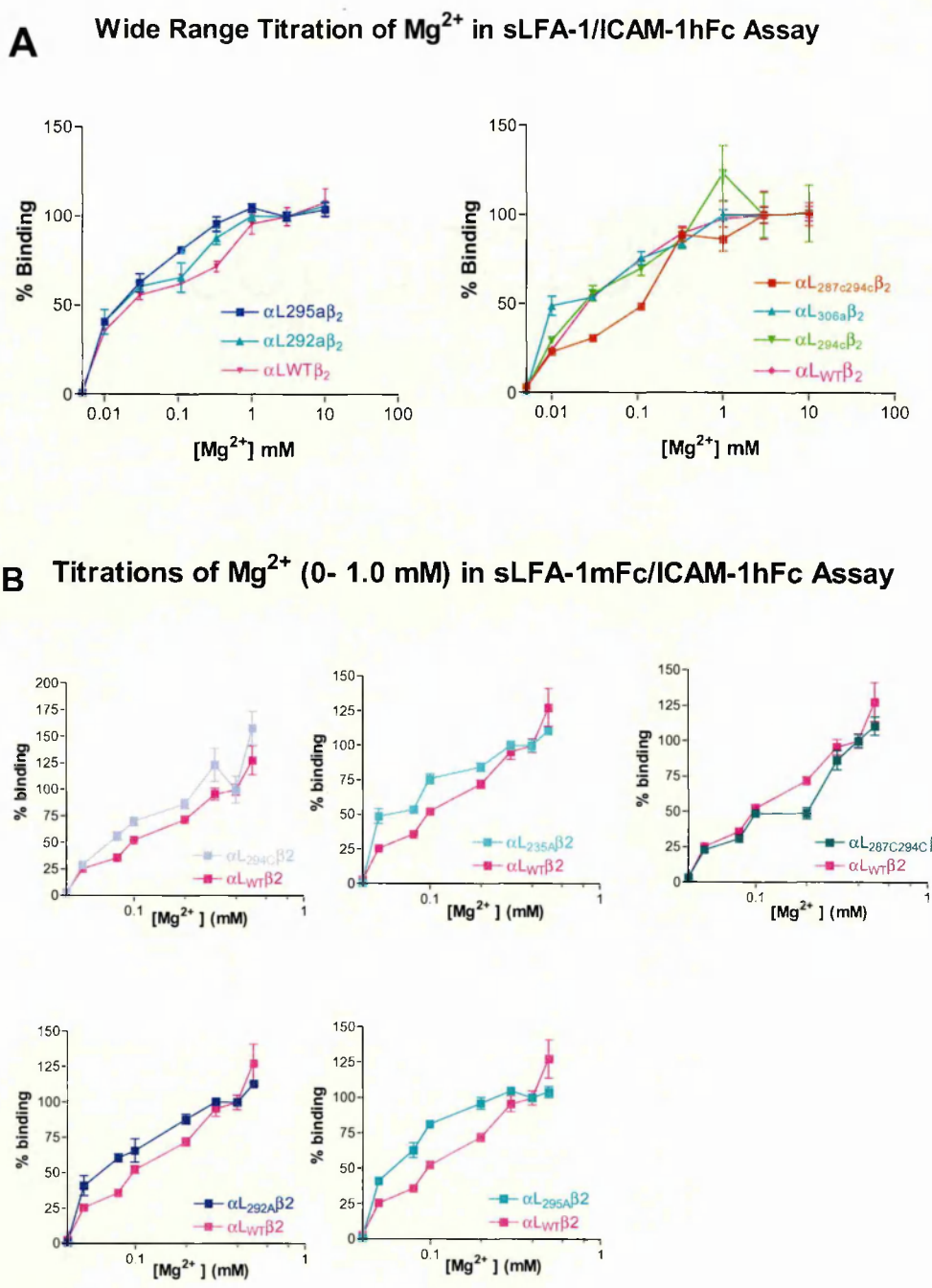

Figure 4.10 **Titrations of Mg^{2+} in the sLFA-1mFc/ICAM-1hFc Assay**. Figure 4.10(A) represents the initial Mg^{2+} titrations carried out to determine the range over which any variation in cation concentration from construct to construct could be detected. Figure 4.10(B) represents titrations between 0-1mM Mg^{2+}. Captured integrin was depleted of divalent cation by washing (x2) in 20mM EDTA/TBS followed by 4 washes in TBS. 50µl of 400ng/ml ICAM-1hFc in TBS/0.1% BSA, pH7.5 was added to each well along with 50µl of twice the required concentration of Mg^{2+} in TBS/0.1% BSA, pH7.5. The results are expressed in terms of percentage binding, with 100% binding defined as the maximal signal seen with optimal concentration of Mg^{2+}. Each data point represents Mean +/-SD (n=3). Data presented in **A** are representative of 1 experiment and **B** are representative of 2 or more independently conducted experiments

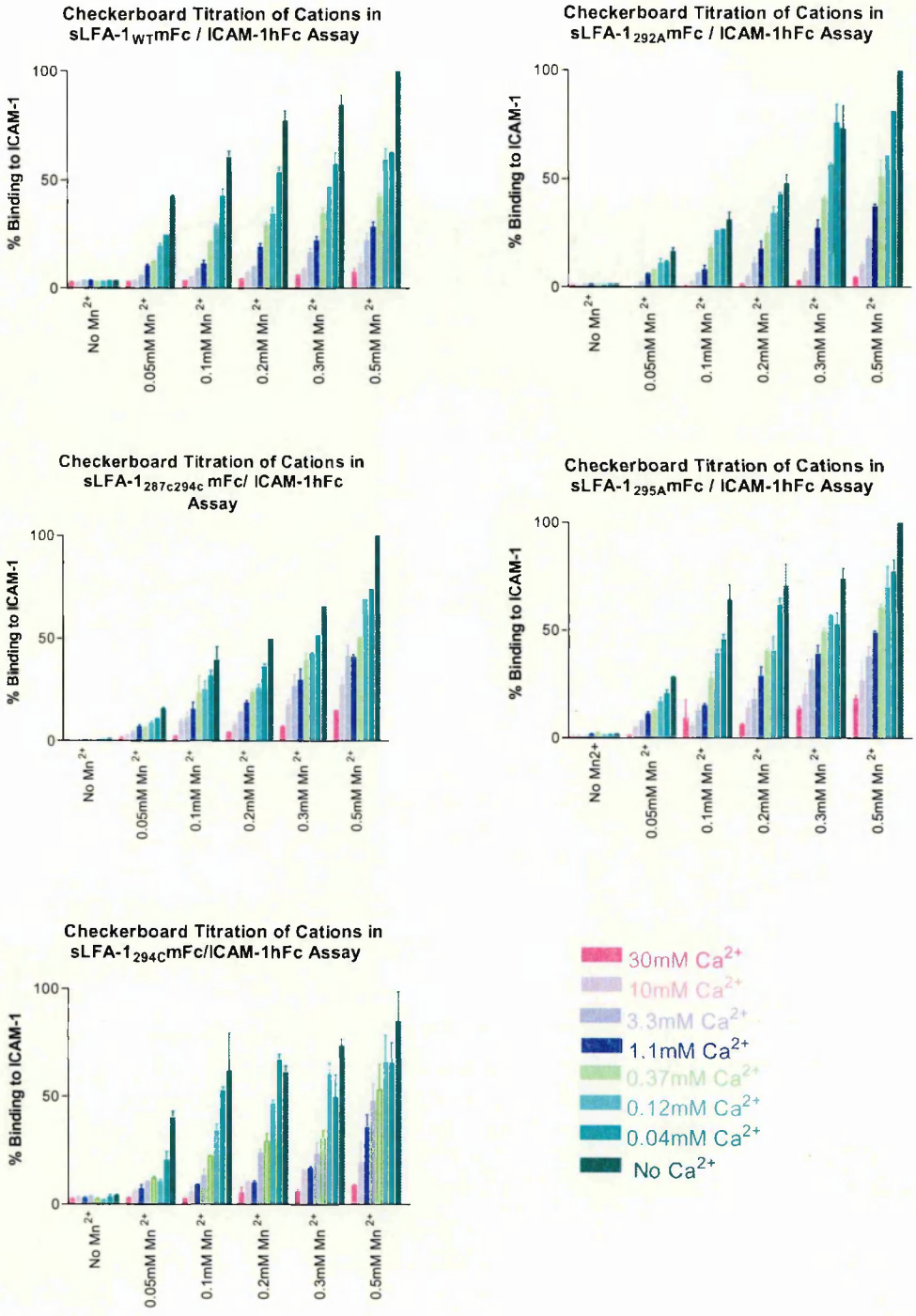

Figure 4.11 **Inhibitory effect of Ca^{2+} on Mn^{2+}-induced binding of LFA-1 to ICAM-1.** Captured integrin was depleted of divalent cation by washing (x2) in 20mM EDTA/TBS followed by 4 washes in TBS. 50µl of 400ng/ml ICAM-1hFc in TBS/0.1% BSA, pH7.5 was added to each well along with 50µl of 2X required concentrations of Ca^{2+} and Mn^{2+} in TBS/0.1% BSA, pH7.5. The results are expressed in terms of percentage binding, with 100% binding defined as the maximal signal seen with optimal concentration of Mn^{2+}. Each data point represents mean +/- SD (n=3) and data presented here are representative of 2 or more independently conducted experiments

4.9 Discussion

This chapter describes the generation of a series of soluble forms of LFA-1 containing mutations within the IDAS of the αL I domain and the effects these mutations have on the activation state of LFA-1 compared to wild type. A soluble active derivative of the integrin α4β1hFc generated by fusing the extracellular regions of the α4 and β1 subunits to separate Fc domains of the human immunoglobulin γ1 has previously been reported (Stephens *et al.*, 2000). Analysis of this construct showed that co-expression of these chimaeric molecules resulted in dimerisation of the α and β subunits, presumably brought about by the CH3 domains of the immunoglobulin and maintained by formation of disulphide bridges in the hinge region (Stephens *et al.*, 2000). A similar method using mouse immunoglobulin Fc (γ1 isotype) domains was utilised in this study to generate a soluble form of LFA-1. Mouse Fc regions rather than human were used as purified ICAM-hFc's were already available and allowed for development of ELISA-based ligand binding assays using anti-mFc capture and anti-hFc reveal. Non-reduced Western blotting analysis of the sLFA-1mFc constructs, in addition to assembly assay results, also confirmed heterodimer formation of the αL and β2 subunits using mFc tails. However, expression levels of many hFc/mFc-tagged soluble integrins have been shown to vary greatly from integrin to integrin, with expression levels of integrins with hFc tails being generally higher (personal communication, V. Perkins). These expression levels also compare unfavourably to levels of soluble LFA-1 expression in CHO-K1 cells of 1.0μg/ml reported by Tominaga *et al.* (1998). In this instance, stop codons were introduced directly before the beginning of the transmembrane domain of both the αL and β2 subunit DNA sequences and no tagging system was employed. That Tominaga's group reported functionally active integrin suggests that dimerisation of the α and β subunits occurs without the need for interacting tails. However, efforts within this laboratory to generate active LFA-1 without tagging was unsuccessful.

Production of a soluble form of LFA-1 using the mFc tagging system also generated a functionally active form of the integrin. While sLFA-1_{WT}mFc bound to ICAM-1hFc in the presence of Mn^{2+} in a concentration-dependent manner only minimal binding was seen when soluble ICAM-2hFc and ICAM-3hFc were used as ligands in the presence of Mn^{2+}. In the case of all three ligands further binding could be stimulated on addition of stimulating mAbs (See Figure 4.5).

Introduction of a range of mutations in and around the IDAS had varied effects on expression and ligand binding of sLFA-1 compared to wild type. Substitutions at residues L295A, F292A and K287C/K294C increased the expression of sLFA-1 over sLFA-1_{WT}mFc as measured by mIgG ELISA and Western blotting analysis. Whether these substitutions increase transcription or translation or stabilise the protein allowing for the increased potential for heterodimer formation is unknown. Interestingly, the double substitution at L295A/I306A, which appeared to be highly expressed as measured by mIgG ELISA, was shown to consist predominantly of β2 homodimers by Western blotting analysis. It has previously been shown (unpublished results) that soluble β2hFc can be expressed independently of the α subunit, and although the number of β2 mAbs that do not require the presence of the α-subunit to bind is limited, binding to both KIM127 and KIM185 has been shown. The introduction of the double substitution may therefore have lead to a misfolding of the αL subunit rendering it unable to pair with the β2 subunit.

Mutational analysis of the IDAS within the context of the soluble integrin confirmed that this region has a major role to play in controlling the affinity of integrin for ligand. This was most evident in binding experiments with ICAM-2 and ICAM-3 where sLFA-1_{WT}mFc was unable to bind ligand above background level in the presence of Mn^{2+} without the addition of activating mAbs, whereas introduction of alanine substitutions at positions L292, L295, I235, I306, a cysteine substitution at residue K294, and a double cysteine substitution at residues K287 and K294, enabled the integrin to bind ligand constitutively. This higher affinity of wild type LFA-1

for ICAM-1 over ICAM-2 and -3 has previously been reported in the literature for both cell surface expressed LFA-1 and isolated I domain with the measured K_D for ICAM-1 (173nM) shown to be ~3 times and ~20 times less than that for ICAM-2 and ICAM-3, respectively (Shimaoka *et al.*, 2001; Labadia *et al.*, 1998; de Fougerolles *et al.*, 1994; Woska *et al.*, 1998). Several attempts to measure the K_D of sLFA-1_{WT}mFc for the 3 ligands, by Biacore, were made during the course of this study but were unsuccessful due to the low concentrations of heterodimer in cell culture supernatants.

Shimaoka *et al.* (2001) have previously shown that the introduction of the double cysteine mutation at positions 287C and 294C promoted the formation of a cysteine bond that appeared to 'lock' the α7 helix in a downward position that resembled the 'open' conformation seen in crystal structures of the αM and α1 I domains when complexed with ligand. This group also showed that soluble I domain containing this double mutation had a ~9000 fold increase in affinity over wild type LFA-1 on binding to ICAM-1. Although the increase in ICAM-1 binding with sLFA-$1_{287C294C}$mFc relative to sLFA-1_{WT}mFc seen in our studies appears to be much lower than that reported by Shimaoka *et al.*, the increased binding is still significant and suggests that other domains within the extracellular region of the integrin may impose constraints on the I domain and thus influence its ability to bind ligand. The increases in ICAM-1 binding appear to be more similar to that seen by Huth *et al.* (2000) on introduction of sLFA-1_{235A} and sLFA-1_{306A} mutations into an LFA-1 COS expression system.

Xiong *et al.* (2000) have previously shown that mutation in the αM I domain at I316 (equivalent to I306 in αL) to glycine increased the affinity of recombinant soluble αM I domain for its ligands and was sufficient to favour the 'open' conformation. The side chain of I306 appears to pack into a hydrophobic pocket between the C-terminal α-helix and the opposing β-sheet in the 'closed' conformation, but due to the downward movement of this helix in the 'open' conformation, this residue cannot pack against the side of the domain in the 'open' conformation and is not visualized in the crystal structure of αM in the 'open' conformation (Lee *et al.*, 1995).

Consistent with observations made from the αM I domain, alanine substitution at I306 of αL in this study also increased adhesion to ICAM-1. While this suggests that I306 has a role to play in restraining the αL I domain in an inactive conformation, the ability of activating mAbs to further increase ligand binding also suggests that altering the chemical nature of the amino acid at position 306 is not sufficient to completely push the equilibrium in favour of the 'open', active conformation.

Arnaout's group (Li *et al.*, 1998) also mutated F302 at the top of the β6-α7 loop in the αM I domain which was shown to be buried in the 'closed' conformation and exposed in the 'open' conformation of the αM I domain crystal structures. This residue is equivalent to F292 in the αL I domain and mutation of F302 to a tryptophan appeared to stabilize the 'open' conformation and increase ligand binding. In our study, sLFA-1_{292A}mFc also showed increased ligand binding compared with sLFA-1_{WT}mFc. Interestingly, binding of sLFA-1_{292A}mFc could be further enhanced on addition of activating mAbs. This result suggests that although mutating F292 to alanine does not 'lock' the I domain in an active conformation, an alanine at this position preferentially shifts the equilibrium towards the active conformation and may represent an intermediate conformation between inactive, 'closed' and active, 'open'. Shimaoka *et al.* (2003) have since shown that in the low affinity, 'closed' conformation, F292 in the αL I domain is buried in a hydrophobic pocket and its removal from this pocket appears to be a key factor in enabling rearrangement at the MIDAS to allow ligand binding. Therefore, by mutating this residue to alanine, the interactions that normally hold it in the hydrophobic pocket are presumably lost and hence no longer hold the I domain in the 'closed' conformation. We hypothesise that an alanine substitution at residue L295, further down on the α7 helix, behaves in a similar way by reducing the number of interactions with sides chains of other residues that would hold it in the inactive, 'closed' state. However, unlike the case with sLFA-1_{292A}mFc, activating mAbs cannot further activate sLFA-1_{295A}mFc.

Interestingly an alanine substitution at position F299 completely abrogated LFA-1 ligand binding even though expression levels of sLFA-1_{299A}mFc were double that seen for sLFA-1_{WT}mFc and the former protein appeared to fold and dimerise efficiently, as evidenced by the assembly assays. The complete lack of ligand binding with this protein, even in the presence of activating mAbs, suggests that the presence of a phenylalanine at this position on the α7 helix has a role to play in forming hydrophobic interactions with other residues both inside and outside the IDAS. There are no previous reports of substitution at the 299 position.

Binding of all mutant forms of sLFA-1mFc to ICAM-1, -2, -3 was fully blocked by DA36. However, the inability of 6.5E to completely block the interaction of sLFA-1_{295A}mFc with ICAM-1 and sLFA-$1_{287c294c}$mFc with all three ligands suggests this mAb favours the 'closed' conformation of the I domain. The epitope of 6.5E has been reported to be located at the top of the β-subunit I-like domain (Huang *et al.,* 2000) and so its ability to block the LFA-1/ICAM interaction is probably through an allosteric mechanism because of the distance between the 6.5E epitope and the ligand binding site epitope. The fact that 6.5E binding was shown by FACS analysis not to be affected by introduction of the 287C294C mutation (Lu *et al.*, 2001) suggests that the shift downwards of the α7 helix hinders the ability of 6.5E to effect allosteric inhibition. When 6.5E is added in the presence of activating mAbs its capacity to block ICAM-1 binding is further reduced and is almost totally abolished in the case of sLFA-$1_{287C294C}$mFc. The reduced capacity of 6.5E to block ligand interactions is unlikely to be due to steric hindrance because of the distance between the epitopes. It is more likely that activating mAbs bind to a proportion of the sLFA-1mFc molecules and stabilizes them in the active state which affects allosteric inhibition by 6.5E. With sLFA-$1_{287C294C}$mFc, the binding of the activating mAbs must further stabilize the active conformation reducing even further the capacity of 6.5E to block through allosteric means.

Results shown here also demonstrated that certain mutant forms of LFA-1 (sLFA-$1_{287C294C}$mFc, sLFA-1_{295A}mFc and sLFA-1_{294C}mFc) cannot be further activated by activating mAbs, which supports and extends previous work using cysteine substitutions that allow the introduction of disulphide bonds and thus lock the I domain in a fully activated form (Shimaoka *et al.*, 2000). It is unlikely, however, that single mutations allow the formation of physical restraints similar to the disulphide bond. Instead, removal of the bulky groups that link the β6 and α7 helix may reduce the energy barrier sufficiently for the α7 helix to shift downward and a take up a position similar to that seen in the locked 'open' conformation of Shimaoka's 287C294C I domain. This has also been suggested by Huth *et al.* (2001) who investigated the effects of a wide range of mutations within the IDAS. They proposed that large hydrophobic amino acids within the IDAS such as I306, I235 and I255 sit in a pocket creating an energy barrier to conformational change in the I domain which stabilizes the 'closed' conformation. On the other hand, hydrophilic amino acids on the surface of the IDAS such as K232, K287, Q303, K304 and K305 appear to stabilize an active state by interacting with other amino acids in LFA-1.

Interestingly, although Shimaoka *et al.* (2001) claim that it is the introduction of the disulphide bond rather than the mutations themselves that generates a constitutively active form of the I domain, the introduction of a single cysteine substitution at position K294 also appears to constitutively activate LFA-1 in our system. This sLFA-1_{294C}mFc protein behaves in a similar manner to sLFA-$1_{287C294C}$mFc and, indeed, cannot be further activated by mAbs. Mutation of K294 to alanine had previously been shown to behave in a similar manner to wild type (Huth *et al.*, 2000) suggesting that the chemical nature of the substitution affects the overall conformation of the IDAS. Shimaoka *et al.* (2001) provide no data on the binding capacity of the 294C mutant within the context of an isolated I domain but expression of full length LFA-1 in a T293 cell system showed it to be constitutively active although wild type LFA-1 behaved in a similar manner.

In contrast, mutation of the K287 residue to cysteine did not appear to alter ligand binding over that seen for wild-type but was inducible by activating Abs. Huth *et al.* (2000) showed that whilst a K287A mutation reduced binding below wild type, increased binding was achieved on addition of an activating mAb. Interestingly, in the present study introduction of the K287F mutation had a detrimental effect on the LFA-1/ligand interaction which could not be rescued by activating mAbs (data not shown). Comparison of the α subunits of the leucocyte integrin family show that this position in all the α subunits, except αL, contains a conserved phenylalanine. Results suggest that a phenylalanine at this position in other members of the β2 family I domains may explain their reduced affinity for ICAM ligands compared to LFA-1.

The determination of the overall conformation of the sLFA-1Fc constructs is beyond the scope of this study. However, because there are no restraining cytoplasmic tails, we hypothesise that the molecule is quite flexible and could oscillate from the 'bent, inactive' conformation to the 'upright, active' conformation, with a proportion of the molecules at any one time primed for ligand binding. This hypothesis is similar to that suggested by Drbal *et al.* (2001) from analysis of their soluble integrins. If this is the case, it could explain the ability of KIM127, KIM185 and MEM148 to further activate sLFA-1_{WT}mFc and several of the mutated forms of sLFA-1mFc since one could postulate that such mAbs bind to integrin flexed in the active conformation and stabilize it. KIM127 and other activating mAbs which bind in the β2 stalk region are thought to work by acting as a wedge to break the α and β domain-domain contacts when in the 'upright active' conformation (Huang *et al.*, 2000). Such a hypothesis would also argue that mutants that cannot be further activated in the presence of mAbs were already in the optimum conformation for ligand binding. In these cases, the preferential positioning of the α7 helix in the downward position may alter the position of the other extracellular domains and hold the construct in the 'upright active' form. The epitopes for the activating mAbs would therefore be available for binding but not required to stabilize the conformation.

Characterisation of Lovastatin / αL I domain interaction by Kallen *et al.* (1999) showed that the main contacts between ligand and protein are formed by the side chains of the residues Leu132, Phe153, Ile235, Tyr257, Lys287, Leu298, Glu301, Leu302 and Lys305. Comparison of the unliganded (Qu and Leahy, 1995) and Lovastatin-bound αL I-domain crystal structure showed that only minor differences, especially in the MIDAS, exist between both structures (Kallen *et al.,* 1999). This suggested that Lovastatin functions by stabilizing the inactive conformation, and results from the present study support this conclusion. Although Lovastatin inhibited the ICAM-1/LFA-1_{WT}mFc interaction by ~75%, the inhibitory capacity of this compound on ICAM-1 binding to sLFA-$1_{287C294C}$mFc, sLFA-1_{295A}mFc and sLFA-1_{294C}mFc was sharply reduced, indicating that the I domains of these mutated forms of sLFA-1 are predominantly in the 'open', active conformation.

It is well established that integrins require divalent cations to support ligand binding (Marlin and Springer, 1986; Dransfield and Hogg, 1989; Dransfield *et al.*, 1990, 1992) and recent crystallographic studies of the I domains with ligand have confirmed that cation binding in the MIDAS is essential for ligand binding. Previous analysis of a soluble α4β1 construct have shown that both Mn^{2+} and Mg^{2+} support VCAM binding, with 1mM Mn^{2+} and >10mM Mg^{2+} required to give maximal binding (Stephens *et al.,* 2000). Data presented here suggests that 0.5mM Mn^{2+} and 1mM Mg^{2+} are required for optimal binding of sLFA-1mFc constructs. Introduction of mutations within the IDAS site do not appear to alter this requirement. Similar results were reported by Shimaoka *et al.* (2001) when comparing the cation requirement of cell expressed LFA-1_{WT} and LFA-$1_{287C294C}$. These findings are not surprising as the IDAS is distal to the MIDAS and no cation binding site that could be affected by the introduction of selected mutations has been identified in the IDAS region.

Several studies have shown that, whilst the divalent cations, Mn^{2+} /Mg^{2+}, are required for ligand binding, Ca^{2+} appears to inhibit LFA-1/ligands interactions (Dransfield *et al.*, 1992; Jackson *et al.*, 1994) and that subtle changes in the ratio between Mn^{2+} /Mg^{2+} and Ca^{2+} may actually be a controlling factor in the activation of LFA-1, and integrins in general (Labadia *et al.*, 1998; Rothlein and Springer, 1986; Stewart *et al.*, 1996). In the present study, Ca^{2+} was shown to inhibit Mn^{2+}-dependent sLFA-1/ICAM-1 binding in a concentration dependent manner suggesting that both cations compete for binding sites on the LFA-1 molecule. The results also show that Ca^{2+} is not capable of supporting ligand binding even at high (mM) concentrations. Similar findings of cation competition were also reported by Labadia *et al.* (1998). Using surface plasmon resonance to measure ligand binding they showed that titration of Ca^{2+} into the millimolar concentration range, in the presence of Mg^{2+}, resulted in a dose dependent decrease in ICAM-1 binding. Measurement of the binding constants of Mg^{2+} and Ca^{2+} (K^{Mg}_{ICAM} (133nM) and K^{Ca}_{ICAM} (11μM) respectively) suggest that, at high concentrations, Ca^{2+} could competitively displace Mg^{2+}. Interestingly, *in vivo* cation concentration measurements have shown that levels of Mg^{2+} increase significantly, with a similar corresponding decrease in the concentration of Ca^{2+}, during injury and trauma and this increase in Mg^{2+} correlates with increased integrin-dependent migration of inflammatory cells to the site of injury (Grzesiak and Pierschbacher, 1995).

Overall, this chapter has demonstrated that the introduction of select mutations within the IDAS can have a major effect on the ability of LFA-1 to bind integrin in a cell free system. While several of the mutations appeared to shift the equilibrium in favour of the 'open' conformation, an alanine substitution at position F299, which although expressed well, had a deleterious effect on ligand binding. The introduction of these mutations and their ability to alter the activation state of LFA-1 also appears to have no effect on the cation requirement of the integrin. In light of these results it is of interest to determine if the introduction of similar mutations, especially the novel single mutations at positions F292 and K294, into a cell surface expressed form of

LFA-1 would behave in a similar manner compared to wild type or whether other factors such as cytoplasmic restraints would over ride their effects.

Chapter 5

Effect of I Domain Mutations on Activation and Binding Properties of LFA-1 in the K562 Cell System

Chapter 5 Effect of I Domain Mutations on Activation and Binding Properties of LFA-1 in the K562 Cell System

5.1 Introduction

Data in chapter 3 showed that introduction of certain mutations within the I domain of soluble forms of LFA-1 lead to an increase in the affinity for its ligands ICAM-1, -2 and -3. Since this system is dependent only on affinity changes arising from conformational changes induced by the mutations, it was of interest to see if such mutations would have the same effect in a cell system. It is known that cell adhesion can have a large avidity component and it is not clear what the effects would be of increasing affinity without necessarily changing the avidity of the interaction.

Previously, this laboratory has generated a K562 cell line expressing full length wild-type LFA-1 (KL4 cell line) and showed it to be functionally active and able to bind the appropriate ligands (Ortlepp, 1997). Other laboratories have also successfully transfected K562 cells with LFA-1 (Bleijs *et al.*, 2000; Lub *et al*, 1997) as well as other members of the integrin family including VLA-4 (Masumoto *et al.*, 1993) and VLA-6 (Delwel *et al.*, 1996). The K562 cell line is a non-adherent human erythroleukaemic cell line originally established by Lozzio and Lozzio (1981) from the pleural effusion of a patient with chronic myelogenous leukaemia. As this cell line also shows no significant expression of β2 integrins (Hickstein *et al.*, 1993) (See Table 5.1) it makes it an ideal cell line in which to study the activation and binding properties of various transfected mutated forms of LFA-1 without interference from other members of the β2 family. The presence of endogenous α5β1 also makes it possible to investigate the extent of crosstalk between α5β1 and LFA-1 within such newly generated cell lines.

Using KL4 cells as our wild type control, the K562 parental cell line was stably transfected with double gene vectors containing full length LFA-1 carrying a range of mutations that had previously been introduced into the soluble-Fc system. This chapter will outline the generation and selection of these cell lines and describe the results obtained from ligand binding studies in the presence and absence of activating and blocking agents.

5.2 Characterisation of K562 Cells

Prior to transfection of K562 cells with the various mutant forms of LFA-1, the cell line was evaluated for expression of α and β integrin chains on the cell surface by flow cytometry using several Abs to the same antigen. Results are shown in Table 5.1.

5.3 Expression of mutant forms of LFA-1 in the K562 cell line

K562 cells were stably transfected using electroporation with double gene vectors encoding β2 and one of the 5 mutations listed in Table 5.2. Individual vectors were DNA sequenced with primers to the I domain region just prior to transfection to verify the presence of the mutation(s). Following positive selection using the G418 selection method, clonal selection was carried out by several rounds of flow cytometry analysis using antibodies to both the α and β chains (HI111 and CTB101) and 6.5E which requires the αβ heterodimer to be correctly folded for detection. Expression of the antibody epitopes is similar for all cell lines except for the $K562_{287C294C}$ cell line, which has much lower expression of the HI111 epitope but has similar CTB101 and 6.5E expression (Fig 5.1). The fact that the single mutation, 294C incorporated into the K562 cell line behaves in a similar manner to the KL4 cell line suggests that either the 287C mutation, or

the combination of both mutations in close proximity to each other, distorts the HI111 epitope and leads to reduced antibody binding.

Ab Name	Antigen	Host Species	Isotype	K562 n=1	K562 n=2
No Ab				ND	2.55
MOPC21	Control	mouse	IgG1	0.1	3.77
BHA2.1	hα2β1	mouse	IgG1	3.25	6.13
Y9A2	hα9β1	mouse	IgG1	ND	7.39
TS2/7	hα1	mouse	IgG1	7.17	8.14
C3II.1	h α3	mouse	IgG1	3.91	4.11
Max68P	h α4	mouse	IgG1	5.75	5.07
TS2/16	h β1	mouse	IgG1	173	103.74
LM609	h αvb3	mouse	IgG1	3.73	9.65
AB1926	h β5	rabbit	polyclonal	3.17	2.59
E7P6	h αvβ6	mouse	IgG1	4.38	5.34
sevenE3	h αIIbβ3	mouse	IgG1	7.72	11.6
AMF-7	h αV	mouse	IgG1	4.55	3.15
BP6	h β7	mouse	IgG1	3.7	3.12
LF61	h αE	mouse	IgG1	5.01	5.27
DA36	αL(I Domain)	mouse	IgG1	3.97	3.4
R7.1	h αL	mouse	IgG1	7.78	7
KIM247	h αM	mouse	IgG1	8.4	9.54
KIM249	h αM	mouse	IgG1	11.02	17.98
KIM185	hβ2	mouse	IgG1	8.3	4.7
KIM202	hβ2	mouse	IgG1	4.08	3.66
KIM215	hβ2	mouse	IgG1	4.01	3.76
6.5E	h αL β2	mouse	IgG1	10.2	9.7
KIM 75	h αM β2	mouse	IgG1	8.46	10.6
αD	h αD	mouse	IgG1	3.96	2.88
15.2	ICAM-1	mouse	IgG1	256.31	109.96
MCA1140	ICAM-2	mouse	IgG1	114.4	38.91
MCA1485	ICAM-3	mouse	IgG1	3.79	ND
Cal3.10	ICAM-3	mouse	IgG1	8.12	8.7
Ig11	VCAM	mouse	IgG1	4.67	4.34
UPC10	gG2a Control	mouse	IgG2a	6.84	5.44
CBR-IC/2	ICAM-2	mouse	IgG2a	46.13	ND
MEM111	ICAM-1	mouse	IgG2a	122.59	64.61
HA5	α5 β1	mouse		133.61	55.1
P1D6	α5	mouse	IgG3	127.94	97.21
sc6597	α6	goat	polyclonal	6.09	5.9
sc6638	β8	goat	polyclonal	4.17	4.22
sc6628	β4	goat	polyclonal	4.62	5.02
Ab3.9	αX	mouse	IgG1		2.46

Table 5.1 **FACS analysis of parental K562 cells.** Results are shown as mean fluorescence intensity in arbitrary units and are from two determinations carried out on separate days. Antibodies that showed high levels of binding are highlighted in red.

Residue	Change	Effect on activity in Soluble system
287 and 294	287K→287C, 294K→294C	>WT
235	235I→235A	>WT
306	306I→306A	>WT
294	294K→294C	>WT
292	292F→292A	>WT

Table 5.2 **List of mutations introduced into LFA-1 and expressed in K562 cells.**

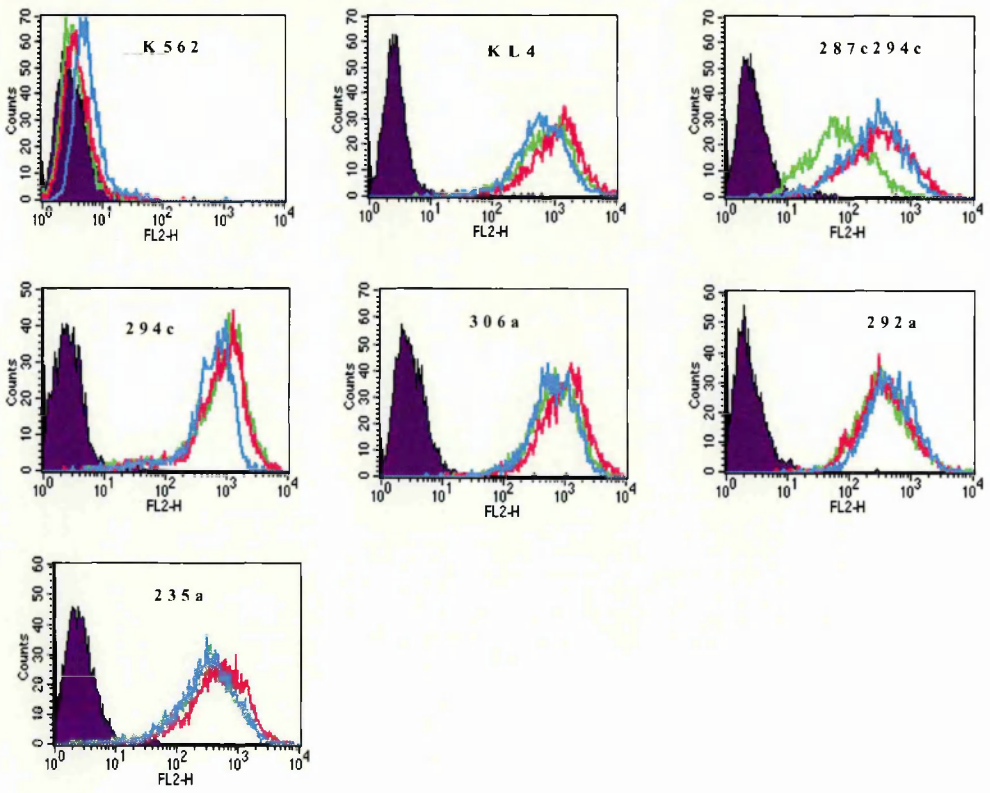

Figure 5.1 **FACS analysis of final stable cell lines chosen for each introduced mutation.** Cells were stained with HI11 (αL)(Green), CTB101 (β2) (Blue), 6.5E(αLβ2) (Pink) or the isotype control MOPC21 (Purple). The above profiles are representative of 6 or more independently performed experiments.

5.4 Binding of LFA-1 Expressing K562 Cells to ICAMs

Chapter 4 showed that the affinity of the soluble-expressed LFA-1 could be dramatically increased when select mutations were introduced into the IDAS of the I domain and it was therefore of interest to see if expression of these mutated forms of LFA-1 on the cell surface would also induce binding in the absence of stimulus. To study the binding of the various LFA-1-expressing K562 cell lines to ICAM ligands, cells were incubated on plates coated with anti-hFc-captured ICAM-1hFc, ICAM-2hFc, or ICAM-3hFc in the presence of cations, activating mAbs, blocking mAbs or other stimulating agents with the degree of cell binding being measured using a simple cell stain.

Figure 5.2 shows binding of transfected K562 cell lines to immobilized ICAM-1hFc. As expected, the untransfected K562 cell line is unable to support ligand binding even in the presence of activating mAbs. The KL4 cell line, which expresses LFA-1_{WT} on the cell surface, is also unable to support ICAM-1hFc binding when the assay is carried out in complete media which contains both Mg^{2+} and Ca^{2+} at concentrations of ~1mM and ~1.8mM respectively. The level of binding is increased when KL4 cells are incubated in media containing 1mM Mn^{2+} but it is only on the addition of activating mAbs KIM127 and KIM185 that maximal binding is achieved with cells expressing wild type LFA-1.

In contrast to results with KL4 cells, all the mutated forms show a significant increase in binding to ICAM-1 in the presence of media alone and this binding is similar to, or greater than, the binding of KL4 cells in the presence of Mn^{2+} (Figure 5.2). The $K562_{287C294C}$ cell line shows approximately a 10-fold increase in binding above KL4, with the other mutated forms showing an increase of between 2- and 5- fold. The binding of all the mutant forms was further enhanced when cells were incubated with 1mM Mn^{2+} and again there is a significant 3-5-fold increase in binding over KL4 cells. Although there is some variation in levels of binding, addition of

KIM127 and KIM185, incubated with media alone or in the presence of Mn^{2+}, led to a similar level of binding with all cell lines.

Binding of the KL4 cell line to ICAM-2hFc and ICAM-3hFc, like ICAM-1hFc, also required the presence of activating mAbs to achieve optimal binding, with only low level binding in the presence of Mn^{2+} and only background binding in media alone. Constitutive binding of $K562_{287C294C}$ and $K562_{235A}$ to ICAM-2 and ICAM-3 in media alone was again observed and this binding was further increased by addition of Mn^{2+}. Although the binding of the $K562_{306A}$, $K562_{294C}$ and $K562_{292A}$ cell lines to ICAM-2 and ICAM-3 is significantly reduced compared to ICAM-1 in media alone, the level of binding was still approximately 2-fold higher than that seen for wild type and addition of 1mM Mn^{2+} restored binding levels of $K562_{294C}$ and $K562_{292A}$ to those seen for the $K562_{287C294C}$ and $K562_{235A}$cell lines. Interestingly, whilst the binding of the $K562_{306A}$ cell line to ICAM-1 in the presence of Mn^{2+} was comparable to the other mutant cell lines, comparison of levels of binding of this cell line with ICAM-2 and ICAM-3 showed ~50% reduced binding. Again, addition of KIM127 increases binding of all cell lines to ICAM-2 and ICAM-3 to similar levels.

These results suggest that introduction of mutations within the IDAS can activate LFA-1 although results shown here indicate that they are not capable of rendering the LFA-1 fully active as judged by the ability of mAbs and Mn^{2+} to further enhance binding. These results are in contrast to those seen with soluble forms of the integrin containing the 278C294C, 295A and 294C mutations. In the soluble system, introduction of these mutations fully activate the soluble integrin in the presence of Mn^{2+} and addition of activating mAbs could not increase binding further.

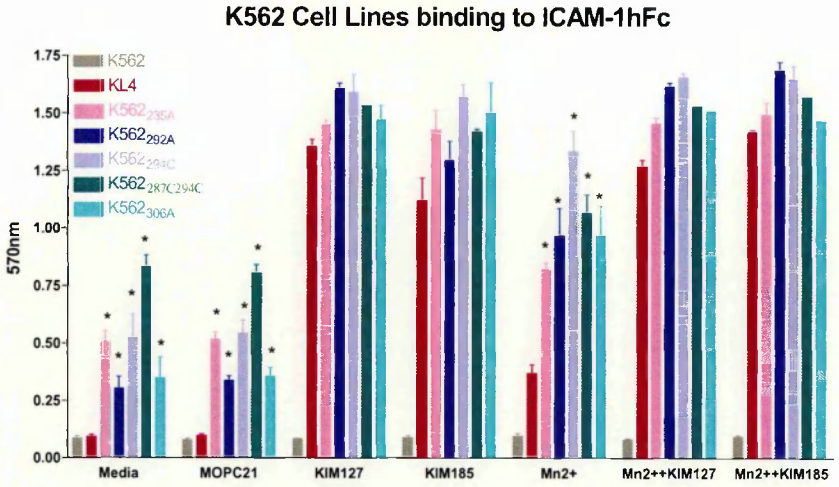

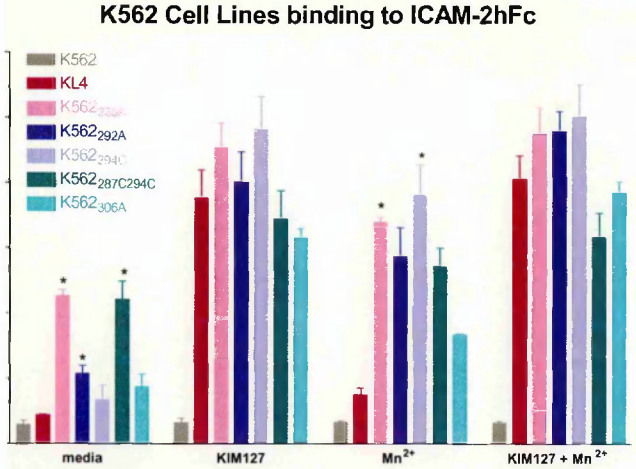

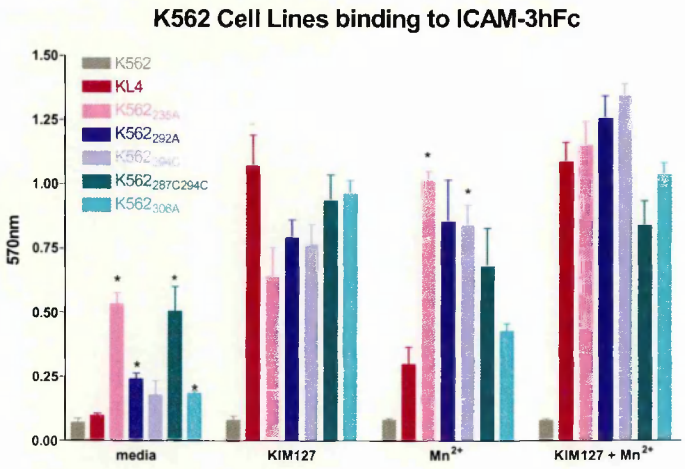

Figure 5.2 **Binding of K562 Cell-Lines to ICAM-1hFc, ICAM-2hFc and ICAM-3hFc.** $5x10^5$/ml of cells were washed and diluted in DMEM (media) alone or containing MOPC21 (control mAb), 1mM Mn^{2+}, 20µg/ml KIM127, 20µg/ml KIM185, 1mM Mn^{2+} + 20µg/ml KIM127 or DMEM containing 1mM Mn^{2+} + 20µg/ml KIM185. The degree of binding was assessed at 570nm using the Rose Bengal Assay. Each data point represents Mean +/- SD (n=3) and the data presented here are representative of that obtained in three other independently performed experiments. Statistical analysis was performed to compare KL4 binding with the other ICAM-1 binding K562 cell lines under the same conditions. * indicates significance $p<0.01$.

5.4.1 Binding of LFA-1 Expressing K562 Cells to ICAMs with blocking mAbs

To confirm that the enhanced binding of the mutants was LFA-1 dependent, the effects of known LFA-1 blocking mAbs were investigated. Figure 5.3 shows the binding profile of the cell lines in the presence of DA36 (αL mAb) and 6.5E (β2 mAb). As predicted DA36 blocked binding of all the LFA-1 expressing cell lines to all three ICAM ligands even when fully activated in the presence of KIM127. However, whilst 6.5E was also capable of significantly blocking the ICAM-1, -2, -3 interactions of KL4, $K562_{292A}$ and $K562_{306A}$ cell lines in the presence of Mn^{2+}, it was not as effective as DA36 in inhibiting ligand binding of the $K562_{287C294C}$ and $K562_{294C}$ cell lines. Also, in the presence of KIM127, the ability of 6.5E to block binding to all three ligands was reduced in all the mutant cell lines. This result is similar to the result seen for the soluble mutant constructs when 6.5E was added in the presence of KIM127 (see Figure 4.7).

5.4.2 Effect of PMA and Cytochalasin D on Ligand binding of K562 Cells

To gain an insight into the role the cytoskeleton might play in restraining the integrin in an inactive state, the effect of cytochalasin D was investigated. Several researchers have reported that addition of cytoskeletal-disrupting agents such as cytochalasin D have an enhancing effect on ligand binding (Van Kyook *et al.*, 1999, Leitinger *et al.,* 2000). This is thought to be due to the untethering of the cytoplasmic domains from cytoskeletal restraints, allowing lateral movement of integrins into clusters which increases the avidity of the integrin for ligand. Figure 5.4, however, shows that cytochalasin D has only a very slight positive effect on binding of all K562 cell lines to ICAM-1hFc. This result suggests that the majority of the integrin-mediated ICAM-binding of the K562 cells does not require an intact cytoskeleton. Phorbol esters such as PMA are known activators of the PKC pathway and have been shown to be a major regulator of 'inside out' signalling-induced integrin-mediated interactions which result in clustering of integrins on the cell surface (Stewart *et al.*, 1996; Lub *et al.*, 1997(a); Chapter 1 Section 5.1).

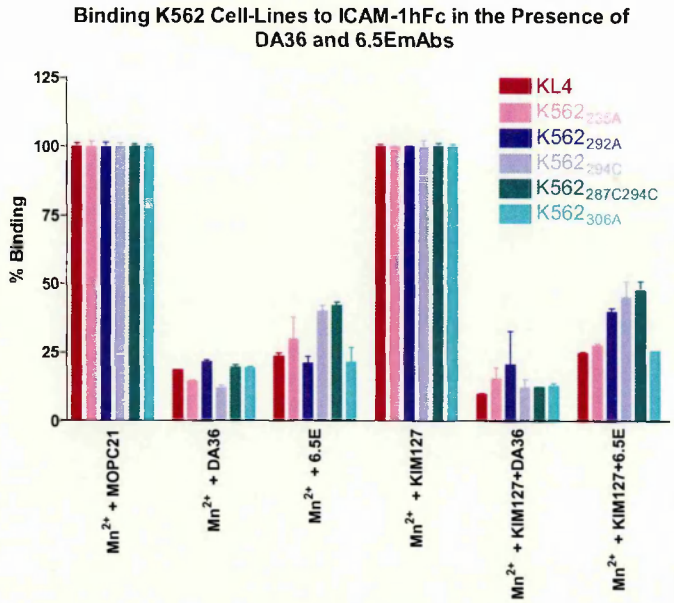

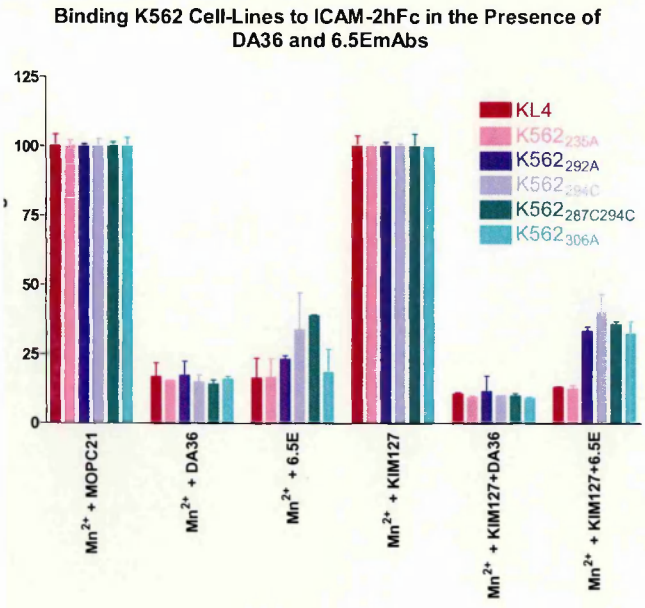

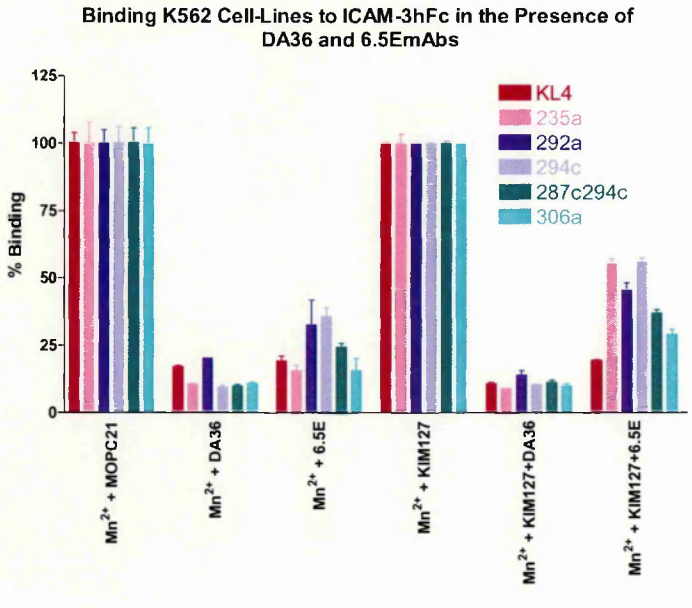

Figure 5.3 **Binding of K562 Cell Lines to ICAM-1, -2, -3 in the presence of DA36 and 6.5E mAbs.** $5x10^5$ /ml of cells were washed and diluted in DMEM containing 1mM Mn^{2+} (control) with or without 20µg/ml KIM127 or MOPC21 (control Mab) to which was added 20µg/ml DA36 or 20µg/ml 6.5E. The degree of binding was assessed at 570nm using the Rose Bengal Assay and 100% represents the binding of the individual cell lines under control conditions in the presence of MOPC21. Each data point represents Mean +/- SD (n=3) and the data presented here are representative of that obtained in three other independently performed experiments.

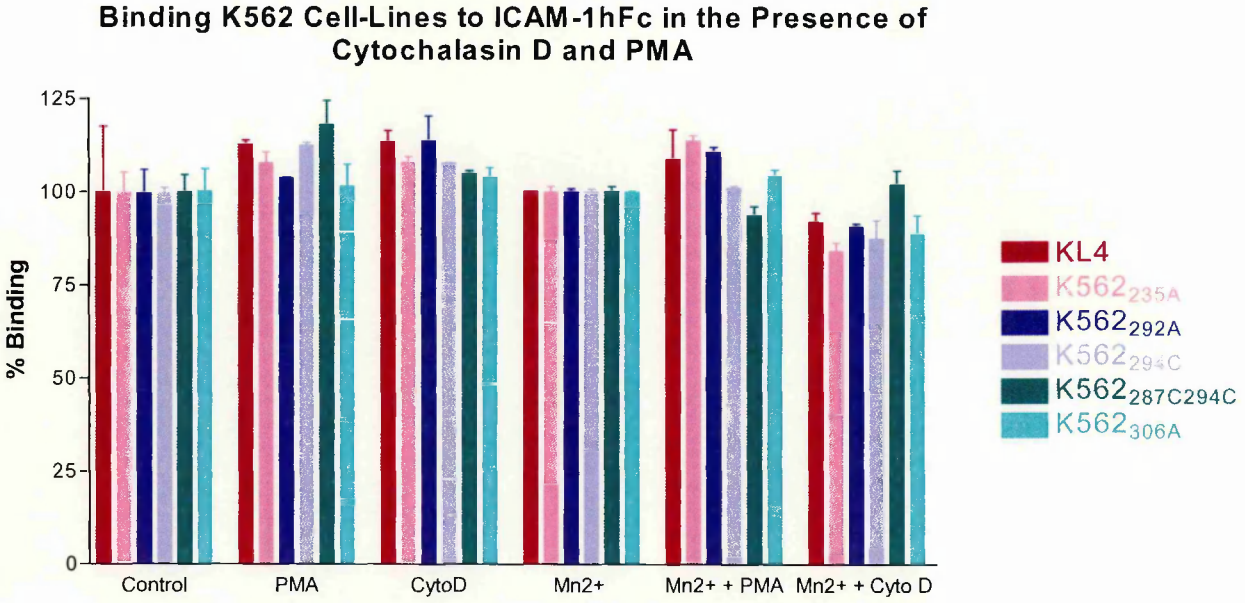

Figure 5.4 **Binding of K562 Cell Lines to ICAM-1hFc in the presence of Cytochalasin D and PMA.** Cells were washed and diluted in DMEM (control) in the presence or absence of 1mM Mn^{2+} with or without 5µg/ml Cytochalasin D (final) or 100ng/ml PMA (final). The degree of binding was assessed at 570nm using the Rose Bengal Assay. 100% represents the binding of the individual cell lines under control conditions both in the presence or absence of Mn^{2+}. Each data point represents mean +/- SD (n=3) and the data presented here are representative of that obtained in three other independently performed experiments.

In this study addition of PMA to most cell lines had a very slight positive effect on ligand binding relative to the control. However these effects were not statistically significant, which suggests that either upregulation of PKC in the K562 system has little effect on LFA-1 activation or that the integrins are already in a clustered state on the cell surface. The inability of PMA to activate K562 transfected cells has previously been noted by Ortlepp *et al.* (1997).

5.5 Integrin Crosstalk

Evidence is now emerging suggesting that integrin 'outside-in' signalling can alter the activity of neighbouring integrins in a process termed 'crosstalk' (Blystone *et al.*, 1994; Leitinger and Hogg, 2000). Several researchers have shown both up- and down-regulation of LFA-1-dependent ligand binding when other integrins are activated on the same cell surface (Van Kooyk *et al.*, 1993(b); Porter and Hogg, 1997; May *et al.*, 2000; Chan *et al.*, 2000).

As mutant forms of LFA-1 expressed in K562 cells appear to be partially activated it was of interest to see if these forms of LFA-1 (or indeed mAb-activated LFA-1) have an effect on the binding of other integrins expressed on K562 cells. Table 5.1 confirmed previously published data (Ortlepp, 1997) that the parental K562 cell line predominantly expresses only one integrin, $\alpha5\beta1$, on its cell surface. FACS analysis of $\alpha5\beta1$ expression on all the LFA-1 expressing cell lines was also carried out and showed that all the transfected cell lines expressed similar levels of $\alpha5\beta1$ (See Figure 5.5). Interestingly, the parental K562 cell line has slightly higher expression levels of $\alpha5\beta1$ compared with the other cell lines. Whether the transfection process caused this reduced expression level in transfected cells is unknown.

Initial analysis of the binding of K562 cells to fibronectin-coated plates showed that binding took place in the presence of media alone but that this could be enhanced by the addition of 1mM Mn^{2+} (Figure 5.6). Cells expressing various IDAS mutations bound to fibronectin in a similar manner to the parental cell line (Figure 5.6). There was slight variation in the binding levels of the transfected cells with the $K562_{235A}$ cell line showing a consistent trend towards increased binding, however, this did not reach statistical significance.

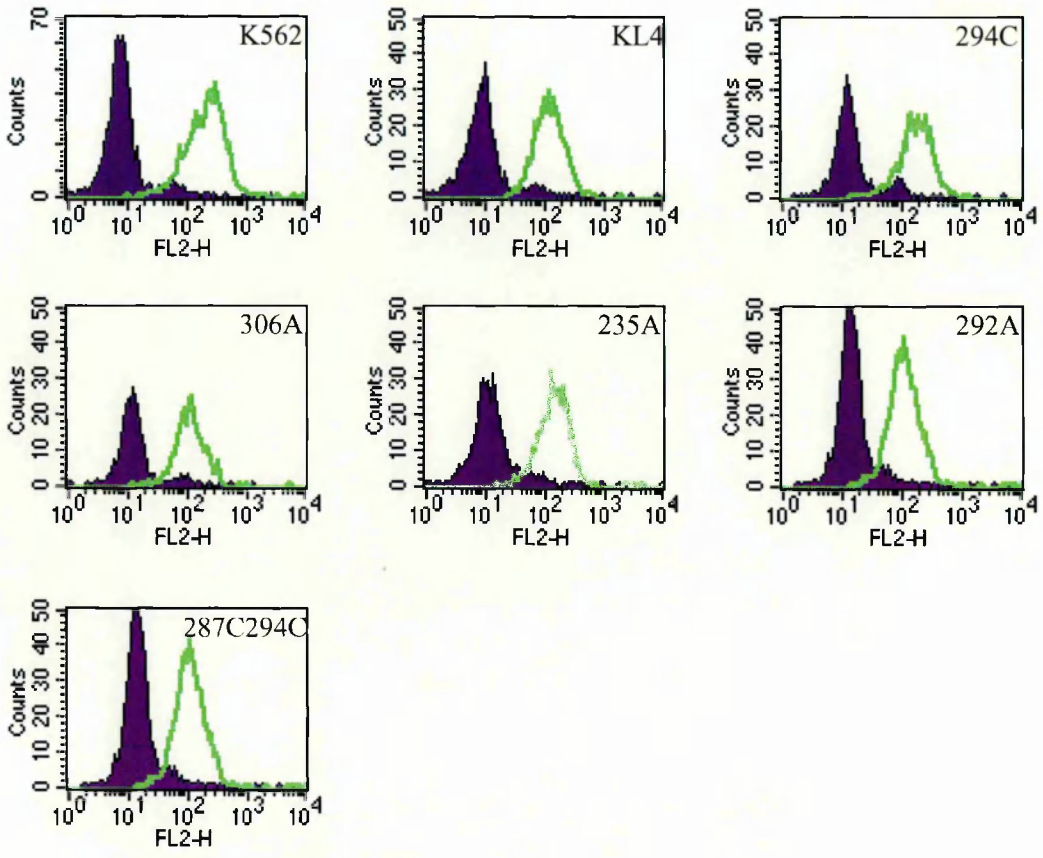

Figure 5.5 **FACS analysis of K562 cells for α5β1 expression.** Cells were stained with SAM-1-PE (α5)(Green) or MAB 1382E-PE (α4) (Purple). The binding of the α4 mAb was used as an isotype control as K562 cell line does not express α4β1. The above profiles are representative of 3 or more independently performed experiments.

Further characterisation of the binding of K562 cells to fibronectin showed that this interaction could be blocked by the α5 mAb, SAM-1 (Figure 5.7). The inability of Max68P to affect the binding of any of the cell lines to fibronectin supports previous findings that α4β1 is not expressed on the K562 cell line (Figure 5.7). The cells could also be further stimulated to bind ligand in the presence of the β1 activating mAb TS2/16. In these experiments, the variations in levels of binding were not statistically significant when compared to the parental K562 cell line. As this cell line does not express LFA-1, it suggests that the activation state of LFA-1 does not affect the binding of α5β1 to fibronectin.

5.5.1 Binding of K562 cells to Fibronectin in the presence of LFA-1 mAbs

Addition of LFA-1 blocking mAbs 6.5E and DA36 had no effect on the capacity of the K562 cell lines to bind fibronectin (Figure 5.8). This was an expected result since the original K562 cell line, which does not express LFA-1, binds in a similar manner to the LFA-1-transfected cell lines. Interestingly, however, maximal activation of the LFA-1-transfected K562 cell lines achieved by the addition of KIM127 appeared to increase the binding of all cell lines to fibronectin (Figure 5.9). The ability of the mAb SAM-1 to completely block this interaction (Figure 5.10) suggests that in the presence of KIM127 this increased binding is $\alpha5\beta1$ dependent and not through some other fibronectin receptor that may be present on the cell surface. This data suggests that LFA-1 may be able to crosstalk to $\alpha5\beta1$ under defined conditions. No such activation was noted for the parental K562 cell line. Data previously shown in Figure 5.2 demonstrated that binding of the LFA-1-expressing K562 cell lines to ICAM in the presence of KIM127 was similar and maximal for all cell lines. This data suggests that, whilst mutations within the IDAS site can increase affinity of LFA-1for ICAM ligands, this level of activation alone is not sufficient to support crosstalk with $\alpha5\beta1$. Effective crosstalk only appears to take place on addition of KIM127 which maximally activates all the cell lines.

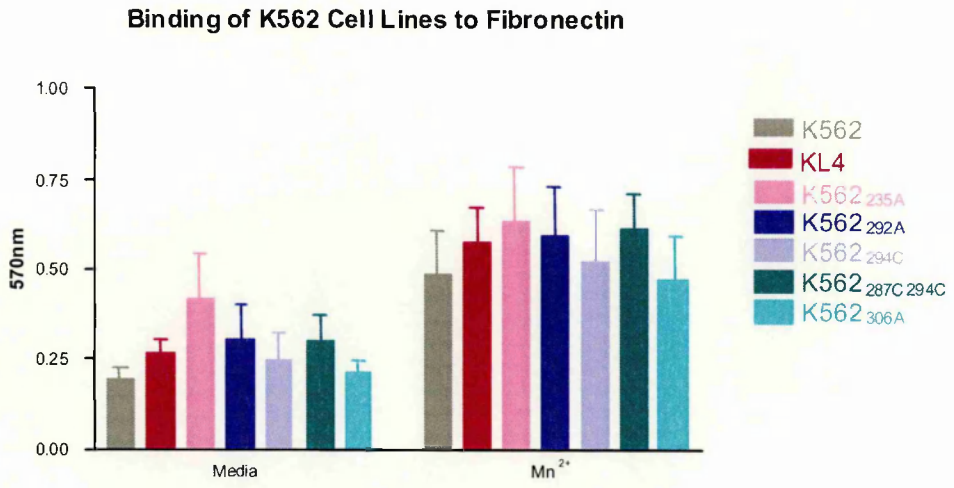

Figure 5.6 **Binding of K562 Cell Lines to Fibronectin.** $5x10^5$ /ml of cells were washed and diluted in DMEM (media) in the presence or absence of 1mM Mn^{2+}. The degree of cell binding to fibronectin coated plates was assessed at 570nm using the Rose Bengal Assay. The data presented here are the mean from 5 independently performed experiments (n=3 for each assay) +/- SD.

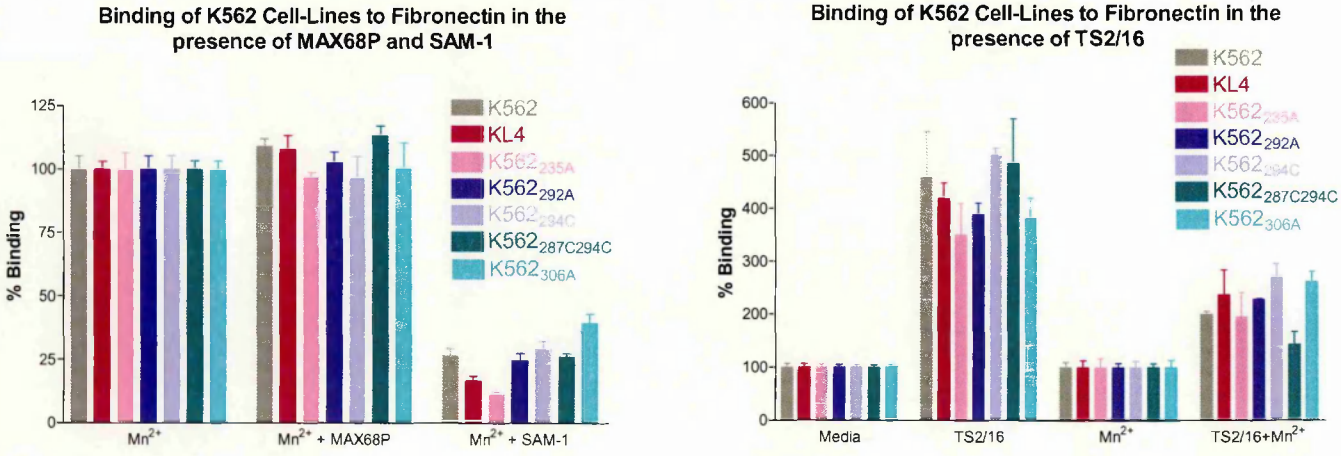

Figure 5.7 **Binding of K562 Cell Lines to Fibronectin in the presence of α5β1 Blocking and Activating mAbs.** In each experiment, 100% represents the binding of the individual cell lines in the presence of the control mAb MOPC21 either in the presence of media (DMEM) or Mn^{2+}. All mAbs were used at 20μg/ml. Each data point represents Mean +/- SD (n=3) and the data presented here are representative of that obtained in three other independently performed experiments.

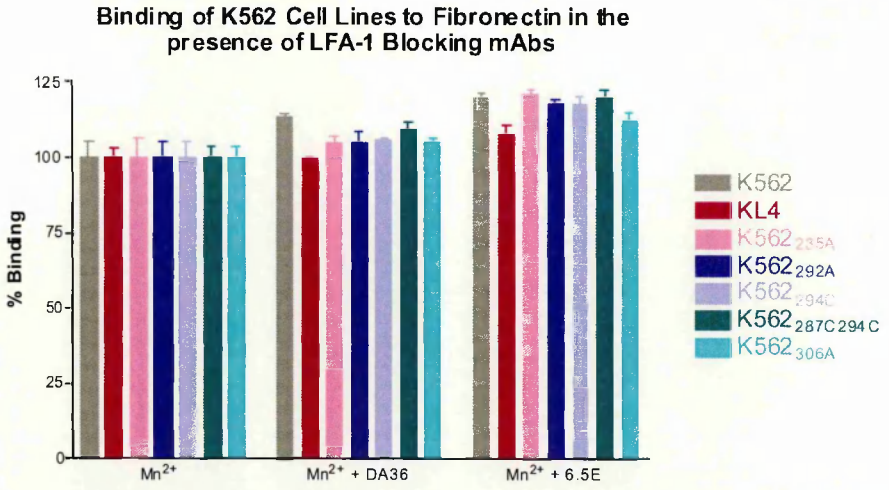

Figure 5.8 **Binding of K562 mutant cell lines to Fibronectin in the presence of LFA-1 Blocking mAbs.** $5x10^5$ /ml of cells were washed and diluted in DMEM (media) in the presence of 1mM Mn^{2+}. In each experiment 100% represents the binding of the individual cell lines in the presence of the control mAb MOPC21. All mAbs were used at 20µg/ml. Each data point represents mean +/- SD (n=3) and the data presented here are representative of that obtained in two other independently performed experiments.

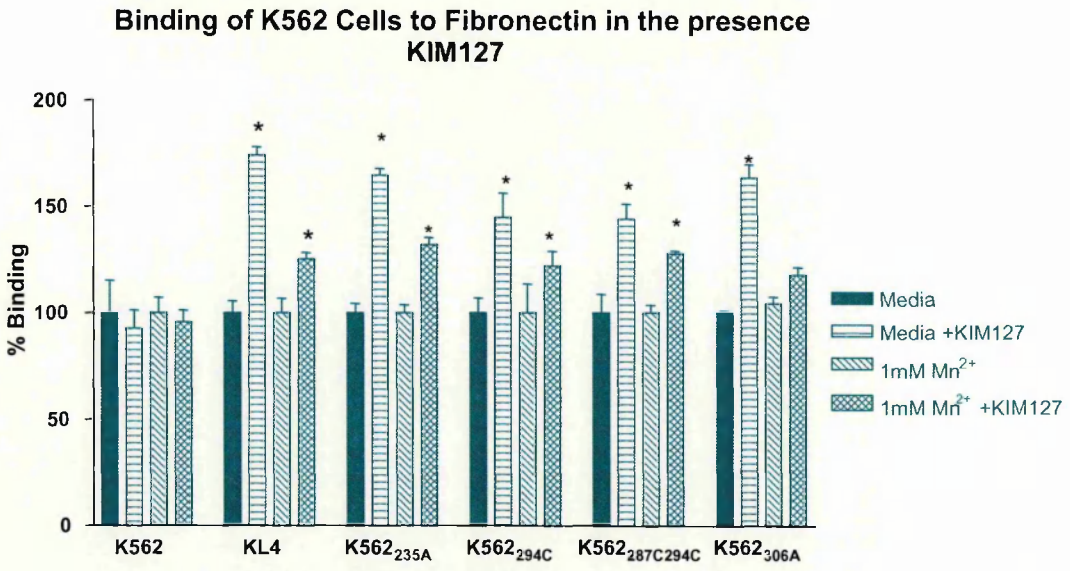

Figure 5.9 **Binding of the K562 cell lines to Fibronectin in the presence of KIM127.** $5x10^5$ /ml of cells were washed and diluted in DMEM media with or without 1mM Mn^{2+} or 20µg/ml KIM127. In this experiment, 100% represents the binding of the individual cell lines either in the presence of media with or without Mn^{2+} and without the presence of KIM127. Each data point represents mean +/- SD (n=4) and is representative of 2 other independently performed experiments. Statistical analysis was performed to compare binding in the absence and presence of KIM127. * indicates significance $p<0.01$.

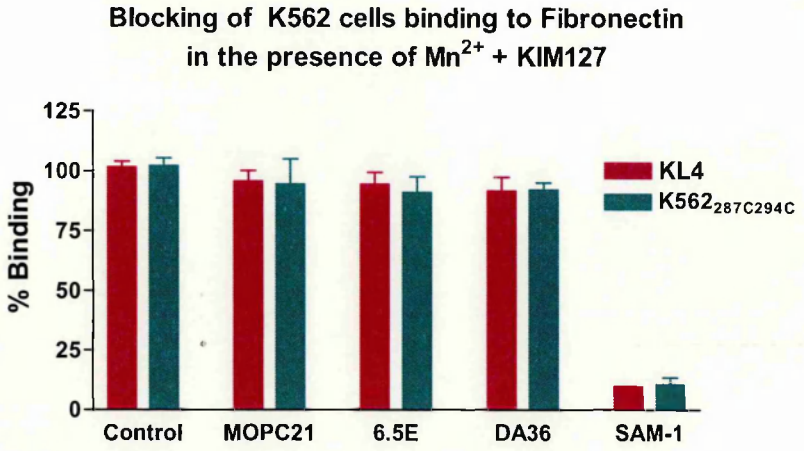

Figure 5.10 Blocking of K562 cells binding to Fibronectin in the presence of $Mn2^{+}$ and KIM127. $5x10^5$ /ml of cells were washed and diluted in DMEM containing 1mM Mn^{2+} and 20µg/ml KIM127 (control) to which was added 20µg/ml 6.5E, 20µg/ml DA36 or 20ug/ml MOPC21. 100% binding represents the binding of the individual cell lines under control conditions. The degree of binding was assessed at 570nm using the Rose Bengal Assay. Each data point represents mean +/- SD (n=3) and is representative of 1 other independently performed experiment.

5.5.2 Binding of cell expressed LFA-1 to ICAM-1 in the presence of α5β1 Abs

Following on from the experiments investigating the effects of LFA-1 activation on the binding of α5β1 to fibronectin, it was of interest to see if addition of α5β1 blocking and activating mAbs had an affect on the activation of $LFA\text{-}1_{WT}$ and the various mutant forms of LFA-1 expressed in K562 cells. Results from binding assays in the presence of the α5 blocking mAb, SAM-1, showed that it had a slight stimulatory effect on the binding of LFA-1 to ICAM-1, although this increase was not statistically significant (Figure 5.11). It is unlikely that any increase in binding could be attributed to the activation state of LFA-1, since the KL4 cell line behaved in a similar manner to $K562_{287C294C}$, the most active mutant with respect to LFA-1 activity. Addition of the activating β1 mAb, TS2/16, also showed a slight increase in K562 ICAM-1 binding, similar to that seen in the presence of SAM-1. On the other hand mAb Max68P, a blocking α4 mAb has a slight inhibitory effect on LFA-1 ligand interaction but this again was- not statistically significant.

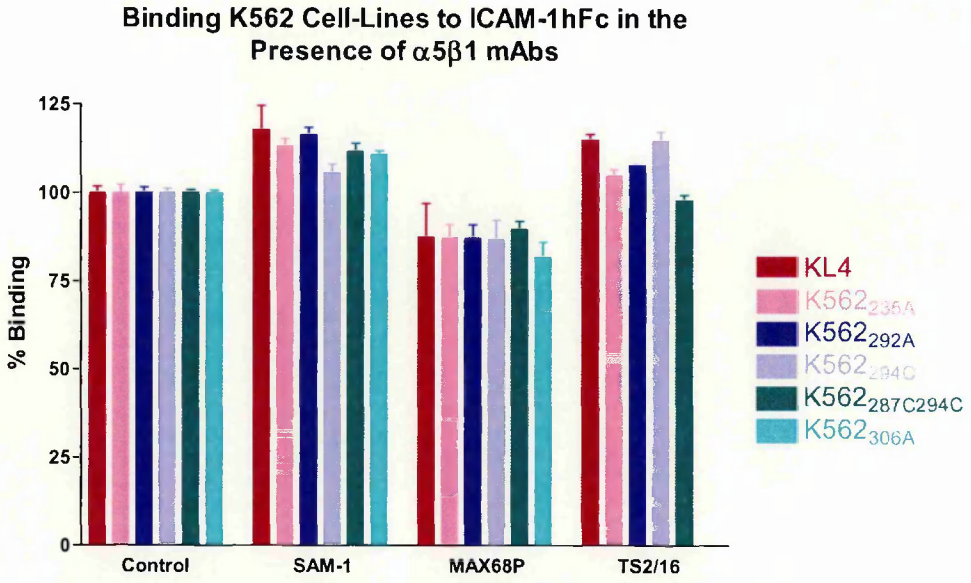

Figure 5.11 **Binding of K562 Cell lines to ICAM-1hFc in the presence of α5β1 mAbs.** Cells were washed and diluted in DMEM containing 1mM Mn^{2+} (control) to which was added 20µg/ml SAM-1, 20µg/ml TS2/16, 20µg/ml Max68P or 20ug/ml MOPC21. 100% binding represents the binding of the individual cell lines under control conditions. The degree of binding was assessed at 570nm using the Rose Bengal Assay. Each data point represents mean +/- SD (n=3) and the data presented here are representative of that obtained in three other independently performed experiments.

5.6 Discussion

In Chapter 4, alanine or cysteine substitutions of residues K287 and K294, K294, I306, L292, F295 and I235 in the I Domain of αL were all shown to have a significant effect on the activation state of the soluble integrin when compared to $sLFA\text{-}1_{WT}mFc$. Generation of a soluble form of LFA-1 allowed for the study of the interaction of the integrin containing such mutations in the context of other domains but without the constraints of the cytoskeleton. A limited characterisation of some of these mutations has previously been investigated by other researchers in a variety of cell systems including T293 cells, COS cells, JB2.7 cells and K562

cells (Ma *et al.*, 2002; Huth *et al*, 2000, Lupher *et al*, 2001). The data presented here extends the characterisation of the known mutants and includes a new mutation at position F292. The K562 cell line was chosen because a K562 cell line expressing LFA-1_{WT} (KL4) had previously been generated and characterised in this laboratory (Ortlepp *et al.*, 1995). It was also selected because the KL4 cell line cell line requires the presence of Mn^{2+} or activating mAbs to stimulate binding to ICAM-1. Therefore, it was expected that the effects of the introduction of mutations that might increase the activity of LFA-1 would be easily detected.

Data generated in this study on the KL4 cell line showed that it was unable to bind the ICAM ligands in media alone and only low levels of binding were seen in the presence of 1mM Mn^{2+}. This data confirms previously reported results showing that transfected LFA-1_{WT} expressed on the cell surface of K562 cells is in a low activation state as judged by its low binding to ICAM-1 and low level binding of antibodies reported to recognise activation epitopes (Mab24 and MEM148) (Ortlepp 1997; Lub *et al.*, 1997(a); Lu *et al.*, 2001(c)). In contrast, expression of cell surface-expressed LFA-1 containing the various amino acid substitutions listed in Table 5.1 upregulated binding to coated-ICAM-1hFc in the presence of media, and this could be further activated in the presence of Mn^{2+}. These results suggest that structural changes in the IDAS site can affect the adhesive function of the integrin when expressed both in the soluble form and as a whole integrin expressed on the cell surface. However, because all of the mutant cell lines could be further activated to bind in the presence of the activating mAbs KIM185 and KIM127 (Figure 5.2), one can conclude that the high affinity state induced by addition of Mn^{2+} is not sufficient to get maximal ligand binding, and that the cytoplasmic tails tethering the integrin to the cell membrane may also have a controlling effect on the activation state of the integrin even when the I domain is locked 'open' as in the case of $K562_{287C294C}$. As hypothesized in Chapter 4, the activating mAbs may act to stabilize the integrin in the active upright form, which is competent to bind ligand thus increasing the ligand binding readout over that seen in the presence of Mn^{2+} alone.

In contrast to the ability of all the mutated forms of LFA-1 used in this study to be further activated in the presence of KIM185 and KIM127, Lu *et al.* (2001(c)) claim that LFA-$1_{287C294C}$ expressed in their K562 cell system is fully activated in the presence of media alone and that activating mAbs or Mn^{2+} cannot further increase this binding. Their result suggests that Mn^{2+} and Mg^{2+} are interchangeable in the MIDAS once the I domain is in the right conformation for ligand binding as suggested by the introduction of the 287C294C mutation. This is further supported by their results from cation studies using the isolated I domain containing the 287C294C mutation since they showed that the level of ICAM-1 binding was comparable in the presence of Mn^{2+} or Mg^{2+} (Lu *et al.*, 2001(d)). In a subsequent paper, they suggest that the cation binding site in the I-like domain of the β2-subunit preferentially binds Mn^{2+}, and it is the binding of Mn^{2+} to this site that induces conformational change within the I-like domain which in turn alters the position of the α7 helix of the I domain, pulling it downward making the I domain competent to bind ligand (Shimaoka *et al.*, 2001).

Interestingly, although they showed that LFA-1_{WT} demonstrated only low level binding when assayed in cell culture media, it could be fully activated in the presence of Mn^{2+} and addition of the activating mAb CBR LFA-1/2 did not further increase the level of binding. In our studies, addition of Mn^{2+} was not sufficient to fully activate wild type LFA-1 expressed on K562 cells since activating mAbs such as KIM127 and KIM185 were needed to fully activate the integrin. The opposing results could be explained by the fact that different activation mAbs were used. Our results confirm data published by Ortlepp *et al.* (1995) where KIM127 and KIM185 were required to demonstrate maximal binding in the presence of Mn^{2+}.

Also similar to the data presented here on the constitutive binding of $K562_{235A}$ and the increased binding in the presence of PMA (Figures 5.2 and Figure 5.4), Lupher *et al.* (2001) reported that ligand binding by LFA-1 containing the I235A mutation in lymphoid cells (JB2.7 cells) was inducible and showed increased binding at lower PMA concentrations relative to wild type. However, while $K562_{235A}$ in our study was shown to bind ligand in the presence of media alone, in their expression system this mutation was unable to support ligand binding under similar conditions. The authors suggest that negative regulation by cytoplasmic interactions, as well as IDAS regulation, control the binding ability of the integrin and that the I235A mutation does not spontaneously induce the activated state of LFA-1. Rather, the mutation may either stabilize the activated state once it forms or destabilize the inactive state and thereby lower the threshold necessary for activation. Both the 294C and I306 mutations have also been previously expressed on the cell surface and shown to be constitutively active. However, in the case of the 294C mutation, a transient T293 system was used which is known to have a high basal level of wild type LFA-1 expression (Lu *et al.*, 2001). In the COS-7 cell system used to express the I306 mutant, integrins are also known to become partially activated without stimulation (Lupher *et al.*, 2001).

As with the LFA-1 constructs expressed in a soluble form, DA36 was capable of blocking all ligand interactions of the LFA-1 expressing K562 cell lines even in the presence of activating mAbs. Its ability to completely block binding to all ligands evaluated suggests that the binding of DA36 can, in some way, directly disrupt the interaction of the MIDAS binding site with ligand. While mAb 6.5E blocked the ICAM-1 interaction (80-90%) with KL4, $K562_{306A}$ and $K562_{292A}$ cell lines when assayed in the presence of Mn^{2+}, the blocking capacity of 6.5E was only ~60-70% with the cell lines $K562_{294C}$, $K562_{287C294C}$ and $K562_{235A}$. In all cases, the addition of the activating mAb KIM127 reduced the ability of 6.5E to block by a further 10-20%. Interestingly, whilst in the soluble system the introduction of the 287C294C mutation appeared to have the greatest influence on the ability of 6.5E to inhibit, in the cell system $K562_{294C}$,

$K562_{287C294C}$ and $K562_{292A}$ all appear to have a similar effect on the ability of 6.5E to inhibit ICAM-1 binding. The profile discussed here with respect to ICAM-1 was also true for all cell lines when ICAM-2 and ICAM-3 were employed apart from the $K562_{235A}$ cell line in the presence of ICAM-3. This cell line behaved in a similar manner to $K562_{294C}$ cells with the ability of 6.5E to block being reduced to approximately 50%. Why this is the case when more or less maximal blocking is achieved with both ICAM-1 and ICAM-2 is unknown.

Addition of cytochalasin D, a chemical agent known to disrupt actin polymerisation, also had no effect on the ability of cell-expressed LFA-1 to bind ligand. The inability of cytochalasin D to alter ligand binding suggests that outside-in signalling subsequent to addition of Mn^{2+} or activating mAbs does not require an intact cytoskeleton.

The ability of LFA-1 to regulate other integrins expressed on the same cell surface has been reported by several researchers (Van Kooyk *et al.*, 1993; Porter and Hogg, 1997; Leitinger *et al.*, 2002). Although K562 cells endogenously express $\alpha5\beta1$, there are no reports to date on the ability of transfected integrins to influence the activation or ligand binding function of this integrin. It was, therefore, of interest to note that addition of the mAb KIM127 to K562 cells expressing LFA-1 caused increased $\alpha5\beta1$-dependent binding to fibronectin. However, in the absence of KIM127 none of the activated forms of LFA-1 alone were capable of significantly modulating $\alpha5\beta1$-mediated fibronectin binding in K562 cells.

On addition of KIM127, all of the LFA-1 transfected cell lines appear to achieve a similar level of activation as demonstrated by similar levels of binding to ICAM-1 (Figure 5.2). In all cases KIM127 seems to promote a higher level of activation than that generated by the I domain mutations alone. The ability of KIM127 to influence the binding of $\alpha5\beta1$ to fibronectin suggests that LFA-1 when expressed on K562 cells must be in a highly activated state to cross talk. These results are consistent with those reported by Leitinger *et al.* (2000). In their study an activated form of LFA-1, generated by deleting the I domain and shown by reporter mAb

binding analysis to resemble activated LFA-1, enhanced binding of both α4β1 and α5β1 to VCAM-1 and fibronectin respectively when expressed in the JB2.7 cell line. This binding could also be further enhanced by the addition of activating β2 mAbs. The inability of our mutant cell lines to enhance α5β1 without the presence of KIM127 suggests either that their activation state is not sufficient to support crosstalk or that the signalling mechanisms within K562 cells are not as finely tuned as in the JB2.7 cell system.

While LFA-1 appears to have an effect on α5β1 ligand binding in our K562 cell system, we found no evidence to suggest that α5β1 had any effect on the activation or ligand binding capacity of LFA-1. While several researchers have shown cross talk leading to LFA-1 activation (Rose *et al.,* 2001; Chan *et al.*; 2000; May *et al.,* 2000), these investigations have primarily focused on the ability of VLA-4 to affect the activation of LFA-1. It would appear therefore that there is another level of complexity allowing for cross talk between some, but not all, neighbouring integrins.

Chapter 6

Effect of I Domain Mutations on Activation and Binding Properties of LFA-1 in the JB2.7 Cell System

Chapter 6 Effect of I Domain Mutations on Activation and Binding Properties of LFA-1 in the JB2.7 Cell System

6.1 Introduction

Although the K562 cell-line is well established for studying the effects of transfected integrins (Andrew *et al.*, 1993; Ortlepp *et al.*, 1995; Stephens *et al.*, 1995; Yalamanchili *et al.*, 2000; Shimaoka *et al.*, 2001; Bleijs *et al.*, 2000; Lub *et al* 1997), published work from Lub *et al.* (1997) has shown that the K562 cell line lacks some of the signalling elements that are known to be required to fully regulate β2 integrin adhesion. While endogenous α5β1 was capable of binding ligand in response to PMA stimulation, β2 integrins expressed in K562 cells were unresponsive even at high concentrations of the phorbol ester. The PKC pathway, which is upregulated by PMA treatment, appears to be involved in the activation of LFA-1 in some cell types (Hibbs *et al.*, 1991) and may therefore also have a role to play in LFA-1 'crosstalk'. If this is the case, the crosstalk described in the previous chapter may not truly represent the process of crosstalk in the majority of cell types. In order to support the K562 cell data, full length LFA-1 containing the αL mutations listed in Table 5.1 were also expressed in the JB2.7 cell line, and the effects of LFA-1 activation on the regulation of other integrins expressed by the cell line were investigated.

The JB2.7 cell line is deficient in the endogenous αL subunit. Originally established to evaluate the extent of interdependence of the α and β subunits for cell surface expression and function, the cell line was generated by treatment of the Jurkat cell line with EMS (ethylmethane sulphonate) followed by selection of clones negative for αL and β2 expression (Weber *et al.*, 1997). Characterisation of the JB2.7 cell line by Weber *et al.* revealed the absence of αL mRNA expression and further biosynthetic studies revealed that the β2 subunit was synthesised and

detectable by immunopercipitation but was not detected by anti-β2 antibodies on the cell surface. Subsequent transfection of this cell line with αL cDNA restored surface expression of LFA-1 and confirmed the requirement of both subunits for presentation on the cell surface. Transfection of αL also reconstituted ligand binding functions of LFA-1 upon stimulation with phorbol esters, suggesting that the chemical mutagenesis methods used to generate the mutant cell line had not affected this cellular signal transduction pathway.

The JB2.7 cell line (which will be referred to as the $JB2.7_{ORG}$ cell line through out the remainder of the thesis) has been used by several researchers to analyse LFA-1-dependent function since it allows for interactions to take place in a 'lymphocyte-like' background (Lupher *et al.*, 2001; Leitinger and Hogg, 2000; Ostermann *et al.*, 2002). More recently Leitinger and Hogg (2000) have reported the ability of LFA-1 to 'crosstalk' to both α5β1 and α4β1 in this cell line. They demonstrated this by using a JB2.7 cell line expressing LFA-1 that lacks an I domain ($JB2.7_{\Delta IDomain}$). Although this form of LFA-1 was unable to support ICAM-1 binding, binding studies with activation reporter mAbs such as mAb24 and NKL1-16 showed that it expressed epitopes generally associated with the active form of the integrin, suggesting that $LFA\text{-}1_{\Delta IDomain}$ had characteristics of a constitutively active integrin. Furthermore, the $JB2.7_{\Delta IDomain}$ cell line demonstrated higher levels of binding to the α5β1 and α4β1 ligands, fibronectin and VCAM-1, relative to a JB2.7 cell line expressing $LFA\text{-}1_{WT}$ ($JB2.7_{LFA\text{-}1WT}$) suggesting that the activation state of LFA-1 had an effect on the ability of other integrins expressed on the same cell surface to bind their respective ligands. Addition of LFA-1 activating mAbs were shown to further increase this 'crosstalk'. Their results are similar to the results shown in the previous chapter where KIM127 appeared to activate LFA-1-expressing K562 cells which in turn upregulated α5β1 binding to fibronectin. In order to determine if activation of LFA-1 through introduction of mutations within the IDAS altered the function of other endogenous integrins expressed on JB2.7 cells, the JB2.7 cell line was transfected with the genes encoding mutant forms of αL and

the binding of the transfected cell lines to fibronectin, VCAM-1 and the ICAMs were compared with that of the JB2.7$_{\Delta IDomain}$ and the JB2.7$_{LFA\text{-}1WT}$ cell lines (both used in the Leitinger study).

6.2 Expression and Characterisation of Mutated Forms of LFA-1 in the JB2.7 Cell Line

JB2.7 cells were stably transfected using electroporation with single gene pEE6 vectors encoding mutated forms of full-length αL (See Section 3.5). Following positive selection using the G418 selection method, clones for use in experiments were selected after several rounds of flow cytometric analysis using mAbs to both the αL and β2 subunits. Clones were selected on the basis of the similarity of their αLβ2, α5β1 and α4β1 expression profiles compared with the JB2.7$_{LFA\text{-}1WT}$ cell line. It was felt that similar integrin expression profiles on all cell lines were required so that direct comparisons of the effects of the introduced mutations within the IDAS could be evaluated. Both the JB2.7$_{LFA\text{-}1WT}$ and JB2.7$_{\Delta IDomain}$ cell lines had previously been selected for similar expression (Leitinger and Hogg, 2000).

The analysis of αLβ2, α5β1 and α4β1 expression on the various JB2.7 cell lines is shown in Figure 6.1 where the MFI values have been tabulated in order to more easily make comparisons across all the cell lines. Since the same parental cell line was used for transfection of the various LFA-1 mutants, the similar expression profiles of α5β1 and α4β1 on all cell lines were as predicted. Also, as expected, both HI111 and Ab38 mAbs which bind to epitopes on the I domain did not bind to either the JB2.7$_{ORG}$ or JB2.7$_{\Delta IDomain}$ cell lines. All other transfected cell lines had a similar profile for Ab38 and HI111 binding apart from the binding of HI111 to the JB2.7$_{287C294C}$ cell line. The reduction in binding of this mAb to LFA-1 containing the 287C294C mutation was also noted with the K562 cell line expressing the same mutation (Figure 5.1 in this thesis; Ma *et al.*, 2002).

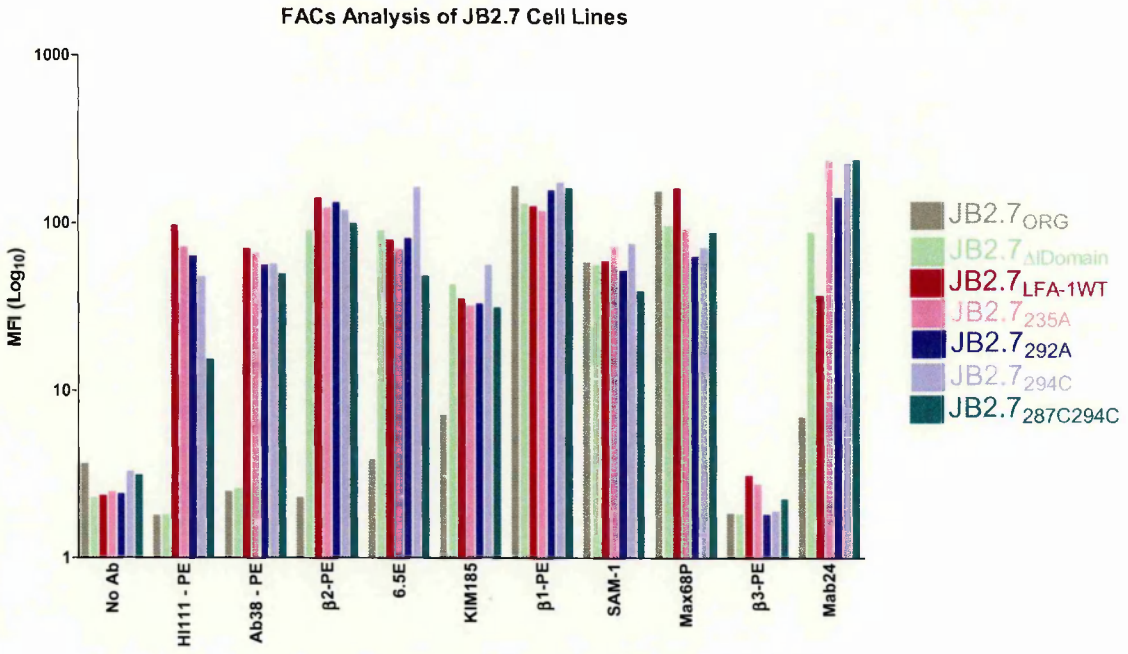

Figure 6.1 **FACS analysis of surface expressed integrins on JB2.7 cell lines.** Expression profiles are tabulated and expressed as geometric Mean Fluorescence Intensity (MFI) units. Several of the mAbs used were directly labeled with PE (phycoerythrin) and required only 1 incubation step whereas with mAbs 6.5E, KIM185, SAM-1 and Max68P, cells were first incubated with the primary mAbs and following 3 washes in FACS buffer where further incubated with a polyclonal anti-mouse Fc-PE labelled Ab. All mAbs were used at 20μg/ml final concentration. The results shown above are representative of 3 or more independently performed experiments performed on different days.

As both the α and β subunits are required for the binding of 6.5E, the ability of this mAb to bind to LFA-1 when it is expressed without the I domain supports previous work which showed that this form of the integrin is correctly folded and that the presence of the I domain is not required for the correct folding of the integrin. The capacity of 6.5E to bind to the same extent to all forms of cell surface-expressed LFA-1 also confirms data from Lu *et al.* (2001(b)) which showed that the 6.5E epitope is available for antibody binding in cell lines containing the 287C294C mutation to the same extent as wild type LFA-1, even though its ability to block ligand binding in this mutation is reduced. Binding of KIM185 also appears to be unaffected by the presence of mutations within the IDAS. Although there is a slightly higher than background level of binding of KIM185 and mAb24 to JB2.7$_{ORG}$, the lack of binding with the other β2 mAbs

and αL mAbs suggests that this may reflect some low level cross-reactivity or non-specific binding. The mAb 24 epitope, which can be induced by divalent cations Mg^{2+} or Mn^{2+}, reflects a conformational change in LFA-1 characteristic of a higher-affinity receptor and is considered to act as an activation reporter (Dransfield and Hogg, 1989; Dransfield *et al.*, 1992(b), Stewart and Hogg, 1996). The mAb24 results shown in Figure 6.1 are similar to those reported by Leitinger and Hogg (2000) in that LFA-1 $JB2.7_{\Delta IDomain}$ demonstrated higher binding in the presence of mAb24 compared with $JB2.7_{LFA\text{-}1WT}$ and is consistent with the $JB2.7_{\Delta IDomain}$ cell line being in a higher activation state than the wild type cell line. Interestingly, all the mutant cell lines showed even higher binding of mAb24 compared with the LFA-1 $JB2.7_{\Delta IDomain}$ cell line, suggesting that the introduction of the IDAS mutations does enhance the activation state of the integrin.

6.3 Binding of JB2.7 Cell Lines to ICAM-1, -2 and -3

Although the mAb24 data suggested that the mutated forms of LFA-1 were more highly activated than $LFA\text{-}1_{WT}$ and also that all mutated cell lines were in a slightly higher activation state than the $JB2.7_{\Delta IDomain}$ cell line, we felt it was prudent to confirm this increased activation above wild type with ICAM binding assays. As expected, both cell lines lacking an αL I domain, $JB2.7_{ORG}$ and $JB2.7_{\Delta IDomain}$, exhibited only background binding to all ICAMs in the presence of Mn^{2+} (Figure 6.2). Ligand binding studies in the presence of media alone also showed that the JB2.7 cell line expressing wild type LFA-1 was unable to bind to any of the three ICAM ligands tested (See Figure 6.2 for ICAM-1 binding). In contrast to this result, and consistent with the K562 cell results, JB2.7 cells transfected with αL containing mutations at positions 287C294C, 294C and 235A did bind to ICAM-1 in media alone and this binding was increased up to 3-fold in the presence of Mn^{2+}. Although $JB2.7_{LFA\text{-}1WT}$ binding to ICAM-1 also

increased approximately 4-fold on addition of Mn^{2+}, the level of binding was still lower than that seen for some of the mutant cell lines.

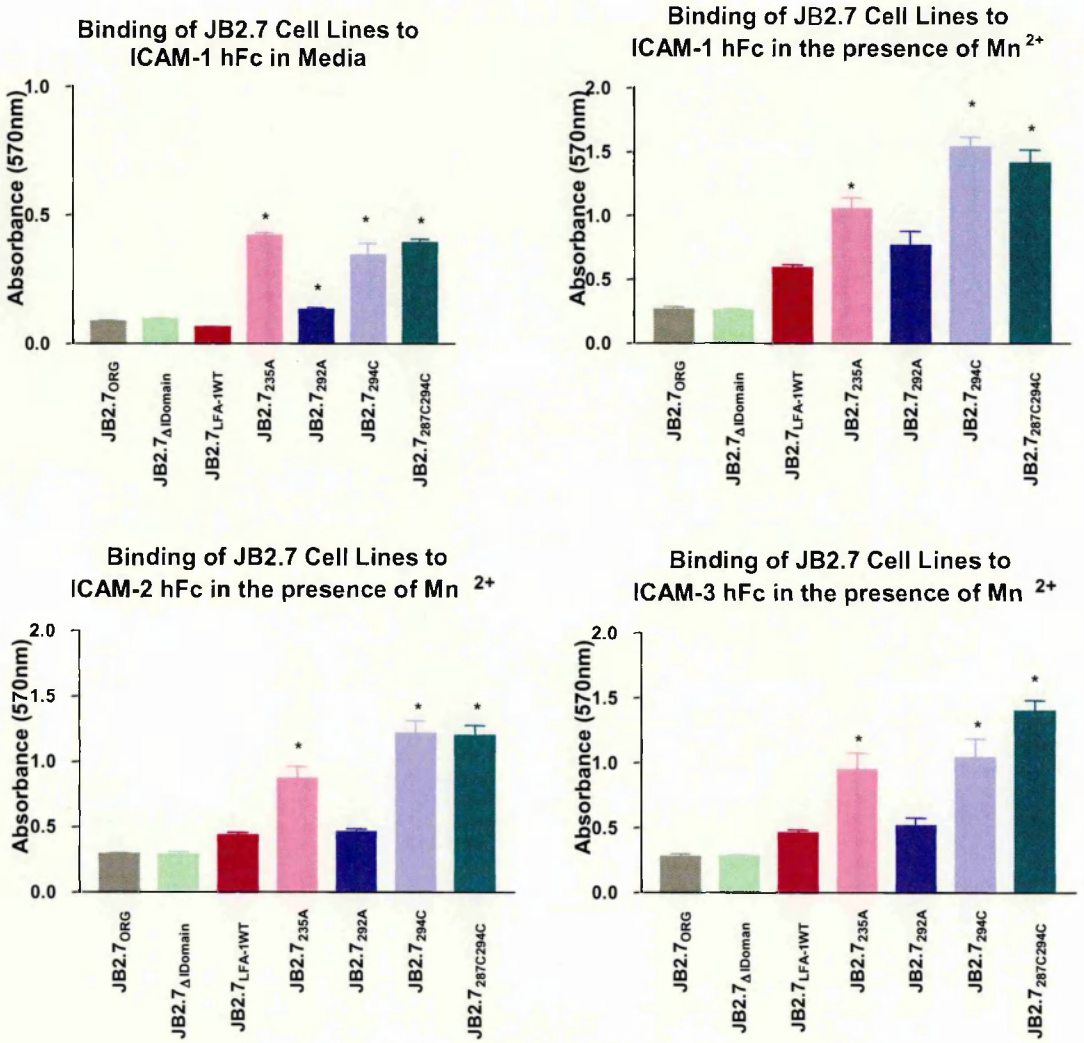

Figure 6.2 **Binding of JB2.7 Cell Lines to ICAM Ligands.** The above graphs show the relative binding of the various cell lines in media (DMEM) +/-Mn^{2+} in the case of ICAM-1hFc and +Mn^{2+} in the case of ICAM-2hFc and ICAM-3hFc. The degree of binding was assessed at 570nm using the Rose Bengal Assay. Each data point presented here represents the mean +/-SD (n=4) and is representative of 3-8 independently performed experiments. Statistical analysis was performed to compare $JB2.7_{LFA\text{-}1WT}$ binding with the other ICAM-1 binding JB2.7 cell lines under the same conditions. * indicates significance $p < 0.01$.

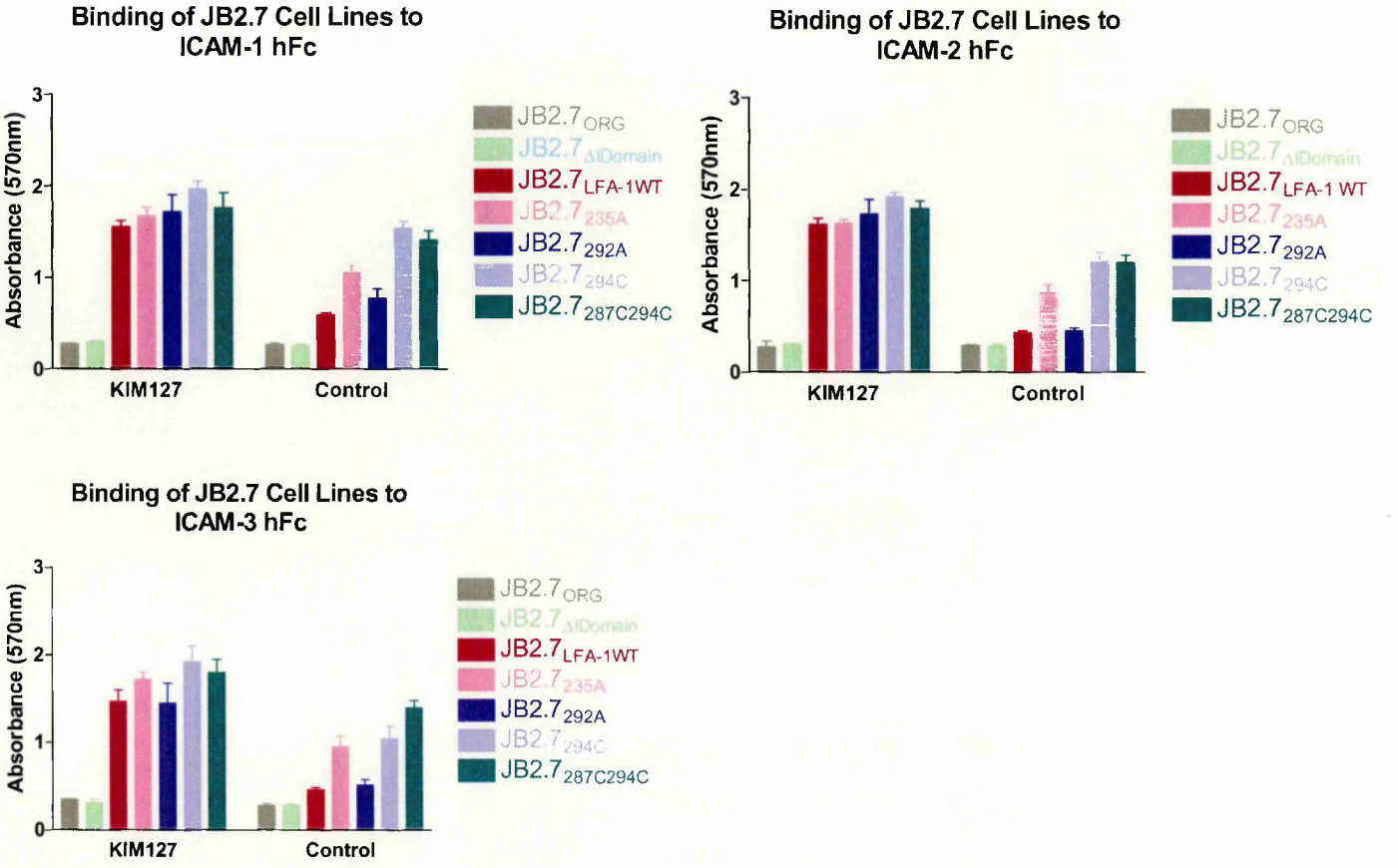

Figure 6.3 **Binding of JB2.7 Cell Lines to ICAM ligands in the presence of KIM127.** The above graphs show the relative binding of the various cell lines in the presence of MOPC21 (Control mAb) or 20μg/ml KIM127 when the assay was carried out in media (DMEM) containing Mn^{2+}. The degree of binding was assessed at 570nm using the Rose Bengal Assay. Each data point represents mean +/-SD (n=3) and these data presented here are representative of that obtained in three other independently performed experiments.

The $JB2.7_{292A}$ cell line bound less than cells transfected with other mutated forms of LFA-1 but binding to ICAM-1 in media was still significantly higher than with cells expressing $LFA\text{-}1_{WT}$. Binding of the $JB2.7_{235A}$ cell line to ICAM-1 did not increase as dramatically as the $JB2.7_{287C294C}$ and $JB2.7_{294C}$ cell lines in the presence of Mn^{2+} although all three cell lines showed equivalent

binding in media alone. Binding of the $JB2.7_{LFA\text{-}1WT}$ and $JB2.7_{292A}$ cell lines to ICAM-2 and ICAM-3 was lower than that seen for binding to ICAM-1, although this binding was still above background levels. The cell lines $JB2.7_{287C294C}$, $JB2.7_{235A}$ and $JB2.7_{294C}$ again showed a higher affinity for ICAM-2 and ICAM-3 over wild type suggesting that the introduction of these mutations has a positive effect on the activation state of the integrin.

On addition of the mAb KIM127 (Figure 6.3), the levels of binding of the $JB2.7_{LFA\text{-}1WT}$ and $JB2.7_{292A}$ cell lines were greatly increased with all ligands tested. Although the cell lines expressing different forms of LFA-1 showed some variations in levels of binding no statistically significant differences between the ICAM-binding cell lines were observed. Although KIM127 did increase the level of binding of both $JB2.7_{287C294C}$ and $JB2.7_{294C}$, this increase in binding was not as dramatic as seen with wild type.

Inhibition of ICAM ligand binding with a metal chelating agent and blocking LFA-1 mAbs confirmed that all ligand interactions were cation and LFA-1 dependent. DA36 was capable of blocking the interaction of all the JB2.7 cell lines with all ICAM ligands (Figure 6.4(a)), even in the presence of KIM127. Similar to results seen for both soluble LFA-1 and K562-expressed LFA-1, 6.5E was unable to completely block ligand binding with some of the mutant forms of LFA-1. Figure 6.4(b) illustrates the binding of the JB2.7 cell lines in the presence of 6.5E. Adhesion of the $JB2.7_{LFA\text{-}1WT}$ and $JB2.7_{292A}$ cell lines was completely blocked by 6.5E in the absence and presence of KIM127. However, binding of the $JB2.7_{287C294C}$ cell line to ICAM-1 was only reduced by ~50% in the presence of Mn^{2+} and the capacity to block was further reduced to ~20% in the presence of KIM127. Similar blocking profiles were shown for ICAM-2 and ICAM-3 (data not shown). Overall, all the cell lines behaved in a similar manner to their equivalent mutations in K562 cells although it does appear that cytoplasmic constraints may have a bigger role to play in JB2.7 cells.

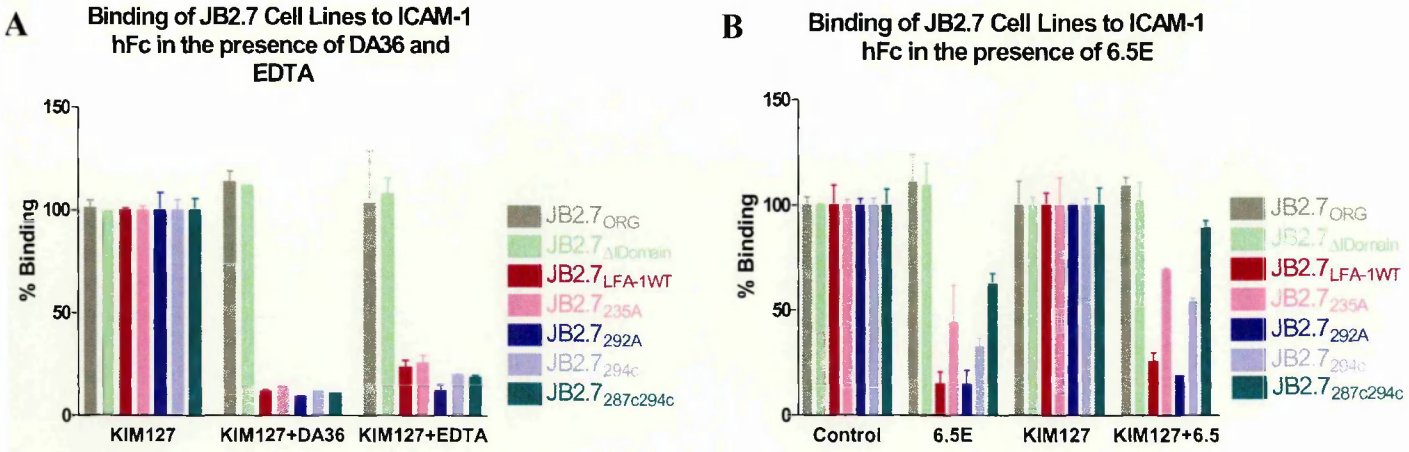

Figure 6.4 **Binding of JB2.7 cell lines in the presence of LFA-1 blocking mAbs and EDTA.** Cells were washed and diluted to $5x10^5$/ml in DMEM containing 1mM Mn^{2+} with or without 20μg/ml KIM127 or MOPC21 (control) to which was added 20μg/ml DA36, 20μg/ml 6.5E or 20mM EDTA. The degree of binding was assessed at 570nm using the Rose Bengal Assay. In experiment A, 100% represents the binding of the individual cell lines in the presence of KIM127 and in experiment B, 100% represents the binding of the individual cell lines in the presence of MOPC21 or KIM127. Each data point represents mean +/- SD (n=3) and the data presented here are representative of 3 other independently performed experiments.

6.3.1. Binding of JB2.7 cells to ICAM-1 in the presence of PMA

The inability of PMA to influence the binding of LFA-1 expressed on K562 cells (Chapter 5, Figure 5.4) suggested that some of the integrin signalling mechanisms may be absent in K562 cells. PMA is a known activator of the PKC pathway and its addition leads to enhanced clustering of integrins on the cell surface (Stewart *et al.*, 1996; Lub *et al.*, 1997; Chapter 1 Section 5.1) and it has been shown in other cell lines (e.g. T cells and JB2.7 cells) to be a major regulator of LFA-1 activation. Before investigating the ability of the mutant cell lines to affect crosstalk in the JB2.7 cell system, the ability of PMA to activate LFA-1 in these cells was checked in order to confirm that a mechanism of LFA-1 activation through inside-out signalling was operational. In this study, addition of PMA to the JB2.7 cell lines did stimulate ligand

binding above that seen for media alone (Figure 6.5). Similar to the data in the presence of Mn^{2+}, the cell lines $JB2.7_{287C294C}$, $JB2.7_{235A}$, and $JB2.7_{294C}$ showed significantly higher levels of binding when compared with wild type cells. Moreover, KIM127 induced comparable levels of binding in all cell lines. This data shows that PMA-induced signalling pathways are operational in JB2.7 cells and that outside-in stimulation with Mn^{2+} yields comparable results to inside-out signalling with PMA in media alone. Finally, in both cases, cells do not appear to be maximally activated since addition of KIM127 can further increase ligand binding.

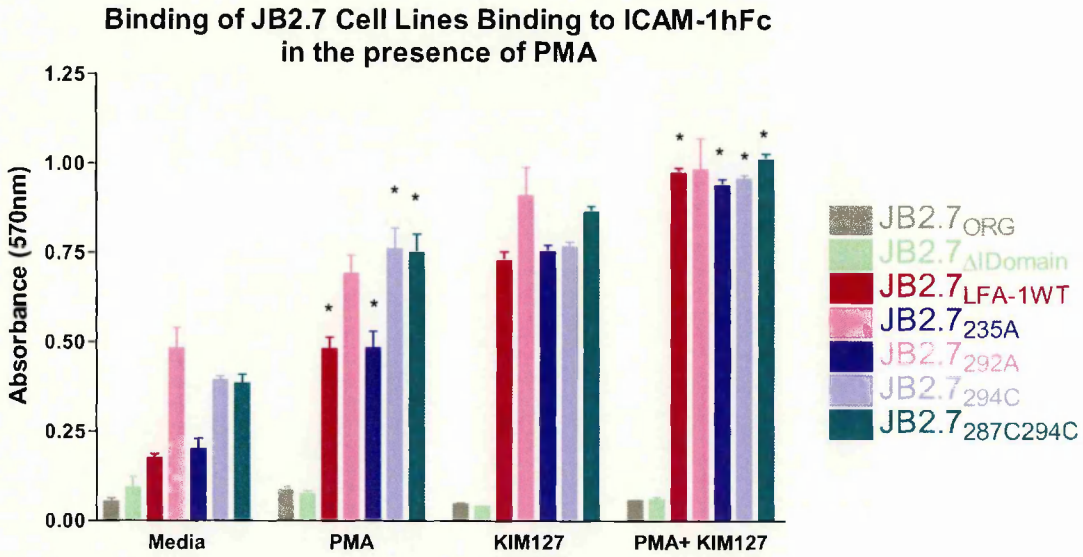

Figure 6.5 **Binding of JB2.7 Cell Lines to ICAM-1hFc in the presence of PMA**. The above graphs show the relative binding of various cell lines with or without KIM127 and with or without PMA when the assay was carried out in media (DMEM). The degree of binding was assessed at 570nm using the Rose Bengal Assay. The data presented here are representative of that obtained in two other independently performed experiments with each data point representing the mean +/-SD (n=4). Statistical analysis was performed to compare binding of each cell line in the presence of Media vs Media+PMA and KIM127 vs KIM127+PMA. * indicates significance $p < 0.05$.

6.4 Binding of JB2.7 Cell Lines to Fibronectin and VCAM-1

Having established that the mutant forms of LFA-1 expressed in JB2.7 cells bind ICAM ligands in a similar manner to the K562 cell lines and that signalling pathways known to be relevant for LFA-1 activation were intact in the JB2.7 cell line, it was therefore of interest to determine if these mutated forms of LFA-1 could support LFA-1 cross talk. Although we demonstrated a statistically significant increase in binding with K562 cells expressing LFA-1 with IDAS mutations compared with KL4 cells, no other reports of crosstalk with K562 cells have been published and in this study only maximally activated LFA-1 was capable of supporting the increase in α5β1 ligand binding. Leitinger and Hogg (2000) reported that JB2.7 cells expressing an activated form of LFA-1 showed increased binding to both fibronectin and VCAM-1 relative to a cell line expressing wild type LFA-1. This finding suggests that an activated form of LFA-1 is capable of influencing the ability of other integrins expressed on the same cell surface to bind ligand. In the present study the level of binding to fibronectin and VCAM-1 of all the JB2.7 cells lines, including cell lines used by Leitinger *et al.*, were compared using an assay which involved assessing colourimetrically the number of cells binding to immobilized ligand. As previously shown (Figure 6.1) levels of α5β1 and α4β1 expression were similar for all JB2.7 cell lines, suggesting that any variation in binding to fibronectin or VCAM would be attributable to the activation state of LFA-1.

In this study, in the presence of media alone, the JB2.7$_{\Delta IDomain}$ cell line did bind to fibronectin to a slightly greater extent than JB2.7$_{LFA\text{-}1WT}$ and JB2.7$_{ORG}$ but this was not statistically significant (Figure 6.6A). However, on binding to VCAM-1 the JB2.7$_{\Delta IDomain}$ cell line did show a statistical difference from the parental cell line (Figure 6.6B). Surprisingly, while all the cell lines expressing mutated LFA-1 molecules exhibited higher mAb24 binding compared with the JB2.7$_{\Delta IDomain}$ cells (Figure 6.1) their binding to both fibronectin and VCAM-1 was not statistically significantly different from cells expressing wild type LFA-1. This suggests that

either the LFA-$1_{\Delta IDomain}$ is in a different activation state from the other forms of LFA-1, or due to the absence of an I domain, its ability to signal is different from that of a more physiological active form of the integrin. In the presence of Mn^{2+}, variation between cell lines in terms of their binding to both VCAM-1 and fibronectin was again observed. However, whilst binding of JB2.$7_{LFA\text{-}1WT}$ and JB2.7_{292A} cells to VCAM-1 was significantly less than binding of the JB2.7_{ORG} cell line, this cannot be attributed to the activation state of LFA-1 since JB2.7_{ORG} (which does not express LFA-1) showed a similar increase in binding compared with the other cell lines expressing LFA-1.

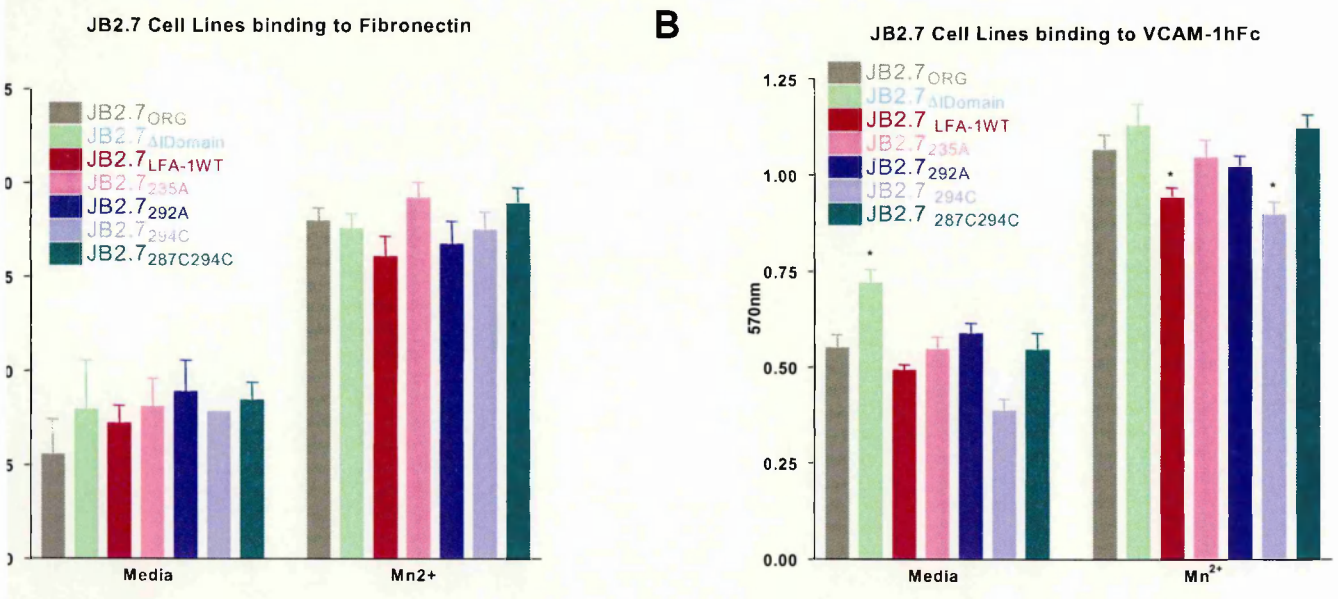

Figure 6.6 **Binding of JB2.7 Cell Lines to Fibronectin and VCAM-1hFc.** Cells were washed and diluted in media (DMEM) in the presence or absence of 1mM Mn^{2+} The degree of cell binding to fibronectin/VCAM-1hFc coated plates was assessed at 570nm using the Rose Bengal Assay. The data presented here are representative of three independently performed experiments and each data point shows mean +/-SD (n=6). Statistical analysis was performed to compare JB2.7_{ORG} binding with the other JB2.7cell lines. * indicates significance $p < 0.05$.

Further characterisation of the binding of JB2.7 cells to fibronectin and VCAM-1 showed that the binding could be completely blocked by the anti-α5 mAb, SAM-1, and the anti-α4 mAb, Max68P respectively (Figure 6.7 & Figure 6.8). Although α4β1 has been shown to bind fibronectin (Chan *et al.*, 1992; Hemler *et al.*, 1990; Humphries *et al.*, 1995), the ability of SAM-1 to completely block this interaction suggests that binding is predominantly α5β1-dependent. The interaction of α5β1 with fibronectin was also completely blocked in the presence of EDTA confirming the requirement of cation for ligand binding (Figure 6.7).

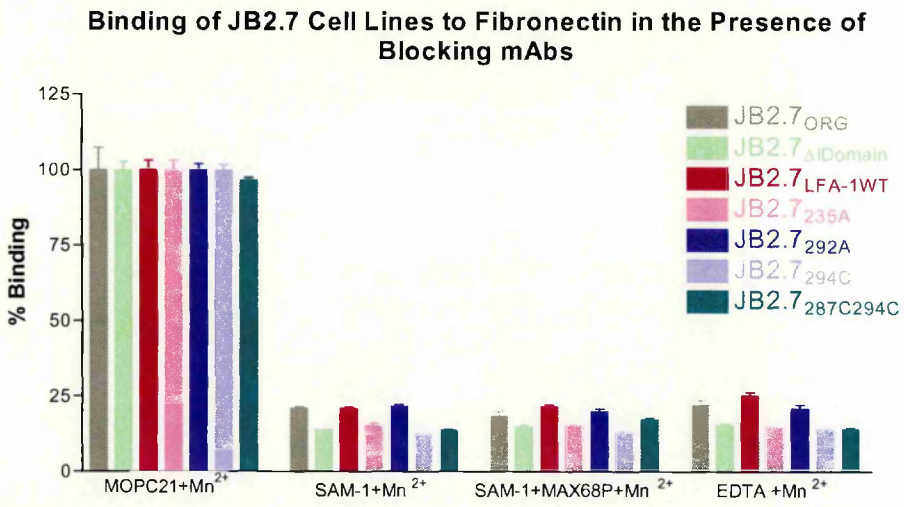

Figure 6.7 **Binding of JB2.7 Cell Lines to Fibronectin in the presence of SAM-1 and EDTA.** In each experiment, 100% represents the binding of the individual cell lines in the presence of the control mAb, MOPC21with 1mM Mn^{2+}. All mAbs were used at 20μg/ml and EDTA was used at 20mM. Each data point represents mean +SD (n=3) and the data presented here are representative of 2 other independently performed experiments.

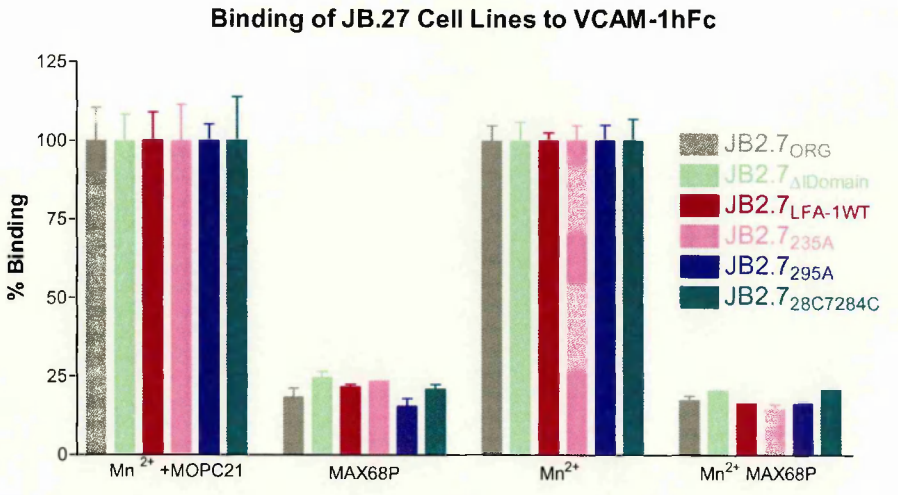

Figure 6.8 **Binding of JB2.7 Cell Lines to VCAM-1hFc in the presence of Max68P.** In each experiment, 100% represents the binding of the individual cell lines in the presence of the control mAb, MOPC21 with or without the presence of Mn^{2+}. All mAbs were used at 20µg/ml. Each data point represents mean +/-SD (n=3) and the data presented are representative of 2 other independently performed experiments.

The activating β1 mAb, TS2/16, was capable of activating both α5β1 and α4β1 which resulted in increased binding to their respective ligands (Figure 6.9 & Figure 6.10). Once again there is slight variation in the relative percentage increase of binding across all the mutants but this variation is unlikely to be attributable to the activation state of LFA-1 since the increase in binding of $JB2.7_{ORG}$ is generally similar to that seen with the other cell lines. The ability of TS2/16 to further increase the binding of all cell lines to fibronectin in the presence of Mn^{2+} also suggests that this integrin is not fully activated with divalent cations alone. In contrast to this result, Mn^{2+} alone appears to be sufficient to fully activate α4β1 since binding to VCAM in the presence of TS2/16 is increased by only 10-15% for all cell lines relative to Mn^{2+} alone.

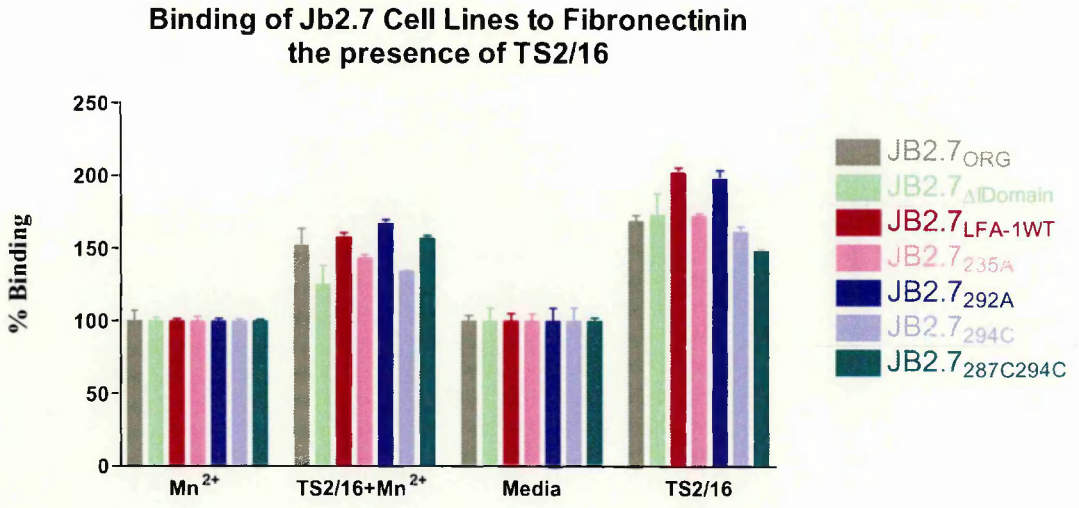

Figure 6.9 **Binding of JB2.7 Cell Lines to Fibronectin in the presence of TS2/16.** Cells were washed and diluted in media (DMEM) with or without 1mM Mn^{2+}. TS2/16 was used at a final concentration of 20μg/ml. In each experiment, 100% represents the binding of the individual cell lines without the presence of mAbs. Each data point represents mean +/- SD (n=3) and the data presented here are representative of 3 other independently performed experiments.

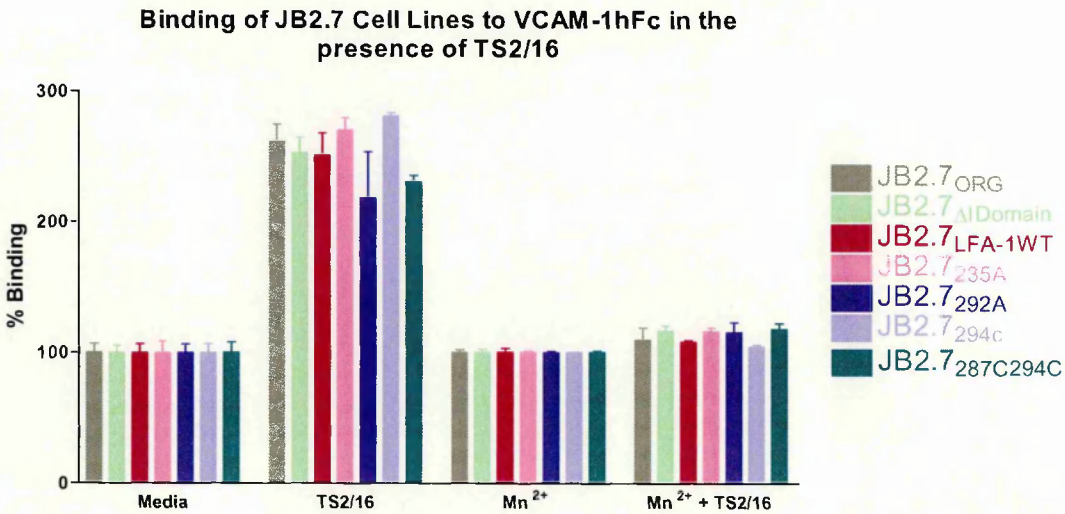

Figure 6.10 **Binding of JB2.7 Cell Lines to VCAM-1hFc in the presence of TS2/16.** Cells were washed and diluted in media (DMEM) with or without 1mM Mn^{2+}. TS2/16 was used at a final concentration of 20μg/ml. In each experiment, 100% represents the binding of the individual cell lines without the presence of mAbs. Each data point represents mean +/- SD (n=3) and the data presented here are representative of 3 other independently performed experiments.

6.4.1. Binding of JB2.7 Cell Lines to Fibronectin in the presence of LFA-1 mAbs

In Chapter 5, addition of KIM127 was shown to increase the binding of LFA-1-expressing K562 cells to fibronectin suggesting that fully activated LFA-1 could affect the activation state of another integrin expressed on the same cell surface. In this chapter we have already shown that, in the presence of KIM127, JB2.7 cells expressing LFA-1 demonstrated increased binding to ICAM ligands relative to cation alone (Figure 6.3). If crosstalk between the integrins was taking place, one might expect to see alterations in the capacity of both α5β1 and α4β1 to bind their respective ligands. However, as seen from Figures 6.11 and 6.12, KIM127 (and KIM185 in the case of VCAM-1 binding) has no significant effect on the ability of either α5β1 to bind fibronectin or α4β1 to bind VCAM-1 when the cells were incubated in media alone. Although there is slight variation between the cell lines in levels of binding in the presence and absence of KIM127, the profile is similar to that seen in the presence of DA36. DA36 is a known blocker of LFA-1 activity and although it is unknown whether the binding of this mAb affects both the binding of ligand and the activation state of LFA-1, or solely the binding of ligand, in this instance it also acts as an isotype control for KIM127. When assays were carried out in the presence of Mn^{2+}, KIM127 also failed to show enhanced binding to fibronectin or VCAM-1 (data not shown).

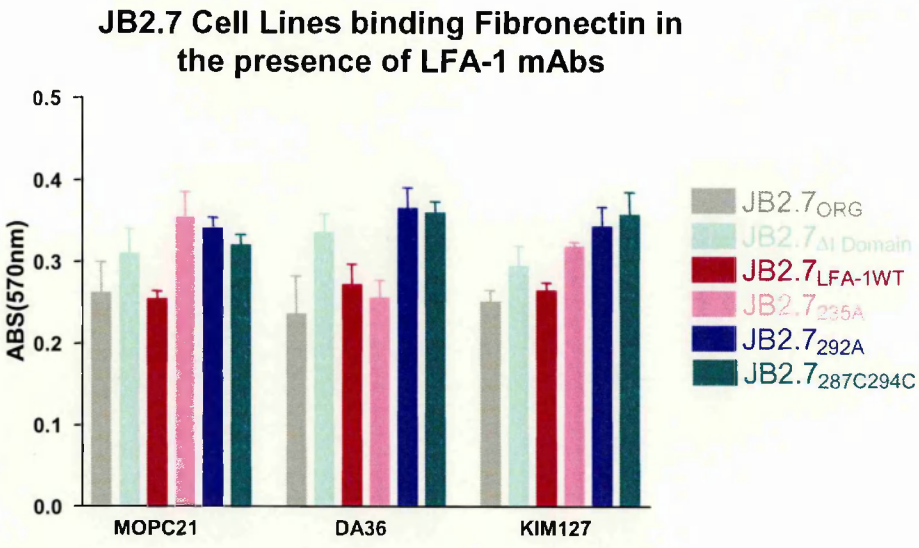

Figure 6.11 **Binding of JB2.7 cell lines to Fibronectin in the presence of LFA-1 mAbs.** All mAbs were used at 20μg/ml and diluted in media (DMEM) with 1mM Mn^{2+} (MOPC21 was used as the control mAb). The degree of binding was assessed at 570nm using the Rose Bengal Assay. Each data point represents mean +/-SD (n=3). The data presented here are representative of 3 other independently performed experiments.

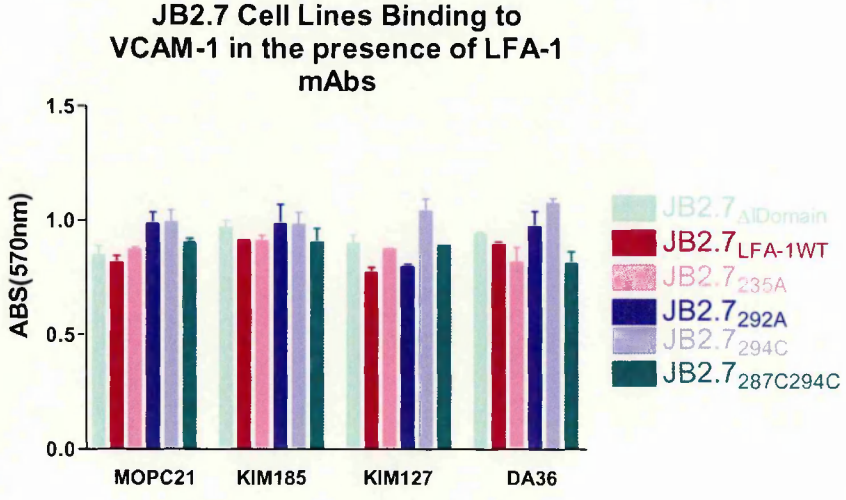

Figure 6.12 **Binding of JB2.7 Cell Lines to VCAM-1hFc in the presence of LFA-1mAbs.** Cells were washed and diluted in media (DMEM) with 1mM Mn^{2+} and all mAbs were used at a final concentration of 20μg/ml. (MOPC21 was used as the control mAb). Each data point represents mean +/-SD (n=3) and the data presented here are representative of 3 other independently performed experiments.

6.4.2. Binding of JB2.7 Cell Lines to ICAM-1 in the presence of α5β1 and α4β1 mAbs

Although there are no published reports of α5β1 and α4β1 crosstalk to αLβ2, we also investigated the ability of both blocking and activating α5β1 and α4β1 mAbs to affect the binding of LFA-1 to ICAM-1 and to determine if the activation state of LFA-1 would affect the extent of any possible crosstalk. However, similar to the results seen in the K562 system, no significant effects were observed, with both blocking and activating α5β1 and α4β1 mAbs exhibiting similar profiles. In all cases $JB2.7_{ORG}$, which lacks expression of LFA-1, gave similar results to the LFA-1-containing cell lines (Figure 6.13).

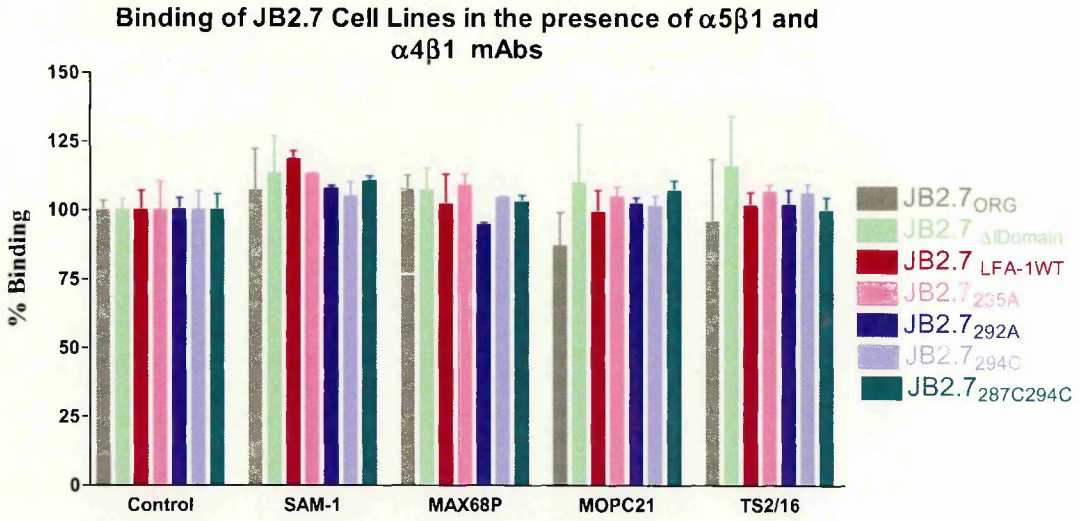

Figure 6.13 **Binding of JB2.7 Cell Lines to ICAM-1 in the presence of α5β1 and α4β1 mAbs.** Cells were washed and diluted in DMEM (media) with 1mM Mn^{2+} followed by the addition of one of the following mAbs SAM-1: α5 blocking mAb; Max68P: α4 blocking mAb; TS2/16: activating β1 mAb or MOPC21 (control mAb) (20μg/ml final concentration). 100% represents the binding of the individual cell lines in the absence of mAb. Each data point represents mean +/-SD (n=3) and the data presented here are representative of 2 other independently performed experiments.

6.5 Discussion

The data presented in Chapter 5 suggested that under certain conditions activated forms of LFA-1 expressed in K562 cells could influence the ability of α5β1 to bind to fibronectin. The work presented in this chapter extends our investigations into LFA-1 crosstalk by looking at the ability of activated forms of LFA-1 to modulate the binding of both α5β1 and α4β1 in the Jurkat derived cell line, JB2.7.

As predicted, the $JB2.7_{ORG}$ and $JB2.7_{\Delta IDomain}$ cell lines which lack functional LFA-1, were unable to support ICAM ligand binding even in the presence of activating mAbs. JB2.7 cells reconstituted with wild type LFA-1 ($JB2.7_{LFA\text{-}1WT}$) were also unable to support binding to the ICAM family members in the presence of media alone. Published data from Weber *et al.* (1997), Lupher *et al.* (2001) and Leitinger and Hogg (2000) support this finding. In all of these reports, stimulating agents such as PMA, Mn^{2+} or activating mAbs were required to activate the integrin. Additions of Mn^{2+} and PMA in this study were also shown to be capable of inducing wild type LFA-1 binding to ICAM-1 although, in both cases, the level of binding could be further increased in the presence of KIM127. Addition of both KIM127 and KIM185 were also shown by Leitinger and Hogg (2000) to further increase binding of wild type LFA-1 to ICAM-1 in the presence of PMA. While there is a statistically significant increase in the ligand binding of the $JB2.7_{292A}$ cell line over the $JB2.7_{LFA\text{-}1WT}$ cell line in the presence of media alone this binding is much reduced compared to the other mutated cell lines in the study. This cell line also showed comparable binding levels to the $JB2.7_{LFA\text{-}1WT}$ cell line in the presence of Mn^{2+} suggesting that in JB2.7 cells the controlling effects of the cytoplasmic domains play a more dominant role than in K562 cells and thus override the capacity of this mutation to activate LFA-1.

Similar to the results seen for the mutated LFA-1-transfected K562 cell lines, the JB2.7$_{294C}$, JB2.7$_{235A}$ and JB2.7$_{287C294C}$ cell lines showed constitutive LFA-1/ICAM-1 binding. This contrasts with work from Lupher *et al.* (2001), which showed that transfection of JB2.7 cells with αL containing the 235A mutation was unable to support ligand binding in the presence of media alone. While the JB2.7$_{294C}$, JB2.7$_{235A}$ and JB2.7$_{287C294C}$ cell lines showed significantly enhanced binding relative to JB2.7$_{WTLFA-1}$, both in the presence of media alone and with 1mM Mn^{2+}, the magnitude of the effects are lower than seen in the K562 cell system. As hypothesized for the 292A mutant, intracellular regular regulation may play a greater role in controlling integrin function in JB2.7 cells than in K562 cells.

Binding of all cell lines expressing LFA-1 was further increased in the presence of KIM127 and, similar to the effects seen with the K562 cell system, the addition of the activating mAb conferred similar levels of binding to all the ICAM-1 binding cell lines. Binding of all the cell lines to ICAM-2 and ICAM-3 followed similar trends to those seen for ICAM-1 binding. Results from blocking studies with 6.5E also support the findings from the K562 experiments.

PMA was capable of stimulating binding of LFA-1-expressing JB2.7 cells to ICAM-1 over and above that seen with media alone. PMA is known to act by inducing clustering of LFA-1 on the cell surface and this result suggests that, in the presence of media containing Mg^{2+}, clustering of the integrin also contributes to ligand binding through avidity changes in the integrin. The concentration of LFA-1 molecules in discreet regions on the cell surface appears to increase the number of interactions with ligand compared to the unclustered state. Since the hierarchy of binding between the various cell lines is maintained in the presence of PMA, it would appear that LFA-1 clusters to the same extent in all cell lines and that the same proportion of LFA-1 molecules are in an active state regardless of whether PMA is present or not. Similar to our results on activation of the JB2.7$_{235A}$ cell line in the presence of PMA, Lupher *et al.* (2001) have also shown that JB2.7 cells expressing LFA-1 with an alanine substitution at I235 demonstrate increased binding to ICAM-1 over wild type in the presence of PMA. Leitinger and Hogg

(2000) have also shown that phorbol esters induce JB2.7$_{LFA\text{-}1WT}$ cells to bind ICAM-1 and that this binding can be further enhanced in the presence of KIM127. In our studies, activation of all cell lines in the presence of PMA could also be further enhanced by the addition of KIM127, and this mAb was capable of activating all cell lines to a similar extent.

Previously, Leitinger and Hogg (2000) showed that removal of the I domain from the αL subunit generates a form of LFA-1 that appears to be in an activated state (as indicated by the binding of activation state reporter mAbs) although its ability to bind ligand is abolished. Using this activated form of LFA-1, they showed that LFA-1 was capable of influencing the ability of other integrins (α5β1 and α4β1) on the same cell surface to bind ligand. This binding could also be further enhanced by the addition of stimulating mAbs. By introducing select mutations within the IDAS, we have also been able to generate activated forms of LFA-1 in the JB2.7 cell system. These cell lines were shown to constitutively bind ligand and display enhanced mAb24 binding when compared with both JB2.7 $_{LFA\text{-}1WT}$ and JB2.7$_{\Delta IDomain}$ cell lines.

We investigated whether these mutated forms of LFA-1 could influence the binding of either α5β1 or α4β1, which are both endogenously expressed on the cell surface of JB2.7 cells, to their respective ligands. The LFA-1 wild type (JB2.7$_{LFA\text{-}1WT}$) and the I domain-less LFA-1 (JB2.7$_{\Delta IDomain}$) cell lines generated in the Leitinger *et al.* studies were also included in our experiments. No significant differences were seen in the ability of any of the cell lines to bind to fibronectin either constitutively or following Mn^{2+}, KIM127 or KIM185 activation. While a small but statistically significant increase in binding of α4β1 to VCAM-1 in media alone was noted in JB2.7$_{\Delta IDomain}$ cells when compared with JB2.7$_{ORG}$ cells, overall, the crosstalk seen in the JB2.7 cells in the presence or absence of activating stimuli was small and based on this data must be considered of dubious physiological relevance.

Whilst the data presented here therefore does not appear to support the conclusions drawn by Leitinger *et al.* there are some potential explanations for the discrepancy. It may be that removal of the I domain forces LFA-1 into a conformation that affects crosstalk signalling pathways and this conformation is not replicated by any of the forms of I domain containing LFA-1 used in this study. However this does not explain the failure of the work reported here to show a difference in fibronectin binding between the JB2.7 cells expressing wild type and the $JB2.7_{\Delta IDomain}$ cell line. It must be noted that the assay system used in the experiments described here does differ from that used by Leitinger *et al.* Their system involved counting ligand-coated beads that remained bound to individual cells after gentle washing and cell fixing. It is possible that this assay is more sensitive and capable of picking up small effects compared to the plate binding methods used in this study. Several attempts were made to carry out the bead-binding format for this study but results were too inconsistent for any firm conclusions to be drawn.

Chapter 7

Discussion

Chapter 7 Discussion

The work reported in this thesis has investigated both the contribution of the IDAS site within the I domain to the activation state of LFA-1 and the effect activated LFA-1 molecules have on the activation state of other integrins expressed on the same cell surface. Through introduction of select mutations within the IDAS site, several activated forms of LFA-1 were generated that showed increased affinity for ligand relative to wild type when expressed both in a soluble form and on the cell surface. Having an activated form of LFA-1 also allowed us to investigate the capacity of LFA-1 to crosstalk with α5β1 and α4β1 on K562 and JB2.7 cells.

At the start of this work, several crystal structures of the αM and α2 I domains had been solved and, depending on the crystallization conditions used, were shown to take up two different conformations. The 'open', or high affinity conformation was observed in crystals that had Mg^{2+} at the MIDAS bound to a glutamate residue from either a ligand (α2) or an adjacent I domain (αM) (Lee *et al.*, 1995; Emsley *et al.*, 2000). The 'open' conformation differed from the 'closed', ligand-free, low affinity structure in terms of the position of residues around the MIDAS but the most dramatic difference was a 10Å downward shift of the α7 helix distal to the MIDAS site. The α7 helix is at the C-terminal end of the I domain and is connected by a flexible linker sequence to the β-propeller.

Through its connection to the main body of the integrin head piece, the IDAS site is now thought to be involved in propagating conformational change to and from the I domain ligand binding site as a result of ligand binding or through conformational change initiated within the cytoplasmic tails as a result of inside-out signalling. As part of this study residues along the length of the α7 helix contained within the IDAS site were mutated, based on the fact that their size and the reactivity of their side chains appeared to preferentially restrain LFA-1 in an inactive conformation. By

substituting these residues with alanine or cysteine, we appeared to be able to artificially shift the equilibrium in favour of the active conformation.

During the course of this work several other groups had also shown that LFA-1 activity could be enhanced by introduction of mutations within the IDAS site. Huth *et al.* (2000) achieved this through the introduction of a series of alanine substitutions in the IDAS site and identified I235 and I306 as residues that appear to preferentially hold the I domain in the 'closed' conformation as substitutions at these positions conferred constitutive activity to LFA-1 expressed on the cell surface. The novel introduction of select cysteine bonds within the IDAS site by Shimaoka *et al.* (2001) also allowed the 'open' and 'closed' conformations seen in the various crystal structures of the αM and α2 I domains to be mimicked within the αL I domain. Results from their ligand binding studies using these restrained I domains reinforced the idea that the downward shift of the α7 helix plays a major role in switching LFA-1 from an inactive to an active state. Indeed when these restraints were introduced into full length LFA-1 expressed on the cell surface, constitutive activity was conferred to the integrin with equivalent levels of binding in the presence of both Mn^{2+} and Mg^{2+} which could not be further enhanced by addition of the activating mAb, CRBLFA-1/2 (Lu *et al.*, 2001, Shimaoka *et al.*, 2001).

In the work reported in this thesis, all of the above mutations along with novel alanine substitutions at positions F292, L295, and F299 were introduced in the αL I domain and were evaluated for their contribution to the proposed conformational changes which take place on integrin activation. F292, L295, and F299 are contained within the loop that connects the β6 strand and α7 helix and it was reasoned that a downward shift of the α7 helix would be associated with radical structural change around these residues and their side chains within the loop in order to facilitate this conformational change. By substituting these residues for alanine residues we proposed that some of the side chain interactions would be removed and that the size change in the case of phenylalanine may introduce more flexibility into this region and therefore lower the energy barrier required to shift the I domain into the active state.

Our findings support the theory that the IDAS site does indeed contribute to the overall activation state of LFA-1. However, we believe also that other factors including attachment to the cell membrane contribute to the activation state and act to restrain the integrin in an inactive form. In our soluble system where the extracellular region of LFA-1 was fused to a Fc moiety, encouraging stable heterodimerisation of the α and β chains by the formation of disulphide bridges in the hinge region of the CH3 domains, LFA-1 constructs containing either the 287C294C double mutation, a single K→C substitution at position 294 or alanine substitutions at F292 or K295 appeared to confer constitutive activity to LFA-1. This was confirmed by the inability of the KIM mAbs and MEM148 to further increase the binding of these constructs to ICAM-1. The introduction of alanine substitutions at residues I235 and I306 also increased ligand binding above wild type but, interestingly, similar to the wild type LFA-1 construct, this binding was further increased by the addition of the activation mAbs. This suggested that even though these mutations shifted the equilibrium further in favour of the active state compared to wild type, it was not sufficient to fully activate the integrin. Whilst alanine substitution of several of the amino acids along the α7-helix appeared to shift the equilibrium towards the active conformation, F299 appears to be essential for the maintenance of the integrity of the ligand binding interface regardless of whether it is in the 'open' or 'closed' conformation. Substitution of this residue to alanine completely abolished the ligand binding capability of LFA-1 although, interestingly expression levels were double that of the wild type construct and antibody binding did not appear to be affected by its absence.

Results published by Lu *et al.* (2001) showed that introduction of a disulphide bond through cysteine substitutions at positions K289 and K294 locked the I domain in a 'closed' conformation, preventing the binding of ligand when expressed as an isolated I domain on the surface of 293T cells. In contrast, in our soluble system this construct behaved in a similar manner to wild type, with further increases in ligand binding shown on the addition of activating mAbs. Addition of a reducing agent such as DTT would have likely adverse affects on LFA-1 due to the presence of several other cysteine bonds in the structure so we were unable to ascertain if indeed the formation

of any of the disulphide bonds did indeed occur. In our hands, single cysteine substitutions at positions 287 and 294 displayed either similar or better ligand binding affinities respectively compared to our wild type construct. This result suggests that, although the formation of the cysteine bond can contribute to the increased affinity for ligand, it is the nature and position of the substitution that is the deciding factor in altering the activation state of LFA-1.

It is widely accepted that the cytoplasmic domains play a central role in the regulation of the adhesive and signalling functions of LFA-1 and whilst the soluble system allowed analysis of the effect of affinity changes that mutations within the IDAS site might confer on LFA-1, the contribution of these domains in the regulation of the whole integrin could not be assessed. To address this, mutations that displayed higher binding activity relative to the wild type construct were introduced into two different cell lines, K562 and JB2.7, both of which have previously been used by other research groups to study the role of LFA-1.

As previously reported by Ortlepp *et al.* (1995) for KL4 cells, wild type LFA-1 expressed on the surface of both K562 and JB2.7 cell lines appeared to be in a low state of activation as judged by its low-level binding to immobilized ICAM ligands. Introduction of the activating mutations used in the soluble system did greatly enhance the capacity of LFA-1 to bind ligand both in media alone and in the presence of Mn^{2+}. The hierarchy of binding of the various forms of cell surface expressed LFA-1 followed a similar pattern to that seen for the soluble constructs although, interestingly, the 294C and 287C294C mutations in both cell lines displayed similar levels of ligand binding in the presence of both Mn^{2+} and Mg^{2+}. This supports the hypothesis discussed above that it is the 294C substitution itself, and not the presence of the disulphide bond, that confers increased affinity to the LFA-1 molecule. In all cases, activating mAbs could further increase affinity for the ICAM ligands, suggesting that other factors were involved in regulating the affinity of LFA-1 for its ligands in the context of the whole integrin. This result also suggests that there is some flexibility in the overall structure of the integrin which is locked on binding of KIM127 into a state favourable for ICAM binding.

By modelling LFA-1 on the crystal structure of αVβ3, Lu *et al.* (2001) showed that the KIM127 epitope was obscured in the 'closed' bent conformation which suggested that it could only bind when the integrin was in the extended conformation. The overall implication is that mAbs such as KIM185 and KIM127 provide rigidity to the extended form of the integrin, and hold it in a conformation that allows ligand to bind.

Through the course of these studies it was noted that the LFA-1 blocking mAb, 6.5E, was unable to fully block ligand binding of some of the mutated forms of LFA-1 when expressed both in soluble and cell-expressed systems. The epitope of 6.5E has been mapped to the top of the β-chain I-like domain and binding studies have shown that both the α and β subunits are required to be present for epitope presentation (Huang *et al.*, 2000). Since flow cytometric analysis showed that the mAb bound to the same extent to all cell lines, the suggestion is that 6.5E inhibits ligand binding either through steric hindrance or through an allosteric mechanism since the epitope is not in the same vicinity as the I domain MIDAS site.

While some groups have reported the ability of PMA to activate LFA-1 expressed on K562 cells, results presented in this study together with data from S.Ortlepp (1997) in this laboratory and Lub *et al.* (1997) do not support this, at least in short term adhesion assays. Findings from Lub *et al.* (1997) suggest that some of the components in the signal transduction pathway linking PKC activation to integrin activation are absent or non-functional in K562 cells, but it must be noted that these components are integrin-specific since PMA can activate some, but not all integrins expressed on K562 cells. This result is in contrast to the results obtained from activation of the LFA-1 expressing JB2.7 cell lines where PMA was able to activated cells transfected with wild type and mutated LFA-1 to a similar extent. The JB2.7 cell line was generated from a Jurkat cell line which, before treatment with EMS (ethylmethane sulphonate), expressed LFA-1 endogenously (Weber *et al.*, 1997). Regardless of the initial activation state of the JB2.7 cell lines expressing different forms of LFA-1, PMA increased the binding of all LFA-1 expressing cell lines while maintaining the hierarchy seen in the presence of media alone. This result is consistent with previous data

suggesting that PMA increases the avidity rather than affinity of LFA-1 for its ligand (Stewart *et al.*, 1996; Van Kooyk *et al.*, 1991; Van Kooyk *et al.*, 1999). The concentration of LFA-1 molecules in discrete regions on the cell surface appears to increase the number of interactions with ligand compared to the unclustered state. Since the hierarchy of binding between the various cell lines is maintained in the presence of PMA, it would appear that the activation state of LFA-1 does not dramatically change its ability to be clustered following PMA treatment.

As well as being one of the main players in the initiation and maintenance of adhesiveness during cell-cell and cell-endothelium contact, integrins are also signalling molecules and signalling pathways initiated through integrin ligand interactions have been shown to be involved in gene expression and cell growth, differentiation and survival (reviewed by Schwartz and Ginsberg, 2003). Evidence is now also emerging which suggests that, in addition to the effects on other receptors on the cell surface, outside-in signals can also alter the activity of neighbouring integrins in a process termed 'crosstalk' (Blystone *et al.*, 1994; Leitinger and Hogg, 2000). Results to date suggest that both the hierarchy and the capacity of an integrin to positively or negatively regulate the function of other integrins is dependent to some extent on the levels of expression of the integrins involved (Diaz-Gonzalez *et al.*, 1996) although further research is required to fully define how crosstalk is initiated and maintained. Work from N. Hoggs's laboratory (Leitinger *et al.*, 2001, Porter and Hogg, 1997) has suggested that LFA-1 can regulate both $\alpha4\beta1$ and $\alpha5\beta1$ in a positive and negative manner depending on the cell type and relative concentrations of each of the integrins involved.

Having identified that alanine or cysteine substitutions within the IDAS site could constitutively activate LFA-1 both in a soluble and cellular environment, further work in this thesis addressed whether activation of LFA-1 in such a manner affected its ability to crosstalk. We showed that when LFA-1 was highly activated in the presence of KIM127, regardless of its initial activation state, adhesion of $\alpha5\beta1$ to fibronectin was increased. No increase in LFA-1 binding to ICAM-1 was noted when $\alpha5\beta1$ was activated suggesting that LFA-1 is the dominant-integrin in the K562

cell system and positively regulates α5β1 activation. Mean Fluorescence Intensity measurements showed that transfected LFA-1 is as highly expressed or even more highly expressed, than α5β1. This is the first report of LFA-1 crosstalk in K562 cells and these cells may employ different control mechanisms relative to the T-cell cell types previously used to investigate crosstalk (Leitinger *et al.*, 2001, Porter and Hogg, 1997).

Whilst the K562 cell line crosstalk data suggests that LFA-1 needs to be highly activated in order to influence the binding of other integrins, there remains the possibility that a reduced level of signalling in this cell line, as suggested by the lack of induced ligand binding in the presence of PMA, would lead to an underestimation of the effect of LFA-1 crosstalk. If this is the case, then, less activated forms of LFA-1 such as our mutated forms of LFA-1, without the presence of activating mAbs, may be sufficient to demonstrate crosstalk in another cell line. Leitinger *et al.* (2001) have previously demonstrated enhanced α5β1- and α4β1- dependent adhesion using an activated form of LFA-1 generated by the deletion of the I domain in the JB2.7 cell line. They showed that, on deletion of the I domain, they could express correctly folded LFA-1 which displayed many of the attributes of an activated form of LFA-1 although it lacked the capacity to bind ligand. Analysis of the activation state of the mutated forms of LFA-1 by mAb24 binding showed that the mAb bound as well or better to our mutant cell lines as to this JB2.7$_{\Delta IDomain}$ cell line.

Disappointingly, our studies did not fully replicate the crosstalk reports of Leitinger *et al.* While we were able to confirm that the JB2.7$_{\Delta IDomain}$ cell line showed significantly more binding to VCAM-1 than that seen for the parental cell line lacking LFA-1 expression (JB2.7$_{ORG}$), our data failed to show a significant increase in binding to fibronectin over the JB2.7$_{ORG}$ cell line. Also, none of the activated forms of LFA-1 generated in this study showed increased binding to VCAM-1 or fibronectin over and above that seen for the JB2.7$_{ORG}$ cell line even when further activated with KIM127. Unlike the situation found in K562 cells, KIM127 treatment of the JB2.7 cells did not stimulate fibronectin binding. Also it was noted that on Mn^{2+} activation JB2.7$_{LFA\text{-}1WT}$ and JB2.7$_{292A}$ cells showed a marginal reduction in fibronectin binding when compared to JB2.7$_{ORG}$ cells. While

the most convincing sign of crosstalk involved the increased binding of the JB2.7$_{\Delta IDomain}$ cell line to VCAM-1, the lack of crosstalk with the other cell lines does bring into question its physiological relevance in the JB2.7 cell line. Although it is possible that LFA-1 lacking an I domain does adopt the conformation of an active LFA-1 molecule and thus mimics real integrin/integrin interactions, our efforts to replicate this with molecules of more obvious physiological relevance were unsuccessful.

While work in this thesis has generated some evidence for integrin crosstalk (most convincingly for KIM127 activated LFA-1 forms interacting with $\alpha5\beta1$), it is clear that from the data presented here and the literature surrounding integrin crosstalk that the phenomenon is complicated and as yet poorly understood. It does not appear that mutations which activate the extracellular domain of LFA-1 can alone result in crosstalk (at least in the cells tested here). This may suggest that integrin clustering plays a key role in crosstalk. The ability of integrins to crosstalk may also be further complicated by cell line specific differences. This is highlighted in this work by what appears to be a clear case of crosstalk in K562 cells that cannot be replicated in JB2.7 cells.

While crosstalk between integrins remains a very attractive theory to explain the regulation of some cellular interactions, the complex nature of such pathways requires additional methodologies to be developed to analysis further the mechanisms involved. Such methodologies include:

1. The development of more sensitive assay systems, possibly using radio-labelling techniques, which could reliably detect small changes in integrin-ligand interactions.
2. Determination of the effects on crosstalk of altering the relative concentration of integrins on the cell surface. Diaz-Gonzalez *et al.* (1996) have previously shown that negative versus positive regulation is dependent on the levels of expression of the integrins involved, with negative regulation controlled by high expression of the dominant integrin. In the context of the work presented in this thesis, this could be investigated by selecting both JB2.7 and K562 wild type and mutated clones expressing different levels of LFA-1 and analysing whether such differences have an effect on the capacity of LFA-1 to regulate the activation

state of other integrins expressed on the same cell surface. The activation state of LFA-1 could also be manipulated in such a system. This may lead to an explanation for the differential ability of LFA-1 to crosstalk in the K562 cells compared with JB2.7 cells.

3. Analysis of the distribution of LFA-1 on the cell surface of the K562 and JB2.7 cell lines. Using confocal microscopy the effects of different activating agents such as PMA, antibodies and cations on the cellular distribution of the integrins involved may help to explain the differences seen in the ability of the two cell types used in this study to initiate crosstalk. Previous work by Leitinger *et al.* (2002) using a similar technique showed that, when activated, LFA-1 homed to lipid rafts which then initiated the entry of other integrins into the rafts through crosstalk.
4. Examination of the availability of adaptor proteins for cytoskeletal connections or components critical for signalling pathways. A detailed analysis of the concentration, activation state and integrin-associated intracellular and cytoskeletal proteins by intracellular staining and immunoprecipitation techniques may help to shed light on the fundamental processes involved in crosstalk. Of special interest would be a study of the phosphorylation profiles over time, not only of the integrin cytoplasmic domains, but also of protein kinases such as Lck, Fyn, and Fak which appear to play important roles in regulating integrin signalling (reviewed in Giancotti *et al.* 2003). The proteolytic state of talin (Valmu *et al.*, 1999; Kupfer *et al.*, 1990) and cytohesin (Geiger *et al.*, 2000) during LFA-1 activation, and analysis of their association with the expressed integrin cytoplasmic tails may also be informative.

The IDAS mutations analysed during the course of these studies showed that this region of the I domain has a significant role to play in the activation state of LFA-1. Further structural analysis now suggests that the I domain may in fact be an intrinsic ligand for the β-I-like domain in I domain-containing integrins and bind in a similar manner to ligands of non I domain-containing

integrins (Alonso *et al.*, 2002; Yang *et al.*, 2004). The conformation of the β-I-like domain appears to be directly influenced by the structural changes brought about by activation of integrins through inside-out signalling. It therefore may be more beneficial to use different activation conformations of the β I-like domain (which could be brought about by introduction of select mutations and activating mAbs) to elucidate the factors involved in LFA-1 crosstalk. Using this approach, a more direct influence of changes in the globular head of the integrin may lead to more defined and measurable changes in intracellular signalling and subsequent crosstalk to other integrins on the cell surface.

Another area of study which may lead to advancement in the understanding of LFA-1 activation and its effects on cellular signalling is the role of the various cation-binding sites that have recently been identified (Xiong *et al.*, 2001; Xiong *et al.*, 2002). Elucidation of the role of cation at each of these sites may help to identify a physiological mechanism of outside-in integrin activation leading possibly to novel signalling pathways and may highlight yet another level of control over the activation state of LFA-1 and integrins in general.

Much progress has been made over the last few years in our understanding of the changes integrins undergo to become functionally active. Nonetheless, further investigation of integrin signalling partners, modes of activation and structural rearrangement may help identify additional points of intervention at which therapeutic agents may be directed. For example, the generation of novel therapeutics that stabilize particular integrin conformations, or competitively interfere with ligand binding, or interfere with signalling pathways. This will be particularly important in the case of LFA-1, which is an important target in the pharmaceutical industry for blocking organ transplantation rejection and treating inflammatory diseases. While monoclonal antibodies have been shown to prolong graft survival in many animal models (Nicolls *et al.*, 2002; Poston *et al.*, 2000; Sarnacki *et al.*, 2000) and to alleviate symptoms of psoriasis in clinical trails (Gottlieb and Bos, 2002, Gottlieb *et al.*, 2002), the identification of low molecular weight inhibitors that can be

administered orally has remained elusive. The identification of further molecularly defined points of intervention, at which such inhibitors may be directed should help this drug discovery process.

Conclusions

The work presented in this thesis has confirmed that mutations in the IDAS of the I domain of LFA-1 can alter the ability of LFA-1 to bind to its ligands. A number of the mutations have confirmed previous literature reports and the results obtained with novel mutations are consistent with currently accepted theories of the interaction of I domains with integrin ligands. Our findings also indicate that alterations to the IDAS site do not cause any major changes in ligand specificity or divalent cation responsiveness.

Whilst the data presented here is consistent with the idea that under certain circumstances the activation state of one integrin can modify the ability of other integrins on the same cell to interact with their ligands it is apparent that the conditions under which crosstalk can occur varies between cell lines. Under the conditions used in this study the introduction of mutations into the LFA-1 I domain currently known to promote ligand binding were not sufficient alone to promote integrin crosstalk in either the K562 or JB2.7 cell systems but in the presence of mAb KIM127, crosstalk between $\alpha 5\beta 1$ and all forms of K562 surface expressed LFA-1 was effectively induced.

Chapter 8

References

Reference List

Acevedo, A., M. A. del Pozo, A. G. Arroyo, P. Sanchez-Mateos, R. Gonzalez-Amaro, and F. Sanchez-Madrid. 1993. Distribution of ICAM-3-bearing cells in normal human tissues. Expression of a novel counter-receptor for LFA-1 in epidermal Langerhans cells. *Am J Pathol.* 143:774-783.

Alonso, J. L., M. Essafi, J. P. Xiong, T. Stehle, and M. A. Arnaout. 2002. Does the integrin alphaA domain act as a ligand for its betaA domain? *Curr.Biol.* 12:R340-R342.

Andrew, D., A. Shock, E. Ball, S. Ortlepp, J. Bell, and M. Robinson. 1993. KIM185, a monoclonal antibody to CD18 which induces a change in the conformation of CD18 and promotes both LFA-1- and CR3-dependent adhesion. *Eur.J Immunol* 23:2217-2222.

Armulik, A., I. Nilsson, G. von Heijne, and S. Johansson. 1999. Determination of the border between the transmembrane and cytoplasmic domains of human integrin subunits. *J Biol.Chem.* 274:37030-37034.

Arnaout, M. A., E. Remold-O'Donnell, M. W. Pierce, P. Harris, and D. G. Tenen. 1988. Molecular cloning of the alpha subunit of human and guinea pig leukocyte adhesion glycoprotein Mo1: chromosomal localization and homology to the alpha subunits of integrins. *Proc.Natl.Acad Sci.U.S.A* 85:2776-2780.

Arnaout, M. A. 2002. Integrin structure: new twists and turns in dynamic cell adhesion. *Immunol Rev.* 186:125-140.

Arnaout, M. A., S. L. Goodman, and J. P. Xiong. 2002. Coming to grips with integrin binding to ligands. *Curr.Opin.Cell Biol.* 14:641-651.

Bailly, P., E. Tontti, P. Hermand, J. P. Cartron, and C. G. Gahmberg. 1995. The red cell LW blood group protein is an intercellular adhesion molecule which binds to CD11/CD18 leukocyte integrins. *Eur.J Immunol* 25:3316-3320.

Baldwin, E. T., R. W. Sarver, G. L. Bryant, Jr., K. A. Curry, M. B. Fairbanks, B. C. Finzel, R. L. Garlick, R. L. Heinrikson, N. C. Horton, L. L. Kelley, A. M. Mildner, J. B. Moon, J. E. Mott, V. T. Mutchler, C. S. Tomich, K. D. Watenpaugh, and V. H. Wiley. 1998. Cation binding to the integrin CD11b I domain and activation model assessment. *Structure.* 6:923-935.

Bazzoni, G., L. Ma, M. L. Blue, and M. E. Hemler. 1998. Divalent cations and ligands induce conformational changes that are highly divergent among beta1 integrins. *J Biol.Chem.* 273:6670-6678.

Beglova, N., S. C. Blacklow, J. Takagi, and T. A. Springer. 2002. Cysteine-rich module structure reveals a fulcrum for integrin rearrangement upon activation. *Nat.Struct.Biol.* 9:282-287.

Bella, J., P. R. Kolatkar, C. W. Marlor, J. M. Greve, and M. G. Rossmann. 1998. The structure of the two amino-terminal domains of human ICAM-1 suggests how it functions as a rhinovirus receptor and as an LFA-1 integrin ligand. *PNAS* 95:4140-4145.

Berg, N. N. and H. L. Ostergaard. 1997. T cell receptor engagement induces tyrosine phosphorylation of FAK and Pyk2 and their association with Lck. *J Immunol* 159:1753-1757.

Berg, R. W., E. Leung, S. Gough, C. Morris, W. P. Yao, S. X. Wang, J. Ni, and G. W. Krissansen. 1999. Cloning and characterization of a novel beta integrin-related cDNA coding for the protein TIED ("ten beta integrin EGF-like repeat domains") that maps to chromosome band 13q33: A divergent stand-alone integrin stalk structure. *Genomics* 56:169-178.

Berlin-Rufenach, C., F. Otto, M. Mathies, J. Westermann, M. J. Owen, A. Hamann, and N. Hogg. 1999. Lymphocyte Migration in Lymphocyte Function-associated Antigen (LFA)-1-deficient Mice. *J.Exp.Med.* 189:1467-1478.

Bilsland, C. A., M. S. Diamond, and T. A. Springer. 1994. The leukocyte integrin p150, 95 (CD11c/CD18) as a receptor for iC3b. Activation by a heterologous beta subunit and localization of a ligand recognition site to the I domain. *J Immunol* 152:4582-4589.

Birner, U., T. B. Issekutz, U. Walter, and A. C. Issekutz. 2000. The role of alpha (4) and LFA-1 integrins in selectin-independent monocyte and neutrophil migration to joints of rats with adjuvant arthritis. *Int.Immunol* 12:141-150.

Bleijs, D. A., M. E. Binnerts, S. J. van Vliet, C. G. Figdor, and Y. van Kooyk. 2000. Low-affinity LFA-1/ICAM-3 interactions augment LFA-1/ICAM-1-mediated T cell adhesion and signaling by redistribution of LFA-1. *J Cell Sci.* 113 (Pt 3): 391-400.

Blystone, S. D., I. L. Graham, F. P. Lindberg, and E. J. Brown. 1994. Integrin alpha v beta 3 differentially regulates adhesive and phagocytic functions of the fibronectin receptor alpha 5 beta 1. *J Cell Biol.* 127:1129-1137.

Blystone, S. D., F. P. Lindberg, S. E. LaFlamme, and E. J. Brown. 1995. Integrin beta 3 cytoplasmic tail is necessary and sufficient for regulation of alpha 5 beta 1 phagocytosis by alpha v beta 3 and integrin-associated protein. *J Cell Biol.* 130:745-754.

Blystone, S. D., S. E. Slater, M. P. Williams, M. T. Crow, and E. J. Brown. 1999. A molecular mechanism of integrin crosstalk: alpha V beta3 suppression of calcium/calmodulin-dependent protein kinase II regulates alpha5beta1 function. *J Cell Biol.* 145:889-897.

Bork, P., T. Doerks, T. A. Springer, and B. Snel. 1999. Domains in plexins: links to integrins and transcription factors. *Trends Biochem.Sci.* 24:261-263.

Bouvard, D., C. Brakebusch, E. Gustafsson, A. Aszodi, T. Bengtsson, A. Berna, and R. Fassler. 2001. Functional consequences of integrin gene mutations in mice. *Circ Res* 89:211-223.

Butcher, E. C., M. Williams, K. Youngman, L. Rott, and M. Briskin. 1999. Lymphocyte trafficking and regional immunity. *Adv.Immunol* 72:209-253.

Cabanas, C. and N. Hogg. 1993. Ligand intercellular adhesion molecule 1 has a necessary role in activation of integrin lymphocyte function-associated molecule 1. *Proc.Natl.Acad Sci.U.S.A* 90:5838-5842.

Calzada, M. J., M. V. Alvarez, and J. Gonzalez-Rodriguez. 2002. Agonist-specific structural rearrangements of integrin alpha IIb beta 3. Confirmation of the bent conformation in platelets at rest and after activation. *J Biol.Chem.* 277:39899-39908.

Campbell, J. J., J. Hedrick, A. Zlotnik, M. A. Siani, D. A. Thompson, and E. C. Butcher. 1998. Chemokines and the arrest of lymphocytes rolling under flow conditions. *Science* 279:381-384.

Casasnovas, J. M. and T. A. Springer. 1995. Kinetics and thermodynamics of virus binding to receptor. Studies with rhinovirus, intercellular adhesion molecule-1 (ICAM-1), and surface plasmon resonance. *J Biol.Chem.* 270:13216-13224.

Casasnovas, J. M., T. A. Springer, J. H. Liu, S. C. Harrison, and J. H. Wang. 1997. Crystal structure of ICAM-2 reveals a distinctive integrin recognition surface. *Nature* 387:312-315.

Casasnovas, J. M., T. Stehle, J. H. Liu, J. H. Wang, and T. A. Springer. 1998. A dimeric crystal structure for the N-terminal two domains of intercellular adhesion molecule-1. *Proc.Natl.Acad Sci.U.S.A* 95:4134-4139.

Casasnovas, J. M., C. Pieroni, and T. A. Springer. 1999. Lymphocyte function-associated antigen-1 binding residues in intercellular adhesion molecule-2 (ICAM-2) and the integrin binding surface in the ICAM subfamily. *Proc.Natl.Acad Sci.U.S.A* 96:3017-3022.

Champe, M., B. W. McIntyre, and P. W. Berman. 1995. Monoclonal antibodies that block the activity of leukocyte function-associated antigen 1 recognize three discrete epitopes in the inserted domain of CD11a. *J Biol.Chem.* 270:1388-1394.

Chan, A. W., M. J. Minski, L. Lim, and J. C. Lai. 1992. Changes in brain regional manganese and magnesium levels during postnatal development: modulations by chronic manganese administration. *Metab Brain Dis.* 7:21-33.

Chan, B. M., M. J. Elices, E. Murphy, and M. E. Hemler. 1992. Adhesion to vascular cell adhesion molecule 1 and fibronectin. Comparison of alpha 4 beta 1 (VLA-4) and alpha 4 beta 7 on the human B cell line JY. *J.Biol.Chem.* 267:8366-8370.

Chan, B. M., V. L. Morris, D. Hangan-Steinman, B. Jarvie, M. Cialacu, J. Laansoo, G. Hunter, W. Wan, and S. Uniyal. 2002. Integrin alpha2beta1 on rat myeloma cells modulates interaction of alpha4beta1 integrin with vascular cell adhesion molecule-1 but not fibronectin. *J Biomater.Sci.Polym.Ed* 13:429-446.

Chan, J. R., S. J. Hyduk, and M. I. Cybulsky. 2000. α4β1 Integrin/VCAM-1 Interaction Activates αLβ2 Integrin-Mediated Adhesion to ICAM-1 in Human T Cells. *J Immunol* 164:746-753.

Cherukuri, A., M. Dykstra, and S. K. Pierce. 2001. Floating the raft hypothesis: lipid rafts play a role in immune cell activation. *Immunity.* 14:657-660.

Claas, C., C. S. Stipp, and M. E. Hemler. 2001. Evaluation of prototype transmembrane 4 superfamily protein complexes and their relation to lipid rafts. *J Biol.Chem.* 276:7974-7984.

Cockett, M. I., C. R. Bebbington, and G. T. Yarranton. 1991. The use of engineered E1A genes to transactivate the hCMV-MIE promoter in permanent CHO cell lines. *Nucleic Acids Res* 19:319-325.

Constantin, G., M. Majeed, C. Giagulli, L. Piccio, J. Y. Kim, E. C. Butcher, and C. Laudanna. 2000. Chemokines trigger immediate beta2 integrin affinity and mobility changes: differential regulation and roles in lymphocyte arrest under flow. *Immunity.* 13:759-769.

Corbi, A. L., T. K. Kishimoto, L. J. Miller, and T. A. Springer. 1988. The human leukocyte adhesion glycoprotein Mac-1 (complement receptor type 3, CD11b) alpha subunit. Cloning, primary structure, and relation to the integrins, von Willebrand factor and factor B. *J.Biol.Chem.* 263:12403-12411.

D'Arcangelo, G., G. G. Miao, S. C. Chen, H. D. Soares, J. I. Morgan, and T. Curran. 1995. A protein related to extracellular matrix proteins deleted in the mouse mutant reeler. *Nature* 374:719-723.

D'Souza, S. E., M. H. Ginsberg, T. A. Burke, S. C. Lam, and E. F. Plow. 1988. Localization of an Arg-Gly-Asp recognition site within an integrin adhesion receptor. *Science* 242:91-93.

Davignon, D., E. Martz, T. Reynolds, K. Kurzinger, and T. A. Springer. 1981. Lymphocyte function-associated antigen 1 (LFA-1): a surface antigen distinct from Lyt-2, 3 that participates in T lymphocyte-mediated killing. *Proc.Natl.Acad Sci.U.S.A* 78:4535-4539.

de Fougerolles, A. R., S. A. Stacker, R. Schwarting, and T. A. Springer. 1991. Characterization of ICAM-2 and evidence for a third counter-receptor for LFA-1. *J Exp.Med.* 174:253-267.

de Fougerolles, A. R. and T. A. Springer. 1992. Intercellular adhesion molecule 3, a third adhesion counter-receptor for lymphocyte function-associated molecule 1 on resting lymphocytes. *J Exp.Med.* 175:185-190.

de Fougerolles, A. R., X. Qin, and T. A. Springer. 1994. Characterization of the function of intercellular adhesion molecule (ICAM)-3 and comparison with ICAM-1 and ICAM-2 in immune responses. *J Exp.Med.* 179:619-629.

de Fougerolles, A. R., 2003. Integrins in Immune and Inflammatory Disease in *I Domains in Integrins, edited by Daoald Gullberg. In press*

de Pereda, J. M., G. Wiche, and R. C. Liddington. 1999. Crystal structure of a tandem pair of fibronectin type III domains from the cytoplasmic tail of integrin alpha 6 beta 4. *EMBO J* 18:4087-4095.

Delwel, G. O., F. Hogervorst, and A. Sonnenberg. 1996. Cleavage of the alpha 6 subunit is essential for activation of the alpha 6 beta1 integrin by phorbol 12-myristate 13-acetate. *J Biol.Chem.* 271:7293-7296.

Diacovo, T. G., A. R. deFougerolles, D. F. Bainton, and T. A. Springer. 1994. A functional integrin ligand on the surface of platelets: intercellular adhesion molecule-2. *J Clin.Invest* 94:1243-1251.

Diamond, M. S. and T. A. Springer. 1994. The dynamic regulation of integrin adhesiveness. *Curr.Biol.* 4:506-517.

Diaz-Gonzalez, F., J. Forsyth, B. Steiner, and M. H. Ginsberg. 1996. Trans-dominant inhibition of integrin function. *Mol.Biol.Cell* 7:1939-1951.

Doussis-Anagnostopoulou, I., L. Kaklamanis, J. Cordell, M. Jones, H. Turley, K. Pulford, D. Simmons, D. Mason, and K. Gatter. 1993. ICAM-3 expression on endothelium in lymphoid malignancy. *Am J Pathol.* 143:1040-1043.

Dransfield, I. and N. Hogg. 1989. Regulated expression of Mg^{2+} binding epitope on leukocyte integrin alpha subunits. *EMBO J* 8:3759-3765.

Dransfield, I., C. Cabanas, J. Barrett, and N. Hogg. 1992a. Interaction of leukocyte integrins with ligand is necessary but not sufficient for function. *J Cell Biol.* 116:1527-1535.

Dransfield, I., C. Cabanas, A. Craig, and N. Hogg. 1992b. Divalent cation regulation of the function of the leukocyte integrin LFA-1. *J Cell Biol.* 116:219-226.

Drbal, K., P. Angelisova, J. Cerny, I. Hilgert, and V. Horejsi. 2001. A novel anti-CD18 mAb recognizes an activation-related epitope and induces a high-affinity conformation in leukocyte integrins. *Immunobiology* 203:687-698.

Du, X., M. Gu, J. W. Weisel, C. Nagaswami, J. S. Bennett, R. Bowditch, and M. H. Ginsberg. 1993. Long range propagation of conformational changes in integrin alpha IIb beta 3. *J Biol.Chem.* 268:23087-23092.

Dustin, M. L. and T. A. Springer. 1989. T-cell receptor cross-linking transiently stimulates adhesiveness through LFA-1. *Nature* 341:619-624.

Dustin, M. L. and J. A. Cooper. 2000. The immunological synapse and the actin cytoskeleton: molecular hardware for T cell signaling. *Nat.Immunol* 1:23-29.

Dustin, M. L. 2002. The immunological synapse. *Arthritis Res* 4 Suppl 3:S119-S125.

Edwards, C. P., M. Champe, T. Gonzalez, M. E. Wessinger, S. A. Spencer, L. G. Presta, P. W. Berman, and S. C. Bodary. 1995. Identification of amino acids in the CD11a I-domain important for binding of the leukocyte function-associated antigen-1 (LFA-1) to intercellular adhesion molecule-1 (ICAM-1). *J Biol.Chem.* 270:12635-12640.

Edwards, C. P., K. L. Fisher, L. G. Presta, and S. C. Bodary. 1998. Mapping the intercellular adhesion molecule-1 and -2 binding site on the inserted domain of leukocyte function-associated antigen-1. *J Biol.Chem.* 273:28937-28944.

Emsley, J., S. L. King, J. M. Bergelson, and R. C. Liddington. 1997. Crystal structure of the I domain from integrin alpha2beta1. *J Biol.Chem.* 272:28512-28517.

Emsley, J., C. G. Knight, R. W. Farndale, M. J. Barnes, and R. C. Liddington. 2000. Structural basis of collagen recognition by integrin alpha2beta1. *Cell* 101:47-56.

Fagerholm, S., T. J. Hilden, and C. G. Gahmberg. 2002. Lck tyrosine kinase is important for activation of the CD11a/CD18-integrins in human T lymphocytes. *Eur.J Immunol* 32:1670-1678.

Faull, R. J., N. L. Kovach, J. M. Harlan, and M. H. Ginsberg. 1994. Stimulation of integrin-mediated adhesion of T lymphocytes and monocytes: two mechanisms with divergent biological consequences. *J Exp.Med.* 179:1307-1316.

Gahmberg, C. G. 1997a. Leukocyte adhesion: CD11/CD18 integrins and intercellular adhesion molecules. *Curr.Opin.Cell Biol.* 9:643-650.

Gahmberg, C. G., M. Tolvanen, and P. Kotovuori. 1997(b). Leukocyte adhesion--structure and function of human leukocyte beta2-integrins and their cellular ligands. *Eur.J Biochem.* 245:215-232.

Galfre, G. and C. Milstein. 1982. Chemical typing of human kappa light chain subgroups expressed by human hybrid myelomas. *Immunology* 45:125-128.

Geiger, C., W. Nagel, T. Boehm, Y. van Kooyk, C. G. Figdor, E. Kremmer, N. Hogg, L. Zeitlmann, H. Dierks, K. S. Weber, and W. Kolanus. 2000. Cytohesin-1 regulates beta-2 integrin-mediated adhesion through both ARF-GEF function and interaction with LFA-1. *EMBO J* 19:2525-2536.

Geijtenbeek, T. B., R. Torensma, S. J. van Vliet, G. C. van Duijnhoven, G. J. Adema, Y. van Kooyk, and C. G. Figdor. 2000. Identification of DC-SIGN, a novel dendritic cell-specific ICAM-3 receptor that supports primary immune responses. *Cell* 100:575-585.

Giancotti, F. G. and G. Tarone. 2003. Positional control of cell fate through joint integrin/receptor protein kinase signaling. *Annu.Rev.Cell Dev.Biol.* 19:173-206.

Ginsberg, M. H., J. D. Wencel, J. G. White, and E. F. Plow. 1983. Binding of fibronectin to alpha-granule-deficient platelets. *J Cell Biol.* 97:571-573.

Ginsberg, M. H., B. Yaspan, J. Forsyth, T. S. Ulmer, I. D. Campbell, and M. Slepak. 2001. A membrane-distal segment of the integrin alpha IIb cytoplasmic domain regulates integrin activation. *J Biol.Chem.* 276:22514-22521.

Gottlieb, A., J. G. Krueger, R. Bright, M. Ling, M. Lebwohl, S. Kang, S. Feldman, M. Spellman, K. Wittkowski, H. D. Ochs, P. Jardieu, R. Bauer, M. White, R. Dedrick, and M. Garovoy. 2000. Effects of administration of a single dose of a humanized monoclonal antibody to CD11a on the immunobiology and clinical activity of psoriasis. *J Am Acad Dermatol* 42:428-435.

Gottlieb, A. B., J. G. Krueger, K. Wittkowski, R. Dedrick, P. A. Walicke, and M. Garovoy. 2002. Psoriasis as a model for T-cell-mediated disease: immunobiologic and clinical effects of treatment with multiple doses of efalizumab, an anti-CD11a antibody. *Arch.Dermatol* 138:591-600.

Gottlieb, A. B. and J. D. Bos. 2002. Recombinantly engineered human proteins: transforming the treatment of psoriasis. *Clin.Immunol* 105:105-116.

Grabovsky, V., S. Feigelson, C. Chen, D. A. Bleijs, A. Peled, G. Cinamon , F. Baleux, F. Arenzana-Seisdedos, T. Lapidot, Y. van Kooyk, R. R. Lobb, and R. Alon. 2000. Subsecond induction of alpha4 integrin clustering by immobilized chemokines stimulates leukocyte tethering and rolling on endothelial vascular cell adhesion molecule 1 under flow conditions. *J Exp.Med.* 192:495-506.

Griggs, D. W., C. M. Schmidt, and C. P. Carron. 1998. Characteristics of cation binding to the I domains of LFA-1 and MAC-1. The LFA-1 I domain contains a Ca^{2+}-binding site. *J Biol.Chem.* 273:22113-22119.

Grzesiak, J. J. and M. D. Pierschbacher. 1995. Shifts in the concentrations of magnesium and calcium in early porcine and rat wound fluids activate the cell migratory response. *J Clin.Invest* 95:227-233.

Hemler, M. E., M. J. Elices, C. Parker, and Y. Takada. 1990. Structure of the integrin VLA-4 and its cell-cell and cell-matrix adhesion functions. *Immunol Rev.* 114:45-65.

Henderson, R. B., L. H. Lim, P. A. Tessier, F. N. Gavins, M. Mathies, M. Perretti, and N. Hogg. 2001. The use of lymphocyte function-associated antigen (LFA)-1-deficient mice to determine the role of LFA-1, Mac-1, and alpha4 integrin in the inflammatory response of neutrophils. *J Exp.Med.* 194:219-226.

Hermand, P., M. Huet, I. Callebaut, P. Gane, E. Ihanus, C. G. Gahmberg , J. P. Cartron, and P. Bailly. 2000. Binding sites of leukocyte beta 2 integrins (LFA-1, Mac-1) on the human ICAM-4/LW blood group protein. *J Biol.Chem.* 275:26002-26010.

Hibbs, M. L., H. Xu, S. A. Stacker, and T. A. Springer. 1991. Regulation of adhesion of ICAM-1 by the cytoplasmic domain of LFA-1 integrin beta subunit. *Science* 251:1611-1613.

Hickstein, D. D., E. Grunvald, G. Shumaker, D. M. Baker, A. L. Back, L. J. Embree, E. Yee, and K. A. Gollahon. 1993. Transfected leukocyte integrin CD11b/CD18 (Mac-1) mediates phorbol ester-activated, homotypic cell:cell adherence in the K562 cell line. *Blood* 82:2537-2545.

Hogg, N. 1991. An integrin overview. *Chem.Immunol* 50:1-12.

Holness, C. L., P. A. Bates, A. J. Little, C. D. Buckley, A. McDowall, D. Bossy, N. Hogg, and D. L. Simmons. 1995. Analysis of the binding site on intercellular adhesion molecule 3 for the leukocyte integrin lymphocyte function-associated antigen 1. *J Biol.Chem.* 270:877-884.

Huang, C. and T. A. Springer. 1995. A binding interface on the I domain of lymphocyte function-associated antigen-1 (LFA-1) required for specific interaction with intercellular adhesion molecule 1 (ICAM-1). *J Biol.Chem.* 270:19008-19016.

Huang, C. and T. A. Springer. 1997. Folding of the beta-propeller domain of the integrin alphaL subunit is independent of the I domain and dependent on the beta2 subunit. *Proc.Natl.Acad Sci.U.S.A* 94:3162-3167.

Huang, C., Q. Zang, J. Takagi, and T. A. Springer. 2000. Structural and functional studies with antibodies to the integrin beta 2 subunit. A model for the I-like domain. *J Biol.Chem.* 275:21514-21524.

Hughes, P. E., F. Diaz-Gonzalez, L. Leong, C. Wu, J. A. McDonald, S. J. Shattil, and M. H. Ginsberg. 1996. Breaking the integrin hinge. A defined structural constraint regulates integrin signaling. *J Biol.Chem.* 271:6571-6574.

Humphries, M. J., J. Sheridan, A. P. Mould, and P. Newham. 1995. Mechanisms of VCAM-1 and fibronectin binding to integrin alpha 4 beta 1: implications for integrin function and rational drug design. *Ciba Found.Symp.* 189:177-191.

Humphries, M. J. 2000. Integrin structure. *Biochem.Soc.Trans.* 28:311-339.

Humphries, M. J. 2002. Insights into integrin-ligand binding and activation from the first crystal structure. *Arthritis Res* 4 Suppl 3:S69-S78.

Huth, J. R., E. T. Olejniczak, R. Mendoza, H. Liang, E. A. Harris, M. L. Lupher, Jr., A. E. Wilson, S. W. Fesik, and D. E. Staunton. 2000. NMR and mutagenesis evidence for an I domain allosteric site that regulates lymphocyte function-associated antigen 1 ligand binding. *Proc.Natl.Acad.Sci.U.S A* 97:5231-5236.

Hynes, R. O. 1992. Integrins: versatility, modulation, and signaling in cell adhesion. *Cell* 69:11-25.

Hynes, R. O. 2002. Integrins: bidirectional, allosteric signaling machines. Cell 110:673-687.

Ihanus, E., L. Uotila, A. Toivanen, M. Stefanidakis, P. Bailly, J. P. Cartron, and C. G. Gahmberg. 2003. Characterization of ICAM-4 binding to the I domains of the CD11a/CD18 and CD11b/CD18 leukocyte integrins. *Eur.J Biochem.* 270:1710-1723.

Imhof, B. A. and D. Dunon. 1995. Leukocyte migration and adhesion. *Adv.Immunol* 58:345-416.

Jackson, A. M., A. B. Alexandroff, M. B. Lappin, K. Esuvaranathan, K. James, and G. D. Chisholm. 1994. Control of leucocyte function-associated antigen-1-dependent cellular conjugation by divalent cations. *Immunology* 81:120-126.

Kakimoto, K., T. Nakamura, K. Ishii, T. Takashi, H. Iigou, H. Yagita, K. Okumura, and K. Onoue. 1992. The effect of anti-adhesion molecule antibody on the development of collagen-induced arthritis. *Cell Immunol* 142:326-337.

Kallen, J., K. Welzenbach, P. Ramage, D. Geyl, R. Kriwacki, G. Legge , S. Cottens, G. Weitz-Schmidt, and U. Hommel. 1999. Structural basis for LFA-1 inhibition upon lovastatin binding to the CD11a I-domain. *J Mol.Biol.* 292:1-9.

Kamata, T., R. Wright, and Y. Takada. 1995. Critical threonine and aspartic acid residues within the I domains of beta 2 integrins for interactions with intercellular adhesion molecule 1 (ICAM-1) and C3bi. *J Biol.Chem.* 270:12531-12535.

Kamata, T., K. K. Tieu, T. Tarui, W. Puzon-McLaughlin, N. Hogg, and Y. Takada. 2002. The role of the CPNKEKEC sequence in the beta 2 subunit I domain in regulation of integrin alpha(L)beta(2) (LFA-1). *J Immunol* 168:2296-2301.

Kelly, T. A., D. D. Jeanfavre, D. W. McNeil, J. R. Woska, Jr., P. L. Reilly, E. A. Mainolfi, K. M. Kishimoto, G. H. Nabozny, R. Zinter, B. J. Bormann, and R. Rothlein. 1999. Cutting edge: a small molecule antagonist of LFA-1-mediated cell adhesion . *J Immunol* 163:5173-5177.

King, D. J., J. R. Adair, S. Angal, D. C. Low, K. A. Proudfoot, J. C. Lloyd, M. W. Bodmer, and G. T. Yarranton. 1992. Expression, purification and characterization of a mouse-human chimeric antibody and chimeric Fab' fragment. *Biochem.J* 281 (Pt 2):317-323.

Kishimoto, T. K., K. O'Connor, A. Lee, T. M. Roberts, and T. A. Springer. 1987. Cloning of the beta subunit of the leukocyte adhesion proteins: homology to an extracellular matrix receptor defines a novel supergene family. *Cell* 48:681-690.

Klickstein, L. B., M. R. York, A. R. Fougerolles, and T. A. Springer. 1996. Localization of the binding site on intercellular adhesion molecule-3 (ICAM-3) for lymphocyte function-associated antigen 1 (LFA-1). *J Biol.Chem.* 271:23920-23927.

Krauss, K. and P. Altevogt. 1999. Integrin leukocyte function-associated antigen-1-mediated cell binding can be activated by clustering of membrane rafts. *J Biol.Chem.* 274:36921-36927.

Krutmann, J., A. Kock, E. Schauer, F. Parlow, A. Moller, A. Kapp, E. Forster, E. Schopf, and T. A. Luger. 1990. Tumor necrosis factor beta and ultraviolet radiation are potent regulators of human keratinocyte ICAM-1 expression. *J Invest Dermatol* 95:127-131.

Kucik, D. F., M. L. Dustin, J. M. Miller, and E. J. Brown. 1996. Adhesion-activating Phorbol Ester Increases the Mobility of Leukocyte Integrin LFA-1 in Cultured Lymphocytes. *J.Clin.Invest.* 97:2139-2144.

Kupfer, A., P. Burn, and S. J. Singer. 1990. The PMA-induced specific association of LFA-1 and talin in intact cloned T helper cells. J Mol.Cell Immunol 4:317-325.

Labadia, M. E., D. D. Jeanfavre, G. O. Caviness, and M. M. Morelock. 1998. Molecular regulation of the interaction between leukocyte function-associated antigen-1 and soluble ICAM-1 by divalent metal cations. *J Immunol* 161:836-842.

Landis, R. C., R. I. Bennett, and N. Hogg. 1993. A novel LFA-1 activation epitope maps to the I domain. *J Cell Biol.* 120:1519-1527.

Larson, R. S., A. L. Corbi, L. Berman, and T. Springer. 1989. Primary structure of the leukocyte function-associated molecule-1 alpha subunit: an integrin with an embedded domain defining a protein superfamily. *J Cell Biol.* 108:703-712.

Larson, R. S. and T. A. Springer. 1990. Structure and function of leukocyte integrins. *Immunol Rev.* 114:181-217.

Lee, J. O., L. A. Bankston, M. A. Arnaout, and R. C. Liddington. 1995a. Two conformations of the integrin A-domain (I-domain): a pathway for activation? *Structure.* 3:1333-1340.

Lee, J. O., P. Rieu, M. A. Arnaout, and R. Liddington. 1995b. Crystal structure of the A domain from the alpha subunit of integrin CR3 (CD11b/CD18). *Cell* 80:631-638.

Legge, G. B., R. W. Kriwacki, J. Chung, U. Hommel, P. Ramage, D. A. Case, H. J. Dyson, and P. E. Wright. 2000. NMR solution structure of the inserted domain of human leukocyte function associated antigen-1. *J Mol.Biol.* 295:1251-1264.

Leitinger, B., A. McDowall, P. Stanley, and N. Hogg. 2000. The regulation of integrin function by Ca(2+). *Biochim.Biophys.Acta* 1498:91-98.

Leitinger, B. and N. Hogg. 2000. Effects of I domain deletion on the function of the beta2 integrin lymphocyte function-associated antigen-1. *Mol.Biol.Cell* 11:677-690.

Leitinger, B. and N. Hogg. 2002. The involvement of lipid rafts in the regulation of integrin function. *J Cell Sci.* 115:963-972.

Lewis, M., H. Kaita, G. Coghlan, S. Philipps, E. Belcher, P. J. McAlpine, G. R. Coopland, and R. A. Woods. 1988. The chromosome 19 linkage group LDLR, C3, LW, APOC2, LU, SE in man. *Ann.Hum.Genet.* 52 (Pt 2):137-144.

Li, R., P. Nortamo, C. Kantor, P. Kovanen, T. Timonen, and C. G. Gahmberg. 1993. A leukocyte integrin binding peptide from intercellular adhesion molecule-2 stimulates T cell adhesion and natural killer cell activity. *J Biol.Chem.* 268 :21474-21477.

Li, R., P. Rieu, D. L. Griffith, D. Scott, and M. A. Arnaout. 1998. Two functional states of the CD11b A-domain: correlations with key features of two Mn^{2+}-complexed crystal structures. *J Cell Biol.* 143:1523-1534.

Liddington, R. C. and M. H. Ginsberg. 2002. Integrin activation takes shape. *J Cell Biol.* 158:833-839.

Lin, E. C., B. I. Ratnikov, P. M. Tsai, C. P. Carron, D. M. Myers, C. F. Barbas, III, and J. W. Smith. 1997. Identification of a region in the integrin beta3 subunit that confers ligand binding specificity. *J Biol.Chem.* 272:23912-23920.

London, E. and D. A. Brown. 2000. Insolubility of lipids in triton X-100: physical origin and relationship to sphingolipid/cholesterol membrane domains (rafts). *Biochim.Biophys.Acta* 1508:182-195.

Lozzio, B. B., C. B. Lozzio, E. G. Bamberger, and A. S. Feliu. 1981. A multipotential leukemia cell line (K-562) of human origin. *Proc.Soc.Exp.Biol.Med.* 166:546-550.

Lu, C., J. Takagi, and T. A. Springer. 2001a. Association of the membrane proximal regions of the alpha and beta subunit cytoplasmic domains constrains an integrin in the inactive state. *J Biol.Chem.* 276:14642-14648.

Lu, C., M. Ferzly, J. Takagi, and T. A. Springer. 2001b. Epitope mapping of antibodies to the C-terminal region of the integrin beta 2 subunit reveals regions that become exposed upon receptor activation. *J Immunol* 166:5629-5637.

Lu, C., M. Shimaoka, M. Ferzly, C. Oxvig, J. Takagi, and T. A. Springer. 2001c. An isolated, surface-expressed I domain of the integrin alphaLbeta2 is sufficient for strong adhesive function when locked in the open conformation with a disulfide bond. *Proc.Natl.Acad Sci.U.S.A* 98:2387-2392.

Lu, C., M. Shimaoka, Q. Zang, J. Takagi , and T. A. Springer. 2001d. Locking in alternate conformations of the integrin alphaLbeta2 I domain with disulfide bonds reveals functional relationships among integrin domains. *Proc.Natl.Acad Sci.U.S.A* 98:2393-2398.

Lu, C. F. and T. A. Springer. 1997. The alpha subunit cytoplasmic domain regulates the assembly and adhesiveness of integrin lymphocyte function-associated antigen-1. *J Immunol* 159:268-278.

Lub, M., Y. van Kooyk, and C. G. Figdor. 1995. Ins and outs of LFA-1. *Immunol Today* 16:479-483.

Lub, M., S. J. van Vliet, S. P. Oomen, R. A. Pieters, M. Robinson, C. G. Figdor, and Y. van Kooyk. 1997(a). Cytoplasmic tails of beta 1, beta 2, and beta 7 integrins differentially regulate LFA-1 function in K562 cells. *Mol.Biol.Cell* 8:719-728.

Lub, M., Y. van Kooyk, S. J. van Vliet, and C. G. Figdor. 1997(b). Dual role of the actin cytoskeleton in regulating cell adhesion mediated by the integrin lymphocyte function-associated molecule-1. *Mol.Biol.Cell* 8:341-351.

Lupher, M. L., Jr., E. A. Harris, C. R. Beals, L. M. Sui, R. C. Liddington, and D. E. Staunton. 2001. Cellular activation of leukocyte function-associated antigen-1 and its affinity are regulated at the I domain allosteric site. *J Immunol* 167:1431-1439.

Luque, A., M. Gomez, W. Puzon, Y. Takada, F. Sanchez-Madrid, and C. Cabanas. 1996. Activated conformations of very late activation integrins detected by a group of antibodies (HUTS) specific for a novel regulatory region (355-425) of the common beta 1 chain. *J Biol.Chem.* 271:11067-11075.

Ly, D. P., K. M. Zazzali, and S. A. Corbett. 2003. De novo expression of the integrin alpha5beta1 regulates alphavbeta3-mediated adhesion and migration on fibrinogen. *J Biol.Chem.* 278:21878-21885.

Ma, Q., M. Shimaoka, C. Lu, H. Jing, C. V. Carman, and T. A. Springer. 2002. Activation-induced conformational changes in the I domain region of lymphocyte function-associated antigen 1. *J Biol.Chem.* 277:10638-10641.

Marlin, S. D. and T. A. Springer. 1987. Purified intercellular adhesion molecule-1 (ICAM-1) is a ligand for lymphocyte function-associated antigen 1 (LFA-1). *Cell* 51:813-819.

Masumoto, A. and M. E. Hemler. 1993. Multiple activation states of VLA-4. Mechanistic differences between adhesion to CS1/fibronectin and to vascular cell adhesion molecule-1. *J Biol.Chem.* 268:228-234.

May, A. E., F. J. Neumann, A. Schomig, and K. T. Preissner. 2000. VLA-4 (alpha(4)beta(1)) engagement defines a novel activation pathway for beta(2) integrin-dependent leukocyte adhesion involving the urokinase receptor. *Blood* 96:506-513.

Mazzone, A. and G. Ricevuti. 1995. Leukocyte CD11/CD18 integrins: biological and clinical relevance. *Haematologica* 80:161-175.

Michishita, M., V. Videm, and M. A. Arnaout. 1993. A novel divalent cation-binding site in the A domain of the beta 2 integrin CR3 (CD11b/CD18) is essential for ligand binding. *Cell* 72:857-867.

Miller, J., R. Knorr, M. Ferrone, R. Houdei, C. P. Carron, and M. L. Dustin. 1995. Intercellular adhesion molecule-1 dimerization and its consequences for adhesion mediated by lymphocyte function associated-1. *J Exp.Med.* 182:1231-1241.

Montoya, M. C., D. Sancho, G. Bonello, Y. Collette, C. Langlet, H. T. He, P. Aparicio, A. Alcover, D. Olive, and F. Sanchez-Madrid. 2002. Role of ICAM-3 in the initial interaction of T lymphocytes and APCs. *Nat.Immunol* 3:159-168.

Montoya, M. C., D. Sancho, M. Vicente-Manzanares, and F. Sanchez-Madrid. 2002. Cell adhesion and polarity during immune interactions. *Immunol Rev.* 186:68-82.

Mould, A. P., S. J. Barton, J. A. Askari, S. E. Craig, and M. J. Humphries. 2003. Role of ADMIDAS cation-binding site in ligand recognition by integrin alpha 5beta 1. *J Biol.Chem.* (E publication)

Muir, T. W., M. J. Williams, M. H. Ginsberg, and S. B. Kent. 1994. Design and chemical synthesis of a neoprotein structural model for the cytoplasmic domain of a multisubunit cell-surface receptor: integrin alpha IIb beta 3 (platelet GPIIb-IIIa). *Biochemistry* 33:7701-7708.

Nagel, W., L. Zeitlmann, P. Schilcher, C. Geiger, J. Kolanus, and W. Kolanus. 1998. Phosphoinositide 3-OH Kinase Activates the beta 2 Integrin Adhesion Pathway and Induces Membrane Recruitment of Cytohesin-1 . *J.Biol.Chem.* 273:14853-14861.

Nicolls, M. R., M. Coulombe, J. Beilke, H. C. Gelhaus, and R. G. Gill. 2002. CD4-dependent generation of dominant transplantation tolerance induced by simultaneous perturbation of CD154 and LFA-1 pathways. *J Immunol* 169:4831-4839.

Nolte, M., R. B. Pepinsky, S. Y. Venyaminov, V. Koteliansky, P. J. Gotwals, and M. Karpusas. 1999. Crystal structure of the alpha1beta1 integrin I-domain: insights into integrin I-domain function. *FEBS Lett.* 452:379-385.

O'Toole, T. E., J. C. Loftus, X. P. Du, A. A. Glass, Z. M. Ruggeri, S. J. Shattil, E. F. Plow, and M. H. Ginsberg. 1990. Affinity modulation of the alpha IIb beta 3 integrin (platelet GPIIb-IIIa) is an intrinsic property of the receptor. *Cell Regul.* 1:883-893.

O'Toole, T. E., Y. Katagiri, R. J. Faull, K. Peter, R. Tamura, V. Quaranta, J. C. Loftus, S. J. Shattil, and M. H. Ginsberg. 1994. Integrin cytoplasmic domains mediate inside-out signal transduction. *J Cell Biol.* 124:1047-1059.

Olinger, M. L. 1989. Disorders of calcium and magnesium metabolism. *Emerg.Med.Clin.North Am* 7:795-822.

Ortlepp, S., P. E. Stephens, N. Hogg, C. G. Figdor, and M. K. Robinson. 1995. Antibodies that activate beta 2 integrins can generate different ligand binding states. *Eur.J Immunol* 25:637-643.

Ortlepp, S.,1997. Leucoctye Integrin Activation by Monoclonal Antibodies. PhD Thesis.

Ostermann, G., K. S. Weber, A. Zernecke, A. Schroder, and C. Weber. 2002. JAM-1 is a ligand of the beta(2) integrin LFA-1 involved in transendothelial migration of leukocytes. *Nat.Immunol* 3:151-158.

Oxvig, C. and T. A. Springer. 1998. Experimental support for a beta-propeller domain in integrin alpha-subunits and a calcium binding site on its lower surface. *Proc.Natl.Acad Sci.U.S.A* 95:4870-4875.

Oxvig, C., C. Lu, and T. A. Springer. 1999. Conformational changes in tertiary structure near the ligand binding site of an integrin I domain. *Proc.Natl.Acad Sci.U.S.A* 96:2215-2220.

Pacifici, R., J. Roman, R. Kimble, R. Civitelli, C. M. Brownfield, and C. Bizzarri. 1994. Ligand binding to monocyte alpha 5 beta 1 integrin activates the alpha 2 beta 1 receptor via the alpha 5 subunit cytoplasmic domain and protein kinase C. *J Immunol* 153:2222-2233.

Petruzzelli, L., L. Maduzia, and T. A. Springer. 1995. Activation of lymphocyte function-associated molecule-1 (CD11a/CD18) and Mac-1 (CD11b/CD18) mimicked by an antibody directed against CD18. *J Immunol* 155:854-866.

Porter, J. C. and N. Hogg. 1997. Integrin cross talk: activation of lymphocyte function-associated antigen-1 on human T cells alters alpha4beta1- and alpha5beta1-mediated function. *J Cell Biol.* 138:1437-1447.

Poston, R. S., R. C. Robbins, B. Chan, P. Simms, L. Presta, P. Jardieu, and R. E. Morris. 2000. Effects of humanized monoclonal antibody to rhesus CD11a in rhesus monkey cardiac allograft recipients. *Transplantation* 69:2005-2013.

Puzon-McLaughlin, W., T. Kamata, and Y. Takada. 2000. Multiple discontinuous ligand-mimetic antibody binding sites define a ligand binding pocket in integrin alpha(IIb)beta(3). *J Biol.Chem.* 275:7795-7802.

Qu, A. and D. J. Leahy. 1995. Crystal structure of the I-domain from the CD11a/CD18 (LFA-1, alpha L beta 2) integrin. *Proc.Natl.Acad Sci.U.S.A* 92:10277-10281.

Qu, A. and D. J. Leahy. 1996. The role of the divalent cation in the structure of the I domain from the CD11a/CD18 integrin. *Structure.* 4:931-942.

Randi, A. M. and N. Hogg. 1994. I domain of beta 2 integrin lymphocyte function-associated antigen-1 contains a binding site for ligand intercellular adhesion molecule-1. *J.Biol.Chem.* 269:12395-12398.

Reilly, P. L., J. R. Woska, Jr., D. D. Jeanfavre, E. McNally, R. Rothlein, and B. J. Bormann. 1995. The native structure of intercellular adhesion molecule-1 (ICAM-1) is a dimer. Correlation with binding to LFA-1. *J Immunol* 155:529-532.

Ridgway, J. B., L. G. Presta, and P. Carter. 1996. 'Knobs-into-holes' engineering of antibody CH3 domains for heavy chain heterodimerization. *Protein Eng* 9:617-621.

Rodriguez-Fernandez, J. L., M. Gomez, A. Luque, N. Hogg, F. Sanchez-Madrid, and C. Cabanas. 1999. The interaction of activated integrin lymphocyte function-associated antigen 1 with ligand intercellular adhesion molecule 1 induces activation and redistribution of focal adhesion kinase and proline-rich tyrosine kinase 2 in T lymphocytes. *Mol.Biol.Cell* 10:1891-1907.

Rose, D. M., J. Han, and M. H. Ginsberg. 2002. Alpha4 integrins and the immune response. *Immunol Rev.* 186:118-124.

Rose, D. M., V. Grabovsky, R. Alon, and M. H. Ginsberg. 2001. The Affinity of Integrin {alpha}4{beta}1 Governs Lymphocyte Migration. *J Immunol* 167:2824-2830.

Roth, J. A. and M. D. Garrick. 2003. Iron interactions and other biological reactions mediating the physiological and toxic actions of manganese. *Biochem.Pharmacol.* 66:1-13.

Rothlein, R., M. L. Dustin, S. D. Marlin, and T. A. Springer. 1986. A human intercellular adhesion molecule (ICAM-1) distinct from LFA-1. *J Immunol* 137:1270-1274.

Rothlein, R. and T. A. Springer. 1986. The requirement for lymphocyte function-associated antigen 1 in homotypic leukocyte adhesion stimulated by phorbol ester. *J Exp.Med.* 163:1132-1149.

Ruoslahti, E. 1996. RGD and other recognition sequences for integrins. *Annu.Rev.Cell Dev.Biol.* 12:697-715.

Sambrook, J., E.F.Fritsch and T.Maniatis. 1989. Molecular Cloning. A Laboratory manual. 2nd Edition. Cold Spring Habour Laboratory Press.

Sampath, R., P. J. Gallagher, and F. M. Pavalko. 1998. Cytoskeletal interactions with the leukocyte integrin beta2 cytoplasmic tail. Activation-dependent regulation of associations with talin and alpha-actinin. *J Biol.Chem.* 273:33588-33594.

Sanchez-Madrid, F., J. A. Nagy, E. Robbins, P. Simon, and T. A. Springer. 1983. A human leukocyte differentiation antigen family with distinct alpha-subunits and a common beta-subunit: the lymphocyte function-associated antigen (LFA-1), the C3bi complement receptor (OKM1/Mac-1), and the p150,95 molecule. *J Exp.Med.* 158:1785-1803.

Sansom, D., J. Borrow, E. Solomon, and J. Trowsdale. 1991. The human ICAM2 gene maps to 17q23-25. Genomics 11:462-464.

Sarnacki, S., F. Auber, C. Cretolle, C. Camby, M. Cavazzana-Calvo, W. Muller, N. Wagner, N. Brousse, Y. Revillon, A. Fischer, and N. Cerf-Bensussan. 2000. Blockade of the integrin alphaLbeta2 but not of integrins alpha4 and/or beta7 significantly prolongs intestinal allograft survival in mice. *Gut* 47:97-104.

Scharffetter-Kochanek, K., H. Lu, K. Norman, N. van Nood, F. Munoz, S. Grabbe, M. McArthur, I. Lorenzo, S. Kaplan, K. Ley, C. W. Smith, C. A. Montgomery, S. Rich, and A. L. Beaudet. 1998. Spontaneous skin ulceration and defective T cell function in CD18 null mice. *J Exp.Med.* 188:119-131.

Shattil, S. J., J. A. Hoxie, M. Cunningham, and L. F. Brass. 1985. Changes in the platelet membrane glycoprotein IIb.IIIa complex during platelet activation. *J.Biol.Chem.* 260:11107-11114.

Shier, P., G. Otulakowski, K. Ngo, J. Panakos, E. Chourmouzis, L. Christjansen, C. Y. Lau, and W. P. Fung-Leung. 1996. Impaired immune responses toward alloantigens and tumor cells but normal thymic selection in mice deficient in the beta2 integrin leukocyte function-associated antigen-1. *J Immunol* 157:5375-5386.

Shier, P., K. Ngo, and W. P. Fung-Leung. 1999. Defective CD8+ T cell activation and cytolytic function in the absence of LFA-1 cannot be restored by increased TCR signaling. *J Immunol* 163:4826-4832.

Shimaoka, M., J. M. Shifman, H. Jing, J. Takagi, S. L. Mayo, and T. A. Springer. 2000. Computational design of an integrin I domain stabilized in the open high affinity conformation. *Nat.Struct.Biol.* 7:674-678.

Shimaoka, M., C. Lu, R. T. Palframan, U. H. von Andrian, A. McCormack, J. Takagi, and T. A. Springer. 2001. Reversibly locking a protein fold in an active conformation with a disulfide bond: integrin alphaL I domains with high affinity and antagonist activity in vivo. *Proc.Natl.Acad Sci.U.S.A* 98:6009-6014.

Shimaoka, M., C. Lu, A. Salas, T. Xiao, J. Takagi, and T. A. Springer. 2002(a). Stabilizing the integrin alpha M inserted domain in alternative conformations with a range of engineered disulfide bonds. *Proc.Natl.Acad Sci.U.S.A* 99:16737-16741.

Shimaoka, M., J. Takagi, and T. A. Springer. 2002(b). Conformational regulation of integrin structure and function. *Annu.Rev.Biophys.Biomol.Struct.* 31:485-516.

Shimaoka, M., T. Xiao, J. H. Liu, Y. Yang, Y. Dong, C. D. Jun, A. McCormack, R. Zhang, A. Joachimiak, J. Takagi, J. H. Wang, and T. A. Springer. 2003. Structures of the alpha L I domain and its complex with ICAM-1 reveal a shape-shifting pathway for integrin regulation. *Cell* 112:99-111.

Smith, J. W. and D. A. Cheresh. 1990. Integrin (alpha v beta 3)-ligand interaction. Identification of a heterodimeric RGD binding site on the vitronectin receptor. *J Biol.Chem.* 265:2168-2172.

Smith, J. W., R. S. Piotrowicz, and D. Mathis. 1994. A mechanism for divalent cation regulation of beta 3-integrins. *J.Biol.Chem.* 269:960-967.

Springer, T. A., M. L. Dustin, T. K. Kishimoto, and S. D. Marlin. 1987. The lymphocyte function-associated LFA-1, CD2, and LFA-3 molecules: cell adhesion receptors of the immune system. *Annu.Rev.Immunol* 5:223-252.

Springer, T. A. 1994. Traffic signals for lymphocyte recirculation and leukocyte emigration: the multistep paradigm. *Cell* 76:301-314.

Springer, T. A. 1997. Folding of the N-terminal, ligand-binding region of integrin alpha-subunits into a beta-propeller domain. *Proc.Natl.Acad Sci.U.S.A* 94:65-72.

Springer, T. A., H. Jing, and J. Takagi. 2000. A novel Ca^{2+} binding beta hairpin loop better resembles integrin sequence motifs than the EF hand. *Cell* 102:275-277.

Springer, T. A. 2002. Predicted and experimental structures of integrins and beta-propellers. *Curr.Opin.Struct.Biol.* 12:802-813.

Staunton, D. E., M. L. Dustin, H. P. Erickson, and T. A. Springer. 1990. The arrangement of the immunoglobulin-like domains of ICAM-1 and the binding sites for LFA-1 and rhinovirus. *Cell* 61:243-254.

Stephens, P. E. and M. I. Cockett. 1989. The construction of a highly efficient and versatile set of mammalian expression vectors. *Nucleic Acids Res* 17:7110.

Stephens, P., J. T. Romer, M. Spitali, A. Shock, S. Ortlepp, C. G. Figdor, and M. K. Robinson. 1995. KIM127, an antibody that promotes adhesion, maps to a region of CD18 that includes cysteine-rich repeats. *Cell Adhes.Commun.* 3:375-384.

Stephens, P. E., S. Ortlepp, V. C. Perkins, M. K. Robinson, and H. Kirby. 2000. Expression of a soluble functional form of the integrin alpha4beta1 in mammalian cells. *Cell Adhes.Commun.* 7:377-390.

Stewart, M. and N. Hogg. 1996. Regulation of leukocyte integrin function: affinity vs. avidity. *J Cell Biochem.* 61:554-561.

Stewart, M. P., C. Cabanas, and N. Hogg. 1996. T cell adhesion to intercellular adhesion molecule-1 (ICAM-1) is controlled by cell spreading and the activation of integrin LFA-1. *J Immunol* 156:1810-1817.

Stewart, M. P., A. McDowall, and N. Hogg. 1998. LFA-1-mediated adhesion is regulated by cytoskeletal restraint and by a Ca^{2+}-dependent protease, calpain. *J Cell Biol.* 140:699-707.

Takagi, J., N. Beglova, P. Yalamanchili, S. C. Blacklow, and T. A. Springer. 2001. Definition of EGF-like, closely interacting modules that bear activation epitopes in integrin beta subunits. *Proc.Natl.Acad Sci.U.S.A* 98:11175-11180.

Takagi, J. and T. A. Springer. 2002. Integrin activation and structural rearrangement. *Immunol Rev.* 186:141-163.

Takagi, J., B. M. Petre, T. Walz, and T. A. Springer. 2002. Global conformational rearrangements in integrin extracellular domains in outside-in and inside-out signaling. *Cell* 110:599-11.

Takahashi, N., S. Ueda, M. Obata, T. Nikaido, S. Nakai, and T. Honjo. 1982. Structure of human immunoglobulin gamma genes: implications for evolution of a gene family. *Cell* 29:671-679.

Tamkun, J. W., D. W. DeSimone, D. Fonda, R. S. Patel, C. Buck, A. F. Horwitz, and R. O. Hynes. 1986. Structure of integrin, a glycoprotein involved in the transmembrane linkage between fibronectin and actin. *Cell* 46:271-282.

Thorne, R. F., J. F. Marshall, D. R. Shafren, P. G. Gibson, I. R. Hart, and G. F. Burns. 2000. The integrins alpha3beta1 and alpha6beta1 physically and functionally associate with CD36 in human melanoma cells. Requirement for the extracellular domain OF CD36. *J Biol.Chem.* 275:35264-35275.

Tian, L., P. Kilgannon, Y. Yoshihara, K. Mori, W. M. Gallatin, O. Carpen, and C. G. Gahmberg. 2000. Binding of T lymphocytes to hippocampal neurons through ICAM-5 (telencephalin) and characterization of its interaction with the leukocyte integrin CD11a/CD18. *Eur.J Immunol* 30:810-818.

Tian, L., H. Nyman, P. Kilgannon, Y. Yoshihara, K. Mori, L. C. Andersson, S. Kaukinen, H. Rauvala, W. M. Gallatin, and C. G. Gahmberg. 2000. Intercellular adhesion molecule-5 induces dendritic outgrowth by homophilic adhesion. *J Cell Biol.* 150:243-252.

Tominaga, Y., Y. Kita, A. Satoh, S. Asai, K. Kato, K. Ishikawa, T. Horiuchi, and T. Takashi. 1998. Affinity and kinetic analysis of the molecular interaction of ICAM-1 and leukocyte function-associated antigen-1. *J Immunol* 161:4016-4022.

Tominaga, Y., Y. Kita, T. Uchiyama, K. Sato, K. Sato, T. Takashi, and T. Horiuchi. 1998. Expression of a soluble form of LFA-1 and demonstration of its binding activity with ICAM-1. *J Immunol Methods* 212:61-68.

Trask, B., A. Fertitta, M. Christensen, J. Youngblom, A. Bergmann, A. Copeland, P. de Jong, H. Mohrenweiser, A. Olsen, A. Carrano, and . 1993. Fluorescence in situ hybridization mapping of human chromosome 19: cytogenetic band location of 540 cosmids and 70 genes or DNA markers. *Genomics* 15:133-145.

Tuckwell, D. S., M. J. Humphries, and A. Brass. 1994. A secondary structure model of the integrin alpha subunit N-terminal domain based on analysis of multiple alignments. Cell Adhes.Commun. 2:385-402.

Tuckwell, D. S. and M. J. Humphries. 1997. A structure prediction for the ligand-binding region of the integrin beta subunit: evidence for the presence of a von Willebrand factor A domain. *FEBS Lett.* 400:297-303.

Valmu, L., M. Autero, P. Siljander, M. Patarroyo, and C. G. Gahmberg. 1991. Phosphorylation of the beta-subunit of CD11/CD18 integrins by protein kinase C correlates with leukocyte adhesion. *Eur.J Immunol* 21:2857-2862.

van Kooyk, Y., van de Wiel-van Kemenade, P. Weder, T. W. Kuijpers, and C. G. Figdor. 1989. Enhancement of LFA-1-mediated cell adhesion by triggering through CD2 or CD3 on T lymphocytes. *Nature* 342:811-813.

van Kooyk, Y., P. Weder, F. Hogervorst, A. J. Verhoeven, G. van Seventer, A. A. te Velde, J. Borst, G. D. Keizer, and C. G. Figdor. 1991. Activation of LFA-1 through a Ca^{2+}-dependent epitope stimulates lymphocyte adhesion. *J Cell Biol.* 112:345-354.

van Kooyk, Y., P. Weder, K. Heije, M. R. de Waal, and C. G. Figdor. 1993(a). Role of intracellular Ca^{2+} levels in the regulation of CD11a/CD18 mediated cell adhesion. *Cell Adhes.Commun.* 1:21-32.

van Kooyk, Y., van de Wiel-van Kemenade, P. Weder, R. J. Huijbens, and C. G. Figdor. 1993(b). Lymphocyte function-associated antigen 1 dominates very late antigen 4 in binding of activated T cells to endothelium. *J Exp.Med.* 177:185-190.

van Kooyk, Y., P. Weder, K. Heije, and C. G. Figdor. 1994. Extracellular Ca^{2+} modulates leukocyte function-associated antigen-1 cell surface distribution on T lymphocytes and consequently affects cell adhesion. *J Cell Biol.* 124:1061-1070.

van Kooyk, Y., S. J. van Vliet, and C. G. Figdor. 1999. The actin cytoskeleton regulates LFA-1 ligand binding through avidity rather than affinity changes. *J Biol.Chem.* 274:26869-26877.

Van, der Vieran, V., H. Le Trong, C. L. Wood, P. F. Moore, T. St John, D. E. Staunton, and W. M. Gallatin. 1995. A novel leukointegrin, alpha d beta 2, binds preferentially to ICAM-3. *Immunity.* 3:683-690.

Van, der Vieran, V, D. T. Crowe, D. Hoekstra, R. Vazeux, P. A. Hoffman, M. H. Grayson, B. S. Bochner, W. M. Gallatin, and D. E. Staunton. 1999. The leukocyte integrin alpha D beta 2 binds VCAM-1: evidence for a binding interface between I domain and VCAM-1. *J Immunol* 163:1984-1990.

Vinogradova, O., A. Velyvis, A. Velyviene, B. Hu, T. Haas, E. Plow, and J. Qin. 2002. A structural mechanism of integrin alpha(IIb)beta(3) "inside-out" activation as regulated by its cytoplasmic face. *Cell* 110:587-597.

Weber, C., J. Kitayama, and T. A. Springer. 1996. Differential regulation of beta 1 and beta 2 integrin avidity by chemoattractants in eosinophils. *Proc.Natl.Acad Sci.U.S.A* 93:10939-10944.

Weber, K. S., M. R. York, T. A. Springer, and L. B. Klickstein. 1997. Characterization of lymphocyte function-associated antigen 1 (LFA-1)-deficient T cell lines: the alphaL and beta2 subunits are interdependent for cell surface expression. *J Immunol* 158:273-279.

Weisel, J. W., C. Nagaswami, G. Vilaire, and J. S. Bennett. 1992. Examination of the platelet membrane glycoprotein IIb-IIIa complex and its interaction with fibrinogen and other ligands by electron microscopy. *J Biol.Chem.* 267:16637-16643.

Weitz-Schmidt, G., K. Welzenbach, V. Brinkmann, T. Kamata, J. Kallen, C. Bruns, S. Cottens, Y. Takada , and U. Hommel. 2001. Statins selectively inhibit leukocyte function antigen-1 by binding to a novel regulatory integrin site. *Nat.Med.* 7:687-692.

Wolf, M., M. B. Delgado, S. A. Jones, B. Dewald, I. Clark-Lewis, and M. Baggiolini. 1998. Granulocyte chemotactic protein 2 acts via both IL-8 receptors, CXCR1 and CXCR2. *Eur.J Immunol* 28:164-170.

Woska, J. R., Jr., M. M. Morelock, D. D. Jeanfavre, G. O. Caviness, B. J. Bormann, and R. Rothlein. 1998. Molecular comparison of soluble intercellular adhesion molecule (sICAM)-1 and sICAM-3 binding to lymphocyte function-associated antigen-1. *J Biol.Chem.* 273:4725-4733.

Xie, J., R. Li, P. Kotovuori, C. Vermot-Desroches, J. Wijdenes, M. A. Arnaout, P. Nortamo, and C. G. Gahmberg. 1995. Intercellular adhesion molecule-2 (CD102) binds to the leukocyte integrin CD11b/CD18 through the A domain. *J Immunol* 155:3619-3628.

Xiong, J. P., R. Li, M. Essafi, T. Stehle, and M. A. Arnaout. 2000. An isoleucine-based allosteric switch controls affinity and shape shifting in integrin CD11b A-domain. *J Biol.Chem.* 275:38762-38767.

Xiong, J. P., T. Stehle, B. Diefenbach, R. Zhang, R. Dunker, D. L. Scott, A. Joachimiak, S. L. Goodman, and M. A. Arnaout. 2001. Crystal structure of the extracellular segment of integrin alpha Vbeta3. *Science* 294:339-345.

Xiong, J. P., T. Stehle, R. Zhang, A. Joachimiak, M. Frech, S. L. Goodman, and M. A. Arnaout. 2002. Crystal structure of the extracellular segment of integrin alpha V beta3 in complex with an Arg-Gly-Asp ligand. *Science* 296:151-155.

Xiong, J. P., T. Stehle, S. L. Goodman, and M. A. Arnaout. 2003. Integrins, cations and ligands: making the connection. *J Thromb.Haemost.* 1:1642-1654.

Xiong, J. P., T. Stehle, S. L. Goodman, and M. A. Arnaout. 2003. New insights into the structural basis of integrin activation. *Blood* 102:1155-1159.

Yalamanchili, P., C. Lu, C. Oxvig, and T. A. Springer. 2000. Folding and function of I domain-deleted Mac-1 and lymphocyte function-associated antigen-1. *J Biol.Chem.* 275:21877-21882.

Yauch, R. L., D. P. Felsenfeld, S. K. Kraeft, L. B. Chen, M. P. Sheetz, and M. E. Hemler. 1997. Mutational evidence for control of cell adhesion through integrin diffusion/clustering, independent of ligand binding. *J Exp.Med.* 186:1347-1355.

Yoshihara, Y., S. Oka, Y. Nemoto, Y. Watanabe, S. Nagata, H. Kagamiyama, and K. Mori. 1994. An ICAM-related neuronal glycoprotein, telencephalin, with brain segment-specific expression. *Neuron* 12:541-553.

Yusuf-Makagiansar, H., M. E. Anderson, T. V. Yakovleva, J. S. Murray, and T. J. Siahaan. 2002. Inhibition of LFA-1/ICAM-1 and VLA-4/VCAM-1 as a therapeutic approach to inflammation and autoimmune diseases. *Med.Res Rev.* 22:146-167.

Zang, Q., C. Lu, C. Huang, J. Takagi, and T. A. Springer. 2000. The top of the inserted-like domain of the integrin lymphocyte function-associated antigen-1 beta subunit contacts the alpha subunit beta -propeller domain near beta-sheet 3. *J Biol.Chem.* 275:22202-22212.

Zhang, W. V., Y. Yang, R. W. Berg, E. Leung, and G. W. Krissansen. 1999. The small GTP-binding proteins Rho and Rac induce T cell adhesion to the mucosal addressin MAdCAM-1 in a hierarchical fashion. *Eur.J Immunol* 29:2875-2885.

hCD18 DNA sequence and protein translation with highlighted regions indicating mutations and insertions required to generated a soluble form of CD18. All oligos and restriction sites used in the process are also highlighted.

Ab LEADER SEQUENCE OLIGO (B6113)

```
GGC CAA GCT TCC GCC ACC ATG GGC ATC AAG ATG GAG TCA CAG ACC CAG
GCG GAC TCC AGC ACA CCG AGG GAC ATG CTG GGC CTG CGC CCC CCA CTG
CGC CTG AGG TCG TGT GGC TCC CTG TAC GAC CCG GAC GCG GGG GGT GAC
A   D   S   S   T   P   R   D   M   L   G   L   R   P   P   L>

GTC TTT GTA TAC ATG TTG CTG TGG TTG TCT GGT GTT GAT GGA
CTC GCC CTG GTG GGG CTG CTC TCC CTC GGG TGC GTC CTC TCT CAG GAG
GAG CGG GAC CAC CCC GAC GAG AGG GAG CCC ACG CAG GAG AGA GTC CTC
L   A   L   V   G   L   L   S   L   G   C   V   L   S   Q   E>

150             160             170             180             190
TGC ACG AAG TTC AAG GTC AGC AGC TGC CGG GAA TGC ATC GAG TCG GGG
ACG TGC TTC AAG TTC CAG TCG TCG ACG GCC CTT ACG TAG CTC AGC CCC
C   T   K   F   K   V   S   S   C   R   E   C   I   E   S   G>

200             210             220             230             240
CCC GGC TGC ACC TGG TGC CAG AAG CTG AAC TTC ACA GGG CCG GGG GAT
GGG CCG ACG TGG ACC ACG GTC TTC GAC TTG AAG TGT CCC GGC CCC CTA
  P   G   C   T   W   C   Q   K   L   N   F   T   G   P   G   D>

                250             260             270             280
CCT GAC TCC ATT CGC TGC GAC ACC CGG CCA CAG CTG CTC ATG AGG GGC
GGA CTG AGG TAA GCG ACG CTG TGG GCC GGT GTC GAC GAG TAC TCC CCG
P   D   S   I   R   C   D   T   R   P   Q   L   L   M   R   G>

290             300             310             320             B6110
TGT GCG GCT GAC GAC ATC ATG GAC CCC ACA AGC CTC GCT GAA ACC CAG
ACA CGC CGA CTG CTG TAG TAC CTG GGG TGT TCG GAG CGA CTT TGG GTC
C   A   A   D   D   I   M   D   P   T   S   L   A   E   T   Q>

340             350             360             370             380
GAA GAC CAC AAT GGG GGC CAG AAG CAG CTG TCC CCA CAA AAA GTG ACG
CTT CTG GTG TTA CCC CCG GTC TTC GTC GAC AGG GGT GTT TTT CAC TGC
E   D   H   N   G   G   Q   K   Q   L   S   P   Q   K   V   T>

390             400             410             420             430
CTT TAC CTG CGA CCA GGC CAG GCA GCA GCG TTC AAC GTG ACC TTC CGG
GAA ATG GAC GCT GGT CCG GTC CGT CGT CGC AAG TTG CAC TGG AAG GCC
 L   Y   L   R   P   G   Q   A   A   A   F   N   V   T   F   R>

440             450             460             470             480
CGG GCC AAG GGC TAC CCC ATC GAC CTG TAC TAT CTG ATG GAC CTC TCC
GCC CGG TTC CCG ATG GGG TAG CTG GAC ATG ATA GAC TAC CTG GAG AGG
 R   A   K   G   Y   P   I   D   L   Y   Y   L   M   D   L   S>
```

```
490           500           510           520
TAC TCC ATG CTT GAT GAC CTC AGG AAT GTC AAG AAG CTA GGT GGC GAC
ATG AGG TAC GAA CTA CTG GAG TCC TTA CAG TTC TTC GAT CCA CCG CTG
Y   S   M   L   D   D   L   R   N   V   K   K   L   G   G   D>

530           540           550           560           570
CTG CTC CGG GCC CTC AAC GAG ATC ACC GAG TCC GGC CGC ATT GGC TTC
GAC GAG GCC CGG GAG TTG CTC TAG TGG CTC AGG CCG GCG TAA CCG AAG
 L   L   R   A   L   N   E   I   T   E   S   G   R   I   G   F>

580           590           600           610           620
GGG TCC TTC GTG GAC AAG ACC GTG CTG CCG TTC GTG AAC ACG CAC CCT
CCC AGG AAG CAC CTG TTC TGG CAC GAC GGC AAG CAC TTG TGC GTG GGA
 G   S   F   V   D   K   T   V   L   P   F   V   N   T   H   P>

630           640           650           660           670
GAT AAG CTG CGA AAC CCA TGC CCC AAC AAG GAG AAA GAG TGC CAG CCC
CTA TTC GAC GCT TTG GGT ACG GGG TTG TTC CTC TTT CTC ACG GTC GGG
 D   K   L   R   N   P   C   P   N   K   E   K   E   C   Q   P>

680           690           700           710           720
CCG TTT GCC TTC AGG CAC GTG CTG AAG CTG ACC AAC AAC TCC AAC CAG
GGC AAA CGG AAG TCC GTG CAC GAC TTC GAC TGG TTG TTG AGG TTG GTC
  P   F   A   F   R   H   V   L   K   L   T   N   N   S   N   Q>

                730           740           750           760
TTT CAG ACC GAG GTC GGG AAG CAG CTG ATT TCC GGA AAC CTG GAT GCA
AAA GTC TGG CTC CAG CCC TTC GTC GAC TAA AGG CCT TTG GAC CTA CGT
F   Q   T   E   V   G   K   Q   L   I   S   G   N   L   D   A>

770           780           790           800           810
CCC GAG GGT GGG CTG GAC GCC ATG ATG CAG GTC GCC GCC TGC CCG GAG
GGG CTC CCA CCC GAC CTG CGG TAC TAC GTC CAG CGG CGG ACG GGC CTC
P   E   G   G   L   D   A   M   M   Q   V   A   A   C   P   E>

820           830           840           850           860
GAA ATC GGC TGG CGC AAC GTC ACG CGG CTG CTG GTG TTT GCC ACT GAT
CTT TAG CCG ACC GCG TTG CAG TGC GCC GAC GAC CAC AAA CGG TGA CTA
 E   I   G   W   R   N   V   T   R   L   L   V   F   A   T   D>

870           880           890           900           910
GAC GGC TTC CAT TTC GCG GGC GAC GGA AAG CTG GGC GCC ATC CTG ACC
CTG CCG AAG GTA AAG CGC CCG CTG CCT TTC GAC CCG CGG TAG GAC TGG
D   G   F   H   F   A   G   D   G   K   L   G   A   I   L   T>

920           930           940           950           960
CCC AAC GAC GGC CGC TGT CAC CTG GAG GAC AAC TTG TAC AAG AGG AGC
GGG TTG CTG CCG GCG ACA GTG GAC CTC CTG TTG AAC ATG TTC TCC TCG
P   N   D   G   R   C   H   L   E   D   N   L   Y   K   R   S>
```

```
970          980          990          1000
AAC GAA TTC GAC TAC CCA TCG GTG GGC CAG CTG GCG CAC AAG CTG GCT
TTG CTT AAG CTG ATG GGT AGC CAC CCG GTC GAC CGC GTG TTC GAC CGA
 N   E   F   D   Y   P   S   V   G   Q   L   A   H   K   L   A>

1010         1020         1030         1040         1050
GAA AAC AAC ATC CAG CCC ATC TTC GCG GTG ACC AGT AGG ATG GTG AAG
CTT TTG TTG TAG GTC GGG TAG AAG CGC CAC TGG TCA TCC TAC CAC TTC
 E   N   N   I   Q   P   I   F   A   V   T   S   R   M   V   K>

1060         1070         1080         1090         1100
ACC TAC GAG AAA CTC ACC GAG ATC ATC CCC AAG TCA GCC GTG GGG GAG
TGG ATG CTC TTT GAG TGG CTC TAG TAG GGG TTC AGT CGG CAC CCC CTC
T   Y   E   K   L   T   E   I   I   P   K   S   A   V   G   E>

1110          1120         1130         1140          1150
CTG TCT GAG GAC TCC AGC AAT GTG GTC CAT CTC ATT AAG AAT GCT TAC
GAC AGA CTC CTG AGG TCG TTA CAC CAG GTA GAG TAA TTC TTA CGA ATG
L   S   E   D   S   S   N   V   V   H   L   I   K   N   A   Y>

1160         1170         1180         1190         1200
AAT AAA CTC TCC TCC AGG GTC TTC CTG GAT CAC AAC GCC CTC CCC GAC
TTA TTT GAG AGG AGG TCC CAG AAG GAC CTA GTG TTG CGG GAG GGG CTG
 N   K   L   S   S   R   V   F   L   D   H   N   A   L   P   D>

    1210         1220         1230         1240
ACC CTG AAA GTC ACC TAC GAC TCC TTC TGC AGC AAT GGA GTG ACG CAC
TGG GAC TTT CAG TGG ATG CTG AGG AAG ACG TCG TTA CCT CAC TGC GTG
 T   L   K   V   T   Y   D   S   F   C   S   N   G   V   T   H>

     1250         1260         1270         1280         1290
AGG AAC CAG CCC AGA GGT GAC TGT GAT GGC GTG CAG ATC AAT GTC CCG
TCC TTG GTC GGG TCT CCA CTG ACA CTA CCG CAC GTC TAG TTA CAG GGC
 R   N   Q   P   R   G   D   C   D   G   V   Q   I   N   V   P>

1300         1310         1320         1330         1340
ATC ACC TTC CAG GTG AAG GTC ACG GCC ACA GAG TGC ATC CAG GAG CAG
TAG TGG AAG GTC CAC TTC CAG TGC CGG TGT CTC ACG TAG GTC CTC GTC
 I   T   F   Q   V   K   V   T   A   T   E   C   I   Q   E   Q>

  1350         1360         1370         1380         1390
TCG TTT GTC ATC CGG GCG CTG GGC TTC ACG GAC ATA GTG ACC GTG CAG
AGC AAA CAG TAG GCC CGC GAC CCG AAG TGC CTG TAT CAC TGG CAC GTC
 S   F   V   I   R   A   L   G   F   T   D   I   V   T   V   Q>

   1400         1410         1420         1430         1440
GTT CTT CCC CAG TGT GAG TGC CGG TGC CGG GAC CAG AGC AGA GAC CGC
CAA GAA GGG GTC ACA CTC ACG GCC ACG GCC CTG GTC TCG TCT CTG GCG
 V   L   P   Q   C   E   C   R   C   R   D   Q   S   R   D   R>
```

```
1450          1460          1470          1480
AGC CTC TGC CAT GGC AAG GGC TTC TTG GAG TGC GGC ATC TGC AGG TGT
TCG GAG ACG GTA CCG TTC CCG AAG AAC CTC ACG CCG TAG ACG TCC ACA
S   L   C   H   G   K   G   F   L   E   C   G   I   C   R   C>

1490          1500          1510          1520          1530
GAC ACT GGC TAC ATT GGG AAA AAC TGT GAG TGC CAG ACA CAG GGC CGG
CTG TGA CCG ATG TAA CCC TTT TTG ACA CTC ACG GTC TGT GTC CCG GCC
D   T   G   Y   I   G   K   N   C   E   C   Q   T   Q   G   R>

1540          1550          1560          1570          1580
AGC AGC CAG GAG CTG GAA GGA AGC TGC CGG AAG GAC AAC AAC TCC ATC
TCG TCG GTC CTC GAC CTT CCT TCG ACG GCC TTC CTG TTG TTG AGG TAG
S   S   Q   E   L   E   G   S   C   R   K   D   N   N   S   I>

  1590          1600          1610          1620          1630
ATC TGC TCA GGG CTG GGG GAC TGT GTC TGC GGG CAG TGC CTG TGC CAC
TAG ACG AGT CCC GAC CCC CTG ACA CAG ACG CCC GTC ACG GAC ACG GTG
 I   C   S   G   L   G   D   C   V   C   G   Q   C   L   C   H>

   1640          1650          1660          1670          1680
ACC AGC GAC GTC CCC GGC AAG CTG ATA TAC GGG CAG TAC TGC GAG TGT
TGG TCG CTG CAG GGG CCG TTC GAC TAT ATG CCC GTC ATG ACG CTC ACA
 T   S   D   V   P   G   K   L   I   Y   G   Q   Y   C   E   C>

1690          1700          1710          1720
GAC ACC ATC AAC TGT GAG CGC TAC AAC GGC CAG GTC TGC GGC GGC CCG
CTG TGG TAG TTG ACA CTC GCG ATG TTG CCG GTC CAG ACG CCG CCG GGC
  D   T   I   N   C   E   R   Y   N   G   Q   V   C   G   G   P>

1730          1740          1750          1760          1770
GGG AGG GGG CTC TGC TTC TGC GGG AAG TGC CGC TGC CAC CCG GGC TTT
CCC TCC CCC GAG ACG AAG ACG CCC TTC ACG GCG ACG GTG GGC CCG AAA
 G   R   G   L   C   F   C   G   K   C   R   C   H   P   G   F>

1780          1790          1800          1810          1820
GAG GGC TCA GCG TGC CAG TGC GAG AGG ACC ACT GAG GGC TGC CTG AAC
CTC CCG AGT CGC ACG GTC ACG CTC TCC TGG TGA CTC CCG ACG GAC TTG
 E   G   S   A   C   Q   C   E   R   T   T   E   G   C   L   N>

1830          1840          1850          1860          1870
CCG CGG CGT GTT GAG TGT AGT GGT CGT GGC CGG TGC CGC TGC AAC GTA
GGC GCC GCA CAA CTC ACA TCA CCA GCA CCG GCC ACG GCG ACG TTG CAT
P   R   R   V   E   C   S   G   R   G   R   C   R   C   N   V>

1880          1890          1900          1910     B3610
TGC GAG TGC CAT TCA GGC TAC CAG CTG CCT CTG TGC CAG GAG TGC CCC
ACG CTC ACG GTA AGT CCG ATG GTC GAC GGA GAC ACG GTC CTC ACG GGG
 C   E   C   H   S   G   Y   Q   L   P   L   C   Q   E   C   P>
```

```
1930          1940          1950          1960
GGC TGC CCC TCA CCC TGT GGC AAG TAC ATC TCC TGC GCC GAG TGC CTG
CCG ACG GGG AGT GGG ACA CCG TTC ATG TAG AGG ACG CGG CTC ACG GAC
 G   C   P   S   P   C   G   K   Y   I   S   C   A   E   C   L>

1970 Sfu I              1990          2000          2010
AAG TTC GAA AAG GGC CCC TTT GGG AAG AAC TGC AGC GCG GCG TGT CCG
TTC AAG CTT TTC CCG GGG AAA CCC TTC TTG ACG TCG CGC CGC ACA GGC
 K   F   E   K   G   P   F   G   K   N   C   S   A   A   C   P>

2020          2030          2040          2050          2060
GGC CTG CAG CTG TCG AAC AAC CCC GTG AAG GGC AGG ACC TGC AAG GAG
CCG GAC GTC GAC AGC TTG TTG GGG CAC TTC CCG TCC TGG ACG TTC CTC
 G   L   Q   L   S   N   N   P   V   K   G   R   T   C   K   E>

  2070          2080          2090          2100          2110
AGG GAC TCA GAG GGC TGC TGG GTG GCC TAC ACG CTG GAG CAG CAG GAC
TCC CTG AGT CTC CCG ACG ACC CAC CGG ATG TGC GAC CTC GTC GTC CTG
 R   D   S   E   G   C   W   V   A   Y   T   L   E   Q   Q   D>

2120          2130          2140          2150          2160
GGG ATG GAC CGC TAC CTC ATC TAT GTG GAT GAG AGC CGA GAG TGT GTG
CCC TAC CTG GCG ATG GAG TAG ATA CAC CTA CTC TCG GCT CTC ACA CAC
 G   M   D   R   Y   L   I   Y   V   D   E   S   R   E   C   V>

2170          2180          2190          2200
GCA GGC CCC AAC ATC GCC GCC ATC GTC GGG GGC ACC GTG GCA GGC ATC
CGT CCG GGG TTG TAG CGG CGG TAG CAG CCC CCG TGG CAC CGT CCG TAG
 A   G   P   N   I   A   A   I   V   G   G   T   V   A   G   I>
                 CAG CTG GGA ACC OLIGO TO INTRODUCE Sal I SITE(B3611)

2210          2220          2230          2240          2250
GTG CTG ATC GGC ATT CTC CTG CTG GTC ATC TGG AAG GCT CTG ATC CAC
CAC GAC TAG CCG TAA GAG GAC GAC CAG TAG ACC TTC CGA GAC TAG GTG
 V   L   I   G   I   L   L   L   V   I   W   K   A   L   I   H>

2260          2270          2280          2290          2300
CTG AGC GAC CTC CGG GAG TAC AGG CGC TTT GAG AAG GAG AAG CTC AAG
GAC TCG CTG GAG GCC CTC ATG TCC GCG AAA CTC TTC CTC TTC GAG TTC
 L   S   D   L   R   E   Y   R   R   F   E   K   E   K   L   K>

2310          2320          2330          2340          2350
TCC CAG TGG AAC AAT GAT AAT CCC CTT TTC AAG AGC GCC ACC ACG ACG
AGG GTC ACC TTG TTA CTA TTA GGG GAA AAG TTC TCG CGG TGG TGC TGC
 S   Q   W   N   N   D   N   P   L   F   K   S   A   T   T   T>

  2360          2370          2380
 GTC ATG AAC CCC AAG TTT GCT GAG AGT TAG
 CAG TAC TTG GGG TTC AAA CGA CTC TCA ATC
  V   M   N   P   K   F   A   E   S   *
```

hCD11a DNA sequence and protein translation with highlighted regions indicating mutations and insertions required to generated a soluble form of CD11a. All oligos and restriction sites used in the process are also highlighted.

Ab LEADER SEQUENCE OLIGO (B6114)

GGC CAA GCT TCC GCC ACC ATG GCT TGG GTG TGG AAC TTG
ATG AAG GAT TCC TGC ATC ACT GTG ATG GCC ATG GCG CTG
TAC TTC CTA AGG ACG TAG TGA CAC TAC CGG TAC CGC GAC
M K D S C I T V M A M A L >

CTA TTC CTG ATG GCA GCT GCC CAA AGT GCC CAA GCA
CTG TCT GGG TTC TTT TTC TTC GCG CCG GCC TCG AGC **TAC AAC CTG GAC**
GAC AGA CCC AAG AAA AAG AAG CGC GGC CGG AGC TCG ATG TTG GAC CTG
L S G F F F F A P A S S Y N L D>

160 180 190 200 210
GTG CGG GGC GCG CGG AGC TTC TCC CCA CCG CGC GCC GGG AGG CAC TTT
CAC GCC CCG CGC GCC TCG AAG AGG GGT GGC GCG CGG CCC TCC GTG AAA
V R G A R S F S P P R A G R H F>

220 230 240 250 260 270
GGA TAC CGC GTC CTG CAG GTC GGA AAC GGG GTC ATC GTG GGA GCT CCA
CCT ATG GCG CAG GAC GTC CAG CCT TTG CCC CAG TAG CAC CCT CGA GGT
G Y R V L Q V G N G V I V G A P>

280 290 300 310 320
GGG GAG GGG AAC AGC ACA GGA AGC CTC TAT CAG TGC CAG TCG GGC ACA
CCC CTC CCC TTG TCG TGT CCT TCG GAG ATA GTC ACG GTC AGC CCG TGT
G E G N S T G S L Y Q C Q S G T>

330 340 350 360 370
GGA CAC TGC CTG CCA GTC ACC CTG AGA GGT TCC AAC TAT ACC TCC AAG
CCT GTG ACG GAC GGT CAG TGG GAC TCT CCA AGG TTG ATA TGG AGG TTC
G H C L P V T L R G S N Y T S K>

380 390 400 410 420
TAC TTG GGA ATG ACC TTG GCA ACA GAC CCC ACA GAT GGA AGC ATT TTG
ATG AAC CCT TAC TGG AAC CGT TGT CTG GGG TGT CTA CCT TCG TAA AAC
Y L G M T L A T D P T D G S I L>

430 440 450 460 470
GCC TGT GAC CCT GGG CTG TCT CGA ACG TGT GAC CAG AAC ACC TAT **CTG**
CGG ACA CTG GGA CCC GAC AGA GCT TGC ACA CTG GTC TTG TGG ATA GAC
A C D P G L S R T C D Q N T Y L>

480 ***B6112*** 490 500 510 520
AGT GGC CTG TGT TAC CTC TTC CGC CAG AAT CTG CAG GGT CCC ATG CTG
TCA CCG GAC ACA ATG GAG AAG GCG GTC TTA GAC GTC CCA GGG TAC GAC
S G L C Y L F R Q N L Q G P M L>

```
      Nar 1          550                560                570
CAG GGG CGC CCT GGT TTT CAG GAA TGT ATC AAG GGC AAC GTA GAC CTG
GTC CCC GCG GGA CCA AAA GTC CTT ACA TAG TTC CCG TTG CAT CTG GAC
Q   G   R   P   G   F   Q   E   C   I   K   G   N   V   D   L>
                                START OF I DOMAIN     B6109

580                590                600                610                620
GTA TTT CTG TTT GAT GGT TCG ATG AGC TTG CAG CCA GAT GAA TTT CAG
CAT AAA GAC AAA CTA CCA AGC TAC TCG AAC GTC GGT CTA CTT AAA GTC
 V   F   L   F   D   G   S   M   S   L   Q   P   D   E   F   Q>

630           640           650           660           670
AAA ATT CTG GAC TTC ATG AAG GAT GTG ATG AAG AAA CTC AGC AAC ACT
TTT TAA GAC CTG AAG TAC TTC CTA CAC TAC TTC TTT GAG TCG TTG TGA
 K   I   L   D   F   M   K   D   V   M   K   K   L   S   N   T>

680           690           700           710           720
TCG TAC CAG TTT GCT GCT GTT CAG TTT TCC ACA AGC TAC AAA ACA GAA
AGC ATG GTC AAA CGA CGA CAA GTC AAA AGG TGT TCG ATG TTT TGT CTT
 S   Y   Q   F   A   A   V   Q   F   S   T   S   Y   K   T   E>

730           740           750           760
TTT GAT TTC TCA GAT TAT GTT AAA TGG AAG GAC CCT GAT GCT CTG CTG
AAA CTA AAG AGT CTA ATA CAA TTT ACC TTC CTG GGA CTA CGA GAC GAC
 F   D   F   S   D   Y   V   K   W   K   D   P   D   A   L   L>

770           780           790           800           810
AAG CAT GTA AAG CAC ATG TTG CTG TTG ACC AAT ACC TTT GGT GCC ATC
TTC GTA CAT TTC GTG TAC AAC GAC AAC TGG TTA TGG AAA CCA CGG TAG
 K   H   V   K   H   M   L   L   L   T   N   T   F   G   A   I>

B8549 830           840           850           860
AAT TAT GTC GCG ACA GAG GTG TTC CGG GAG GAG CTG GGG GCC CGG CCA
TTA ATA CAG CGC TGT CTC CAC AAG GCC CTC CTC GAC CCC CGG GCC GGT
 N   Y   V   A   T   E   V   F   R   E   E   L   G   A   R   P>

870           B8553         890           900           910
GAT GCC ACC AAA GTG CTT ATC ATC ATC ACG GAT GGG GAG GCC ACT GAC
CTA CGG TGG TTT CAC GAA TAG TAG TAG TGC CTA CCC CTC CGG TGA CTG
 D   A   T   K   V   L   I   I   I   T   D   G   E   A   T   D>
                       235

      920           930           940           950           960
AGT GGC AAC ATC GAT GCG GCC AAA GAC ATC ATC CGC TAC ATC ATC GGG
TCA CCG TTG TAG CTA CGC CGG TTT CTG TAG TAG GCG ATG TAG TAG CCC
 S   G   N   I   D   A   A   K   D   I   I   R   Y   I   I   G>

            970           980           990           1000
ATT GGA AAG CAT TTT CAG ACC AAG GAG AGT CAG GAG ACC CTC CAC AAA
TAA CCT TTC GTA AAA GTC TGG TTC CTC TCA GTC CTC TGG GAG GTG TTT
 I   G   K   H   F   Q   T   K   E   S   Q   E   T   L   H   K>
```

```
1010          1020          1030          1040          1050
TTT GCA TCA AAA CCC GCG AGC GAG TTT GTG AAA ATT CTG GAC ACA TTT
AAA CGT AGT TTT GGG CGC TCG CTC AAA CAC TTT TAA GAC CTG TGT AAA
 F   A   S   K   P   A   S   E   F   V   K   I   L   D   T   F>
                                        287     289         292

1060          1070          1080          1090          1100
GAG AAG CTG AAA GAT CTA TTC ACT GAG CTG CAG AAG AAG ATC TAT GTC
CTC TTC GAC TTT CTA GAT AAG TGA CTC GAC GTC TTC TTC TAG ATA CAG
 E   K   L   K   D   L   F   T   E   L   Q   K   K   I   Y   V>
     294 295           299                           306

          1120          1130          1140          1150
ATT GAG GGC ACA AGC AAA CAG GAC CTG ACT TCC TTC AAC ATG GAG CTG
TAA CTC CCG TGT TCG TTT GTC CTG GAC TGA AGG AAG TTG TAC CTC GAC
 I   E   G   T   S   K   Q   D   L   T   S   F   N   M   E   L>
END OF I DOMAIN

1160          1170          1180          1190          1200
TCC TCC AGC GGC ATC AGT GCT GAC CTC AGC AGG GGC CAT GCA GTC GTG
AGG AGG TCG CCG TAG TCA CGA CTG GAG TCG TCC CCG GTA CGT CAG CAC
 S   S   S   G   I   S   A   D   L   S   R   G   H   A   V   V>

B8550              1220          1230                1240
GGG GCA GTA GGA GCC AAG GAC TGG GCT GGG GGC TTT CTT GAC CTG AAG
CCC CGT CAT CCT CGG TTC CTG ACC CGA CCC CCG AAA GAA CTG GAC TTC
 G   A   V   G   A   K   D   W   A   G   G   F   L   D   L   K>

1250          1260          1270          1280          1290
GCA GAC CTG CAG GAT GAC ACA TTT ATT GGG AAT GAA CCA TTG ACA CCA
CGT CTG GAC GTC CTA CTG TGT AAA TAA CCC TTA CTT GGT AAC TGT GGT
 A   D   L   Q   D   D   T   F   I   G   N   E   P   L   T   P>

B8554              1310          1320          1330          1340
GAA GTG AGA GCA GGC TAT TTG GGT TAC ACC GTG ACC TGG CTG CCC TCC
CTT CAC TCT CGT CCG ATA AAC CCA ATG TGG CAC TGG ACC GAC GGG AGG
 E   V   R   A   G   Y   L   G   Y   T   V   T   W   L   P   S>

1350          1360          1370          1380          1390
CGG CAA AAG ACT TCG TTG CTG GCC TCG GGA GCC CCT CGA TAC CAG CAC
GCC GTT TTC TGA AGC AAC GAC CGG AGC CCT CGG GGA GCT ATG GTC GTG
 R   Q   K   T   S   L   L   A   S   G   A   P   R   Y   Q   H>

1400          1410          1420          1430          1440
ATG GGC CGA GTG CTG CTG TTC CAA GAG CCA CAG GGC GGA GGA CAC TGG
TAC CCG GCT CAC GAC GAC AAG GTT CTC GGT GTC CCG CCT CCT GTG ACC
 M   G   R   V   L   L   F   Q   E   P   Q   G   G   G   H   W>
```

```
1450          1460          1470          1480
AGC CAG GTC CAG ACA ATC CAT GGG ACC CAG ATT GGC TCT TAT TTC GGT
TCG GTC CAG GTC TGT TAG GTA CCC TGG GTC TAA CCG AGA ATA AAG CCA
 S   Q   V   Q   T   I   H   G   T   Q   I   G   S   Y   F   G>

1490          1500          1510          1520          1530
GGG GAG CTG TGT GGC GTC GAC GTG GAC CAA GAT GGG GAG ACA GAG CTG
CCC CTC GAC ACA CCG CAG CTG CAC CTG GTT CTA CCC CTC TGT CTC GAC
 G   E   L   C   G   V   D   V   D   Q   D   G   E   T   E   L>

1540          1550          1560  B8551   1580
CTG CTG ATT GGT GCC CCA CTG TTC TAT GGG GAG CAG AGA GGA GGC CGG
GAC GAC TAA CCA CGG GGT GAC AAG ATA CCC CTC GTC TCT CCT CCG GCC
 L   L   I   G   A   P   L   F   Y   G   E   Q   R   G   G   R>

1590          1600          1610          1620          1630
GTG TTT ATC TAC CAG AGA AGA CAG TTG GGG TTT GAA GAA GTC TCA GAG
CAC AAA TAG ATG GTC TCT TCT GTC AAC CCC AAA CTT CTT CAG AGT CTC
 V   F   I   Y   Q   R   R   Q   L   G   F   E   E   V   S   E>

1640          1650          1660          1670          1680
CTG CAG GGG GAC CCC GGC TAC CCA CTC GGG CGG TTT GGA GAA GCC ATC
GAC GTC CCC CTG GGG CCG ATG GGT GAG CCC GCC AAA CCT CTT CGG TAG
 L   Q   G   D   P   G   Y   P   L   G   R   F   G   E   A   I>

1690      B8555               1710          1720
ACT GCT CTG ACA GAC ATC AAC GGC GAT GGG CTG GTA GAC GTG GCT GTG
TGA CGA GAC TGT CTG TAG TTG CCG CTA CCC GAC CAT CTG CAC CGA CAC
 T   A   L   T   D   I   N   G   D   G   L   V   D   V   A   V>

1730          1740          1750          1760          1770
GGG GCC CCT CTG GAG GAG CAG GGG GCT GTG TAC ATC TTC AAT GGG AGG
CCC CGG GGA GAC CTC CTC GTC CCC CGA CAC ATG TAG AAG TTA CCC TCC
 G   A   P   L   E   E   Q   G   A   V   Y   I   F   N   G   R>

1780          1790          1800          1810          1820
CAC GGG GGG CTT AGT CCC CAG CCA AGT CAG CGG ATA GAA GGG ACC CAA
GTG CCC CCC GAA TCA GGG GTC GGT TCA GTC GCC TAT CTT CCC TGG GTT
 H   G   G   L   S   P   Q   P   S   Q   R   I   E   G   T   Q>

1830          1840          1850          1860          1870
GTG CTC TCA GGA ATT CAG TGG TTT GGA CGC TCC ATC CAT GGG GTG AAG
CAC GAG AGT CCT TAA GTC ACC AAA CCT GCG AGG TAG GTA CCC CAC TTC
 V   L   S   G   I   Q   W   F   G   R   S   I   H   G   V   K>

1880          1890          1900          1910          1920
GAC CTT GAA GGG GAT GGC TTG GCA GAT GTG GCT GTG GGG GCT GAG AGC
CTG GAA CTT CCC CTA CCG AAC CGT CTA CAC CGA CAC CCC CGA CTC TCG
 D   L   E   G   D   G   L   A   D   V   A   V   G   A   E   S>
```

```
1930          1940          1950          1960
CAG ATG ATC GTG CTG AGC TCC CGG CCC GTG GTG GAT ATG GTC ACC CTG
GTC TAC TAG CAC GAC TCG AGG GCC GGG CAC CAC CTA TAC CAG TGG GAC
Q   M   I   V   L   S   S   R   P   V   V   D   M   V   T   L>

1970          1980          1990          2000          B8552
ATG TCC TTC TCT CCA GCT GAG ATC CCA GTG CAT GAA GTG GAG TGC TCC
TAC AGG AAG AGA GGT CGA CTC TAG GGT CAC GTA CTT CAC CTC ACG AGG
 M   S   F   S   P   A   E   I   P   V   H   E   V   E   C   S>

2020          2030          2040          2050          2060
TAT TCA ACC AGT AAC AAG ATG AAA GAA GGA GTT AAT ATC ACA ATC TGT
ATA AGT TGG TCA TTG TTC TAC TTT CTT CCT CAA TTA TAG TGT TAG ACA
Y   S   T   S   N   K   M   K   E   G   V   N   I   T   I   C>

2070          2080          2090 B8556          2110
TTC CAG ATC AAG TCT CTC TAC CCC CAG TTC CAA GGC CGC CTG GTT GCC
AAG GTC TAG TTC AGA GAG ATG GGG GTC AAG GTT CCG GCG GAC CAA CGG
F   Q   I   K   S   L   Y   P   Q   F   Q   G   R   L   V   A>

2120          2130          2140          2150          2160
AAT CTC ACT TAC ACT CTG CAG CTG GAT GGC CAC CGG ACC AGA AGA CGG
TTA GAG TGA ATG TGA GAC GTC GAC CTA CCG GTG GCC TGG TCT TCT GCC
N   L   T   Y   T   L   Q   L   D   G   H   R   T   R   R   R>

2170          2180          2190          2200
GGG TTG TTC CCA GGA GGG AGA CAT GAA CTC AGA AGG AAT ATA GCT GTC
CCC AAC AAG GGT CCT CCC TCT GTA CTT GAG TCT TCC TTA TAT CGA CAG
G   L   F   P   G   G   R   H   E   L   R   R   N   I   A   V>

2210          2220          2230          2240          2250
ACC ACC AGC ATG TCA TGC ACT GAC TTC TCA TTT CAT TTC CCG GTA TGT
TGG TGG TCG TAC AGT ACG TGA CTG AAG AGT AAA GTA AAG GGC CAT ACA
 T   T   S   M   S   C   T   D   F   S   F   H   F   P   V   C>

2260          2270          2280          2290          2300
GTT CAA GAC CTC ATC TCC CCC ATC AAT GTT TCC CTG AAT TTC TCT CTT
CAA GTT CTG GAG TAG AGG GGG TAG TTA CAA AGG GAC TTA AAG AGA GAA
 V   Q   D   L   I   S   P   I   N   V   S   L   N   F   S   L>

2310          2320          2330          2340          2350
TGG GAG GAG GAA GGG ACA CCG AGG GAC CAA AGG GCG CAG GGC AAG GAC
ACC CTC CTC CTT CCC TGT GGC TCC CTG GTT TCC CGC GTC CCG TTC CTG
W   E   E   E   G   T   P   R   D   Q   R   A   Q   G   K   D>

    2360          2370          B8557          2390          2400
ATA CCG CCC ATC CTG AGA CCC TCC CTG CAC TCG GAA ACC TGG GAG ATC
TAT GGC GGG TAG GAC TCT GGG AGG GAC GTG AGC CTT TGG ACC CTC TAG
I   P   P   I   L   R   P   S   L   H   S   E   T   W   E   I>
```

```
            2410          2420          2430          2440
CCT TTT GAG AAG AAC TGT GGG GAG GAC AAG AAG TGT GAG GCA AAC TTG
GGA AAA CTC TTC TTG ACA CCC CTC CTG TTC TTC ACA CTC CGT TTG AAC
 P   F   E   K   N   C   G   E   D   K   K   C   E   A   N   L>


2450          2460      2470    B8559         2490
AGA GTG TCC TTC TCT CCT GCA AGA TCC AGA GCC CTG CGT CTA ACT GCT
TCT CAC AGG AAG AGA GGA CGT TCT AGG TCT CGG GAC GCA GAT TGA CGA
 R   V   S   F   S   P   A   R   S   R   A   L   R   L   T   A>

2500          2510          2520          2530          2540
TTT GCC AGC CTC TCT GTG GAG CTG AGC CTG AGT AAC TTG GAA GAA GAT
AAA CGG TCG GAG AGA CAC CTC GAC TCG GAC TCA TTG AAC CTT CTT CTA
 F   A   S   L   S   V   E   L   S   L   S   N   L   E   E   D>

2550          2560          2570          2580          2590
GCT TAC TGG GTC CAG CTG GAC CTG CAC TTC CCC CCG GGA CTC TCC TTC
CGA ATG ACC CAG GTC GAC CTG GAC GTG AAG GGG GGC CCT GAG AGG AAG
A   Y   W   V   Q   L   D   L   H   F   P   P   G   L   S   F>

 2600          2610          2620          2630          2640
CGC AAG GTG GAG ATG CTG AAG CCC CAT AGC CAG ATA CCT GTG AGC TGC
GCG TTC CAC CTC TAC GAC TTC GGG GTA TCG GTC TAT GGA CAC TCG ACG
R   K   V   E   M   L   K   P   H   S   Q   I   P   V   S   C>

 2650          2660          2670          2680
GAG GAG CTT CCT GAA GAG TCC AGG CTT CTG TCC AGG GCA TTA TCT TGC
CTC CTC GAA GGA CTT CTC AGG TCC GAA GAC AGG TCC CGT AAT AGA ACG
E   E   L   P   E   E   S   R   L   L   S   R   A   L   S   C>

 2690          2700          2710          2720          2730
AAT GTG AGC TCT CCC ATC TTC AAA GCA GGC CAC TCG GTT GCT CTG CAG
TTA CAC TCG AGA GGG TAG AAG TTT CGT CCG GTG AGC CAA CGA GAC GTC
N   V   S   S   P   I   F   K   A   G   H   S   V   A   L   Q>

 2740  B8558           2760          2770          2780
ATG ATG TTT AAT ACA CTG GTA AAC AGC TCC TGG GGG GAC TCG GTT GAA
TAC TAC AAA TTA TGT GAC CAT TTG TCG AGG ACC CCC CTG AGC CAA CTT
 M   M   F   N   T   L   V   N   S   S   W   G   D   S   V   E>

 2790          2800          2810  B3606                   2830
TTG CAC GCC AAT GTG ACC TGT AAC AAT GAG GAC TCA GAC CTC CTG GAG
AAC GTG CGG TTA CAC TGG ACA TTG TTA CTC CTG AGT CTG GAG GAC CTC
 L   H   A   N   V   T   C   N   N   E   D   S   D   L   L   E>

 2840          2850          2860          2870          2880
GAC AAC TCA GCC ACT ACC ATC ATC CCC ATC CTG TAC CCC ATC AAC ATC
CTG TTG AGT CGG TGA TGG TAG TAG GGG TAG GAC ATG GGG TAG TTG TAG
 D   N   S   A   T   T   I   I   P   I   L   Y   P   I   N   I>
```

```
2890          2900          2910          2920
CTC ATC CAG GAC CAA GAA GAC TCC ACA CTC TAT GTC AGT TTC ACC CCC
GAG TAG GTC CTG GTT CTT CTG AGG TGT GAG ATA CAG TCA AAG TGG GGG
 L   I   Q   D   Q   E   D   S   T   L   Y   V   S   F   T   P>

2930          2940          2950          2960              BamH I
AAA GGC CCC AAG ATC CAC CAA GTC AAG CAC ATG TAC CAG GTG AGG ATC
TTT CCG GGG TTC TAG GTG GTT CAG TTC GTG TAC ATG GTC CAC TCC TAG
 K   G   P   K   I   H   Q   V   K   H   M   Y   Q   V   R   I>

2980          2990          3000          3010          3020
CAG CCT TCC ATC CAC GAC CAC AAC ATA CCC ACC CTG GAG GCT GTG GTT
GTC GGA AGG TAG GTG CTG GTG TTG TAT GGG TGG GAC CTC CGA CAC CAA
 Q   P   S   I   H   D   H   N   I   P   T   L   E   A   V   V>

3030          3040          3050          3060          3070
GGG GTG CCA CAG CCT CCC AGC GAG GGG CCC ATC ACA CAC CAG TGG AGC
CCC CAC GGT GTC GGA GGG TCG CTC CCC GGG TAG TGT GTG GTC ACC TCG
 G   V   P   Q   P   P   S   E   G   P   I   T   H   Q   W   S>

3080          3090          3100          3110      B3607
GTG CAG ATG GAG CCT CCC GTG CCC TGC CAC TAT GAG GAT CTG GAG AGG
CAC GTC TAC CTC GGA GGG CAC GGG ACG GTG ATA CTC CTA GAC CTC TCC
 V   Q   M   E   P   P   V   P   C   H   Y   E   D   L   E   R>

      3130          3140          3150          3160
CTC CCG GAT GCA GCT GAG CCT TGT CTC CCC GGA GCC CTG TTC CGC TGC
GAG GGC CTA CGT CGA CTC GGA ACA GAG GGG CCT CGG GAC AAG GCG ACG
 L   P   D   A   A   E   P   C   L   P   G   A   L   F   R   C>

3170          3180          3190          3200      B3608
CCT GTT GTC TTC AGG CAG GAG ATC CTC GTC CAA GTG ATC GGG ACT CTG
GGA CAA CAG AAG TCC GTC CTC TAG GAG CAG GTT CAC TAG CCC TGA GAC
 P   V   V   F   R   Q   E   I   L   V   Q   V   I   G   T   L>

3220          3230          3240          3250          3260
GAG CTG GTG GGA GAG ATC GAG GCC TCT TCC ATG TTC AGC CTC TGC AGC
CTC GAC CAC CCT CTC TAG CTC CGG AGA AGG TAC AAG TCG GAG ACG TCG
 E   L   V   G   E   I   E   A   S   S   M   F   S   L   C   S>

3270          3280          3290          3300          3310
TCC CTC TCC ATC TCC TTC AAC AGC AGC AAG CAT TTC CAC CTC TAT GGC
AGG GAG AGG TAG AGG AAG TTG TCG TCG TTC GTA AAG GTG GAG ATA CCG
 S   L   S   I   S   F   N   S   S   K   H   F   H   L   Y   G>

3320          3330          3340          3350          3360
AGC AAC GCC TCC CTG GCC CAG GTT GTC ATG AAG GTT GAC GTG GTG TAT
TCG TTG CGG AGG GAC CGG GTC CAA CAG TAC TTC CAA CTG CAC CAC ATA
 S   N   A   S   L   A   Q   V   V   M   K   V   D   V   V   Y>
```

```
3370              3380              3390              3400
GAG AAG CAG ATG CTC TAC CTC TAC GTG CTG AGC GGC ATC GGG GGG CTG
CTC TTC GTC TAC GAG ATG GAG ATG CAC GAC TCG CCG TAG CCC CCC GAC
 E   K   Q   M   L   Y   L   Y   V   L   S   G   I   G   G   L>
             TCC AGC TGA ATT  OLIGO TO INTRODUCE Sal I SITE(B3609)

 3410          3420          3430          3440          3450
CTG CTG CTG CTG CTC ATT TTC ATA GTG CTG TAC AAG GTT GGT TTC TTC
GAC GAC GAC GAC GAG TAA AAG TAT CAC GAC ATG TTC CAA CCA AAG AAG
 L   L   L   L   L   I   F   I   V   L   Y   K   V   G   F   F>

 3460          3470          3480          3490          3500
AAA CGG AAC CTG AAG GAG AAG ATG GAG GCT GGC AGA GGT GTC CCG AAT
TTT GCC TTG GAC TTC CTC TTC TAC CTC CGA CCG TCT CCA CAG GGC TTA
 K   R   N   L   K   E   K   M   E   A   G   R   G   V   P   N>

 3510          3520          3530          3540          3550
GGA ATC CCT GCA GAA GAC TCT GAG CAG CTG GCA TCT GGG CAA GAG GCT
CCT TAG GGA CGT CTT CTG AGA CTC GTC GAC CGT AGA CCC GTT CTC CGA
 G   I   P   A   E   D   S   E   Q   L   A   S   G   Q   E   A>

 3560          3570          3580          3590          3600
GGG GAT CCC GGC TGC CTG AAG CCC CTC CAT GAG AAG GAC TCT GAG AGT
CCC CTA GGG CCG ACG GAC TTC GGG GAG GTA CTC TTC CTG AGA CTC TCA
 G   D   P   G   C   L   K   P   L   H   E   K   D   S   E   S>

3610
GGT GGT GGC AAG GAC TGA
CCA CCA CCG TTC CTG ACT
 G   G   G   K   D   *>
```